Calcium signalling mechanisms in regulating mesenchymal stem cell functions

Fatema Zahed Mousawi

Submitted in accordance with the requirements for the degree of Doctor of Philosophy

The University of Leeds

School of Biomedical Sciences

June, 2019

Acknowledgement

First and foremost, I would like to express my sincerest gratitude to my supervisor, Dr. Lin-Hua Jiang, who gave me the great opportunity to work with him and join his research group. I am very grateful for his patience, invaluable assistance and guidance during the planning and development of this research work, his intellectual support at every stage of my PhD study and his willingness to give his time so generously. This thesis would not have been finished without his supervision, guidance and altruistic.

I would like to extend my sincere thanks to Dr. Sreenivasan Ponnambalam for being my assessor and for his instructive and informative pieces of advice. I am also grateful for Dr. Xuebin Yang for being my second supervisor. I must also thank Dr. Hongsen Peng, who provided the cells used in this study. I would like to acknowledge the Kuwait Government for supporting my PhD with a fully-funded scholarship.

I would also like to thank all members of the Dr. Jiang research group both past and present, Dr. Sharifa Alawieyah Syed Mortadza, Yunjie Hao, Dr. Madiha Khalid, Dr. Xin Li and Harneet Mankoo for the their selfless assistance, technical support, moral support, especially during working until late hours, and for their abilities in turning the hard times into enjoyable times in the lab. I also wish to thank Antony Chan and Faheem Shaik for their practical suggestions and technical support.

I am very grateful to my beloved family and friends for their support during my PhD. I especially wish to express my love and greatest gratitude for my precious mother (Om-Sayed Ahmed) for her great role in my life in always supporting me, believing in me and pushing me forward for better. Warmest thanks also go to my best friends, Maali Al-Ahmad, Jumana AL-Qallaf, Nada Abuarab and Areej Al-Zahrani, without whom I would never have been able to achieve so much through their constant motivations as well as support and allowing me to vent out frustration during my PhD. Finally, a special thank you to a special person, Mohsen Al-Abdullah, who has been the best supporter, keeping me positive and being a good listener all the way throughout writing my thesis. I couldn't have done this without you all. Thank you all.

Publications

Jiang, L.-H., Hao, Y., Mousawi, F., Peng, H. and Yang, X. 2017. Expression of P2 purinergic receptors in mesenchymal stem cells and their roles in extracellular nucleotide regulation of cell functions: P2 receptors in MSC functions. *Journal of Cellular Physiology*. **232**(2), pp.287–297.

Jiang, L.-H., Mousawi, F., Yang, X. and Roger, S. 2017. ATP-induced Ca^{2+}-signalling mechanisms in the regulation of mesenchymal stem cell migration. *Cellular and Molecular Life Sciences*. **74**(20), pp.3697–3710.

Khalid, M., Brisson, L., Tariq, M., Hao, Y., Guibon, R., Fromont, G., Mortadza, S.A.S., Mousawi, F., Manzoor, S., Roger, S. and Jiang, L.-H. 2017. Carcinoma-specific expression of P2Y11 receptor and its contribution in ATP-induced purinergic signalling and cell migration in human hepatocellular carcinoma cells. *Oncotarget*. **8**(23), pp.37278–37290.

Peng, H., Hao, Y., Mousawi, F., Roger, S., Li, J., Sim, J.A., Ponnambalam, S., Yang, X. and Jiang, L.-H. 2016. Purinergic and store-operated Ca^{2+} signalling mechanisms in mesenchymal stem cells and their roles in ATP-induced stimulation of cell migration: ATP-induced Ca^{2+} signalling in MSC migration. *Stem Cells*. **34**(8), pp.2102–2114.

Manuscript accepted and under revision

Mousawi, F., Peng, H., Li, J., Ponnambalam, S., Roger, S., Zhao, H.C., Yang, X. and Jiang, L.-H. (2019) Chemical activation of the Piezo1 channel drives mesenchymal stem cell migration via inducing ATP release and activation of P2 receptor purinergic signalling. *Stem Cells* (accepted).

Wei, L.*, Mousawi, F.*, Li, D., Roger, S., Li, J., Yang, X. and Jiang, L.-H. (2019) ATP release and P2 receptor signalling in Piezo1 channel-dependent mechanoregulation. *Frontiers in Pharmacology* (under revision) (*co-first author).

Abstract

Extracellular ATP is one of the most common signalling molecules that induce an increase in the intracellular Ca^{2+} concentration ($[Ca^{2+}]_i$) via P2 receptors, namely ligand-gated ion channels P2X and/or G protein-coupled P2Y receptors. ATP is shown to evoke robust Ca^{2+} signalling in mesenchymal stem cells (MSCs) and regulate MSC proliferation, migration and differentiation. However, there are noticeable discrepancies in the mechanisms underlying ATP-induced Ca^{2+} signalling and regulation of MSC functions. Furthermore, the Ca^{2+}-dependent downstream signalling pathways in ATP-induced regulation of MSC functions are poorly understood. MSCs have been documented to release ATP in response to mechanical stimulation, but the mechanism mechanosensing and mediating ATP release remains elusive. The studies presented in this thesis, using human dental pulp-derived MSCs (hDP-MSCs), aimed to investigate ATP-induced purinergic Ca^{2+} signalling and Ca^{2+}-dependent signalling pathways in regulating cell migration and adipogenic differentiation and examine the hypothesis that the mechanically activated Ca^{2+}-permeable Piezo1 channel regulates hDP-MSC migration via ATP release and activation of the P2 receptors.

The study presented in chapter 3, first of all, showed that exposure to ATP increased cell migration, using wound healing and trans-well migration assays. Exposure to BzATP and NF546, a P2Y11 selective agonist, also enhanced cell migration. ATP-induced cell migration was inhibited by PPADS, a P2 generic antagonist. It was also reduced by KN-93, a CaMKII inhibitor, chelerythrine chloride, a PKC inhibitor, and PF431396, a PYK2 inhibitor, and furthermore, by U0126, an inhibitor MEK/ERK, and SB202190, a p38 MAPK inhibitor. Collectively, these results provide evidence to confirm the recent findings that extracellular ATP stimulates hDP-MSC migration and identify CaMKII, PKC, PYK2 and MAPKs as downstream signalling pathways in transducing ATP-induced Ca^{2+} signalling to cell migration.

The study in chapter 4 focused on the Piezo1 channel in hDP-MSCs. Piezo1 mRNA and protein expression were detected using RT-PCR and immunostaining, respectively. Exposure to Yoda1, a chemical activator of the Piezo1 channel, elevated the $[Ca^{2+}]_i$ via

Ca^{2+} influx. Yoda1-induced Ca^{2+} response was inhibited by ruthenium red and GsMTx4, two structurally different Piezo1 inhibitors, or Piezo1-specific siRNA, supporting the functional expression of the Piezo1 channel. Exposure to Yoda1 stimulated cell migration, which was inhibited by Piezo1-specific siRNA. Yoda1-induced cell migration was also prevented by apyrase, an ATP-scavenger as well as PPADS, suggesting that Piezo1 channel activation stimulates cell migration via ATP release and activation of the P2 receptors. Consistently, Yoda1-induced cell migration was inhibited by KN-93, chelerythrine chloride, PF431396, and U0126, indicating engagement of CaMKII, PKC and PYK2 and MEK/ERK as Ca^{2+}-dependent downstream signalling mechanisms.

The study presented in chapter 5 started with examining the molecular mechanisms participating in ATP-induced Ca^{2+} signalling. ATP-induced increase in the $[Ca^{2+}]_i$ in extracellular Ca^{2+}-containing solution was inhibited by PPADS. ATP and BzATP induced increases in the $[Ca^{2+}]_i$ in extracellular Ca^{2+}-free as well as Ca^{2+}-containing solutions. ADP and NF546 also evoked an increase in the $[Ca^{2+}]_i$. These results support a significant role for the P2X7, P2Y1 and P2Y11 receptors in ATP-induced Ca^{2+} signalling. The study, next, examined the expression of these receptors and also the P2Y2 receptor during adipogenic differentiation. There was an increase in the P2Y1 and a decrease in the P2Y2 mRNA expression, but no alteration in the expression of the P2Y11 and P2X7 after hDP-MSC adipogenesis. Exposure to ATP during adipogenesis resulted in a significant increase in adipogenic differentiation, examined using oil red O staining and, furthermore, up-regulation of the P2Y11 expression with no effect on the other receptors. Moreover, ATP-induced adipogenic differentiation was reduced by KN-93 and PF431396, suggesting the involvement of CaMKII and PYK2 in ATP-induced upregulation of adipogenesis.

In summary, the studies presented in this thesis gain a better understanding of ATP-induced Ca^{2+} downstream signalling pathways in the regulation of MSC migration and adipogenic differentiation, and also provide evidence to support an important role for the Piezo1 channel in regulating MSC migration via ATP release and subsequent activation of P2 receptors. Such information should be useful for the development of better use of MSCs in tissue engineering and cell-based therapies.

Table of Contents

List of Tables

List of Figures

List of Abbreviations

µg	Microgram
µl	Microliter
µm	Micrometer
µM	Micromolar
2-APB	2-Aminoethoxydiphenyl borate
2-MeSADP	2-Methylthio-ADP
2-MeSATP	2-Methylthioadenosine 5’-triphosphate
5-BDBD	5-(3-Bromophenyl)-1,3-dihydro-2H-benzofuro[3,2-e]-1,4-diazepin-2-one
αβMeATP	α,β-methylene ATP
ABC	ATP-binding cassette
AC	Adenylyl cyclase
ACh	Acetylcholine
ADP	Adenosine 5'-diphosphate
ALP	Alkaline phosphatase
AM	Acetoxymethyl
AMP	Adenosine monophosphate
Ap4A	Diadenosine tetraphosphate
AT-MSCs	Adipose tissue-derived MSCs
ATP	Adenosine 5’-triphosphate
ATPγS	Adenosine-5'-(γ-thio)-triphosphate
BBG	Brilliant blue G
BM-MSCs	Bone marrow-derived MSCs
BMP2	Bone morphogenetic protein 2
bp	Base pairs
BrdU	5-Bromo-20-deoxyuridine

BzATP	2′(3′)-O-(4-benzoylbenzoyl)-ATP
Ca^{2+}	Calcium ion
$CaCl_2$	Calcium chloride solution
CaM	Calmodulin
CaMKII	Calmodulin-dependent kinase II
cAMP	Cyclic AMP
CCK-8 assay	Cell counting-kit-8 assay
CD	Cluster of differentiation antigen
cDNA	Complementary DNA
CEBPα/β	CCAAT/enhancer binding protein α/β
CED	C-terminal extracellular domain
CO_2	Carbon dioxide
CRAC channels	Ca^{2+}-release-activated Ca^{2+} channels
C_t	Cycle threshold
CTC	Chelerythrine chloride
CTD	C-terminal domain
CTL	Control
DAG	Diacylglycerol
DAPI	4',6-diamidino-2-phenylindole
DCC receptor	Deleted in colorectal cancer receptor
DMEM	Dulbecco’s modified Eagle’s medium
DNA	Deoxyribonucleic acid
D-PBS	Dulbecco’s phosphate buffered saline
DP-MSCs	Dental pulp-derived MSCs
EC_{50}	Concentration of agoist evoking half of the maximal response
ECM	Extracellular matrix
EDTA	Ethylene diamine tetraacetic acid

EGTA	Ethylene glycol tetraacetic acid
E-NPPs	Ecto-nucleotide pyrophosphohydrolases/phosphodiesterases
E-NTPDases	Ecto-nucleoside triphosphate diphosphohydrolases
ER	Endoplasmic reticulum
ERK	Extracellular signal-regulated kinase
ESCs	Embryonic stem cells
FABP4	Fatty acid binding protein 4
Fam38	Family with sequence similarity 38
FBS	Foetal bovine serum
FITC	Fluorescein isothiocyanate
g	Gravitational force
GPCRs	G-protein-coupled receptors
G-proteins	Guanosine nucleotide-binding proteins
GsMTx4	Grammostola spatulata mechanotoxin 4
HEPES	N-(2-hydroxyethyl) piperazine-N'-(2-ethanulfonic acid)
HLA-DR	Human leucocyte antigen class II cell surface receptor
HP	Hydrostatic pressure
IBMX	Isobutyl-methylxanthine
IC_{50}	Concentration inhibiting agonist-induced response by 50%
IH	Inner helix
IL-1receptor	Interleukin-1 receptor
IL-1β	Interleukin-1β
IP_3	Inositol 1,4,5-triphosphate
IP_3R	IP_3 receptor
iPSCs	Induced pluripotent stem cells
ISCT	International Society for Cellular Therapy
iso-PPADS	2,5-Disulfonate isomer PPDAS

JNK	Jun N-terminal kinase
K^+	Potassium ion
Kb	Kilo base
KCl	Potassium chloride
Klf-4	Kruppel like factor-4
LIPUS	Low-intensity pulsed ultrasound
LPA	Lysophosphatidic acid
LPAR	Lysophosphatidic acid receptor
LPL	Lipoprotein lipase
mAChR	Muscarinic acetylcholine receptor
MAPK	Mitogen-activated protein kinase
MEK	Mirogen-activated protein kinase kinase
mg/kg/day	Milligrams per kilogram per day
$MgCl_2$	Magnesium chloride
mM	Millimolar
mRNA	Messenger RNA
MSCs	Mesenchymal stem cells
MTT	Methylthiazol tetrazolium
mU/ml	Milliunits per milliliter
Na^+	Sodium ion
NaCl	Sodium chloride
NAD	Nicotinamide adenine dinucleotide
NFAT	Nuclear factor of activated T cells
nm	Nanometers
nM	Nanomolar
Oct-3/4	Octamer binding transcription factor-3/4
OD	Optical density

OH	Outer helix
oxATP	Oxidized ATP
PA	Pluronic acid
Pax6	Paired box 6
PBS	Phosphate-buffered saline
PDBu	Phorbol 12,13-dibutyrate
PDLSCs	Periodontal ligament stem cells
PFA	Paraformaldehyde
PH	Peripheral region
Pi	Phosphate
PIP_2	Phosphatidylinositol 4,5-biphosphate
PKC	Protein kinase C
PLC	Phospholipase C
PMA	Phorbol 12-myristate 13-acetate
PPADS	Pyridoxal-phosphate-6-azophenyl-2',4'-disulfonate
PPARγ	Peroxisome proliferator-activated receptor γ
PPi	Pyrophosphate
PYK2	Proline-rich tyrosine kinase 2
R^2	Coefficient of determination
rcf	Relative centrifugal force
RNA	Ribonucleic acid
RR	Ruthenium red
RT-PCR	Reverse transcription-polymerase chain reaction
Runx2	Runt related transcription factor 2
S.E.M.	Standard error of mean
SBS	Standard buffer solution
SERCA	Sarcoplasmic/endoplasmic reticulum Ca^{2+}-ATPase

siRNA	Small interfering RNA
SOC entry	Store-operated Ca^{2+} entry
Sox-2	Sex determining region Y box-2
Sox-9	Sex determining region Y box-9
SR	Sarcoplasmic reticulum
SSEA	Stage-specific embryonic antigen
Stim1	Stromal interaction molecule 1
TAE	Tris acetate EDTA
TE buffer	Tri-EDTA buffer
TM	Transmembrane segments
TNF-α	Tumor necrosis factor-α
TNP-ATP	2,3-O-(2,4,6-trinitrophenyl) ATP
Tuj1	Neuron-specific class III β-tubulin
U/ml	Units per milliliter
UC-MSCs	Umbilical cord-derived MSCs
UDP	Uridine diphosphate
Up4U	Diuridine tetraphosphate
UTP	Uridine -5'-triphosphate
UTPγS	Uridine 5'-O-3-thiotriphosphate
[3H] thymidine	Tritium-labeled thymidine
$[Ca^{2+}]_i$	Intracellular Ca^{2+} concentration

CHAPTER 1
General Introduction

1.1 A brief introduction to Ca^{2+} signalling

Virtually in all cell types, intracellular calcium ion (Ca^{2+}) is a well-defined primary second messenger to initiate signalling cascades in the control and regulation of diverse events ranging from fertilization, embryonic development, cell proliferation, differentiation, migration, death, muscle contraction, to gene expression (Berridge et al., 2000; Berridge et al., 2003; Ding et al., 2012; Lembong et al., 2017; Morrell et al., 2018). Concentrations of the intracellular Ca^{2+} ($[Ca^{2+}]_i$) can range from ~100 nM under rest conditions (Clapham, 2007), while the concentration of extracellular Ca^{2+} is ~1-2 mM (Samtleben et al., 2013) and, therefore, there is a large Ca^{2+}gradient between inside and outside the cell. There are several mechanisms to maintain the basal $[Ca^{2+}]_i$, such as the plasma membrane Ca^{2+}-ATPase pump and the sodium ion (Na^+)-Ca^{2+} exchanger that involves driving cytosolic Ca^{2+} out of the cell and also the sarcoplasmic/endoplasmic reticulum Ca^{2+}-ATPase (SERCA) pump that is crucial for transporting cytosolic Ca^{2+} into the endoplasmic reticulum (ER) or sarcoplasmic reticulum (SR) in muscle cells (Clapham, 2007). A variety of extracellular chemical, mechanical and biological stimuli have been shown to regulate intracellular Ca^{2+} signalling via acting on specified mechanisms or coupling intrinsic signalling mechanisms (Bootman, 2012; Kim et al., 2015; Artemenko et al., 2016). Numerous mechanisms have been identified that increase in the $[Ca^{2+}]_i$ via stimulating extracellular Ca^{2+} influx or intracellular Ca^{2+} release (Berridge et al., 2000; Kawano et al., 2002; Berridge et al., 2003). The former mechanism model demonstrated extracellular Ca^{2+} entry is mediated via plasma membrane Ca^{2+} permeable ion channels (Berridge et al., 2000; Kawano et al., 2002; Clapham, 2007; Coste et al., 2010). Subsequently, the later mechanism established intracellular Ca^{2+} release occurs from the ER that represents the largest intracellular Ca^{2+} store (Berridge et al., 2003), with the Ca^{2+} concentration to be ~100-800 μM (Samtleben et al., 2013).

Extracellular nucleotides, particularly adenosine 5'-triphosphate (ATP), act as autocrine and/or paracrine signalling molecules leading to an increase in the $[Ca^{2+}]_i$. ATP-induced increase in the $[Ca^{2+}]_i$ is mediated by the P2 family of purinergic receptors located on the cell surface (Burnstock and Ulrich, 2011). According to the pharmacological, functional and molecular properties, P2 receptors can be further divided into two distinctive subfamilies, namely P2X and P2Y (Ralevic and Burnstock, 1998). The P2X receptors are ionotropic receptors that function as ATP-gated Ca^{2+}-permeable cationic channels (North, 2002), whereas the P2Y receptors are metabotropic receptors that are coupled to the trimeric guanosine nucleotide-binding proteins (G-proteins) and thus belong to the G-protein-coupled receptors (GPCRs) superfamily (Abbracchio et al., 2006). ATP-induced P2 purinergic signalling with a consequent increase in the $[Ca^{2+}]_i$ can initiate intracellular signalling pathways and thereby determine or regulate a wide array of cellular functions (North, 2002; Burnstock and Ulrich, 2011).

Cells are continuously exposed to mechanical forces that are integrated by the plasma membrane, cytoskeleton, extracellular matrix (ECM), adhesion proteins and ion channels to influence biological processes at the molecular and cellular levels, such as gene expression, adhesion, migration and cell fate, which are essential to maintain tissue homeostasis (Kim et al., 2009). It has been extensively documented that ATP is released from different cell types in response to various physical, chemical and biological stimuli. Mechanical stimulus is well-recognized to cause ATP release and subsequent increase in the $[Ca^{2+}]_i$ (Katz et al., 2006; Riddle et al., 2007; Katz et al., 2008; Sun et al., 2013; Weihs et al., 2014; Shibukawa et al., 2015: Wang et al., 2016; Albarrán-Juárez et al., 2018). The Piezo1 channel, a newly-discovered mechanosensitive or mechanically activated Ca^{2+}-permeable cationic channel (Coste et al., 2010; Coste et al., 2012), has been shown to sense mechanical stimuli and transduce into intracellular Ca^{2+} signals via mediating extracellular Ca^{2+} influx (Miyamoto et al., 2014; Hung et al., 2016). Interestingly, emerging evidence also supports a role of the Piezo1 channel in mediating mechanical induction of Ca^{2+} signalling via ATP release and subsequent activation of P2 receptors (Wang et al., 2016; Albarrán-Juárez et al., 2018).

In this Introduction chapter, I will firstly present an overview of the P2 receptors and their roles in ATP-induced Ca^{2+} signalling, and also the Piezo1 channel and its role in mediating mechanical induction of ATP release and subsequent activation of P2 purinergic signalling. Secondly, I will introduce mesenchymal stem cells (MSCs), which the research described in this thesis will focus on, and discuss the current knowledge regarding the expression of P2X and P2Y receptors and Piezo1 channel in MSCs, and their roles in the regulation of MSC functions. It is well-recognized that Ca^{2+} signalling regulation of cell functions depends on Ca^{2+}-sensitive protein kinases and downstream signalling pathways. Therefore, in the final section, I will discuss the roles of Ca^{2+}-sensitive protein kinases and downstream signalling pathways in the regulation of MSC functions.

1.2 ATP-induced purinergic Ca^{2+} signalling

1.2.1 ATP release and metabolism

ATP is better known to be present intracellularly as the main source of cellular energy and indispensable for a living cell. Extracellular ATP was proposed as a signalling molecule mediating purinergic neurotransmission in 1972 by Burnstock (Burnstock et al., 1972), a concept that remained controversial until molecular identification of the first receptors for ATP in early 1990 (Burnstock, 2013). The cytosolic concentration of ATP is in the range of 2-5 mM (Orriss et al., 2009), whereas the concentration of extracellular ATP surrounding cells under *in vitro* culture conditions or *in vivo* is in the nanomolar range (Praetorius and Leipziger, 2009). It is well-recognized that ATP is released from most cell types into the extracellular milieu at the site of tissue damage and inflammation. ATP is also released from healthy cells, as has shown in neurons, astrocytes, endothelial cells, urothelial cells, macrophages, osteoblasts and odontoblasts (Bowler et al., 2001; Bodin and Burnstock, 2001; Lazarowski, 2003; Agresti et al., 2005a; Abbracchio et al., 2006; Orriss et al., 2009; Praetorius and Leipziger, 2009; Lazarowski, 2012; Tu et al., 2014). Although the mechanisms mediating ATP release are not fully understood, several release mechanisms have been proposed, such as transportation via ATP-release channels including connexion hemi-gap junction channels and pannexin channels, ATP-binding cassette (ABC) transporters, and secretion via exocytosis of ATP-containing vesicles as well as plasma membrane-derived ATP-containing macrovesicles (Figure 1.1A)

(Schwiebert, 2001; Bodin and Burnstock, 2001; Striedinger et al., 2007; Burnstock and Verkhratsky, 2009; Praetorius and Leipziger, 2009; Dou et al., 2012; Lohman and Isakson, 2014; Egbuniwe et al., 2014; Di Virgilio and Adinolfi, 2017). There is evidence that intracellular Ca^{2+} can trigger the vesicular release of ATP (Striedinger et al., 2007; Praetorius and Leipziger, 2009; Dou et al., 2012).

Almost all cell types, including MSCs, express a group of plasma membrane ecto-enzymes that catalyze ATP hydrolysis (Figure 1.1B) (Abbracchio et al., 2006; Jiang et al., 2017a). Thus, extracellular ATP is readily hydrolyzed into adenosine diphosphate (ADP), adenosine monophosphate (AMP) and adenosine by members of the ecto-nucleoside triphosphate diphosphohydrolases (E-NTPDases) family, such as E-NTPDase 1 (apyrase or CD39) and NTPDase 2 (ecto-ATPase or CD39L1). ATP can be converted to AMP by the ecto-nucleotide pyrophosphohydrolases/phosphodiesterases (E-NPPs) family, and AMP to adenosine by ecto-5'-nucleotidases (CD73).

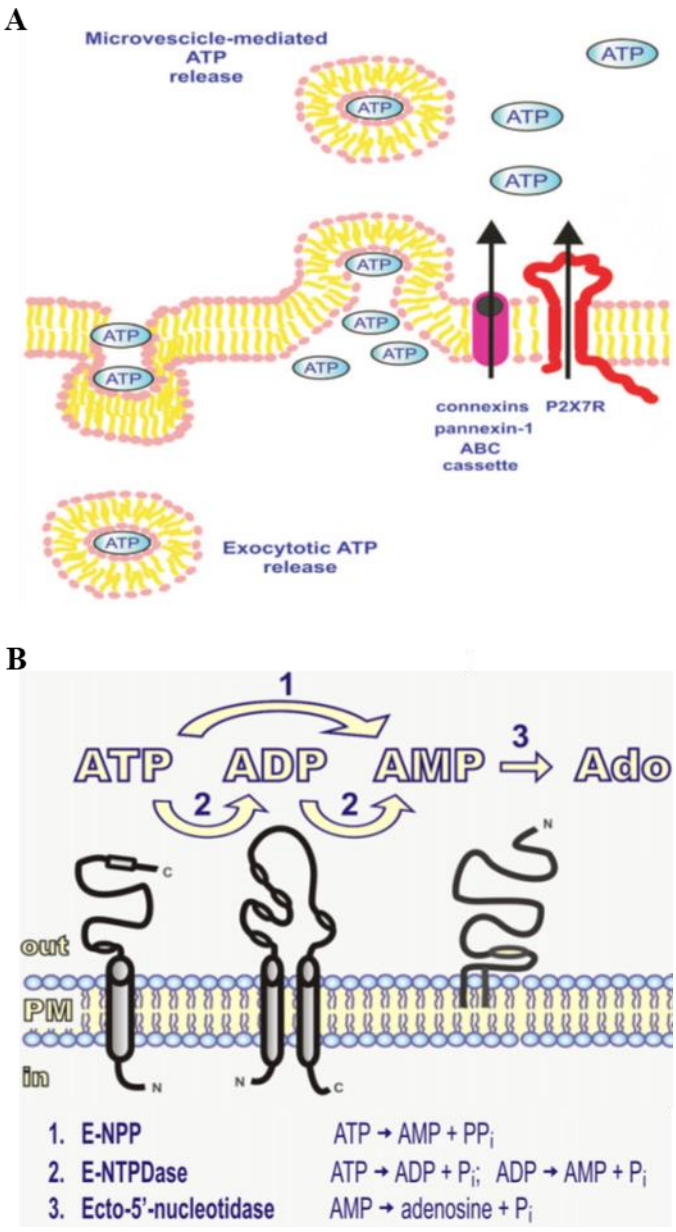

Figure 1.1 Proposed mechanisms mediate ATP release and degradation
(A) ATP can be released into extracellular space via ATP-containing vesicles (exocytosis), plasma membrane-derived macrovesicles. ATP can be also transported out of the cell through connexion hemi-gap junction and pannexin channels, ATP-binding cassette (ABC), or through P2X7 receptor (adapted from Di Virgilio and Adinolfi, 2017). (B) Extracellular ATP is hydrolyzed to AMP and pyrophosphate (PPi) by ecto-nucleotide pyrophosphohydrolase/phosphodiesterase (E-NPP) that possesses a short N-terminal intracellular domain, a single transmembrane domain, and a large extracellular domain, and to ADP, AMP and phosphate (Pi) by ecto-nucleoside triphosphate diphosphohydrolase (E-NTPDase) that possesses N- and C-terminal transmembrane domains. AMP is further hydrolyzed to adenosine and Pi by a glygosylphosphatidylinositol-anchoring phospholipid ecto-5'-nucleotidase (adapted from Yegutkin, 2008).

1.2.2 P2X receptors

As introduced above, P2X receptors are ATP-gated Ca^{2+}-permeable cationic channels that upon activation mediate Ca^{2+} influx to elevate the $[Ca^{2+}]_i$ (Figure 1.2A). P2X-mediated influx of Na^+ and Ca^{2+} and efflux of potassium ions (K^+) can also cause membrane depolarization that induces activation of voltage-gated Ca^{2+} channels, particularly in excitable cells, to increase the $[Ca^{2+}]_i$ (North, 2002). Since this mechanism does not involve production and diffusion of a second messenger within the cytosol or plasma membrane, the P2X receptors mainly mediate rapid responses to extracellular ATP (Burnstock et al., 2010).

Seven distinctive mammalian genes have been identified to encode seven P2X receptor subunits (P2X1-P2X7), which range in length from 384 (P2X4) to 595 (P2X7) amino acid residues (North, 2002; North and Jarvis, 2013). The P2X receptors are trimeric protein complexes. Each subunit possesses similar membrane topology consisting of intracellular N- and C-termini, and two α-helical transmembrane segments (TM1 and TM2) connected by a large extracellular loop composed of ~ 280 amino acid residues (Figure 1.2B) (Hattori and Gouaux, 2012). P2X1-P2X7 can form functional homotrimeric receptors, with the exception of P2X6 (Kaebisch et al., 2015). Except for P2X7, they can also assemble heterotrimeric receptors, for examples, P2X1/2, P2X1/4, P2X1/5, P2X2/3, P2X2/4, P2X2/5, P2X2/6 (Jiang, 2012; Kaebisch et al., 2015). Three ATP molecules bind to the extracellular part of P2X receptors at the inter-subunit interface. ATP binding induces conformational changes in the extracellular part that are transduced to the transmembrane domains, leading to the opening of the ion-permeating pathway that is formed by the TM2 segment from each of the three subunits (Figure 1.2B) (Hattori and Gouaux, 2012; Mansoor et al., 2016).

The P2X receptors are exclusively activated by extracellular ATP with varying potency, which is often determined by the ATP concentration that induces 50% of the maximal response (EC_{50}). The EC_{50} values of ATP range from 70 nM at the P2X1 receptor to ≥100 μM at the P2X7 receptor (Jarvis and Khakh, 2009). There are several synthetic ATP analogues that act as the P2X receptor agonists.

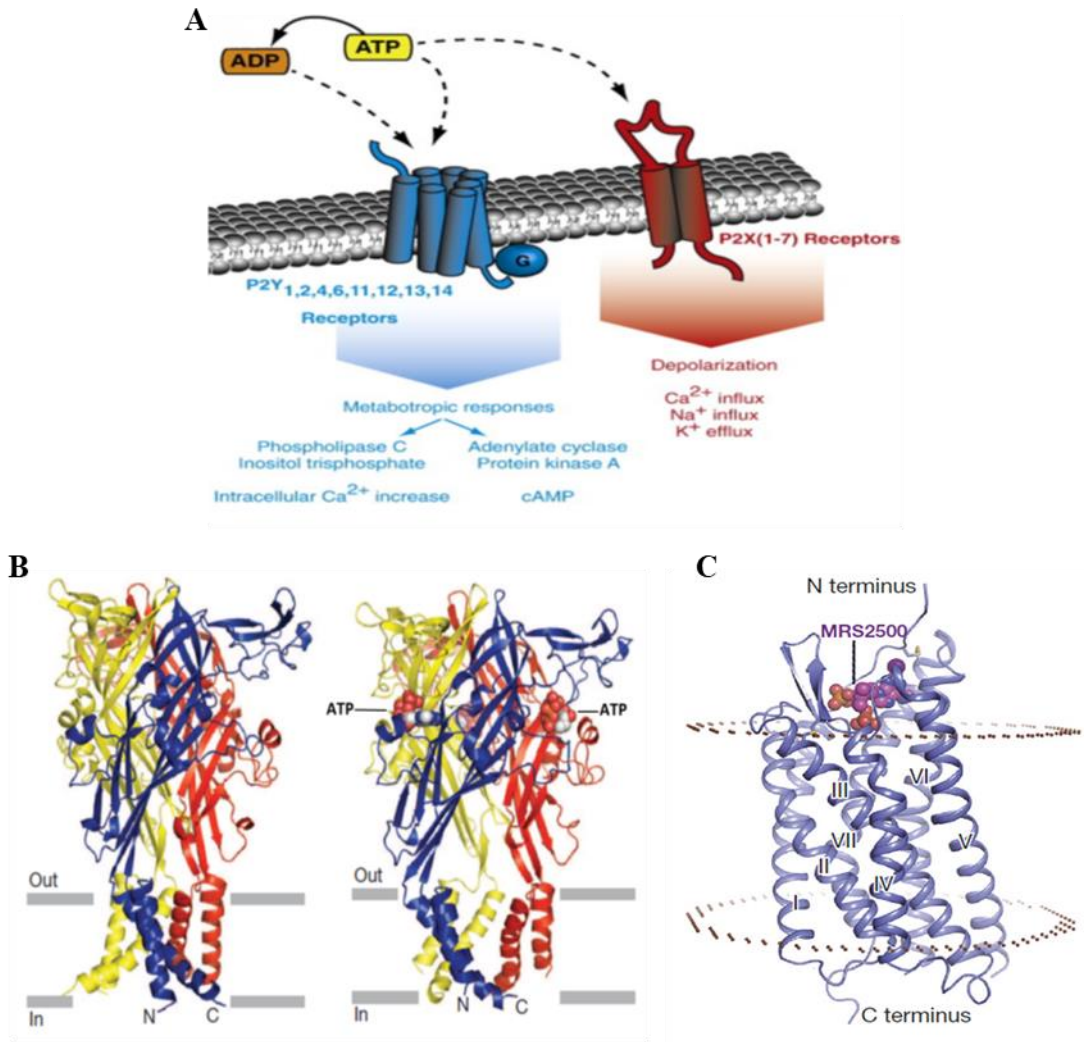

Figure 1.2 P2 purinergic receptor family and their architecture

(A) Extracellular ATP is an agonist for the P2X receptors, while ATP and its metabolite ADP can activate the P2Y receptors. Activation of the P2X receptors results in an influx of extracellular Na^+ and Ca^{2+} and efflux of K^+, thereby increasing the intracellular Ca^{2+} concentration and causing membrane depolarization. Activation of P2Y receptors leads to signal transduction via PLC activation, IP_3 generation and intracellular Ca^{2+} release to increase the intracellular Ca^{2+} concentration, and alternatively coupled to activation or inhibition of adenylate cyclase that regulates cAMP production (Adapted from Baroja-Mazo et al., 2013). (B) The zebrafish P2X4 receptor structure, with each subunit represented in a different color. Each subunit consists of short intracellular N- and C-termini (which are truncated in the structure) and two domains joined by a large extracellular loop. ATP, shown in sphere representation, binds to the subunit-interface and causes conformational changes in the extracellular domains that are transduced to the transmembrane domains, leading to opening the ion-permeating pathway (Adapted from Hattori and Gouaux, 2012). (C) The human P2Y1 receptor structure, illustrating the seven-transmembrane helical domains with short extracellular N- and intracellular C-termini, and binding of MRS2500 antagonist, shown in sphere presentation, to the extracellular N-terminus (Adapted from Zhang et al., 2015).

For example, 2-methylthioadenosine 5'-triphosphate (2-MeSATP), like ATP, activates all P2X receptors, including P2X1 (EC_{50} = 70 nM), P2X3 (EC_{50} = 0.3 μM) P2X4 (EC_{50} = 10 μM) and P2X7 (EC_{50} = 100 μM) receptors. α,β-methylene ATP (αβMeATP) acts as an agonist for P2X1 (EC_{50} = 0.3 μM) and P2X3 (EC_{50} = 0.8 μM) receptors. 2',3'-O(benzoyl-4-benzoyl)-ATP (BzATP) exhibits a potency (EC_{50} = 20 μM) that is about 5 times greater than ATP (EC_{50} ≥100 μM) at the P2X7 receptors but is equipotent or less potent than ATP at other P2X receptors, such as P2X1 (EC_{50} = 0.3 nM) (Jarvis and Khakh, 2009).

Surmain and pyridoxal-phosphate-6-azophenyl-2',4'-disulfonate (PPADS) are two generic antagonists that antagonize all P2X receptors, except the P2X4 receptor (Jarvis and Khakh, 2009; Syed and Kennedy, 2012). PPDAS 2,5-disulfonate isomer, *iso*-PPADS, is a selective antagonist for P2X receptors (Zhang et al., 2019). Numerous P2X subtype-selective antagonists have been developed. For example, NF279, a suramin analogue, is a P2X1 selective antagonist with the concentration that inhibits 50% of agonist-induced receptor response (IC_{50}) of 9-19 nM (Rettinger et al., 2000; Jarvis and Khakh, 2009). It can also antagonize other P2X receptors at micromolar concentrations, including P2X2 (IC_{50} ~ 30 μM), P2X3 (IC_{50} ~ 50 μM), P2X4 (IC_{50} > 100 μM) and P2X7 (IC_{50} ~ 20 μM) (Rettinger et al., 2000; Jarvis and Khakh, 2009). PSB-12062 (IC_{50} ~1.4 μM) and 5-BDBD (IC_{50} ~ 1.6 μM) represent two P2X4 selective antagonists (Stokes et al., 2017). 2,3-O-(2,4,6-trinitrophenyl) ATP (TNP-ATP) antagonizes P2X1 (IC_{50} ~ 6 nM), P2X2 (IC_{50} ~ 1 μM), P2X3 (IC_{50} ~ 1 nM) and P2X4 (IC_{50} ~ 15 μM) receptors (Jarvis and Khakh, 2009). A large number of P2X7 selective antagonists have been identified (Jiang, 2012; Jiang, et al., 2017b; Jiang et al., 2017a), including oxidized ATP (oxATP) (IC_{50} ~ 100 μM) (North and Jarvis, 2013), brilliant blue G (BBG) (IC_{50} ~ 10-100 nM) (Jiang et al., 2000), AZ11645373 (IC_{50} ~ 5-20 nM), A438079 (IC_{50} ~ 126-500 nM), A740003 (IC_{50} ~ 18 nM), KN-62 (IC_{50} ~ 40-130 nM) and AZ10606120 (IC_{50} < 10 nM) (Jiang et al., 2012). Some of these P2X7 antagonists are species-specific, for example, AZ11645373 (Stokes et al., 2006) and KN-62 (Donnelly-Roberts et al., 2009) are human P2X7 (hP2X7), selective antagonists.

The P2X receptors are expressed in many types of cells, both excitable cells like neurons and muscle cells and non-excitable cells like bone cells, endothelial cells and immune cells, where they mediate a variety of physiological processes, such as synaptic neurotransmission, muscle contraction, regulation of blood pressure and immune responses, and numerous pathophysiological processes, such as pain, inflammatory diseases, and cancer metastasis (Jarvis and Khakh, 2009; Burnstock et al., 2010; Burnstock, 2013; Burnstock, 2018). In addition, the P2X receptors have been shown to regulate cell proliferation, differentiation and migration (Burnstock et al., 2010). Interestingly, some studies indicated that the P2X7 receptor mediates ATP release in different cell types (Figure 1.1A) (Suadicani, 2006; Brandao-Burch et al., 2012).

1.2.3 P2Y receptors

The P2Y receptors are 308 to 377 amino acid residues long (Abbracchio et al., 2006), and the tertiary structure consists of seven transmembrane domains with short extracellular N- and intracellular C-termini (Figure 1.2A and C) (Ralevic and Burnstock, 1998). There are eight mammalian P2Y subtypes (P2Y1, P2Y2, P2Y4, P2Y6 and P2Y11-P2Y14) that exhibit preferential activation by different nucleotides (Ralevic and Burnstock, 1998; Abbracchio et al., 2006) via binding to the extracellular N-terminus (Jacobson et al., 2015). For instance, ATP activates the P2Y1, P2Y2, P2Y4 and P2Y11 receptors, ADP activates P2Y1, P2Y12 and P2Y13 receptors, UTP activates the P2Y2 and P2Y4 receptors, UDP activates the P2Y6 receptor, and UDP and nucleotide sugars, such as UDP-glucose and UTP-galactose, selectively activate the P2Y14 receptor (Abbracchio et al., 2006; Nishimura et al., 2017). ATP acts as a full agonist at the P2Y2 and P2Y11 receptors and partial agonist at the P2Y1 receptor (Burnstock, 2007; Jacobson et al., 2015; von Kügelgen and Hoffmann, 2016). ATP may also act as an antagonist at the human, but not rat, P2Y4 receptor (Kennedy et al., 2000).

There are several P2Y subtype selective agonists. For example, 2-methylthio-ADP (2-MeSADP) (EC_{50} ~ 8 nM) and (N)-methanocarba analogue of 2-MeSADP (MRS2365) (EC_{50} ~ 0.4 nM) (Ilatovskaya et al., 2013) are selective agonists with higher potency than ADP (EC_{50} ~ 8 μM) at the P2Y1 receptor (Webb et al., 1996). BzATP can also act as a

partial agonist at the P2Y1 receptor with an EC_{50} of 8.7 μM (Ilatovskaya et al., 2013). Moreover, there are several P2Y2 selective agonists, including 2-thio-UTP (EC_{50} ~ 35 nM) (Ko et al., 2008), γ-thiophosphate UTP (UTPγS) (EC_{50} ~ 0.24 μM), diquafosol, INS365 (Up4U) (EC_{50} ~ 0.1 μM) (Jacobson et al., 2009) and diadenosine-tetraphosphate (Ap4A) (EC_{50} ~ 0.7 μM) (Lazarowski et al., 1995). Furthermore, it has been reported that BzATP (EC_{50} ~10 μM) and γ-thiophosphate ATP (ATPγS) (EC_{50} ~ 13.5 μM) are more potent agonists than ATP (EC_{50} ~ 65 μM) at the P2Y11 receptor (Communi et al., 1999). Nicotinamide adenine dinucleotide (NAD^+) is a P2Y11 receptor agonist in a concentration range of 1-100 μM (Moreschi et al., 2006), and NF546 (EC_{50} ~ 0.53 μM) is a potent agonist for the P2Y11 receptor over the other P2Y receptors (Meis et al., 2010).

The P2Y receptors are antagonized by generic P2 antagonists, suramin (P2Y1, P2Y2, P2Y6 and P2Y11-P2Y13) and PPADS (P2Y1, P2Y4, P2Y6 and P2Y13) (von Kügelgen and Hoffmann, 2016). P2Y subtype-specific antagonists have been also developed. For example, MRS2179 (IC_{50} ~ 0.3 μM), MRS2279 (IC_{50} ~ 52 nM) and MRS2500 (IC_{50} ~ 1 nM) are P2Y1 specific antagonists (Jacobson et al., 2009). PSB-416 (IC_{50} ~ 22 μM) (von Kügelgen and Hoffmann, 2016), AR-C126313 (IC_{50} ~ 1 μM) (Jacobson et al., 2009) and AR-C118925XX (IC_{50} ~ 1 μM) (Rafehi et al., 2017) are P2Y2 specific antagonists. NF157 (IC_{50} ~ 0.46 μM) (Ullmann et al., 2005) and NF340 (IC_{50} ~ 0.37 μM) (Meis et al., 2010) are P2Y11 specific antagonists.

In contrast to the P2X receptors, the responses mediated by the P2Y receptors are usually longer due to the fact that they are coupled to the trimeric G-proteins (composed of α, β and γ subunits) to generate intracellular second messengers (Figure 1.2A). The P2Y receptors can be grouped based on the G_α proteins that they are coupled to and the downstream signal transduction pathways. The P2Y1, P2Y2, P2Y4, P2Y6 and P2Y11 receptors are coupled to the $G_{\alpha,q/11}$ protein, activating membrane-bound phospholipase C (PLC) to generate inositol 1,4,5-triphosphate (IP_3) and diacylglycerol (DAG) from membrane lipid phosphatidylinositol 4,5-biphosphate (PIP_2). IP_3 binds to the Ca^{2+} release channel IP_3 receptors (IP_3R) in the ER membrane and induces ER Ca^{2+} release into the cytoplasm (Ralevic and Burnstock, 1998). P2Y receptor-induced reduction in the ER Ca^{2+}

can induce store-operated Ca^{2+} (SOC) entry via the Ca^{2+}-release-activated Ca^{2+} (CRAC) channels. The CRAC channels are composed of the plasma membrane Ca^{2+} channel pore-forming protein Orai1 and the ER Ca^{2+} sensor stromal interaction molecule 1 (Stim1) protein within the ER membrane. A reduction in the ER Ca^{2+} promotes Stim1 to aggregate, translocate to the ER-plasma membrane junction and interact with Orai1, resulting in the activation of CRAC (Zhang et al., 2005; Park et al., 2009). The ER Ca^{2+} release and refilling are important in the generation of intracellular Ca^{2+} oscillations (Dolmetsch et al., 1998). In addition to the $G_{\alpha,q/11}$, the P2Y11 receptor is coupled to the $G_{\alpha,s}$ protein, resulting in activation of adenylyl cyclase (AC) and increase in the cyclic AMP (cAMP) level (Abbracchio et al., 2006). On the other hand, the P2Y12-P2Y14 receptors are coupled to the $G_{\alpha/i}$ protein and their activation thus leads to inhibition of AC activity and thereby reduction in the cAMP level (Abbracchio et al., 2006; Kaebisch et al., 2015). It is worth mentioning that activation of the P2Y receptors also leads to Ca^{2+} influx and subsequent increase in the $[Ca^{2+}]_i$ via activating non-selective cationic channels (Sugasawa et al., 1996; Wu and Mori, 1999; Tolhurst et al., 2005). The $G_{\beta\gamma}$ dimers can regulate the $[Ca^{2+}]_i$ via inhibiting voltage-gated Ca^{2+} channels to decrease Ca^{2+} influx (Van Kolen and Slegers, 2006; Zamponi and Currie, 2013).

The P2Y receptors are expressed in many types of cells, such as endothelial, epithelial, bone, brain, muscle and immune cells, and mediate a variety of cell functions (Abbracchio et al., 2006). For examples, activation of the P2Y1 receptor stimulates osteoclast activity and bone resorption, and activation of the P2Y2 receptor inhibits bone formation by osteoblast (Hoebertz et al., 2002). Activation of the P2Y1 (Agresti et al., 2005a; Agresti et al., 2005b) and P2Y2 (Wiedon et al., 2012; Chadet et al., 2014) receptors promotes migration of oligodendrocyte progenitor cells (Agresti et al., 2005a; Agresti et al., 2005b), smooth muscle cells (Wiedon et al., 2012) and breast cancer cells (Chadet et al., 2014). The P2Y receptors are expressed in stem cells and involved in the regulation of cell proliferation, differentiation and migration (Glaser et al., 2012).

1.3 Piezo1 channel and its role in mechanical induction of ATP release

The Piezo1 channel is a novel mechanosensitive or mechanically activated Ca^{2+}-permeable cationic channel. It was firstly identified by showing that small interfering RNA (siRNA) knockdown of the Piezo1 (also named Fam38a) reduced pressure-induced currents in Neuro2A mouse neuroblastoma cells (Coste et al., 2010). A second gene encoding a related protein, Piezo2 (also named Fam38b), was cloned in dorsal root ganglia neurons and the Piezo2 protein can also form a mechanically activated channel (Coste et al., 2010).

The Piezo channels are large integral membrane proteins and structurally unrelated to other known proteins (Coste et al., 2010; Coste et al., 2012). The human Piezo1 and Piezo2 proteins consist of 2521 and 2752 amino acid residues, respectively, and share ~50% identity at the amino acid level (Wu et al., 2017). The mouse Piezo1 comprises 2457 amino acid residues (Ge et al., 2015). The three-dimensional structures comprising the large and central part of the mouse Piezo1 channel have been recently resolved using cryo-electron microscopy (Ge et al., 2015; Guo and MacKinnon, 2017; Saotome et al., 2018; Zhao et al., 2019). The Piezo1 channel is a homotrimer (Figure 1.3A) (Ge et al., 2015; Saotome et al., 2018; Zhao et al., 2019). Each subunit of the Piezo1 channel is thought to contain intracellular N- and C-termini and 38 transmembrane segments (Figure 1.3B) (Zhao et al., 2019). It has a propeller-like structure (Figure 1.3A) that contains N-terminal extracellular blade domains and transmembrane domains (Zhao et al., 2019). The blades are supported by the intracellular beam and anchor domains that surround a central ion-conducting pore (Figure 1.3C) (Ge et al., 2015; Saotome et al., 2018). The C-terminal part of the Piezo1 channel is composed of the transmembrane domain outer helix (OH), the C-terminal extracellular domain (CED), the transmembrane domain inner helix (IH), and the intracellular C-terminal domain (CTD), and necessary for the formation of the ion-conducting pore. The N-terminal extracellular blades sense mechanical stimuli and govern mechanical gating of the ion-conducting pore (Ge et al., 2015; Bae et al., 2016; Zhao et al., 2016; Zhao et al., 2019).

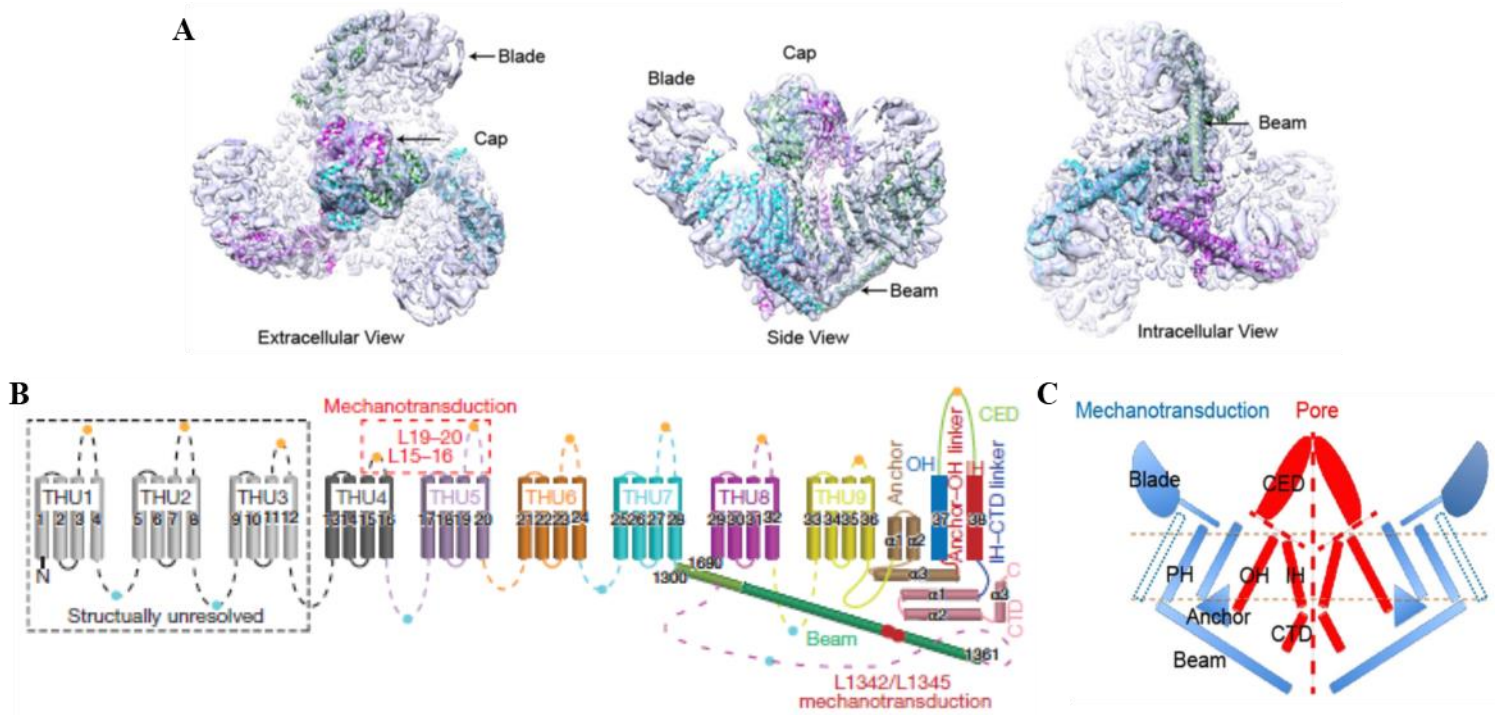

Figure 1.3 Overall structure of Piezo1 channel

The structure and working module of the mouse Piezo1 channel. (A) Top, side and bottom views of the trimeric three-bladed, propeller-shaped structure, with distinct regions labelled (Adapted from Xu, 2016). (B) Membrane topology model of the mouse Piezo1 protein consisting of 38 transmembrane domains. The extracellular loops, L15-16 and L19-20, have an important role in the mechanical activation of the Piezo1 channel. The intracellular loops, L1342 and L1345, are required to govern mechanical gating composed of extracellular blades, intracellular beam and anchor domains. The last two transmembrane regions determine a putative hydrophobic pore comprising the outer helix (OH), C-terminal extracellular domain (CED), transmembrane domain inner helix (IH), and intracellular C-terminal domain (CTD). The N-terminal 12 transmembrane domains remain unresolved in the structure (Adapted from Zhao et al., 2019). (C) The architectural model of the mouse Piezo1 channel (only two out of three subunits are shown), consisting of the putative central pore (in red) and the peripheral regions (PH) (in blue). The featured structures are labelled. The red dashed lines indicate potential ion-permeating pathway (Adapted from Xu, 2016).

Two models have been proposed to mediate transduction of the mechanical forces into conformational changes and channel opening, transmission through lipid bilayer membrane tension, and through ECM and/or intracellular cytoskeleton (Ranade et al., 2015; Wu et al., 2017; Murthy et al., 2017). The Piezo1 channel is directly gated by lipid bilayer membrane tension in response to extracellular mechanical stimuli (Pathak et al., 2014; Murthy et al., 2017). There is evidence to suggest that the Piezo1 channel can be gated by cell-generated intracellular forces via actin-myosin contraction in the absence of extracellular mechanical stimuli (Pathak et al., 2014; Nourse and Pathak, 2017; Ellefsen et al., 2019).

A wide range of external mechanical techniques have been utilized to study the mechanotransduction signalling of Piezo1 channel-induced Ca^{2+} entry, including cell indentation (Coste et al., 2010), pressure generating membrane stretching (Coste et al., 2010; Miyamoto et al., 2014; Pathak et al., 2014; Lewis and Grandl, 2015), flow fluid shear stress (Li et al., 2014; Ranade et al., 2014; Wang et al., 2016; Albarrán-Juárez et al., 2018), osmotic stress (Syeda et al., 2016), tissue compression (Jin et al., 2015) and traction forces (Ellefsen et al., 2019). The main limitation of such external mechanical stimuli is that the amount of force required to activate the Piezo1 channel cannot be accurately determined (Parpaite and Coste, 2017). They were the only means to activate the mechanosensitive Piezo1 channel until the identification of Yoda1, a synthetic chemical that selectively activates the Piezo1 channel with EC_{50} of 26.6 µM (Syeda et al., 2015). Yoda1 can activate the Piezo1 channel reconstituted in an artificial membrane in the absence of other cellular components (Syeda et al., 2015). It has been shown that a region between 1961 and 2063 amino acid residues in the C-terminus is required for Yoda1-induced activation of the Piezo1 channel (Lacroix et al., 2017), but the Yoda1-binding site remains elusive. Nonetheless, these observations support the notion that Yoda1 interacts directly with and gate the Piezo1 channel. Discovery of Yoda1 has greatly facilitated and will continue to facilitate better understanding the role of the Piezo1 channel in physiological and disease processes.

Up to date, there is no Piezo1 channel-specific inhibitor. Studies have shown that ruthenium red (RR), a polycationic ion known to be an inhibitor at several ion channels, can block the Piezo1 channel currents (Coste et al., 2010; Coste et al., 2012) with IC_{50} of 5.4 μM (Bagriantsev et al., 2014). Mutation of the glutamate residue within the pore region of the Piezo1 channel results in loss of RR blockade, suggesting RR as a channel pore blocker (Zhao et al., 2016). A 34-amino acid peptide *Grammostola spatulata* mechanotoxin 4 (GsMTx4) isolated from the venom of a tarantula spider is the first specific blocker for mechanically activated currents (Suchyna et al., 2000). GsMTx4 has been shown as a channel gating modifier acting on the extracellular side of the Piezo1 channel with IC_{50} of ~ 0.3 μM (Bae et al., 2011). There is evidence to suggest that GsMTx4 may inhibit the Piezo1 channel by modulating lipids surrounding the channel to decrease the efficiency of force transduction from the membrane bilayer to the channel (Suchyna et al., 2000; Gnanasambandam et al., 2017). GsMTx4 is a non-specific inhibitor of Piezo1 channel (Bowman et al., 2007) and nonetheless, it has become a useful pharmacological tool for studying the physiological and pathological roles of the Piezo1 channel.

The Piezo1 channel is expressed mainly in non-sensory cells, such as endothelial cells, epithelial bladder and kidney cells, neural progenitor cells (Murthy et al., 2017) periodontal ligament cells (Jin et al., 2015). It is also expressed in MSCs as discussed below. The Piezo1 channel has been shown to be mainly localized in the plasma membrane (Coste et al., 2010; Miyamoto et al., 2014; Etem et al., 2018), and there is some evidence to suggest that the Piezo1 channel is also present in the membrane of ER (McHugh et al., 2010; McHugh et al., 2012), cytoplasm near the nucleus (Miyamoto et al., 2014) and nuclear envelope (Gudipaty et al., 2017). Recent studies have implicated that Piezo1 channel-mediated Ca^{2+} influx regulates cell proliferation, migration, and differentiation in response to external mechanical stimuli (McHugh et al., 2012; Liu and Lee, 2014; Li et al., 2014; Pathak et al., 2014; Hung et al., 2016; Ellefsen et al., 2019). For example, human neural stem/progenitor cells preferably differentiate toward neurons when cultured on stiff substrates as compared on soft substrate. Activation of the Piezo1 channel by the high traction forces generated in cells on the stiff substrates is important in determining substrate stiffness-dependent differentiation of human neural stem/progenitor

cells into neurons (Pathak et al., 2014). Recent studies have shown a role of the Piezo1 channel in stimulating cell proliferation in gastric cancer cells (Zhang et al., 2018a), mouse embryonic stem cells (del Mármol et al., 2018) and kidney epithelial cells (Gudipaty et al., 2017). Moreover, activation of the Piezo1 channel can enhance migration of human umbilical vein endothelial cells (Li et al., 2014; Zhang et al., 2017), gastric cancer cells (Yang et al., 2014; Zhang et al., 2018a), malignant MCF-7 breast cancer cells (Li et al., 2015a) and invasive A375-SM melanoma cancer cells (Hung et al., 2016). Intriguingly, an early study reported that activation of the Piezo1 channel suppressed migration of small cell lung cancer cells (McHugh et al., 2012).

As introduced above, ATP is released from many types of cells in response to diverse forms of mechanical stimuli. Emerging evidence supports an important role of the Piezo1 channel in mediating mechanical induction of ATP release. For example, activation of the Piezo1 channel by mechanical stretch induced Ca^{2+} influx in urothelial cells and ATP release resulting in bladder contraction (Miyamoto et al., 2014). Shear stress-induced activation of the Piezo1 channel mediates Ca^{2+} entry and subsequent ATP release from red blood cells (Cinar et al., 2015). A similar role for the Piezo1 channel was identified in endothelial cells, where mechanical and chemical activation of the Piezo1 channel promotes ATP release through the pannexin channels and subsequent activation of the P2Y2 receptor, resulting in vasodilation (Wang et al., 2016). MSCs are highly mechanosensitive (Engler et al., 2006; Riddle et al., 2007; Lee et al., 2011; Yuan et al., 2012; Suhr et al., 2013; Sun et al., 2013; Yuan et al., 2013; Liu and Lee, 2014; Li et al., 2018; Goetzke et al., 2018). As discussed below, it is well-demonstrated that MSCs can release ATP in response to mechanical stimulation *in vitro* and *in vivo* (Riddle et al., 2007, 2007; Sun et al., 2013; Weihs et al., 2014), and there is increasing evidence to show expression of the Piezo1 channel in MSCs (Gao et al., 2017; Sugimoto et al., 2017). However, it is unknown whether activation of the Piezo1 channel evokes ATP release from MSCs. In the present study (chapter 4), I will explore the role of the Piezo1 channel in mediating ATP release in human dental pulp-derived MSCs (hDP-MSCs).

1.4 Mesenchymal stem cells

Stem cells have unique abilities of self-renewal and differentiation into specific cell lineages during development and growth. In addition, stem cells are important in maintaining healthy tissues, and repairing and regenerating damaged or diseased tissues, therefore, holding great promise for regenerative medicine (Laird et al., 2008). Stem cells reside in a dynamic, specialized microenvironment with a distinctive anatomical localization in the tissue, termed 'stem cell niche', which provides essential signals required for stem cell functions. In addition to stem cells themselves, the supporting cells, ECM, and signalling molecules in the niche together contribute to maintain the undifferentiated state of stem cells and regulate the balance between self-renewal and differentiation (Fuchs et al., 2004; Scadden, 2006; Chagastelles and Nardi, 2011; Gattazzo et al., 2014). Stem cells, based on their origins, can be divided into embryonic stem cells (ESCs) and adult stem cells (Chagastelles and Nardi, 2011; Kaebisch et al., 2015). Alternatively, stem cells can be classified, according to their differentiation capacity, into totipotent, pluripotent and multipotent cells (Chagastelles and Nardi, 2011; Kaebisch et al., 2015; Sudulaguntla et al., 2016). Totipotent stem cells, such as fertilized egg (zygote cell) and blastocyst, are able to produce all cell types in an organism, including extraembryonic tissues outside the embryo body, such as placenta (Sudulaguntla et al., 2016). Pluripotent stem cells, like ESCs, possess the ability to differentiate into almost any of the three germ layers: ectoderm (such as neural and skin cells), mesoderm (such as blood, bone and muscle cells), and endoderm (such as lung, thyroid, and pancreatic cells) (Chagastelles and Nardi, 2011; Kaebisch et al., 2015). ESCs express pluripotency genes (e.g., octamer binding transcription factor-3/4 (Oct-3/4), Rex-1, sex determining region Y box-2 (Sox-2), Nanog, and stage-specific embryonic antigen-3 (SSEA-3) and SSEA-4), and can be maintained in undifferentiated state and undergo unlimited expansion in cultures due to the expression of high levels of telomerase (Chagastelles and Nardi, 2011; Sudulaguntla et al., 2016). In addition to ESCs, induced pluripotent stem cells (iPSCs), as their name suggests, are pluripotent cells and they were first generated in 2006 from adult somatic cells by genetic reprogramming to express several transcription factors (e.g., Oct-3/4, Sox-2, c-Myc and Kruppel like factor-4 (Klf-4) that are potentially involve in pluripotency (Takahashi and Yamanaka, 2006). The number of necessary transcription

factors depends on the cell sources. For example, progenitor and stem cells need fewer transcription factors for the reprogramming process (Kaebisch et al., 2015). Like ESCs, iPSCs are pluripotent and have the ability to self-renew (Leeanansaksiri et al., 2016). They represent an attractive alternative to ESCs in clinical applications, without ethical issues associated with using embryonic tissue to isolate ESCs (Chagastelles and Nardi, 2011; Leeanansaksiri et al., 2016) or immune rejection (Narsinh et al., 2011; Leeanansaksiri et al., 2016). However, it is known that both ESCs and iPSCs can induce tumor formation upon transplantation (Chagastelles and Nardi, 2011; Narsinh et al., 2011; Leeanansaksiri et al., 2016). Accordingly, the potential use of iPSCs in clinical applications is still under investigation (Leeanansaksiri et al., 2016; Sudulaguntla et al., 2016). Multipotent stem cells, such as hematopoietic stem cells, neuronal stem cells and MSCs, can differentiate into limited cell lineages. They are involved in the repair and maintenance of the tissues in which they reside (Augello et al., 2007; Liu et al., 2009; Kaebisch et al., 2015).

MSCs represent the most commonly studied adult stem cells. They are present in a small number in the mesenchymal stromal cell population and can self-renew and differentiate (Figure 1.4) (Caplan, 1991; Pittenger et al., 1999; Dominici et al., 2006). MSCs were initially discovered as a subset of cells derived from bone marrow that showed the ability to attach to the plastic surface and form colonies (Pittenger et al., 1999). Such bone marrow-derived MSCs (BM-MSCs) express cell surface markers (e.g., CD71, CD90 and CD106) and exhibit chondrogenic, osteogenic and adipogenic differentiation *in vitro* under inducing conditions. In addition to the ability of the tri-lineage differentiation, some studies suggest that BM-MSCs possess an ability to differentiate into other mesenchymal lineages, including myocytes, cardiomyocytes, and also into cells of non-mesodermal origin, such as hepatocytes, insulin-producing cells and neurons (Liu et al., 2009), which may result from a very small number of embryonic like-stem cells in MSC preparations (Bhartiya et al., 2013). However, it remains questionable whether BM-MSCs can differentiate to mature or functional cells. For example, BM-MSC-derived neuron-like cells lack the expression of voltage-gated ion channels and deficient in generating action potentials (Hofstetter et al., 2002). BM-MSCs are most commonly used MSCs but bear some limitations, such as the painful procedure that patients can experience during tissue isolation and the limited proliferative capacity (Huang et al., 2009). Increasing efforts are

therefore devoted to exploring other sources. It is now known that MSCs can be isolated from several other tissues, such as adipose tissue, amniotic fluid and membrane, skin, skeletal muscle, dental tissues including dental follicle, dental pulp and apical papilla, peripheral blood, umbilical cord blood, Wharton's jelly, synovial fluid, cartilage, spleen and thymus (Figure 1.4) (Liu et al., 2009; Kaebisch et al., 2015; Sudulaguntla et al., 2016).

MSCs from adipose, umbilical cord and dental pulp tissues have gained increasing attention due to the fact that they are readily obtainable (Huang et al., 2009; Scarfì, 2014). Adipose tissue-derived MSCs (AT-MSCs) (Zuk et al., 2002), umbilical cord-derived MSCs (UC-MSCs) (Huang et al., 2009) and DP-MSCs (Gronthos et al., 2000) possess a high proliferative capacity. Overall, there is an inverse relation between the age of donors and the proliferative capacity and differentiation potential of MSCs (Kretlow et al., 2008; Huang et al., 2009; Via et al., 2012; Scarfì, 2014). Similar to BM-MSCs, AT-MSCs and UC-MSCs can differentiate into osteoblasts, adipocytes, chondrocytes, cardiomyocytes-like cells, neuron-like cells and Schwann cell-like cells (Argentati et al., 2018). DP-MSCs can also undergo adipogenesis, osteogenesis, chondrogenesis and neurogenesis (Gronthos et al., 2002; Perry et al., 2008; Grottkau et al., 2010). It is noteworthy that stem cells derived from dental pulp originate from the migratory multipotent neural crest cells that give rise to different tissues of craniofacial region, including bone, neurons, cartilage teeth, and connective tissues, such as adipocytes (Luan et al., 2009; Janebodin et al., 2011; Zippel et al., 2012). DP-MSCs have become a promising source of MSCs in regenerative medicine (Tatullo et al., 2015) because of their feasible isolation and expansion *in vitro*, high proliferative and multipotent differentiation capacities, even after temporary cryopreservation (Perry et al., 2008).

There are significant disparities in studies using different MSC preparations. In order to make the results more comparable or interpretable as possible, the Mesenchymal and Tissue Stem Cell Committee of the International Society for Cellular Therapy (ISCT) proposes the following minimal criteria for MSCs (Dominici et al., 2006). Firstly, cells should possess the ability to adhere to plastic surface when maintained in standard culture conditions. Secondly, cells should express positive markers, such as CD105, CD73 and

CD90, and lack expression of hematopoietic and endothelial markers CD45, CD34, CD14 or CD11b, CD79α or CD19 and HLA-DR. Finally, cells have to show the ability to differentiate into adipocytes, chondrocytes and osteocytes.

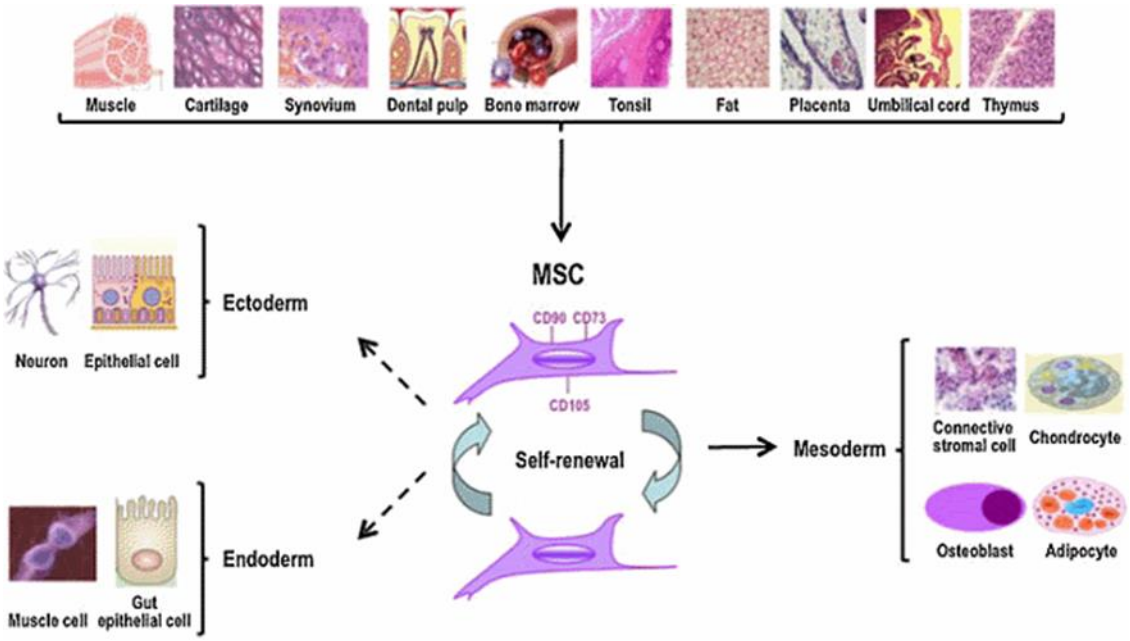

Figure 1.4 Diagram of tissue sources and multiple differentiation potentials of MSCs MSCs can be isolated from various tissues, and express positive cell surface markers (e.g., CD73, CD90 and CD105). They can self-renew and differentiate into mesoderm lineages, including connective stromal cells, osteoblasts, chondrocytes and adipocytes. MSCs have been shown in some studies to demonstrate the potential of differentiating into ectoderm cells, such as neuron and epithelial cells, and endoderm cells, including muscle and gut epithelial cells (www.cancerlink.ru/enmesenchymalstem.html).

Due to the simple isolation procedure, abundant sources, *in vitro* expansion, the ability of self-renewal, migration to damaged tissues, and differentiation into tissue-specific lineages, the ability to secrete stimulatory molecules and the ability to modulate immune responses, MSCs have promising applications in tissue engineering and regenerative medicine (Huang et al., 2009; Wang et al., 2012; Kim and Cho, 2013; Farini et al., 2014; Sudulaguntla et al., 2016). In particular, MSCs are considered as an important stem cell source for the cell-based treatment of various disease conditions. Preclinical studies continue to demonstrate the beneficial effects of MSCs. For example, administration of BM-MSCs via lumbar puncture into the lesion site improved spinal cord injury by

secreting trophic factors, such as nerve growth factor that is known to regulate proliferation and neuronal differentiation (Hawryluk et al., 2012). Furthermore, the role of MSCs in improving heart diseases, such as myocardial infarction, has been demonstrated and attributed to their ability of *in vitro* differentiation into cardiomyocyte-like cells (Toma et al., 2002; Williams et al., 2013; Ghoraishizadeh et al., 2014; Argentati et al., 2018) that spontaneously beat *in vitro* (Planat-benard et al., 2004; Williams et al., 2013; Malandraki-Miller et al., 2018) and involved in direct replacement of myocardial tissue after myocardial infarction using an *in vivo* model, resulting in reduced infarct size (Hatzistergos et al., 2010; Williams et al., 2013). Additionally, *in vivo* studies demonstrated the ability of transplanted MSCs to secrete a wide array of factors (e.g., insulin-like growth factor-1, stem cell-derived factor, prostaglandin E_2) which can suppress the immune function, inhibit fibrosis and apoptosis, or stimulate proliferation and differentiation of endogenous cardiac stem cells (Hatzistergos et al., 2010; Williams et al., 2013). Despite highly promising results, preclinical studies have revealed that treatment of heart diseases is limited by a low efficacy rate of MSC migration/homing and functionality of cardiomyocyte-like cells (Williams et al., 2013). For example, differentiation of MSCs into beating cardiomyocytes does not mean that these cells can develop into mature cardiomyocytes in the healthy heart as they have immature Na^+ and Ca^{2+} handling mechanisms due to the lack expression of voltage-gated Na^+ and Ca^{2+} channels (Wei et al., 2012). Moreover, transplantation of BM-MSCs in the eye vitreous cavity can also improve retinal regeneration in rats (Tzameret et al., 2014) and protect glaucoma in ageing rats (Hu et al., 2013). Consistently, clinical trials have shown the therapeutic potential of using MSCs, for example, in improving bone structure and function in patients with osteogenesis imperfecta (Rastegar et al., 2010; Kim and Cho, 2013). There are promising results of using MSCs to treat liver injury and cirrhosis, multiple sclerosis, rheumatoid arthritis, and system lupus erythematosus (Kim and Cho, 2015; Tsolaki and Yannaki, 2015). Up to date, 249 completed clinical trials using MSCs have been published in public clinical trial database and 70 clinical trials are still ongoing (www.clinicaltrials.gov), indicating a strong interest in MSC-based therapy.

1.5 ATP-induced purinergic Ca^{2+} signalling in MSCs

It has been proposed that ATP is present in the stem cell niche (Burnstock and Ulrich, 2011). This notion has gained support by the findings that ATP is released constitutively from MSCs or in response to mechanical or chemical stimulation, in part via the connexion hemi-gap junction channels or vesicular exocytosis (Kawano et al., 2006; Riddle et al., 2007; Coppi et al., 2007; Burnstock and Ulrich, 2011; Kwon, 2012; Sun et al., 2013; Biver et al., 2013; Weihs et al., 2014). After release, extracellular ATP acts as an autocrine/paracrine signalling molecule that induces an increase in the $[Ca^{2+}]_i$ in MSCs (Coppi et al., 2007; Riddle et al., 2007; Sun et al., 2013; Weihs et al., 2014). As described below, there is an increasing evidence to support the expression of the P2X and P2Y receptors in MSCs and demonstrate their significant roles in mediating ATP-induced Ca^{2+} signalling and regulation of cell proliferation, differentiation and migration (Kawano et al., 2006; Coppi et al., 2007; Ferrari et al., 2011; Zippel et al., 2012; Ciciarello et al., 2013; Sun et al., 2013; Trubiani et al., 2014; Weihs et al., 2014; Noronha-Matos et al., 2014; Li et al., 2015b; Peng et al., 2016; Li et al., 2016; Zhang et al., 2019).

Expression of ATP-sensitive P2 receptors has been examined in MSCs from several tissues, such as bone marrow (Kawano et al., 2006; Riddle et al., 2007; Coppi et al., 2007; Ferrari et al., 2011; Noronha-Matos et al., 2012; Sun et al., 2013; Noronha-Matos et al., 2014), adipose tissue (Zippel et al., 2012; Kotova et al., 2018; Ali et al., 2018), umbilical cord blood (Tu et al., 2014), periodontal ligament (Trubiani et al., 2014; Xu et al., 2019) and dental pulp (Peng et al., 2016; Zhang et al., 2019). Studies have examined receptor expression at the mRNA level using real-time reverse transcription-polymerase chain reaction (RT-PCR), at the protein level using western blotting or immunostaining, and/or at the functional level by measuring ATP or specific agonist-induced currents or Ca^{2+} responses. Table 1.1 summarizes the expression of P2X and ATP-sensitive P2Y receptors in MSCs and the methods used to show their expression. Figure 1.5 illustrates the roles of the major P2X and P2Y receptors in ATP-induced purinergic Ca^{2+} signalling in MSCs.

1.5.1 Expression of P2X receptors in MSCs

As discussed earlier, extracellular ATP opens the P2X receptor ion channels (Figure 1.5). It was reported that ATP induced inward currents in human BM-MSCs (hBM-MSCs) using patch-clamp recording, and treatment with P2 generic antagonist PPADS reduced ATP-induced inward currents (Coppi et al., 2007). These results suggest functional expression of the P2X receptor(s), however, the molecular identity of the receptor(s) mediating ATP-induced currents was not established. Subsequent independent studies have reported expression of different P2X receptors in MSCs from different tissues (Table 1.1) (Riddle et al., 2007; Ferrari et al., 2011; Noronha-Matos et al., 2012; Zippel et al., 2012; Sun et al., 2013; Noronha-Matos et al., 2014; Trubiani et al., 2014; Peng et al., 2016; Ali et al., 2018; Xu et al., 2019; Zhang et al., 2019). The mRNA transcripts for all the P2X receptors, with the exception of P2X2, were detected using real-time RT-PCR in hBM-MSCs (Ferrari et al., 2011). The protein expression of P2X1, P2X4 and P2X7 in hBM-MSCs was also demonstrated by western blotting. Despite detectable mRNA expression, no protein expression was detected for P2X3, P2X5 and P2X6 (Ferrari et al., 2011). The protein expression of P2X7 was also detected in hBM-MSCs from other studies using western blotting (Riddle et al., 2007; Sun et al., 2013) and immunofluorescence (Noronha-Matos et al., 2012; Noronha-Matos et al., 2014). Functional expression of the P2X7 receptor was further demonstrated using Ca^{2+} imaging to measure ATP or other agonist-induced Ca^{2+} responses in hBM-MSCs, in combination with using selective antagonists to inhibit the receptor function or using P2X-specific siRNA to reduce the receptor expression. ATP induced a biphasic increase in the $[Ca^{2+}]_i$, consisting of a transient component followed by a sustained component (Riddle et al., 2007; Ferrari et al., 2011; Noronha-Matos et al., 2014). Ferrari et al. (2011) also demonstrated that BzATP induced a biphasic increase in the $[Ca^{2+}]_i$, with the transient increase attenuated and the sustained increase abolished in extracellular Ca^{2+}-free solution, indicating a major contribution of extracellular Ca^{2+} influx to the sustained increase in the $[Ca^{2+}]_i$. The same study also showed that αβMeATP induced an increase in the $[Ca^{2+}]_i$, suggesting expression of the P2X receptors containing P2X1 and/or P2X3 subunits in hBM-MSCs (Ferrari et al., 2011). However, ATP-evoked increase in the $[Ca^{2+}]_i$ was significantly inhibited by treatment with P2X7 selective antagonist KN-62 or irreversible P2X7 inhibitor oxATP. Treatment

with oxATP also blocked BzATP-induced increase in the $[Ca^{2+}]_i$ (Ferrari et al., 2011). These results indicate an important role for the P2X7 receptor in mediating ATP-induced Ca^{2+} response. Further, it was shown in a separate study using hBM-MSCs that ATP and BzATP induced membrane blebbing and large pore formation (Noronha-Matos et al., 2014), which are characteristics of the P2X7 receptor activation (Virginio et al., 1999; Wei et al., 2016). Treatment with P2X7 selective antagonist A438079, significantly reduced ATP and BzATP-induced increase in the $[Ca^{2+}]_i$, and BzATP-induced large pore formation, suggesting functional expression of the P2X7 receptor in hBM-MSCs (Noronha-Matos et al., 2014).

Expression of P2X receptors was also examined in MSCs from other tissues. Analysis of the mRNA transcripts revealed a consistent expression of P2X4 and P2X7 in hAT-MSCs (Zippel et al., 2012; Ali et al., 2018; Kotova et al., 2018). The results examining the mRNA expression of P2X1-P2X3, P2X5 and P2X6 remain controversial. For example, the P2X1 mRNA was detected in two recent independent studies (Ali et al., 2018; Kotova et al., 2018), but was not in an early study (Zippel et al., 2012). The P2X2 mRNA expression was reported in one recent study (Kotova et al., 2018) but was not in other two studies (Zippel et al., 2012; Ali et al., 2018). Similarly, the P2X3 mRNA was observed in one study (Zippel et al., 2012), but was not in two recent studies (Ali et al., 2018; Kotova et al., 2018). Expression of the P2X5 and P2X6 mRNA in hAT-MSCs was shown by two different studies (Zippel et al., 2012; Ali et al., 2018), but was not by another group (Kotova et al., 2018). Moreover, the protein expression of P2X1, P2X4, P2X5 and P2X7 was detected in hAT-MSCs using immunofluorescence (Ali et al., 2018). The P2X5 and P2X7 protein expression were also detected in hAT-MSCs by another study using western blotting and the protein expression of P2X6 was also reported in the same study (Zippel et al., 2012). Functional expression of the P2X receptors in hAT-MSCs was examined in this study. It was shown that ATP-induced an increase in the $[Ca^{2+}]_i$, which was prevented by treatment with suramin and P2X selective antagonist NF279 (Zippel et al., 2012). A recent study has shown that ATP-induced Ca^{2+} response in hAT-MSCs was insensitive to P2X4 selective antagonist PSB-12062 and P2X7 selective antagonist A438079, ruling out the role of the P2X4 and P2X7 receptors in mediating ATP-evoked increase in the $[Ca^{2+}]_i$

(Ali et al., 2018). In human periodontal ligament stem cells (hPDLSCs), studies so far have only focused on the P2X7 receptor (Trubiani et al., 2014; Xu et al., 2019), and have consistently documented the P2X7 expression at the level of mRNA and protein using real-time RT-PCR and western blotting, respectively (Trubiani et al., 2014; Xu et al., 2019). Functional expression of the P2X7 receptor in hPDLSCs was demonstrated using Ca^{2+} imaging; BzATP induced an increase in the $[Ca^{2+}]_i$ and larger pore formation, both of which were reduced by treatment with oxATP, indicating functional expression of the P2X7 receptor (Trubiani et al., 2014). In hUC-MSCs, expression of the mRNA transcripts for P2X1, P2X4-P2X7, with the exception of P2X2 and P2X3, was detected using real-time RT-PCR (Tu et al., 2014). With regard to hDP-MSCs, the mRNA expression has been analyzed in our recent study using real-time RT-PCR, revealing the mRNA transcripts for P2X4, P2X6 and P2X7, but not P2X1-P2X3 and P2X5 (Peng et al., 2016). The protein expression of the P2X3 and P2X7 receptors has been demonstrated in hDP-MSCs using immunofluorescence in another recent study (Zhang et al., 2019). Our study has demonstrated that ATP and BzATP induced increases in the $[Ca^{2+}]_i$ in a concentration-dependent manner in hDP-MSCs (Peng et al., 2016). However, there was no Ca^{2+} response to αβMeATP, consistence with no expression of P2X1 and P2X3. In addition, ATP-induced increase in the $[Ca^{2+}]_i$ was insensitive to inhibition by P2X4 selective antagonist 5-BDBD. In contrast, the increases in the $[Ca^{2+}]_i$ evoked by ATP and BzATP were attenuated by treatment with P2X7 selective antagonist AZ11645373, and by siRNA-mediated knockdown of the P2X7 expression, indicating functional expression of the P2X7 receptor and its contribution in mediating ATP-induced Ca^{2+} signalling in hDP-MSCs (Peng et al., 2016).

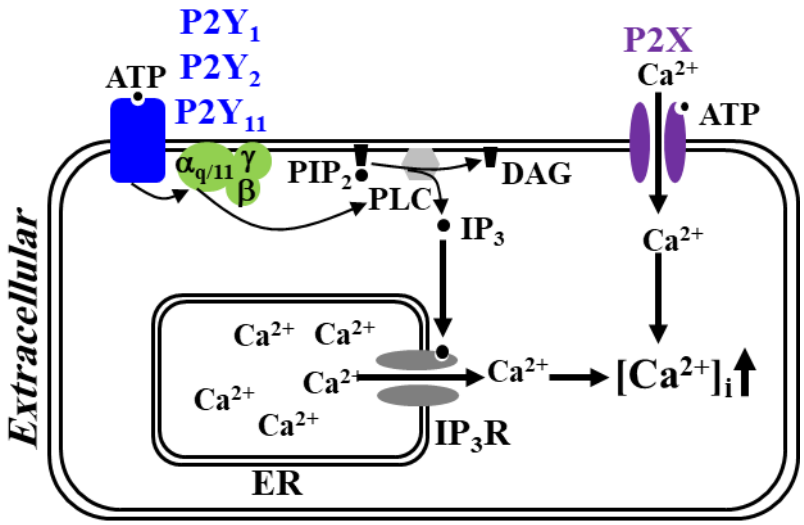

Figure 1.5 Schematic diagram illustrates the molecular mechanisms of ATP-induced P2 receptor-mediated Ca^{2+} signalling in MSCs
ATP can activate the P2X receptors, mainly the P2X7 receptor, allowing Ca^{2+} influx and subsequent increase in the concentration of intracellular Ca^{2+} ($[Ca^{2+}]_i$). ATP can also activate the P2Y1, P2Y2 and/or P2Y11 receptors, resulting in sequential activation of the $G_{\alpha,q/11}$, membrane-bound phospholipase C (PLC), conversion of membrane lipid phosphatidylinositol 4,5-biphosphate (PIP_2) into inositol triphosphate (IP_3) and diacylglycerol (DAG). IP_3 diffuses through the cytosol to bind to the IP_3 receptor (IP_3R) in the endoplasmic reticulum (ER) mediating Ca^{2+} release to increase the $[Ca^{2+}]_i$ (Modified from Jiang et al., 2017a).

1.5.2 Expression of P2Y receptors in MSCs

As introduced earlier, extracellular ATP acts as a partial or full agonist at P2Y1, P2Y2 and P2Y11 receptors. They are coupled to the $G_{\alpha,q/11}$-PLC-IP_3R signalling and thus activation of these receptors can trigger intracellular Ca^{2+} release, resulting in an increase in the $[Ca^{2+}]_i$ (Figure 1.5). As summarized in Table 1.1, studies were conducted on MSCs isolated from different tissues to determine the expression of these P2Y receptors at the mRNA, protein and function levels.

Several studies investigated the expression of the ATP-sensitive P2Y receptors in BM-MSCs. The mRNA transcripts for P2Y1, P2Y2 and P2Y11 were detected using real-time RT-PCR (Ferrari et al., 2011; Fruscione et al., 2011). The protein expression of the P2Y1 receptor was reported in hBM-MSCs by two research groups using western blotting (Ferrari et al., 2011) or immunofluorescence (Noronha-Matos et al., 2012; Noronha-Matos

et al., 2014), but not in an early study using western blotting (Riddle et al., 2007). The protein expression was shown using immunofluorescence staining or western blotting for the P2Y2 (Riddle et al., 2007; Ferrari et al., 2011; Noronha-Matos et al., 2012) and P2Y11 receptors (Riddle et al., 2007; Ferrari et al., 2011). There is compelling evidence to support the functional expression of the P2Y1, P2Y2 and P2Y11 receptors and their roles in ATP-induced Ca^{2+} signalling in hBM-MSCs. For instance, an early study showed spontaneous intracellular Ca^{2+} oscillations in hBM-MSCs, which were abolished by treatment with U73122, a PLC inhibitor, as well as treatment with P2 generic antagonist PPADS or P2Y1 selective inhibitor APPS, but not P2X receptor inhibitor 8-SPT (Kawano et al., 2006). These results support an important role of the P2Y1 receptor in an autocrine/paracrine Ca^{2+} signalling mechanism, in which ATP induces activation of the P2Y1-$G_{\alpha,q/11}$-PLC signalling pathway and triggers ER Ca^{2+} release and subsequent Ca^{2+}-dependent release of ATP into extracellular space (Kawano et al., 2006). Consistently, a separate study using patch-clamp recording showed that externally applied ATP induced Ca^{2+}-dependent outward K^+ currents in hBM-MSCs and such currents were blocked by treatment with PPADS and P2Y1 selective antagonist MRS2179, indicating that ATP-induced activation of the P2Y1-$G_{\alpha,q/11}$-PLC signalling pathway induces release of Ca^{2+}, which in turn activates Ca^{2+}-dependent K^+ outward currents (Coppi et al., 2007). Functional expression of the P2Y1, P2Y2 and P2Y11 receptors in hBM-MSCs was also examined in another study by measuring Ca^{2+} responses to ATP, BzATP and ADP (Ferrari et al., 2011). All these agonists evoked a significant increase in the $[Ca^{2+}]_i$ in extracellular Ca^{2+}-free solution as well as in extracellular Ca^{2+}-containing solution. These results are consistent with the results of examining the receptor expression using real-time RT-PCR and western blotting and, taken together, support expression of the P2Y1, P2Y2 and P2Y11 receptors in hBM-MSCs (Ferrari et al., 2011). Functional expression of the P2Y11 receptor in hBM-MSCs was further supported by investigating Ca^{2+} response to NAD^+ (Fruscione et al., 2011). NAD^+ induced an increase in the $[Ca^{2+}]_i$, which was abolished by treatment with P2Y11 selective antagonist NF157 or by siRNA-mediated knockdown of the P2Y11 receptor expression (Fruscione et al., 2011).

Table 1.1 Summary of the expression of ATP-sensitive P2 receptors in hMSCs

MSC type	P2 receptors expressed	Methods	References
hBM-MSCs	P2X1, P2X3-P2X7	RT-PCR, western blotting, immune-staining, calcium imaging	Riddle et al., 2007; Ferrari et al., 2011; Noronha-Matos et al., 2012; Sun et al., 2013; Noronha-Matos et al., 2014.
	P2Y1, P2Y2, P2Y11	RT-PCR, western blotting, immune-staining, calcium imaging, patch-clamp recording	Kawano et al., 2006; Coppi et al., 2007; Ferrari et al., 2011; Fruscione et al., 2011; Noronha-Matos et al., 2012; Noronha-Matos et al., 2014
hAT-MSCs	P2X1, P2X3-P2X7	RT-PCR, western blotting, immune-staining, calcium imaging	Zippel et al., 2012; Ali et al., 2018; Kotova et al., 2018
	P2Y1, P2Y2, P2Y11	RT-PCR, western blotting, immune-staining, calcium imaging	Zippel et al., 2012; Ali et al., 2018; Kotova et al., 2018
hPDLSCs	P2X7	RT-PCR, western blotting, immune-staining, calcium imaging	Trubiani et al., 2014; Xu et al., 2019
hUC-MSCs	P2X1, P2X4-P2X7	RT-PCR	Tu et al., 2014
hDP-MSCs	P2X3, P2X4, P2X6, P2X7	RT-PCR, immune-staining, calcium imaging, patch-clamp recording	Peng et al., 2016; Zhang et al., 2019
	P2Y1, P2Y2, P2Y11	RT-PCR, immune-staining, calcium imaging, patch-clamp recording	Peng et al., 2016; Zhang et al., 2019

Studies have also examined the expression of the ATP-sensitive P2Y receptors in hAT-MSCs and hDP-MSCs. In hAT-MSCs, the expression of P2Y1, P2Y2 and P2Y11 was detected at the mRNA level using real-time RT-PCR (Zippel et al., 2012; Ali et al., 2018; Kotova et al., 2018) and also at the protein level using western blotting (Zippel et al., 2012) or immunofluorescence (Ali et al., 2018; Kotova et al., 2018). The study by Zippel et al. (2012) found that ATP-induced increase in the $[Ca^{2+}]_i$ in hAT-MSCs was prevented by treatment with suramin. Like ATP, exposure to P2Y1 agonist 2-MeSADP, but not P2Y11 agonist NF546, induced an increase in the $[Ca^{2+}]_i$, suggesting functional expression of the P2Y1 receptor in hAT-MSCs (Zippel et al., 2012). A recent study has reported that ATP-induced increase in the $[Ca^{2+}]_i$ in hAT-MSCs was also attenuated by treatment with P2Y2 antagonist AR-C118925XX, suggesting functional expression of the P2Y2 receptor (Ali et al., 2018). Another recent study has shown that ATP-induced Ca^{2+} response in hAT-MSCs was suppressed by treatment with P2Y11 antagonist NF340 as well as treatment with U73122 or 2-APB, an IP_3R blocker, suggesting functional expression of the P2Y11 receptor (Kotova et al., 2018). In hDP-MSCs, mRNA expression for P2Y1 and P2Y11 was consistently detected in hDP-MSCs from multiple donors using real-time RT-PCR, but the P2Y2 transcript was detectable in some but not all donors, as reported in our previous study (Peng et al., 2016). A very recent study has reported the P2Y2 protein expression in hDP-MSCs using immunofluorescence (Zhang et al., 2019). The role of the P2Y1, P2Y2 and P2Y11 receptors in mediating ATP-induced Ca^{2+} response in hDP-MSCs has been further examined in our recent study. ATP, ADP and BzATP were effective in evoking an increase in the $[Ca^{2+}]_i$ in extracellular Ca^{2+}-free and Ca^{2+}-containing solutions (Peng et al., 2016). ATP-induced increase in the $[Ca^{2+}]_i$ was attenuated by siRNA-mediated knockdown of the P2Y1 or P2Y11 receptor expression, and ADP-induced increase in the $[Ca^{2+}]_i$ was also reduced by siRNA-mediated knockdown of the P2Y1 receptor expression, supporting functional expression of the P2Y1 and P2Y11 receptors and their contribution in mediating ATP-induced Ca^{2+} response in hDP-MSCs (Peng et al., 2016). The recent study by Zhang et al. (2019) has demonstrated using patch-clamp recording that ATP-induced inward currents were completely abolished by treatment with suramin, but not P2X antagonist *iso*-PPADS (Zhang et al., 2019). As mentioned above, this study has demonstrated P2Y2 protein

expression, but it remains unclear whether the P2Y2 receptor is critical in mediating ATP-induced inward currents (Zhang et al., 2019).

In summary, studies have shown ATP-induced Ca^{2+} signalling in MSCs from several tissue origins. In terms of the P2X receptors, there is consistent evidence to support the functional expression of the P2X7 receptor and its important role in mediating ATP-induced Ca^{2+} signalling. Most studies support the functional expression of the P2Y1, P2Y2 and P2Y11 receptors and their contribution in ATP-induced Ca^{2+} signalling in MSCs. There are noticeable differences in the results reported by different studies, which could be attributed in part to the differences in tissue origins, age and gender of donors, and *in vitro* culture conditions as well as the techniques used to examine the receptor expression.

1.6 Role of P2 receptors in ATP-induced regulation of MSC functions

Many studies have examined the regulation by extracellular ATP of MSC functions such as proliferation, viability, migration and differentiation, and the role of ATP-sensitive P2 receptors in such regulations.

1.6.1 Cell proliferation and viability

Studies have evaluated the effects of extracellular ATP, released endogenously or applied exogenously, on proliferation and viability of MSCs from different tissues. An early study showed, by using 5-bromo-20-deoxyuridine (BrdU) labelling assay, that exogenously applied ATP at 25, 100, and 250 μM or endogenously released ATP from hBM-MSCs accelerated cell proliferation via inducing an increase in the $[Ca^{2+}]_i$, activation of Ca^{2+}-sensitive calcineurin and subsequent nuclear translocation of nuclear factor of activated T cells (NFAT) (Riddle et al., 2007). Consistently, a recent study has shown, by using cell counting and Ki67 staining, that cell proliferation and survival of hDP-MSCs were increased during 24-72 hours by blocking ATP degradation with 100 μM ARL 67156, an ectonucleotidase inhibitor, indicating that endogenously released ATP promotes proliferation and survival of hDP-MSCs (Zhang et al., 2019). This study has further

investigated the role of the P2 receptors in ATP-induced regulation of MSC proliferation and viability. The number of hDP-MSCs at 24, 48 and 72 hours was significantly reduced by treatment with 100 μM suramin. The cell number was also significantly reduced at 72 hours, albeit was not at 24 and 48 hr, by inhibiting P2X receptors with 100 μM *iso*-PPADS (Zhang et al., 2019). These results suggest that ATP stimulates cell proliferation in part via the P2X receptors (Zhang et al., 2019). This study has demonstrated the protein expression of the P2X3, P2X7 and P2Y2 receptors, however, it was not established whether or which of these receptors mediated ATP-induced regulation of cell proliferation of hDP-MSCs (Zhang et al., 2019).

It is noted that several other studies have reported opposing or no effect of ATP on MSC proliferation. For example, Coppi et al. (2007) showed that spontaneously released ATP from hBM-MSCs attenuated cell proliferation, determined by cell counting, and inclusion of 10 μM ATP in culture medium also reduced cell proliferation (Coppi et al., 2007). Furthermore, the cell number was increased by treatment with PPADS or P2Y1 antagonist MRS2179, suggesting that endogenously released ATP inhibits cell proliferation via the P2Y1 receptor (Coppi et al., 2007). Another study showed that exposure to ATP at low concentrations (1-100 μM) was without effect on proliferation of hBM-MSCs but treatment with 1 mM ATP resulted in significant inhibition of cell proliferation (Ferrari et al., 2011). This study further revealed that exposure to 1 mM ATP resulted in down-regulation of the expression of genes related to cell proliferation and up-regulation of the expression of growth arrest genes and cell cycle inhibitors. ATP-induced inhibitory effects were abrogated by treatment with 1 U/ml apyrase, an ATP scavenger enzyme (Ferrari et al., 2011). In the study by Fruscione et al. (2011), it was shown neither addition of 50 μM ATP nor treatment with 1 or 5 mU/ml apyrase had significant effects on hBM-MSC proliferation (Fruscione et al., 2011). A recent study has reported that BzATP applied at 5-25 μM did not alter the number of rat BM-MSCs (rBM-MSCs) using cell counting-kit-8 (CCK-8) assay (Li et al., 2015b). Consistent with this, we have shown that hDP-MSCs proliferated at a similar rate in the absence or in the presence of ATP at 0.3-300 μM, using both cell counting and methylthiazol tetrazolium (MTT) assays (Peng et al., 2016).

Another recent study examining hPDLSCs shows that exposure to 30-300 μM BzATP considerably reduced cell viability determined by MTT assay (Trubiani et al., 2014).

In summary, there are significant discrepancies in the results reported by different studies, which could be in part attributed to the differences in the ATP concentrations applied and treatment duration, the receptor expression levels in MSCs, and also the assays used. Therefore, it remains inconclusive whether ATP regulates MSC proliferation and viability.

1.6.2 Cell migration

The ability of MSCs to migrate to destination tissues or lesion sites is crucial for normal tissue morphogenesis and homeostasis and also important for MSC-based therapies (Tuan et al., 2003; Ferrari et al., 2011; Burnstock and Ulrich, 2011; Rodrigues et al., 2014). Studies have gathered increasing evidence to show that ATP stimulates MSC migration. For example, in the study by Ferrari et al. (2011) using trans-well migration assay, inclusion of 1 mM ATP to the upper chamber increased hBM-MSC migration and also enhanced the chemotactic response to chemokine CXC-12 applied in the lower chamber (Ferrari et al., 2011). When added to the lower chamber as a chemotactic stimulus, ATP alone had no effect on cell migration but enhanced the chemotactic activity of chemokine CXC-12 in attracting hBM-MSCs (Ferrari et al., 2011). Additionally, pretreatment with ATP at 1 mM increased the homing rate of hBM-MSCs to bone marrow in immunocompromised mice (Ferrari et al., 2011). A separate study by Fruscione et al. (2011) also using trans-well migration assay found that treatment with ATP at 1-10 μM or addition of ATP in the lower chamber stimulated hBM-MSC migration. While these studies provide evidence to demonstrate that ATP can enhance cell migration *in vitro* (Ferrari et al., 2011; Fruscione et al., 2011) and the homing capacity of hBM-MSCs *in vivo* (Ferrari et al., 2011), the P2 receptor(s) mediating ATP-induced stimulation of cell migration was(were) not identified. Our recent study has shown in hDP-MSC using wound healing assay that exposure to ATP at 30 μM accelerated cell migration (Peng et al., 2016). ATP-stimulated cell migration was inhibited by treatment with PPADS and hP2X7 selective antagonist AZ11645373 or by specific siRNA targeting the P2X7, P2Y1 or

P2Y11 receptor, suggesting that these receptors participate in mediating ATP-induced stimulation of hDP-MSC migration (Peng et al., 2016). In the present study (chapter 3), I further examined the Ca^{2+}-dependent signalling pathways engaged in such ATP-induced regulation of hDP-MSCs.

1.6.3 Cell differentiation

1.6.3.1 Adipogenic differentiation

Several studies have investigated the effects of ATP on adipogenic differentiation of MSCs. For example, exposure of hAT-MSCs to ATP (10-100 μM) during adipogenic differentiation reduced the formation of fat droplets, a characteristic of adipocytes or an indicator of adipogenic differentiation, visualized by oil red O staining (Zippel et al., 2012). Conversely, treatment with 5 U/ml apyrase enhanced adipogenic differentiation of hAT-MSCs (Zippel et al., 2012). As shown in a separate study, exposure of rBM-MSCs to 125 μM BzATP during adipogenic differentiation suppressed the expression of adipogenic genes, such as peroxisome proliferator-activated receptor γ (PPARγ), fatty acid binding protein 4 (FABP4) and adipsin, as well as formation of fat droplets (Li et al., 2015b). This study has further shown that in ovariectomized mice, as a model for osteoporosis, the number of bone marrow adipocytes was reduced by intraperitoneal injection of BzATP (Li et al., 2015b). However, a study using hBM-MSCs showed that treatment with 1 mM ATP prior to adipogenic differentiation enhanced the expression of PPARγ and CCAAT/enhancer binding protein α/β (CEBPα/β) and formation of fat droplets after adipogenic differentiation (Ciciarello et al., 2013).

The role of the P2X receptors in ATP-induced regulation of adipogenic differentiation in MSCs has been examined in the above-mentioned studies. ATP-induced increase in the expression of PPARγ and CEBPα/β in hBM-MSCs was not influenced by treatment with hP2X7 selective antagonist KN-62, largely excluding a possible role of the P2X7 receptor in ATP-induced regulation of adipogenesis (Ciciarello et al., 2013). However, BzATP-induced inhibition of the expression of PPARγ, FABP4 and adipsin in rBM-MSCs was attenuated by treatment with P2X7 selective antagonist BBG and also with P2X7-specific

siRNA, indicating that activation of the P2X7 receptor leads to inhibition of adipogenic differentiation (Li et al., 2015b). Zippel et al. (2012) showed that ATP-induced increase in the $[Ca^{2+}]_i$ in hAT-MSCs remained unchanged after adipogenic differentiation and ATP-induced Ca^{2+} responses in undifferentiated and differentiated hAT-MSCs were reduced by treatment with suramin and P2X antagonist NF279. These results suggest no significant change in the functional expression of P2X receptors during adipogenic differentiation (Zippel et al., 2012). However, increasing evidence suggests changes in the mRNA and/or protein expression of the P2X receptors during adipogenic differentiation. For examples, while the expression of P2X3-P2X5 and P2X7 remained similar, the expression of P2X6 at the mRNA and protein levels was increased in hAT-MSCs during adipogenesis, suggesting a possible role for the P2X6 receptor in committing adipogenic differentiation (Zippel et al., 2012). The mRNA and protein expression levels of P2X7, determined using real-time RT-PCR and western blotting, were down-regulated in rBM-MSCs after adipogenic differentiation, suggesting a role for the P2X7 receptor in adipogenic differentiation (Li et al., 2015b).

The role of ATP-sensitive P2Y receptors in regulating MSC adipogenesis was also investigated using selective agonist and/or antagonist in combination with examining the expression of P2Y receptors and/or adipogenic genes. For example, ATP-induced increase in the expression of adipogenic genes and formation of fat droplets in hBM-MSCs cultured in adipogenic differentiation inducing medium were inhibited by treatment with P2Y1 selective antagonist MRS2279, but not with P2Y11 selective antagonist NF340, favoring a critical role of the P2Y1 receptor in ATP-induced regulation of adipogenic differentiation (Ciciarello et al., 2013). There is evidence to suggest changes in the expression of the P2Y receptors during adipogenic differentiation. For example, the P2Y11 mRNA and protein expression levels in hAT-MSCs were up-regulated after adipogenic differentiation (Zippel et al., 2012). The P2Y2 mRNA expression in rBM-MSCs was also up-regulated after adipogenic differentiation (Li et al., 2016). In this present study (Chapter 5), I examine ATP-induced regulation of adipogenic differentiation in hDP-MSCs, the expression of the P2Y1, P2Y2, P2Y11 and P2X7 receptors during

ATP-induced adipogenic differentiation, and the roles of Ca^{2+}-dependent signalling pathways in ATP-induced regulation of adipogenic differentiation.

1.6.3.2 Osteogenic differentiation

Studies have also examined the effects of extracellular ATP in regulating osteogenic differentiation of MSCs derived from different tissue origins and provide consistent evidence to support that ATP stimulates osteogenic differentiation. For example, treatment of hAT-MSCs during osteogenic differentiation with 5 U/ml apyrase reduced matrix mineralization, indicating that ATP promotes osteogenic differentiation (Zippel et al., 2012). As shown in another study, treatment of hBM-MSCs with 1 μM ATP in basal media increased the alkaline phosphatase (ALP) activity, production of osteocalcin, and mineralization of bone extracellular matrix (Sun et al., 2013). A separate study reported that treatment of rBM-MSCs with 125 μM BzATP during osteogenic differentiation up-regulated the expression of osteogenic genes, such as runt related transcription factor 2 (Runx2), ALP and osteopontin, as well as formation and mineralization of bone extracellular matrix (Li et al., 2015b). The same study also showed that the number and volume of trabecular bone were increased by intraperitoneal injection of 5 mg/kg/day BzATP in ovariectomized mice (Li et al., 2015b). Further, a more recent study has demonstrated that exposure to 100 μM BzATP induced an increase in the expression of ALP, Runx2 and osteocalcin in hPDLSCs cultured in osteogenic differentiation inducing medium (Xu et al., 2019), leading to the suggestion that activation of the P2X7 receptor stimulates osteogenic differentiation. Consistently, a study by Noronha-Matos et al. (2014) found that treatment of hBM-MSCs with 100 μM BzATP during osteogenic differentiation enhanced the ALP activity, expression of Runx2 and osterix, and mineralization of bone extracellular matrix (Noronha-Matos et al., 2014). Of notice, an early study by the same group showed that application of 100 μM ATP decreased the ALP activity in hBM-MSCs cultured in osteogenic differentiation media (Noronha-Matos et al., 2012).

Several studies have investigated the role of the P2X receptors in mediating the effect of ATP on osteogenic differentiation and provide evidence to support a significant role of the P2X7 receptor. Two studies by the same research group showed that the P2X7 protein expression was detected at the early stage (7 days in osteogenesis inducting medium) of osteogenic differentiation of hBM-MSCs but declined afterwards (Noronha-Matos et al., 2012; Noronha-Matos et al., 2014). These findings are consistent with a decrease in ATP-induced Ca^{2+} responses and BzATP-evoked membrane blebbing in hBM-MSCs after osteogenic induction for 21 days compared to those in cells after osteogenic induction for 7 days, indicating that P2X7 receptor promotes the osteogenic commitment of MSCs (Noronha-Matos et al., 2012; Noronha-Matos et al., 2014). Another study demonstrated that treatment with KN-62 or P2X7-specific siRNA significantly reduced or completely abolished ATP-induced increase in the ALP activity, production of osteocalcin, and mineralization of bone extracellular matrix in hBM-MSCs cultured in basal media (Sun et al., 2013). It was also reported that treatment of hBM-MSCs with P2X7 selective antagonist A438079 inhibited BzATP-induced increase in the ALP activity, expression of Runx2 and osterix, and mineralization of bone extracellular matrix (Noronha-Matos et al., 2014). A recent study in rBM-MSCs has shown that treatment with P2X7 selective antagonist BBG or P2X7-specific siRNA prevented BzATP-induced up-regulation of the expression of Runx2, ALP and osteopontin, formation and mineralization of bone extracellular matrix, indicating an important role of the P2X7 receptor in mediating BzATP-induced osteogenesis differentiation (Li et al., 2015b). A more recent study in hPDLSCs has demonstrated that treatment with BBG or A740003 inhibited BzATP-induced increase in the expression of ALP, Runx2 and osteocalcin, indicating that activation of the P2X7 receptor stimulates osteogenic differentiation (Xu et al., 2019). However, Zippel et al. (2012) showed that overexpression of the P2X7 receptor in hAT-MSCs led to reduced ALP activity (Zippel et al., 2012). Changes in the expression of the P2X receptors in MSCs during osteogenic differentiation have been documented. For example, the expression of P2X5 at the mRNA and protein level was up-regulated, while the expression of P2X6 and P2X7 was down-regulated in hAT-MSCs during osteogenesis (Zippel et al., 2012). However, two recent studies show that the P2X7 expression at the mRNA and protein levels was up-regulated in rBM-MSCs (Li et al., 2015b) and hPDLSC during osteogenesis (Xu et al., 2019).

The role of the ATP-sensitive P2Y receptors in regulating MSC osteogenesis has been also investigated using agonist and/or antagonist in combination with examining the expression of the P2Y receptors and/or osteogenic genes. For example, treatment of hAT-MSCs with suramin and PPADS during osteogenic differentiation inhibited mineralization of bone extracellular matrix, which was rescued by application of exogenous ATP, suggesting an involvement of ATP-sensitive P2 receptors in osteogenic differentiation (Zippel et al., 2012). However, it was not clearly established which P2 receptor(s) mediate(s) the inhibition of osteogenic differentiation by suramin and PPADS (Zippel et al., 2012). A separate study reported that the P2Y1 protein expression was detected at the early stage of osteogenic differentiation (7 days in osteogenesis inducing medium) of hBM-MSCs but declined afterwards (Noronha-Matos et al., 2012). These findings are consistent with a decrease in ATP-induced Ca^{2+} responses in hBM-MSCs after osteogenic induction for 21 days compared to those in cells after osteogenic induction for 7 days. In addition, pre-treatment of hBM-MSCs, cultured for 7 days in osteogenesis inducing medium, with MRS2179 totally abolished ATP-induced Ca^{2+} responses, indicating that the P2Y1 receptor promotes osteogenic commitment (Noronha-Matos et al., 2012). Interestingly, overexpression of the P2Y1 or P2Y2 receptor suppressed osteogenesis of hAT-MSCs (Zippel et al., 2012). Furthermore, changes in the expression of the P2Y receptors during osteogenesis were investigated. The P2Y1 expression at the mRNA and protein levels was down-regulated in hAT-MSCs (Zippel et al., 2012) and hBM-MSCs after osteogenic differentiation (Noronha-Matos et al., 2012). The P2Y2 expression at both mRNA and protein levels was also down-regulated after osteogenic differentiation in hAT-MSCs (Zippel et al., 2012) and rBM-MSCs (Li et al., 2016), but up-regulated at the protein level in hBM-MSCs (Noronha-Matos et al., 2012).

1.6.3.3 Chondrogenic differentiation

The current knowledge regarding the regulation of chondrogenic differentiation of MSC by ATP and P2 purinergic signalling is limited. An early study reported that ATP-induced increase in the $[Ca^{2+}]_i$ enhanced the expression of chondrogenic genes, including aggrecan, collagen type II and sex determining region Y box-9 (Sox-9) in mouse BM-MSCs (mBM-MSCs) after chondrogenic differentiation (Kwon. 2012). These effects were

lost upon treatment with P2X4 selective antagonist 5-BDBD, indicating that ATP induces Ca^{2+} influx via the P2X4 receptor and subsequent chondrogenic differentiation in mBM-MSCs (Kwon, 2012). Two independent studies provide evidence to show that endogenously released ATP through the connexin hemi-channels activates the P2 receptors and stimulates the accumulation of collagen type II and chondrogenic differentiation of hBM-MSCs (Gadjanski and Vunjak-Novakovic, 2013) and pig BM-MSCs (Steward et al., 2016).

1.6.3.4 Neural and glial differentiation

There is some evidence to suggest that extracellular ATP regulates differentiation of MSCs into neural and glial lineages. Tu et al. (2014) showed that exogenously applied or endogenously released ATP increased the expression of neuron-specific class III β-tubulin (Tuj1) and paired box 6 (Pax6) and stimulated neural differentiation of hBM-MSCs (Tu et al., 2014). Treatment with TNP-ATP, which is known to inhibit several P2X receptors, including P2X1, P2X2, P2X3 and P2X4 receptors (Jiang et al., 2000), prevented ATP-induced expression of these neurogenic genes and neural differentiation of hBM-MSCs, suggesting that P2X receptors mediate ATP-induced stimulation of neural differentiation (Tu et al., 2014). A separate study showed that exposure of rAT-MSCs to ATP enhanced differentiation into Schwann cell-like cells, which exhibited the expression of glial markers and growth factors and the ability to produce myelin and induce neurite outgrowth (Faroni et al., 2013). The same study demonstrated that glial differentiation of rAT-MSCs was accompanied by up-regulated expression of P2X4 and P2X7 protein. Furthermore, ATP induced currents in Schwann cell-like cells, which were inhibited by treatment with P2X7 selective antagonist AZ10606120, demonstrating functional expression of the P2X7 receptor (Faroni et al., 2013).

In summary, an increasing number of studies have examined regulation by ATP of MSC differentiation in basal media or under specific differentiation conditions and the role of the P2 receptors in such regulation. Overall, it is evident that the results are, to various degree, discrepant. Such discrepancies may be in part attributed to the differences in MSCs used. Nonetheless, there is evidence to suggest that ATP-induced activation of the P2Y1

and P2Y2 receptors up-regulates adipogenic differentiation, whereas activation of the P2X7 receptor down-regulates adipogenic differentiation. ATP stimulates osteogenesis mainly via the P2X7 receptor and, by contrast, activation of the P2Y2 receptor down-regulates osteogenic differentiation. Thus, activation of the P2X7 and P2Y2 receptors imposes opposite regulation of adipogenic and osteogenic differentiation, consistent with the notion that MSC differentiation into adipocytes and osteoblasts is often mutually excluded (Chen et al., 2016). There is evidence to show that ATP promotes MSC differentiation into chondroblasts via the P2X4 receptor. Finally, ATP enhances MSC differentiation into neuron-like cells via the P2X1 and P2X4 receptors, and Schwann cell-like cells via the P2X7 receptor.

1.7 Expression of Piezo1 channel in MSCs and its role in regulating cell functions

There is a strong evidence that MSCs are mechanosensitive, exhibiting the ability to sense and transduce mechanical signals from their niche and convert them into intracellular signalling mechanisms to regulate cell functions (Lee et al., 2011; Liu and Lee, 2014; Li et al., 2018; Goetzke et al., 2018). For example, hBM-MSCs were shown to commit a specific cell lineage and phenotype due to the extreme sensitivity to matrices with tissue-like stiffness (Engler et al., 2006). It was found that hBM-MSCs migrated and differentiated towards neuron-like cells when cultured on soft substrates that mimic the brain, muscle cells on modestly stiff substrates that mimic muscles, and bone cells on rigid substrates that mimic collagenous bone (Engler et al., 2006). In addition, hBM-MSC proliferation was increased by fluid flow (Riddle et al., 2007) and shockwaves (Suhr et al., 2013), and hAT-MSC proliferation was also increased by shockwaves (Weihs et al., 2014). Similarly, migration of hBM-MSCs, as shown using the scratch wound healing assay, was simulated by shear stress (Yuan et al., 2012; Yuan et al., 2013) and shockwaves (Suhr et al., 2013). In another study, hBM-MSCs differentiation into osteoblasts was significantly enhanced after exposure to shockwaves (Sun et al., 2013). These observations indicate that MSC functions are highly regulated by mechanical stimuli.

Recent studies have drawn attention to the Piezo1 channel in MSCs. The protein expression of Piezo1 was shown using western blotting in rDP-MSCs and rPDLSCs by

Gao et al. (2017). The Piezo1 protein expression was up-regulated in rDP-MSCs, but not rPDLSCs, upon stimulation by mechanical low-intensity pulsed ultrasound (LIPUS), indicating that Piezo1 is responsive to LIPUS in rDP-MSCs (Gao et al., 2017). Mechanically activated currents were inhibited by treatment with RR, suggesting a role for Piezo1 in mediating such mechanically activated currents (Gao et al., 2017). Moreover, as shown using BrdU labelling assay, exposure to LIPUS induced proliferation of rDP-MSCs that was inhibited by treatment with RR, suggesting a role of the Piezo1 channel in mediating mechanical regulation of MSC proliferation (Gao et al., 2017). The expression of Piezo1 at the mRNA and protein levels was also demonstrated in hBM-MSCs and MSC-like cells, UE7T-13 and SDP11 cells, using real-time RT-PCR and western blotting, respectively (Sugimoto et al., 2017). The Piezo1 mRNA expression was increased after hydrostatic pressure (HP) (Sugimoto et al., 2017). Exposure of MSC-like cells to HP or Yoda1 consistently enhanced the expression of bone morphogenetic protein 2 (BMP2) and osteogenic differentiation, and suppressed the expression of adipogenic marker lipoprotein lipase (LPL) expression and adipogenic differentiation (Sugimoto et al., 2017). Treatment with Piezo1-specific siRNA inhibited osteogenic differentiation and induced adipogenic differentiation. In addition, treatment of hBM-MSCs with GsMTx4 inhibited HP loading and Yoda1-induced BMP2 expression and osteogenic differentiation (Sugimoto et al., 2017). These results collectively suggest that the Piezo1 channel plays a role in regulating osteogenic and adipogenic differentiation of MSCs.

As already discussed above, MSCs are known to release ATP in response to mechanical stimuli such as fluid flow-induced shear stress and shockwaves, and one interesting role for the Piezo1 channel that has emerged from recent studies is to mediate or regulate ATP release. It is interesting to know whether the Piezo1 channel plays a similar role in mediating ATP release from MSCs. In the present study (chapter 4), I investigate the expression of the Piezo1 channel in hDP-MSCs and its role in regulating cell migration, particularly its role in promoting ATP release from hDP-MSCs.

1.8 Ca^{2+}-dependent downstream signalling in MSC functions

Intracellular Ca^{2+} as a second messenger can induce or regulate a number of Ca^{2+}-dependent signalling pathways. Protein kinase C (PKC), proline-rich tyrosine kinase 2 (PYK2) and calmodulin kinase II (CaMKII) represent three Ca^{2+}-sensitive protein kinases. Activation of these kinases is important in mediating Ca^{2+}-dependent activation of downstream signalling cascades, particularly mitogen-activated protein kinases (MAPKs), a serine/threonine kinase family composed of extracellular signal-regulated kinase (ERK), p38 kinase and Jun N-terminal kinase (JNK) (Kim and Choi, 2010). In this section, I will introduce PKC, PYK2 and CaMKII and discuss the roles of these kinases and the MAPKs signalling pathways in the regulation of cell proliferation, differentiation and migration, focusing mainly on MSCs. Figure 1.7 summarizes such Ca^{2+}-dependent downstream pathways in the regulating MSC functions to be discussed in this section.

1.8.1 PKC

PKCs are serine/threonine kinases that can be grouped into three classes according to their sensitivity to activation by Ca^{2+} and DAG. Conventional PKCs, including PKCα, β1, β2 and γ, are activated via both Ca^{2+} and DAG, and novel PKCs, comprising PKCδ, ε, η, θ and μ, are activated by DAG but insensitive to Ca^{2+}, while atypical PKCs, composed of PKCζ, λ/ί and μ, are insensitive to both Ca^{2+} and DAG (Reyland, 2009; Singh et al., 2017). Conventional PKCs, particularly PKCα that exhibits ubiquitous expression (Webb et al., 2000) and has been most extensively studied (Kang, 2014; Singh et al., 2017), have important roles in the crosstalk between multiple signalling pathways regulating cell functions. Studies often depend on using calphostin C and chelerythrine, broad PKC inhibitors targeting conventional, novel and atypical PKCs, and also conventional PKC specific inhibitors, such as staurosporine (PKCα and γ), bisindolylmaleimide (PKCα, β1, β2 and γ), Gὸ6983 (PKCα, β and γ) and Gὸ6976 (PKCα and PKCβ).

As introduced above, activation of the $G_{\alpha,q/11}$-coupled P2Y receptors, including ATP-sensitive P2Y1, P2Y2 and P2Y11, results in an increase in the $[Ca^{2+}]_i$ and generation of DAG (Figure 1.5), leading to activation of PKC. It has been reported that mechanically

released ATP induced activation of the P2Y2 receptor in osteoblast-like cells, resulting in a subsequent increase in the $[Ca^{2+}]_i$ and activation of PKC and downstream MAPK signalling pathways (Katz et al., 2006; Katz et al., 2008). Moreover, it was shown that activation of the P2Y2 receptor induced by ATP in human endometrial stromal cells (Chang et al., 2008) or UTP in glioma cells (Tu et al., 2000) triggered activation of PKC and the MAPK kinase (MEK)/ERK downstream signalling pathway. In addition to P2Y receptors, it is known that PKC can be activated via other $G_{\alpha,q/11}$-IP_3R-DAG/Ca^{2+} release signalling GPCRs, such as muscarinic acetylcholine (ACh) receptors (mAChRs) by ACh (Tang et al., 2012), sphingosine-1-phosphate (S1P) receptor by S1P (Liu et al., 2010) and lysophosphatidic acid (LPA) receptors by LPA (Ryu and Han, 2015). PKCs can also be directly activated by DAG-mimicking compounds, such as phorbol 12-myristate 13-acetate (PMA) and phorbol 12,13-dibutyrate (PDBu) (Liu et al., 2010).

The role of PKC in the regulation of cell proliferation has been demonstrated in different cell types, such as glioma cells (Tu et al., 2000), endometrial stromal cells (Chang et al., 2008) and osteoblastic cells (Swarthout et al., 2001; Ghayor et al., 2005). Regulation by PKC of MSC proliferation has also been reported. For example, exposure to 17β-estradiol promoted proliferation of hMSCs of undefined tissue origin, measured by using radioactively tritium-labeled thymidine ([^{3}H] thymidine) incorporation assay and fluorescence-activated cell sorting of cells stained with propidium iodide, and the effect was inhibited by treatment with bisindolylmaleimide and staurosporine, suggesting a role of PKC in mediating 17β-estradiol-induced regulation of cell proliferation (Yun et al., 2009). However, it remains unknown how 17β-estradiol activates PKC. In contrast, it was shown in a separate study using Alamar blue assay that treatment with PKC activator PMA or PDBu inhibited proliferation of hBM-MSCs, whereas treatment with S1P had no effect (Liu et al., 2010). Another study reported that exposure of hMSCs from undefined tissue to high glucose (25 mM) increased the $[Ca^{2+}]_i$ via unidentified mechanism(s) and stimulated cell proliferation, determined using [^{3}H] thymidine incorporation assay (Ryu et al., 2010a). High glucose-induced increase in cell proliferation was attenuated by bisindolylmaleimide and staurosporine, indicating the involvement of PKC activation in high glucose-induced cell proliferation (Ryu et al., 2010a). A subsequent study using

PicoGreen assay, however, reported that treatment with Gö6983 induced no effect on proliferation of hBM-MSCs cultured in medium containing high glucose (25 mM) (Tsai et al., 2013). Such discrepancies may be attributed to the difference in stimuli used, duration of PKC activation, PKC isoforms and localization, and downstream signalling pathways that depends on PKC (Nishizuka, 1992; Clark et al., 2004; Rácz et al., 2006; Black and Black, 2012; Heckman et al., 2017). Some of the studies described above further showed that PKC acts as an upstream of the MAPK signalling pathway(s) in the regulation of cell proliferation of MSCs. For example, high glucose-induced activation of the MEK/ERK and p38 MAPK, examined by western blotting, was inhibited by treatment with bisindolylmaleimide and staurosporine (Ryu et al., 2010a). Additionally, pre-treatment with MEK/ERK inhibitor, PD98059, and p38 inhibitor, SB203580, blocked high glucose-induced hMSC proliferation (Ryu et al., 2010a). Similarly, 17β-estradiol-induced activation of MEK/ERK, also determined by western blotting, was attenuated by treatment with bisindolylmaleimide and staurosporine (Yun et al., 2009). Pre-treatment with PD98059 reduced 17β-estradiol-induced proliferation of hMSCs (Yun et al., 2009). These findings suggest that PKC-mediated activation of downstream MEK/ERK and p38 MAPK signalling pathways is involved in regulating MSC proliferation (Yun et al., 2009; Ryu et al., 2010a).

It is also known that PKC plays a role in cell differentiation. PKC activation has been shown to stimulate osteogenesis of osteoblast-like cells (Costessi et al., 2005; Katz et al., 2006; Katz et al., 2008), adipogenesis of pre-adipocytes (Fleming et al., 1998; Nishizuka et al., 2008) and chondrogenesis of chick limb bud mesenchymal cells (Choi et al., 1995; Lim et al., 2003). Consistently, PKC activation has also been shown to regulate MSC differentiation. For example, treatment with PMA and PDBu inhibited, whereas treatment with Gö6976 promoted, the ALP expression in hBM-MSCs (Liu et al., 2010). The same study also showed that treatment with ionomycin to increase the $[Ca^{2+}]_i$ decreased the ALP expression during osteogenic differentiation. These results consistently support the negative effect of Ca^{2+}-induced PKC activation on osteogenesis (Liu et al., 2010). There is evidence to suggest that PKC activation has a positive role in regulating adipogenic differentiation. For example, pretreatment of hBM-MSCs with high glucose stimulated the expression of LPL during adipogenesis, which was reduced by treatment with PKC

inhibitor Gö6983 (Tsai et al., 2013). In the same study, it was also shown that PKC activation following exposure to high glucose had a negative effect on chondrogenesis differentiation of hBM-MSCs that was reversed by PKC inhibitor Gö6983, resulting in increased expression of aggrecan and collagen type II (Tsai et al., 2013). Two separate studies showed that PMA-induced PKC activation stimulated differentiation of hDP-MSCs (Király et al., 2009) and hBM-MSCs (Scintu et al., 2006) into neuron-like cells expressing neuron-specific enolase.

The role of PKC in promoting cell migration has been documented in different cell types, including intestinal epithelial cells (Sumagin et al., 2013), glioblastoma cells (Nomura et al., 2007) and HeLa cells (Gao et al., 2014). A similar role for PKC has also been demonstrated in MSCs. For example, LPA promoted lamellipodia formation and cell migration in hUC-MSCs, which was blocked by treatment with staurosporine and bisindolylmaleimide, indicating that PKC activation mediates LPA-induced cell migration (Ryu and Han, 2015). Similarly, interleukin-1β (IL-1β) via activation of the IL-1 receptor stimulated lamellipodia formation and migration of hUC-MSCs, and such an effect was prevented by treatment with calphostin C or Gö6976, as well as treatment with BAPTA/AM, a Ca^{2+} chelator, supporting a critical role for Ca^{2+}-sensitive PKC in IL-1β-induced stimulation of cell migration (Lin et al., 2015). Exposure of rBM-MSCs to ACh accelerated cell migration, which was blocked by treatment with staurosporine or Gö6976 and also by siRNA-mediated knockdown of PKCα and PKCβ, as well as treatment with IP_3R inhibitor 2-APB. These results collectively support the notion that induction of the mAChR-$G_{\alpha,q/11}$-IP_3R-DAG/Ca^{2+} release signalling pathway and subsequent activation of PKC mediate ACh-induced increase cell migration in the trans-well migration assay (Tang et al., 2012). Consistently, as shown in another study, direct activation of PKC by PMA increased migration of rBM-MSCs using cell adhesion and spreading assays (Song et al., 2013). The same study further demonstrated that injection of PMA-treated rBM-MSCs into rats improved ischemia-induced myocardial infarction, supporting the role of PKC activation in promoting MSC migration *in vivo* (Song et al., 2013). It is known that netrin-1 can activate the deleted in colorectal cancer (DCC) receptor to stimulate the PLC-IP_3R signalling (Xie et al., 2006). A recent study shows that treatment with netrin-1 increased

hUC-MSC migration, assessed by wound healing and trans-well migration assays, that was attenuated by staurosporine and bisindolylmaleimide, suggesting the engagement of PKC in netrin-1 induced cell migration (Lee et al., 2014).

Some of the above-described studies provide evidence to show that PKC-dependent increase in MSC migration in response to various stimuli is mediated through downstream MAPK signalling pathway(s). For example, IL-1β-induced activation of MEK/ERK in hUC-MSCs, examined by western blotting, was prevented by treatment with calphostin C and Gὸ6976, and Ca^{2+} chelator, BAPTA/AM (Lin et al., 2015). Furthermore, IL-1β-induced hUC-MSC migration was inhibited by treatment with MEK/ERK inhibitors, U0126 and PD98059 (Lin et al., 2015). Likewise, ACh-induced activation of MEK/ERK, determined by western blotting, was inhibited by treatment with a 2-APB, staurosporine, Gὸ6976, and PKCα as well as PKCβ-specific siRNA in rBM-MSCs (Tang et al., 2012). Additionally, treatment with PD98059 prevented ACh-induced rBM-MSC migration (Tang et al., 2012). Furthermore, netrin-1-induced activation of MEK/ERK and JNK MAPKs, assessed by western blotting, was blocked by treatment with bisindolylmaleimide and staurosporine in hUC-MSCs (Lee et al., 2014). The role of MEK/ERK and JNK was also examined in netrin-1-induced hUC-MSC migration showing that treatment with PD98059 and the JNK inhibitor, SP600125, prevented cell migration (Lee et al., 2014). Collectively, these findings suggest that PKC-mediated activation of downstream MEK/ERK and JNK MAPK signalling pathways regulate MSC migration (Lin et al., 2015; Tang et al., 2012; Lee et al., 2014).

1.8.2 PYK2

PYK2, also known as related adhesion focal tyrosine kinase, is a cytoplasmic Ca^{2+}-sensitive non-receptor tyrosine kinase and can also be activated by PKC-mediated phosphorylation (Lev et al., 1995). PYK2 is also well-recognized for its role in mediating Ca^{2+}-dependent induction of the MAPK signalling pathways in many types of cells, such as neuronal cells, embryonic kidney cells, and astrocytes (Lev et al., 1995; Blaukat et al., 1999; Wang and Reiser, 2003). PYK2 is readily activated by various stimuli that increase the $[Ca^{2+}]_i$. For example, activation induced by ATP or UTP of the P2Y2-$G_{\alpha,q/11}$-IP_3R-

DAG/Ca^{2+} release signalling pathway elevated the $[Ca^{2+}]_i$ to trigger sequential activation of PYK2 and the MEK/ERK signalling pathway in neuronal cells (Soltoff et al., 1998). Treatment with Ca^{2+} chelators, EGTA and BAPTA/AM, reduced phosphorylation and activation of PYK2, suggesting that PYK2 activation is Ca^{2+}-dependent (Soltoff et al., 1998). UTP-induced activation of the P2Y2-$G_{\alpha,q/11}$-IP_3R-DAG/Ca^{2+} release signalling pathway in astrocytoma cells expressing the recombinant P2Y2 receptor induced PYK2 activation (Liu et al., 2004). It was also reported that mechanical stretch-induced Ca^{2+} influx in smooth muscle cells activated PYK2 and downstream Ras/ERK signalling pathway and, in addition, such stretch-induced PYK2 activation was reduced by treatment with BAPTA/AM, supporting Ca^{2+}-dependent activation of PYK2 (Iwasaki et al., 2003).

PYK2 plays an important role in promoting cell proliferation, as shown in astrocytes (Wang et al., 2002; Wang and Reiser, 2003), osteoblast-like cells (Boutahar et al., 2004) and hepatocellular carcinoma cells (Sun et al., 2008). There is strong evidence to show that PYK2 activation also promotes migration of epithelial cells (Block et al., 2010), endothelial cells (Kuwabara et al., 2004), cervical cancer cells (Chen et al., 2011) and hepatocellular carcinoma cells (Sun et al., 2008). However, the role of PYK2 in regulating MSC proliferation and migration is unclear.

The current understanding regarding the role of PYK2 in regulating cell differentiation is limited. However, there is some evidence to show an important role of PKY2 in regulating MSC osteogenic differentiation. Two independent studies have found that mBM-MSCs derived from PYK2-deficient mice possessed a greater ability of osteoblast differentiation than wild-type cells under osteogenesis inducing conditions *in vitro* (Buckbinder et al., 2007; Eleniste et al., 2016). Consistently, knockdown of the PYK2 expression in mBM-MSCs and transfection with adenovirus expressing PYK2-specific short-hairpin RNA or expressing a kinase-inactive PYK2 mutant in hMSCs of undefined tissue origin increased the ALP activity during osteogenic differentiation (Buckbinder et al., 2007). These results consistently support PYK2-mediated negative regulation of osteogenesis.

1.8.3 CaMKII

Calmodulin (CaM) is a ubiquitous intracellular Ca^{2+}-binding protein and changes its conformation upon Ca^{2+} binding. Serine/threonine kinase CaMKII represents the major target for Ca^{2+}/CaM (Agell et al., 2002; Zayzafoon, 2006). As illustrated in studies discussed below, CaMKII inhibitors such as KN-93 and KN-62 are commonly used to study the role of CaMKII in regulating cell functions.

Studies using a different type of cells have shown that activation of CaMKII positively regulates cell proliferation, for example, in colon cancer cells (Wang et al., 2008; Li et al., 2009) and melanoma cancer cells (Umemura et al., 2014). However, a recent study has found that treatment with KN-93 resulted in no effect on proliferation of rBM-MSCs (Qu et al., 2015).

The role of CaMKII in regulating cell differentiation has been examined, for example, osteogenic differentiation of murine C2C12 myoblast cells (Seo et al., 2009; Choi et al., 2013) and osteoblast-like cells (Zayzafoon et al., 2005) and adipogenesis of embryonic stem cells (Szabo et al., 2009) and 3T3 pre-adipocytes (Visweswaran et al., 2015). There is accumulating evidence to support an important role for CaMKII in regulating MSC differentiation. For example, inhibition of CaMKII in hBM-MSCs by treatment with KN-93 suppressed the downstream MEK/ERK signalling pathway and mineralization of bone extracellular matrix during osteogenic differentiation (Shin et al., 2008). Conversely, as shown in a separate study, activation of CaMKII, as a result of Ca^{2+} influx through the voltage-gated Ca^{2+} channels that were activated by potassium chloride (KCl)-induced membrane depolarization (Pasek et al., 2015), promoted the Rux2 expression after osteogenic differentiation MSC-like cells, ST2 cells (Takada et al., 2007). The same study also showed that activation of CaMKII by KCl through the voltage-gated Ca^{2+} channels suppressed the PPARγ activity during adipogenic differentiation of MSC-like cells (Takada et al., 2007). In contrast, a recent study has reported that inhibition of CaMKII by treatment with KN-62 or KN-93 reduced lipid accumulation and the expression of PPARγ and CEBPα porcine BM-MSCs (pBM-MSCs) during adipogenesis (Zhang et al., 2018b). Regarding the role of CaMKII in the regulation of chondrogenesis, treatment of

rBM-MSCs with KN-93 during chondrogenic induction increased the mRNA expression level of several cartilage markers, including collagen type II, aggrecan and Sox-9, suggesting that CaMKII activation inhibits chondrogenic differentiation (Qu et al., 2015).

CaMKII has shown to positively regulate migration of fibroblast cells (Easley et al., 2008) breast cancer cells (Chi et al., 2016) and melanoma cancer cells (Umemura et al., 2014). There is evidence to show that Ca^{2+}-induced activation of CaMKII regulates MSC migration. In hBM-MSCs, exposure to LPA stimulated cell migration via activation of the LPAR-$G_{\alpha,q/11}$-IP_3R-Ca^{2+} release signalling pathway, and such LPA-induced effect was completely blocked by treatment with KN-93, suggesting critical involvement of CaMKII in mediating LPA-induced stimulation of hBM-MSC migration (Song et al., 2010). Consistently, another study showed that inhibition of CaMKII by treatment with KN-93 suppressed hBM-MSC migration (Shin et al., 2008).

In the present study, I have examined the role of the above-discussed downstream Ca^{2+}-sensitive kinases and downstream MEK/ERK and p38 MAPK signalling pathways in ATP-induced P2 receptor-dependent regulation of cell migration (chapter 3), Yoda1-induced Piezo1 channel-dependent regulation cell migration (chapter 4), and also ATP-induced P2 receptor-dependent regulation of adipogenic differentiation (chapter 5) in hDP-MSCs.

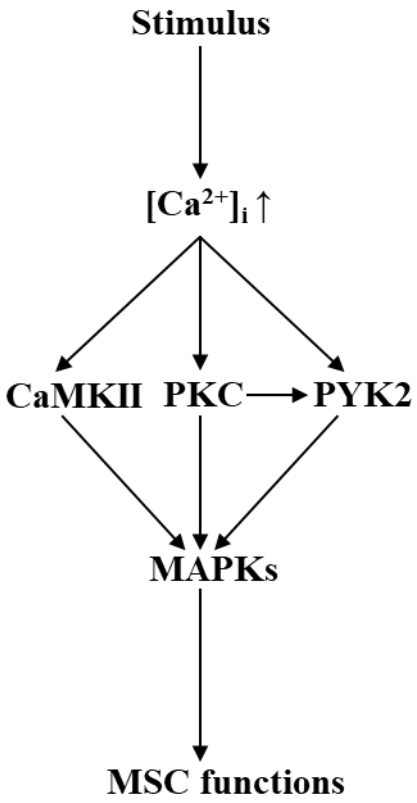

Figure 1.6 Schematic summary of the Ca^{2+}-dependent signalling pathways in regulating MSC functions
Different stimuli induce an increase in the $[Ca^{2+}]_i$ that can stimulate Ca^{2+}-sensitive protein kinases, calmodulin kinase II (CaMKII), protein kinase C (PKC), proline-rich tyrosine kinase 2 (PYK2), and the downstream mitogen-activated protein kinases (MAPKs) signalling pathways. PYK2 can be also activated by PKC. Activation of these signalling pathways leads to regulation of MSC functions, including cell proliferation, differentiation and migration, as discussed in detail in the text (section 1.5).

1.9 Aim and objectives of the study

The overall aim of this study is to provide a better understanding of the Ca^{2+}-signalling mechanisms in the regulation of MSC functions. My study particularly investigates the hypothesis that ATP-sensitive P2 receptors have a role in regulating migration and adipogenic differentiation of hDP-MSCs and that extracellular ATP regulates such MSC functions through Ca^{2+}-dependent downstream signalling pathways, and also examines the hypothesis that activation of the Piezo1 channel regulates hDP-MSC migration via inducing ATP release and activation of the P2 receptors and downstream Ca^{2+}-dependent

proteins. The specific objectives of the study using multidisciplinary approaches including the following:

1. To investigate the role of ATP-sensitive P2 receptors and downstream Ca^{2+}-dependent signalling pathways in mediating ATP-induced regulation of hDP-MSC migration, using trans-well and wound healing assays (Chapter 3).

2. To examine the expression and function of the Piezo1 channel in hDP-MSCs, using real-time RT-PCR, immunostaining and Ca^{2+} imaging, and the role of the Piezo1 channel and downstream Ca^{2+}-dependent signalling pathways on hDP-MSCs migration, using siRNA transfection and wound healing assay (Chapter 4).

3. To assess the expression of the P2Y1, P2Y2, P2Y11 and P2X7 receptors during ATP-induced regulation of adipogenic differentiation of hDP-MSCs, using real-time RT-PCR, and the role of the downstream Ca^{2+}-dependent signalling pathways in mediating ATP-induced regulation of adipogenic differentiation, using oil red O staining (Chapter 5).

CHAPTER 2

Materials and Methods

2.1 Materials

2.1.1 Chemicals

General chemicals and reagents used, including culture medium and antibodies, are summarized in Table 2.1.

Table 2.1 Summary of chemicals and reagents

Chemicals	**Supplier**
Cell culture	
Ethanol	VWR International
Dulbecco's modified Eagle's medium (DMEM) supplemented with GlutaMAX™-I	Invitrogen
Foetal bovine serum (FBS)	Invitrogen/PLL
Penicillin-streptomycin	Sigma-Aldrich
Dulbecco's phosphate buffered saline (D-PBS)	Lonza
0.05% Trypsin-EDTA solution	Invitrogen, Sigma
FLEX-Station recording	
Sodium chloride (NaCl)	Fisher Scientific
Potassium chloride (KCl)	Fisher Scientific
Calcium chloride solution ($CaCl_2$)	Sigma-Aldrich
Magnesium chloride solution ($MgCl_2$)	Sigma-Aldrich
N-(2-hydroxyethyl) piperazine-N'-(2-ethanulfonic acid) (HEPES)	Fisher Scientific
D-Glucose	VWR International
Milli-Q® distilled water	Millipore
Ethylene glycol tetraacetic acid (EGTA)	Sigma-Aldrich
Fura-2/acetoxymethyl (AM)	Invitrogen
Pluronic acid® F-127 (PA)	Invitrogen
Adenosine 5'-triphosphate disodium salt (ATP)	Sigma-Aldrich

Adenosine 5’-triphosphate disodium salt (ADP)	Sigma-Aldrich
2′-&3′-O-(4-benzoyl-benzoyl)-ATP (BzATP)	Sigma-Aldrich
NF546	Tocris Bioscience
α,β-methylene ATP (αβmeATP)	Sigma-Aldrich
Yoda1	Tocris Bioscience
Pyridoxalphosphate-6-azophenyl-2',4'-disulfonic acid (PPADS)	Tocris Bioscience
Grammostola spatulata mechanotoxin 4 (GsMTx4)	Tocris Bioscience
Ruthenium red (RR)	Merck
Ionomycin	Cayman Chemical
Adipogenic differentiation	
Isobutyl-methylxanthine (IBMX)	Sigma-Aldrich
Dexamethasone	Sigma-Aldrich
Insulin	Invitrogen
Indomethacin	Sigma-Aldrich
Oil red O dye	Sigma-Aldrich
Isopropanol	Sigma-Aldrich
Paraformaldehyde (PFA)	Sigma-Aldrich
Hoechst 33342	Cell Signalling Technology
Immunostaining	
Goat serum	Sigma-Aldrich
Triton® X-100	Sigma-Aldrich
Rabbit anti-Piezo1 antibody	Proteintech
Fluorescein isothiocyanate (FITC)-conjugated goat anti-rabbit IgG antibody	Sigma-Aldrich
Slow Fade® Gold antifade reagent with DAPI (4',6-diamidino-2-phenylindole)	Invitrogen
DNA quantitation	
20x Tris-EDTA (TE) buffer	Invitrogen

DNA standards	Invitrogen
Picogreen reagent	Invitrogen
Real-time RT-PCR	
RNAqueous™ Micro kit	Invitrogen
TURBO DNA-free kit	Invitrogen
High Capacity RNA-to-cDNA kit	ThermoFisher Scientific
SensiMix™ SYBR & Fluorescein kit	BIOLINE
Agarose	Fisher Scientific
Tris-base	Sigma-Aldrich
Glacial acetic acid	Fisher Scientific
Ethidium bromide	Sigma-Aldrich
6x gel loading buffer	Biolabs
100 bp DNA ladder	Biolabs
Piezo1-specific siRNA	Ambion
Negative control siRNA #1	Ambion
Negative control siRNA	Dharmacon
Lipofectamine® RMAiMAX transfection reagent	Invitrogen
Opti-MEM™ reduced serum medium	ThermoFisher Scientific
Cell migration assay	
Falcon® cell culture inserts, 8.0-μm pore size	Corning
Culture-insert 2 wells	Ibidi
KN-93	Sigma-Aldrich
Chelerythrine chloride (CTC)	Tocris Bioscience
PF431396	Tocris Bioscience
U0126	Cayman Chemical
SB202190	Tocris Bioscience
Apyrase from potatoes	Sigma-Aldrich

2.1.2 Culture media and solutions

All culture media and solutions are summarized in Table 2.2. Solutions were prepared with Milli-Q deionized water and, if necessary, sterilized by using 0.22-μm filters.

Table 2.2 Summary of culture media and solutions

Cell culture	
Basal medium	DMEM supplemented with GlutaMAX™-I, 10% FBS, and 100 unit/ml penicillin and 100 μg/ml streptomycin
Adipogenic differentiation	
Adipogenic differentiation inducing medium	Basal medium supplemented with 0.5 mM IBMX, 10 μM dexamethasone, 10 μg/ml insulin and 200 μM indomethacin
4% PFA solution	Diluted from 37% PFA with PBS
0.5% oil red O stock solution	5 mg/ml oil red O powder dissolved in isopropanol
0.3% oil red O working solution	Prepared freshly by diluting 0.5% oil red O stock solution with distilled water
DNA content determination	
TE buffer	10 mM Tris-HCl and 1 mM EDTA, pH 8.0
FLEX-Station recording	
Standard buffer solution (SBS) containing calcium (in mM)	NaCl 134, KCl 5, $CaCl_2$ 1.5, $MgCl_2$ 1.2, HEPES 2.38, glucose 8, in distilled water, pH 7.4
SBS without calcium (in mM)	NaCl 134, KCl 5, $MgCl_2$ 1.2, HEPES 2.38, glucose 8, EGTA 0.4, in distilled water, pH 7.4
10% PA solution	10% (w:v) PA dissolved in DMSO
Loading buffer	SBS containing 4 μM Fura-2/AM and 0.04% PA
Immunostaining	
Blocking solution	PBS containing 10% (v:v) goat serum
Permeabilization solution	PBS containing 0.3% (v:v) Triton X-100

Hoechst 33342 staining solution	1 mg/ml stock solution in distilled water
siRNA transfection	
siRNA	20 µM stock in nuclease-free water
Agarose gel preparation	
10 mg/ml ethidium bromide	0.1 g dissolved in 10 ml distilled water
Tris Acetate EDTA (TAE) buffer	40 mM Tris-base, 0.114% (v:v) glacial acetic acid, and 1 mM EDTA, in distilled water, pH 8.0
2% DNA agarose gel	2% (w:v) agarose in TAE buffer and containing 0.5 µg/ml ethidium bromide

2.2 Methods

2.2.1 Cell culture

The hDP-MSCs used in this study were isolated from the molar teeth from two female donors of 9 and 32-year-old and two male donors of 22 and 20-year-old, named as 9F, 32F, 22M and 20M, respectively, from our previous study (Peng et al., 2016). The frozen cells were removed from a liquid nitrogen cryostat and thawed immediately by incubating at 37ºC. The completely thawed cell suspension was transferred into a T-25 flask containing 5 ml basal medium (Table 2.2). After cells were settled down during incubation for 24 hours at 37ºC and 5% CO_2 in a tissue culture incubator, the basal medium was replaced with a fresh basal medium. Cells, when reaching around 80-90% confluency, were sub-cultured. The old media was aspirated, and cells were washed with D-PBS (Lonza) and covered with 0.05% Trypsin-EDTA solution (Invitrogen). Cells were incubated at 37ºC for 3-5 minutes or until cells were detached. An equal amount of basal media was added, and cells were collected by centrifugation at 300 relative centrifugal force (rcf) for 5 minutes. The cell pellet was gently re-suspended in basal medium. The cells were cultured in basal medium in T25 and T75 flasks with the medium replaced every 3-4 days until ~90% confluency was reached. Cells within the fourth to sixth passages were used in the study.

2.2.2 Real-time reverse transcription-polymerase chain reaction (RT-PCR)

Cells were seeded at 8 x 10^4 per well in 6-well plates. Cells, when reaching ~90% confluency, were collected, and total RNA was extracted using a RNAqueous™-Micro kit and treated with a TURBO DNA-free kit (Invitrogen) to remove DNA contamination according to the manufacturer's instructions. The RNA concentration and purity were determined, using a Nanodrop 2000c spectrophotometer (ThermoFisher Scientific). Approximately 0.6 µg RNA was reverse-transcribed into cDNA in 20 µl reaction volume using a High Capacity RNA-to-cDNA kit (ThermoFisher Scientific). The same procedure was carried out for preparing the negative control with Master Mix without reverse transcriptase (ThermoFisher Scientific). The reverse transcription was performed using a Mastercycler Gradient polymerase chain reaction (PCR) machine (Eppendorf) at 37ºC for 60 minutes. Reactions were stopped at 95ºC for 5 minutes and held at 4ºC. The resulting cDNA was stored frozen at -20ºC for further analysis using real-time RT-PCR. Real-time RT-PCR was performed in a PCR machine (ROTOR-Gene model 6000, Corbett Research) using a SensiMix™ SYBR & Fluorescein kit (Bioloine) according to the manufacturer's instructions. The cDNA samples were amplified using primers specific to the target genes as shown in Table 2.3. The PCR reaction in a total volume of 20 µl, containing 1.66 µl of the cDNA sample, 10 µl of 2x SenisMix™ SYBR & Fluorescein, 0.5 µl of 10 µM forward primers, and 0.5 µl of 10 µM reverse primers. The real-time RT-PCR protocol consisted of 95°C for 10 minutes, 45 cycles of 95°C for 10 seconds, 60°C for 15 seconds and 72°C for 20 seconds, followed by a final melting step from 72°C to 95°C. Data were analyzed using ROTOR-Gene 6000 series software 1.7. The cycle threshold (C_t) value was set at 0.2, representing the minimal cycle number based on the point, where the fluorescence signal grows above the background level (Heid et al., 1996). The mRNA expression level for the gene under investigation was normalized to that of β-actin based on the following equation (Livak and Schmittgen, 2001):

$$\text{Normalized expression: } 2^{[-(Ct_{\text{target gene}} - Ct_{\beta\text{-actin}})]}.$$

The PCR products were also analyzed by electrophoresis on 2% agarose gels. To prepare agarose gels, the required amount of agarose was added in 1x TAE buffer and heated in a microwave until agarose was completely dissolved. After the agarose gel solution temperature was lowered to 50-60ºC, ethidium bromide (10 mg/ml) with a final

concentration of 0.5 μg/ml was added and mixed by gently swirling. Then, the agarose gel solution was gently poured into a gel casting tray and a comb was inserted to form the sample wells. Once the gel was formed at room temperature, the comb was gently removed, and the gel was transferred into the tank of the electrophoresis apparatus containing and submerged in 1x TAE buffer. Samples were prepared by mixing 10 μl PCR products with 2 μl 6x loading buffer (Biolabs). The 100 bp DNA ladder solution was prepared by mixing 2 μl stock solution (500 μg/ml, Biolabs) with 2 μl 6x gel loading buffer and 8 μl distilled water. DNA samples and DNA ladder were loaded into the sample wells, and the gel was run at a voltage of 90 V for 45 minutes. The DNA in the gel was visualized and gel images were captured using a G:BOX gel imaging system (SYNGENE). The expected sizes of the PCR products are listed in Table 2.3.

Table 2.3 Primers used for PCR

Primers	**Sequences (5'-3')**	**Expected sizes**
β-actin forward primer	TTGAGACCTTCAACACCC	300
β-actin reverse primer	TCTCTTGCTCGAAGTCC	
P2X7 forward primer	AAAACAGAAGGCCAAGAGCA	176
P2X7 reverse primer	CACCAGGCAGAGACTTCACA	
P2Y1 forward primer	CCGGCTGTCTACATCTTGGT	152
P2Y1 reverse primer	GGCAGAGTCAGCACGTACAA	
P2Y2 forward primer	CCACCTGCCTTCTCACTAGC	163
P2Y2 reverse primer	TGGGAAATCTCAAGGACTGG	
P2Y11 forward primer	AGGGCAAAGTGATGTTCCAC	175
P2Y11 reverse primer	CCCTCCAGGCTCTTCTTTCT	
Piezo1 forward primer	AGATCTCGCACTCCAT	182
Piezo1 reverse primer	CTCCTTCTCACGAGTCC	

2.2.3 Immunostaining

Cells were plated in 24-well plate with approximately 20,000 cells on each coverslip placed in 24-well plates and incubated for 48 hours prior to use. Cells were washed twice with PBS and fixed with 4% PFA for 20 minutes. After washing with PBS three times, cells were permeabilized in PBS containing 0.3% Triton X-100 and incubated for 5 minutes. Next, cells were washed three times with PBS, blocked with PBS containing 10% goat serum for 1 hour at room temperature. Cells were incubated with the primary rabbit anti-Piezo1 antibody (Proteintech) at a dilution of 1:100 overnight at 4ºC. After washing with PBS three times, cells were incubated with the secondary FITC-conjugated goat anti-rabbit IgG antibody (Sigma-Aldrich) at 1:500 at room temperature for 1 hour in dark. After washing with PBS and rinsing with water, cells were mounted with anti-fade mounting medium containing DAPI (Invitrogen). Fluorescent images were captured using an EVOS® Cell Imaging System (ThermoFisher Scientific) or Zeiss LSM880 confocal microscope and ZEN software, and analyzed using ImageJ.

2.2.4 Measurement of intracellular Ca^{2+} concentration

The intracellular Ca^{2+} level was measured using a FLEX-Station III plate reader (Molecular Devices). Cells were seeded at 40,000 cells per well in 96-well plates (SARSTEDT, Germany) and incubated for 24 hours. Cells were washed with Ca^{2+}-containing SBS (Table 2.2) and incubated with SBS containing 4 μM Fura-2/AM and 0.04% PA (Invitrogen) at 37ºC for 45 minutes in dark. Cells were washed with SBS twice and incubated for 30 minutes with 160 μl or 200 μl Ca^{2+}-containing or Ca^{2+}-free SBS (Table 2.2). A 96-well U-bottom compound plate (Greiner Bio-one) was prepared in advance with the correct layout, concentrations, and volumes of solutions (up to 200 μl each well), where ATP, ADP, BzATP and NF546 were used in experiments studying the effects of these purinergic agonists on the $[Ca^{2+}]_i$ and Yoda1 was used in experiments studying the role of the Piezo1 channel on the $[Ca^{2+}]_i$. The cell assay plate, the compound plate and pipette tips were loaded into the FLEX-Station machine, recordings were made using software Softmax Pro (Molecular Devices). In experiments studying the effects of PPADS and GsMTx4 on an agonist-induced increase in the $[Ca^{2+}]_i$, cells were treated for 30 minutes before addition of agonist. To test the effect of RR on Yoda1-induced increases

in the $[Ca^{2+}]_i$, cells were treated with RR for 5 minutes before addition of Yoda1. In experiments studying the effect of Yoda1 on cells transfected with siRNA, cells were exposed to 5 µM ionomycin at the end of recordings. The FLEX-Station machine uses tips to transfer compounds from the compound plate to designated wells in the cell assay plate during the recording; 40 µl or 50 µl compound at 5x working solutions was added to each well for cells bathed in a solution volume of 160 µl or 200 µl respectively. Intracellular Ca^{2+} levels were monitored by measuring the ratio of fluorescence intensity at emission of 510 nm that was alternatively excited by 340 nm and 380 nm (F340/F380). Data analysis was carried out using OriginPro 9.1. All agonists and antagonist stock solutions were diluted in the SBS to the final concentrations indicated in the figures and text.

2.2.5 Trans-well cell migration assay

Cell migration was examined in the trans-well assay, using Falcon® inserts with a pore size of 8 µm. Cells were seeded at a density of 50,000 per insert in 200 µl DMEM culture medium with 2% FBS in the upper chamber. The lower chamber was loaded with 500 µl the same culture medium as the upper chamber. Test compounds including ATP, BzATP and NF546 were applied to the medium in the lower chamber at indicated concentrations to examine their effects on cell migration. In order to study the effect of PPADS on cell migration, cells were pre-treated for 30 minutes at 37ºC. PPADS was also added to the lower chamber and present throughout the experiment. After 24 hour incubation at 37ºC and 5% CO_2, the cells migrated onto the opposite side of the insert facing the lower chamber were stained with Hoechst 33342 (5 ng/ml) for 30 minutes at 37ºC. Afterwards, migrated cells were fixed in 500 µl 4% PFA for 30 minutes at room temperature. Inserts were rinsed with PBS and non-migrated cells were wiped off by using a cotton pad. After the insert surface being dry, images were taken with a fluorescent microscope EVOS® system using transmitted light and blue fluorescence (390-400 nm). The number of migrated cells in 5 randomly chosen areas were counted using ImageJ. Cell migration was presented by expressing the migrated cell number under test conditions as % of that under control conditions.

2.2.6 Wound healing assay

Cell migration was also examined using the wound healing assay. The wound was created by using an insert with two chambers (ibidi), placed in the middle of each well of 24-well plates. Cells were seeded at 20,000-25,000 cells per chamber and incubated for 12-16 hours. The insert was lifted up carefully, and cells were gently washed with D-PBS to remove the floating or loosely-attached cells. Fresh DMEM culture medium supplemented with 2% FBS without or with containing test compounds (Yoda1 and ATP) at indicated concentrations were added into each well. For the experiments testing the effect of an inhibitor, cells were pre-treated with the inhibitor at indicated concentrations (KN-93, CTC, PF431396, U0126, SB202190, apyrase and PPADS) for 30 minutes at 37ºC. Phase contrast images were captured using an EVOS® system at 0, 24, 48 and 72 hours. The wound area was obtained by measuring the wound edge using TScratch software, and the wound narrowing area was derived from the difference between the initial wound width and the wound width.

2.2.7 Transfection with siRNA

Cells were seeded at 40,000 cells per well in 96-well plates and 24-well plates for FLEX-Station recording and wound healing assay, respectively, or at 80,000 cells per well in 6-well plates for real-time RT-PCR. After 24 hours, cells were transfected with 30 nM siRNA targeting the Piezo1 gene (siPiezo1) (Ambion) or siControl (siCTL). Two siCTL were used, siControl#1 from Ambion, and non-targeting control siRNA from Dharmacon. Table 2.4 summarizes the cell densities, siRNA and Lipofectamine® RNAiMAX used for transfections. For Ca^{2+} imaging experiments, 3 µl 20 µM siRNA and 10 µl Lipofectamine® RNAiMAX were separately diluted in 400 µl Opti-MEM medium. For wound healing assay, 3 µl 20 µM siRNA and 6 µl Lipofectamine® RNAiMAX were separately diluted in 400 µl Opti-MEM medium. For real-time RT-PCR experiments, 3 µl 20 µM siRNA and 15 µl Lipofectamine® RNAiMAX were separately diluted in 400 µl Opti-MEM medium. Diluted siRNA duplex and diluted Lipofectamine® RNAiMAX were mixed and incubated for 20 minutes at room temperature and supplemented with 1.2 ml basal medium, without antibiotics (penicillin and streptomycin), to make the final volume of transfection medium to be approximately 2 ml. Cells in each well were covered with the transfection medium

with the volume shown in Table 2.4 and incubated at 37ºC. After incubation for 6 hours, the transfection medium was replaced with a fresh basal medium. Cells were used for measurements of the $[Ca^{2+}]_i$ after 24 hours, wound healing assays after 48 hours, and real-time RT-PCR after 72 hours, post-transfection. The difference in Piezo1 mRNA expression in cells transfected with siPiezo1 relative to that in cells transfected with siCTL was calculated using the $2^{-\Delta\Delta Ct}$ method, where $\Delta\Delta C_t = [(Ct_{Piezo1} - Ct_{\beta\text{-actin}})_{siPiezo1} - (Ct_{Piezo1} - Ct_{\beta\text{-actin}})_{siCTL}]$ (Livak and Schmittgen, 2001).

Table 2.4 Cell density, siRNA and Lipofectamine® RNAiMAX used for transfections

	Cells/well	20 µM siRNA (µl)	Lipofectamine® RNAiMAX (µl)	Transfection medium/well (µl)
96-well plate	40,000	0.15	0.5	100
24-well plate	40,000	0.75	1.5	500
6-well plate	80,000	1.5	7.5	1000

2.2.8 Adipogenic differentiation

Cells were plated into 24-well or 6-well plates with 40,000 and 80,000 cells per well, respectively and maintained in a basal medium until ~70-80% confluency. To induce adipogenic differentiation, the basal medium was replaced with adipogenic differentiation inducing medium. In some experiments, cells were also treated with 30 µM ATP. In experiments determining the effects of the downstream Ca^{2+}-dependent signalling pathways on ATP-induced stimulation of cell migration, cells were pre-treated with PF431396 and KN-93 for 30 minutes at 37ºC before applying ATP. Cells were incubated for 21 days, during which the medium was replaced every 3-4 days. After 21 days, oil red O staining was carried out, as described in the next section. Real-time RT-PCR was also carried out, as described above in section 2.2.3, to study the expression of P2Y1, P2Y2, P2Y11 and P2X7 receptors before and after adipogenic differentiation.

2.2.9 Oil red O staining assay

The oil red O staining assay was conducted to detect the formation of fat droplets, an indicator of adipogenic differentiation, as described in a previous study (Perry et al., 2008). After incubated for three weeks in basal or adipogenic differentiation inducing media as described in section 2.2.8, cells were washed with PBS and fixed with 4% PFA at room temperature for 30 minutes. Then, cells were rinsed twice with distilled water and incubated with 60% isopropanol at room temperature for 5 minutes. After isopropanol was removed, cells were stained with 0.3% oil red O (Table 2.2) for 15 minutes. Next, cells were rinsed extensively with distilled water to remove the staining solution and further stained with Hoechst 33342 at a final concentration of 5 µg/ml for 30 minutes in dark. Fat droplet staining in red and Hoechst 33342 staining in blue were captured using an EVOS® system using red fluorescence channel (586-615 nm) and blue fluorescence channel (390-400 nm), respectively. Images were analyzed using ImageJ. Adipogenic differentiation was determined by quantitating the fat droplets using the following protocols adapted from a previous study (Basseri et al., 2009). Cells in each well were distained by incubating with 100 µl isopropanol and rotating at room temperature for 15 minutes to remove oil red O from the fat droplets. The isopropanol solutions were transferred into a clear, flat bottom 96-well plate (Greiner Bio-One) and the oil red O content was determined by a VersaMax Microplate Reader (Varioskan™) at the wavelength of 510 nm (OD_{510}). The distained cells were washed with distilled water and collected for DNA content determination, as described below.

2.2.10 DNA content determination

Cells were washed with PBS and 200 µl PBS containing 0.01% (v:v) Triton X-100 was added into each wall. Cells were collected using a cell scraper and transferred into Eppendorf tubes and frozen at -20ºC until required or lysed immediately by freezing-thawing cycles. Collected cells were subjected to four cycles of freezing-thawing procedures, where samples were rapidly frozen by immersion in liquid nitrogen for 3 minutes and then thawed at 90°C water bath for 3 minutes. Cell lysates were collected by centrifugation at 10,000 *g* for 15 minutes and cellular debris were discarded. Samples were stored at -20°C or used immediately for Picogreen DNA quantification assay. For each

condition, 20 µl lysate was transferred into 8 wells in a flat, clear bottom 96-well plate (Greiner Bio-One). For each well, 80 µl TE buffer (Table 2.2) was added to make up a total volume of 100 µl. The DNA standard solutions (Life technologies) were prepared at 0, 25, 50, 100, 200, 300, 400, 500 ng/ml and 100 µl was transferred into the 96-well plate with 3 wells for each concentration. Then, an equivalent volume (100 µl) of Picogreen (Life technologies), diluted at 1:200 in TE buffer, was added into each well and incubated for 5 minutes in dark. The fluorescence was measured using a micro-plate reader (Varioskan™) with the excitation wavelength of 480 nm and the emission wavelength of 520 nm. The DNA content (ng/ml) was determined, based on the DNA standard curve that showed a linear relationship between the absorption values and DNA concentration ($R^2 \sim 0.99$). The Adipogenic differentiation was expressed by the OD_{510} value (oil red O content from the same well) per ng/ml DNA in each sample.

2.3 Data analysis

All data are presented as mean ± standard error of mean (S.E.M.), where appropriately, with n indicating the number of independent experiments and N indicating the number of cells or wells of cells from all preparations. Statistical analysis was performed by using OriginPro 9.1 software, and unpaired Student's t-test was used for comparisons between two groups and one-way ANOVA followed by Fisher's post *hoc test* was used for comparisons among multiple groups, with $p < 0.05$ being indicative of significance.

CHAPTER 3

Ca^{2+}-dependent downstream signalling mechanisms in ATP-induced stimulation of hDP-MSC migration

3.1 Introduction

A previous study reported that extracellular ATP enhanced hBM-MSC migration under *in vitro* condition and their *in vivo* homing capability to the bone marrow of immune-deficient mice (Ferrari et al., 2011). Our recent study provides evidence to support that ATP-induced activation of the P2X7, P2Y1 and P2Y11 receptors and subsequent increases in the $[Ca^{2+}]_i$ regulate the migration of hDP-MSC (Peng et al., 2016). There is also evidence to show that Ca^{2+} release from ER and subsequent SOC entry are also involved in inducing cell migration in rBM-MSCs and hDP-MSCs (Tang et al., 2012; Peng et al., 2016).

As discussed in section 1.8 and summarized in Figure 1.6 in the Introduction chapter, previous studies have gathered a large body of evidence to show that activation of PKC, PYK2 and CaMKII, and the MAPKs as downstream signalling pathways are important in mediating Ca^{2+} signalling regulation of cell migration. However, the knowledge regarding the roles of these signalling pathways in the regulation of MSC migration is increasing. For example, it was shown that inhibition of CaMKII by KN-93 prevented LPA-induced activation of the LPAR-$G_{\alpha,q/11}$-IP_3R-Ca^{2+} release signalling pathway and stimulation of hBM-MSC migration (Song et al., 2010). Consistently, another study reported that inhibition of Ca^{2+}/CaMKII by KN-93 suppressed hBM-MSC migration (Shin et al., 2008). ACh-induced an increase in the $[Ca^{2+}]_i$ and subsequent activation of PKC led to stimulation of rBM-MSC migration (Tang et al., 2012). Recent studies have also shown that PKC activation is critical in mediating IL-1β (Lin et al., 2015), LPA (Ryu and Han, 2015) and netrin-1 (Lee et al., 2014) induced an increase in hUC-MSC migration. Moreover, PMA-induced activation of PKC resulted in increased cell migration of rBM-MSCs (Song et al., 2013). There is also evidence to show significant involvement of MEK/ERK in hUC-MSC migration induced by stromal cell-derived factor-1 (Ryu et al.,

2010b), netrin-1 (Lee et al., 2014) and IL-1β (Lin et al., 2015) and rBM-MSC migration stimulated by ACh (Tang et al., 2012). It was also shown that p38 MAPK mediates hUC-MSC migration induced by stromal cell-derived factor-1 (Ryu et al., 2010b) and arachidonic acid (Oh et al., 2015), hBM-MSC migration induced by high mobility group box 1 (Lin et al., 2016) and rBM-MSC migration induced by tumor necrosis factor-α (TNF-α) (Fu et al., 2009). Moreover, an important role of p38 MAPK signalling pathway has been reported to mediate shear stress-induced stimulation of hBM-MSC migration (Yuan et al., 2012; Yuan et al., 2013). As mentioned earlier, our recent study has shown that ATP-induced Ca^{2+} signalling is critical in stimulating hDP-MSC migration (Peng et al., 2016). Therefore, the study presented in this chapter aimed to confirm our recent findings that ATP stimulates hDP-MSC migration and then investigate the role of PKC, PYK2, CaMKII and MAPKs as Ca^{2+}-dependent downstream signalling mechanisms in mediating ATP-induced stimulation of hDP-MSC migration.

3.2 Results

3.2.1 Effect of ATP on cell migration

Our recent study has demonstrated, using the wound healing assay, that exposure to ATP promotes hDP-MSC migration (Peng et al., 2016). The present study confirmed and extended this finding using trans-well migration and wound healing assays to analyze the effect of ATP on hDP-MSCs. In trans-well migration assay, exposure to 30 μM ATP induced an increase in cell migration in hDP-MSCs from 9F (Figure 3.1A and B). Similar results were obtained in cells from 20M (Figure 3.1C) and 22M (Figure 3.1D). Figure 3.1E summarizes the mean data from 9 independent experiments using all three donors, showing a statistically significant increase in cell migration in the presence of ATP. In the wound healing assay, cell migration was faster after exposure of hDP-MSCs from 9F to 30 μM ATP for 24, 48 and 72 hours (Figure 3.2A and B). Similar results were observed in cells from 22M (Figure 3.2C). Figure 3.2D summarizes the mean data from 10 independent experiments, as percentage of that under control conditions at the same time points in parallel experiments (Figure 3.2D). These results from both assays provide consistent evidence to support that ATP significantly stimulates cell migration in hDP-MSCs as reported from our recent study (Peng et al., 2016).

3.2.2 Effect of PPADS on ATP-induced cell migration

Our recent study shows that prior treatment with 30 μM PPADS resulted in inhibition of ATP-induced stimulation of migration of hDP-MSCs (Peng et al., 2016). Such results have been confirmed in the present study, using trans-well migration (Figure 3.3) and wound healing assay (Figure 3.4). Similar results were obtained in trans-well assay using cells from 9F (Figure 3.3A and B) and 22M (Figure 3.3C) and analysis of the mean data from 3 independent experiments shows that treatment with 30 μM PPADS completely prevented ATP-induced increase in cell migration (Figure 3.3D). Likewise, wound healing assay showed that pretreatment of hDP-MSCs from 22M with 30 μM PPADS abolished ATP-induced stimulation cell migration (Figure 3.4). However, parallel experiments using hDP-MSCs from 9F and 22M revealed that treatment with 30 μM PPADS in the absence of ATP was without significant effect on cell migration (Figure 3.5). Similarly, there was no effect of treatment with PPADS alone in wound healing assay using hDP-MSCs from 22M (Figure 3.6). These results provide clear evidence to support that ATP enhances cell migration in hDP-MSCs via the P2 receptor, consistent with our recent study (Peng et al., 2016).

3.2.3 Effects of BzATP and NF546 on cell migration

Experiments were performed to examine the effect of exposure to BzATP and NF546 on hDP-MSC migration using the trans-well assay. As introduced above (sections 1.2.2 and 1.2.3), BzATP is more potent than ATP at the P2X7 receptor and can also act as an agonist at the P2Y1 and P2Y11 receptors, and NF546 is a selective agonist for the P2Y11 receptor. Figure 3.7A shows that exposure to 30 μM BzATP increased cell migration of hDP-MSCs from 9F (Figure 3.7A and B) and from 22M (Figure 3.7C). The mean data from 4 independent experiments using these two donors is shown in Figure 3.7D. Figure 3.8A and B show that exposure to 10 μM NF546 resulted in increased cell migration of hDP-MSCs from 22M. Similar results were obtained in cells from 9F (Figure 3.8C). The mean data from 3 independent experiments using the two donors shown is shown in Figure 3.8D. Taken together, these results show exposure to BzATP or NF546 significantly stimulates cell migration, providing further evidence to support the conclusion that the P2X7, P2Y1

and P2Y11 receptors participate is mediated in ATP-induced increase in cell migration in hDP-MSCs (Peng et al., 2016).

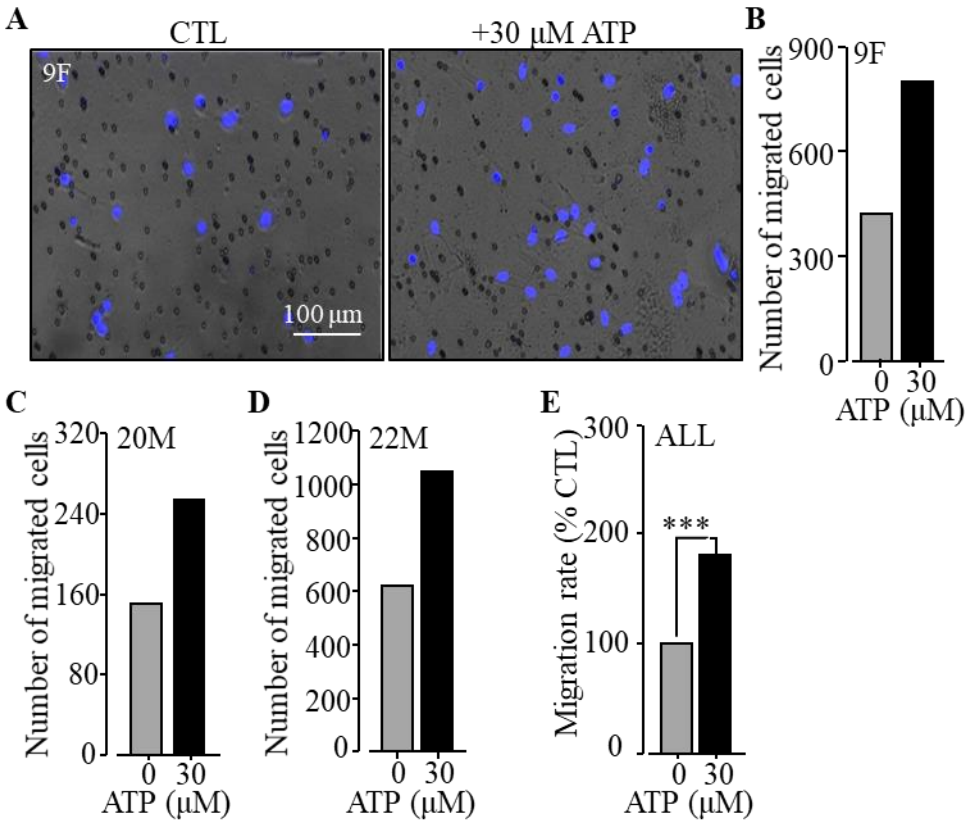

Figure 3.1 ATP increases hDP-MSC migration in trans-well migration assay.
(A) Representative images of trans-well migration assay showing migration of cells from 9F after being stained with Hoechst 33342 in the absence of (CTL) and presence of 30 μM ATP in the culture medium. (B-D) Quantitative analysis of the number of migrated cells in 5 random fields from the following donors: 9F (N = 2 wells) (B), 20M (N = 2 wells) (C), 22M (N = 2 wells) (D) in 1 set of experiment. (E) Summary of the cell migration rate by expressing the migrated cell number as percentage of that under control conditions from 9 independent experiments using cells from 9F, 20M and 22M. ***, $p < 0.001$ compared to control cells.

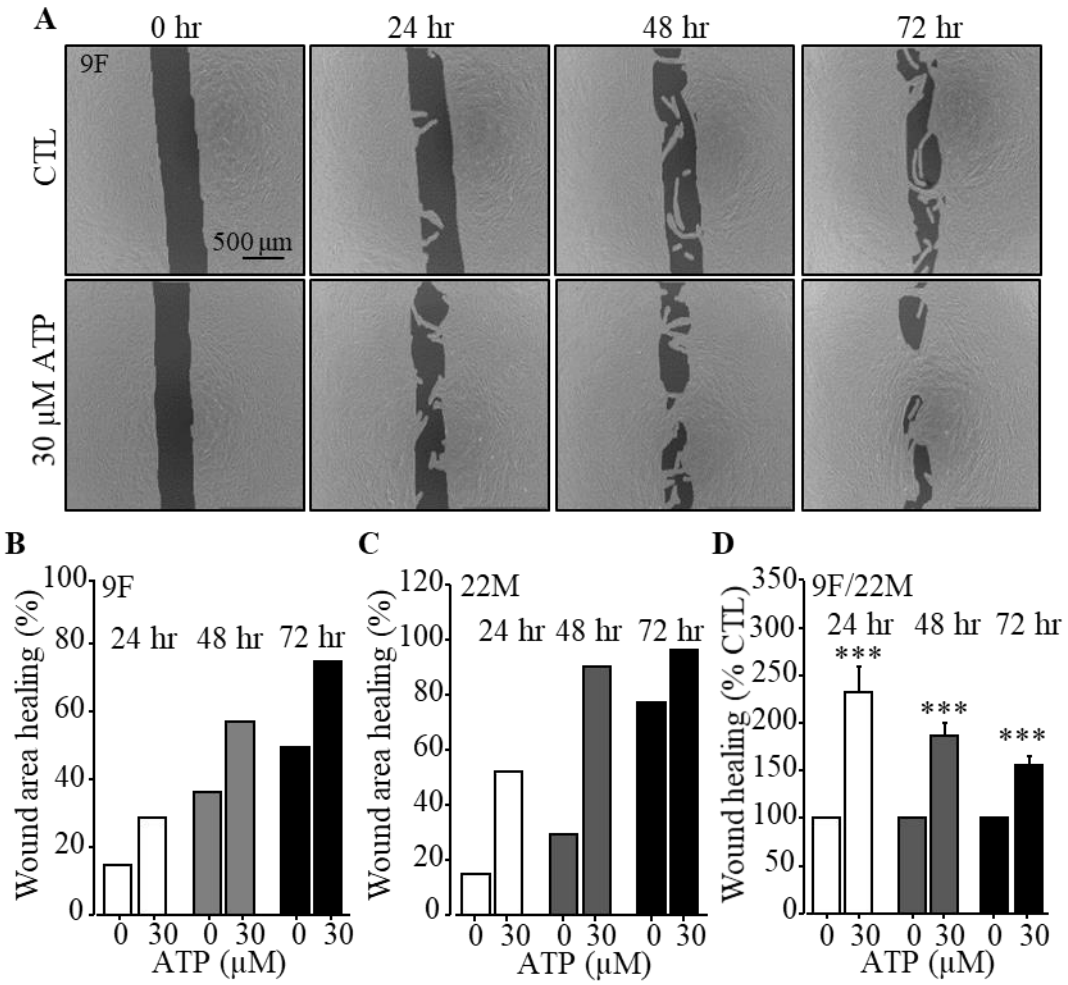

Figure 3.2 ATP increases hDP-MSC migration in wound healing assay.
(A) Representative images of wound healing assay showing the wound areas at 0, 24, 48 and 72 hours, using cells from donor 9F in the absence of (CTL) and presence of 30 µM ATP in the culture medium. (B, C) Quantitative analysis of wound area healing using cells from 9F (N = 2 wells) (B) and 22M (N = 2 wells) (C) in 1 set of experiment. (D) Summary of the mean data with wound healing presented as percentage of that under control conditions at the same time points in parallel experiments, from 10 independent experiments using cells from 9F and 22M. ***, $p < 0.001$ compared to control cells.

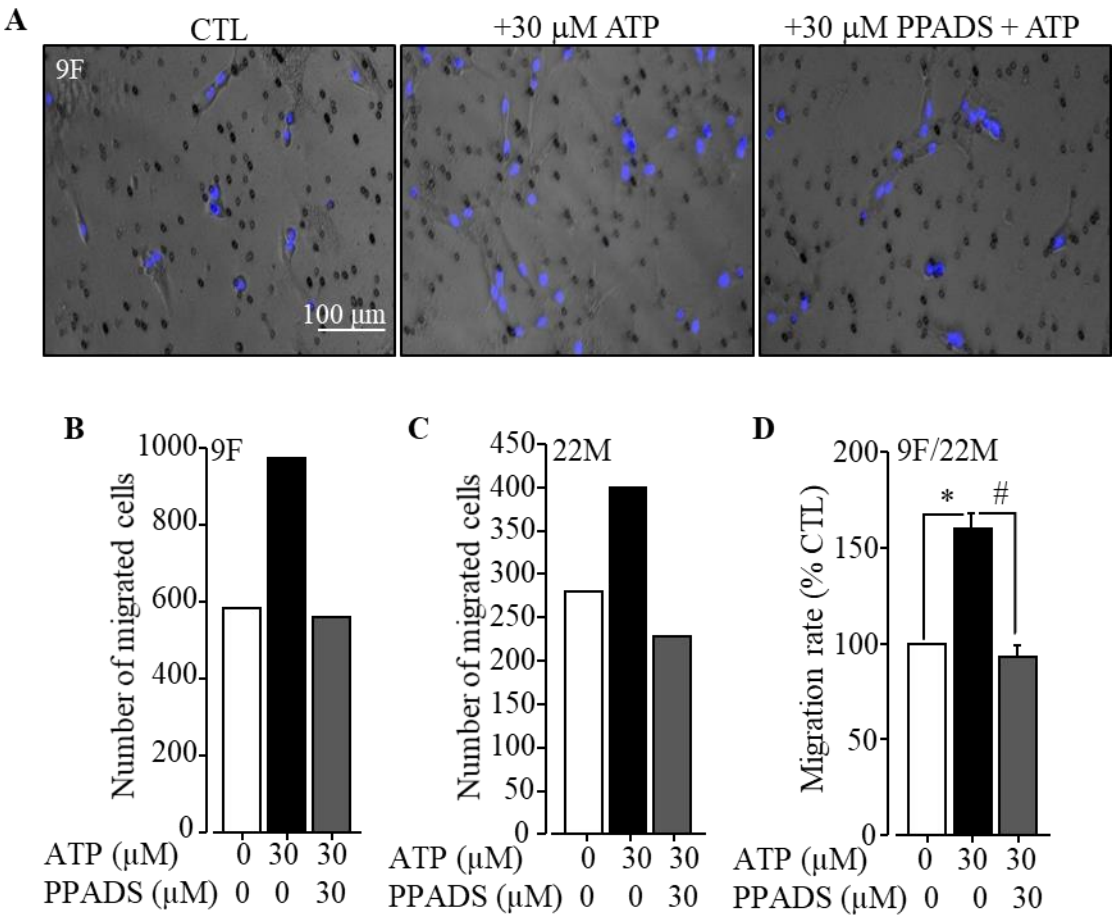

Figure 3.3 Inhibition of ATP-induced hDP-MSC migration by PPADS in trans-well migration assay.

(A) Representative images of trans-well migration assay showing migration of cells from 9F after being stained with Hoechst 33342 in the absence of (CTL) and presence of 30 μM ATP in the culture medium, without or with treatment with 30 μM PPADS before and during exposure to ATP. (B-C) Quantitative analysis of the number of migrated cells in 5 random fields from 9F (N = 2 wells) (B) and 22M (N = 2 wells) (C) in 1 set of experiment. (D) Summary of the cell migration rate by expressing the migrated cell number as percentage of that under control conditions from 3 independent experiments using cells from 9F and 22M. *, $p < 0.05$ compared to control cells. #, $p < 0.05$ compared to cells treated with ATP alone.

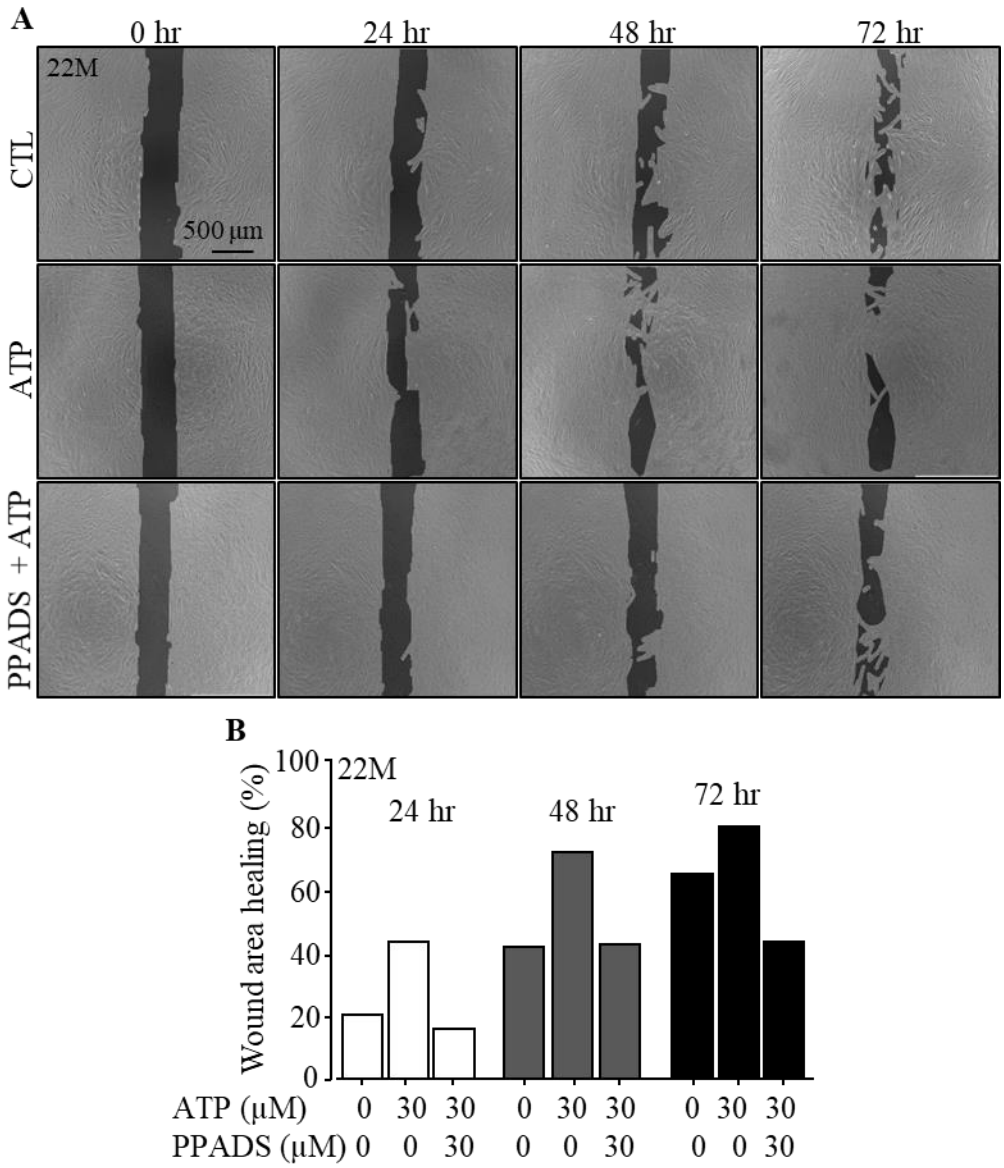

Figure 3.4 Inhibition of ATP-induced hDP-MSC migration by PPADS in wound healing assay.

(A) Representative images of wound healing assay showing wound areas at 0, 24, 48 and 72 hours, using cells from 22M in the absence of (CTL) and presence of 30 µM ATP in the culture medium without or with treatment with 30 µM PPADS before and during exposure to ATP. (B) Quantitative analysis of wound area healing from 2 wells in 1 set of experiment using cells from 22M.

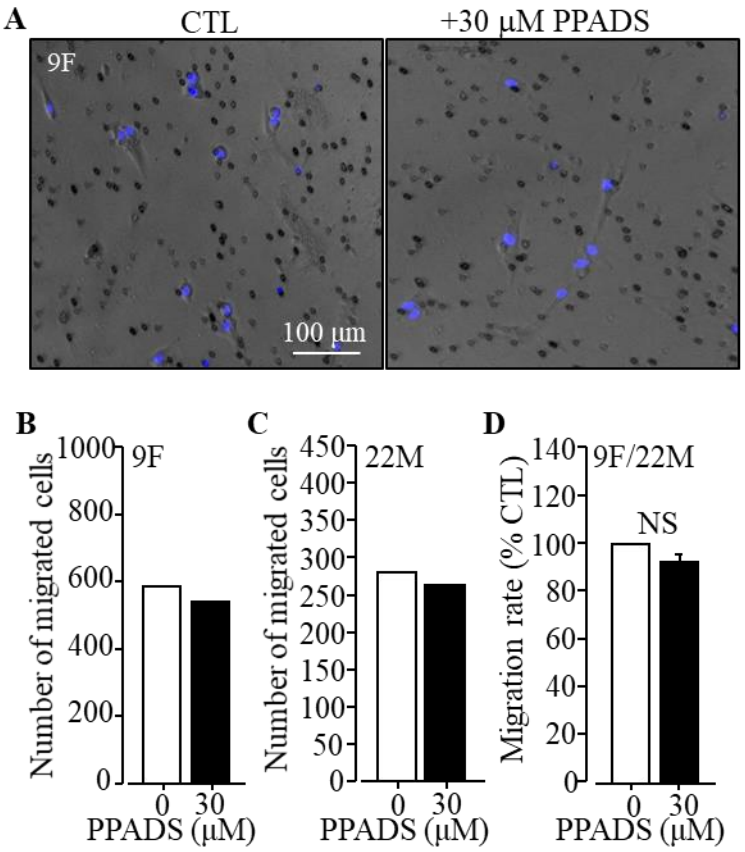

Figure 3.5 No effect of PPADS on hDP-MSC migration in trans-well migration assay. (A) Representative images of trans-well migration assay showing migration of cells from 9F stained with Hoechst 33342 in the absence of (CTL) and presence of 30 μM PPADS in the culture medium. (B, C) Quantitative analysis of the number of migrated cells in 5 random fields from 9F (N = 2 wells) (B) and 22M (N = 2 wells) (C) in 1 set of experiments. (D) Summary of the cell migration rate by expressing the migrated cell number as percentage of that under control conditions from 3 independent experiments using cells from 9F and 22M. NS, no significant difference.

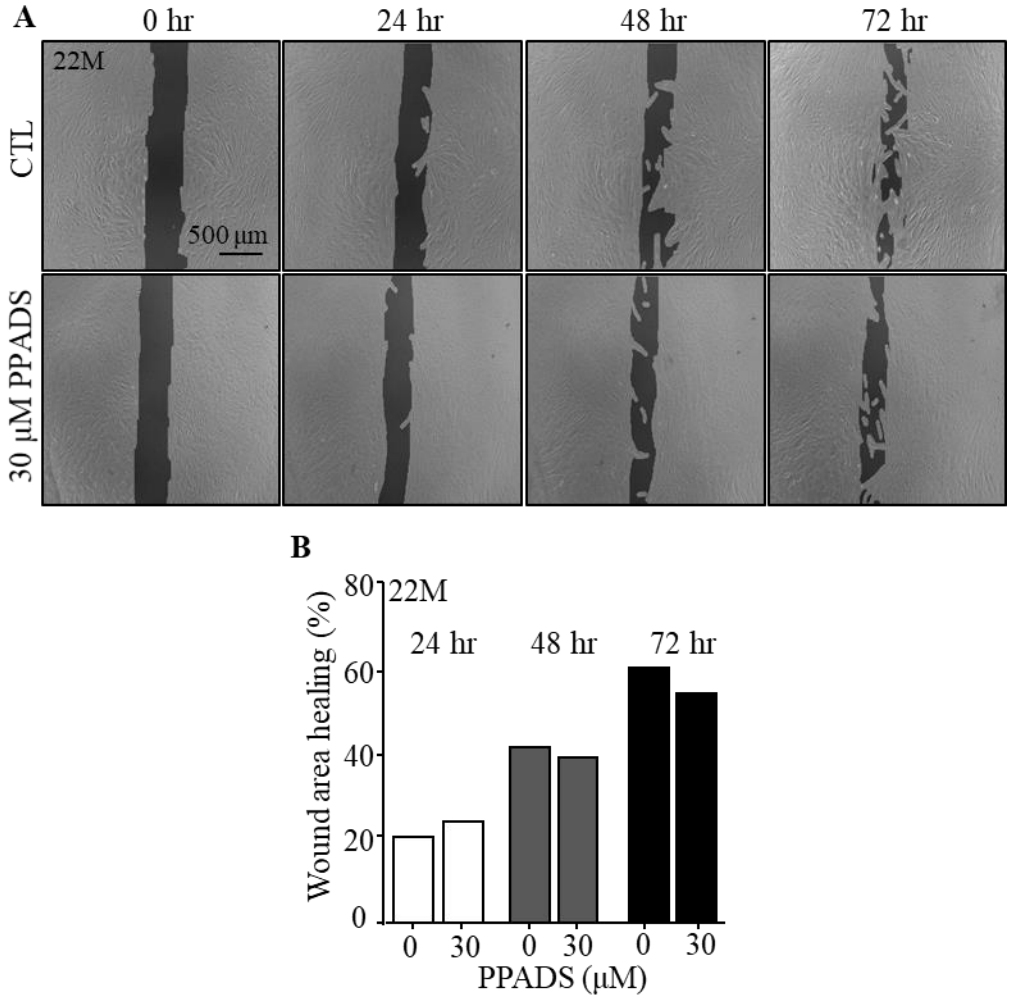

Figure 3.6 No effect of PPADS on hDP-MSC migration in wound healing assay.
(A) Representative images of wound healing assay showing wound areas at 0, 24, 48 and 72 hours, using cells from 22M in the absence of (CTL) and presence of 30 µM PPADS in the culture medium. (B) Quantitative analysis of wound area healing from 2 wells in 1 set of experiment using hDP-MSCs from 22M.

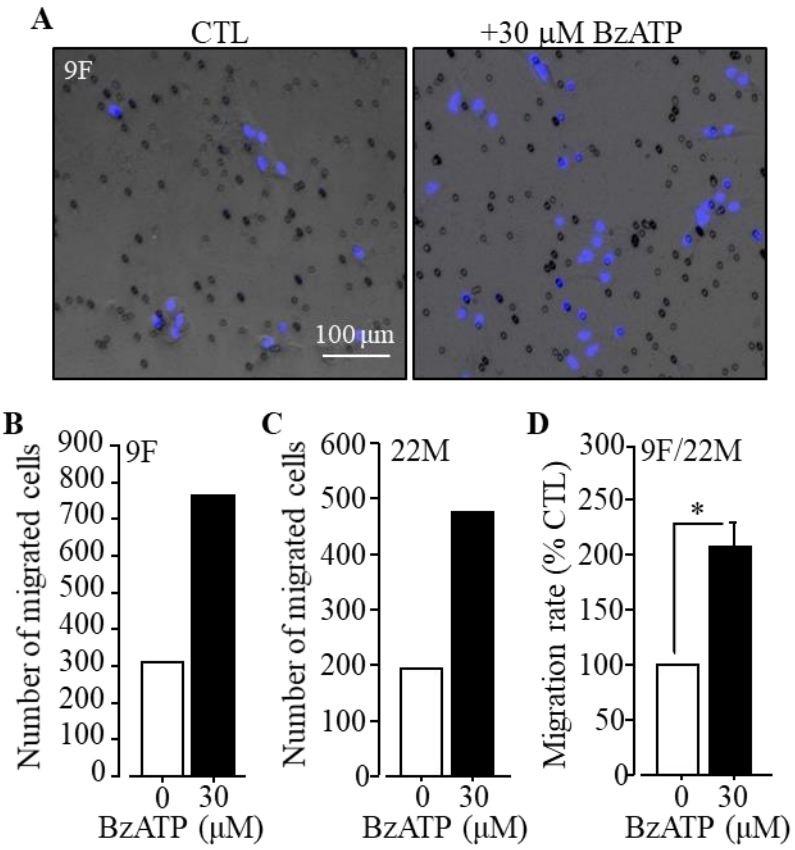

Figure 3.7 BzATP stimulates hDP-MSC migration in trans-well migration assay.
(A) Representative images of trans-well migration assay showing migration of cells from 9F stained with Hoechst 33342 in the absence of (CTL) and presence of 30 μM BzATP in the culture medium. (B, C) Quantitative analysis of the number of migrated cells in 5 random fields from 9F (N = 2 wells) (B) and 22M (N = 2 wells) (C) in 1 set of experiment. (D) Summary of the cell migration rate by expressing the migrated cell number as percentage of that under control conditions from 4 independent experiments using cells from 9F and 22M. *, $p < 0.05$ compared to control cells.

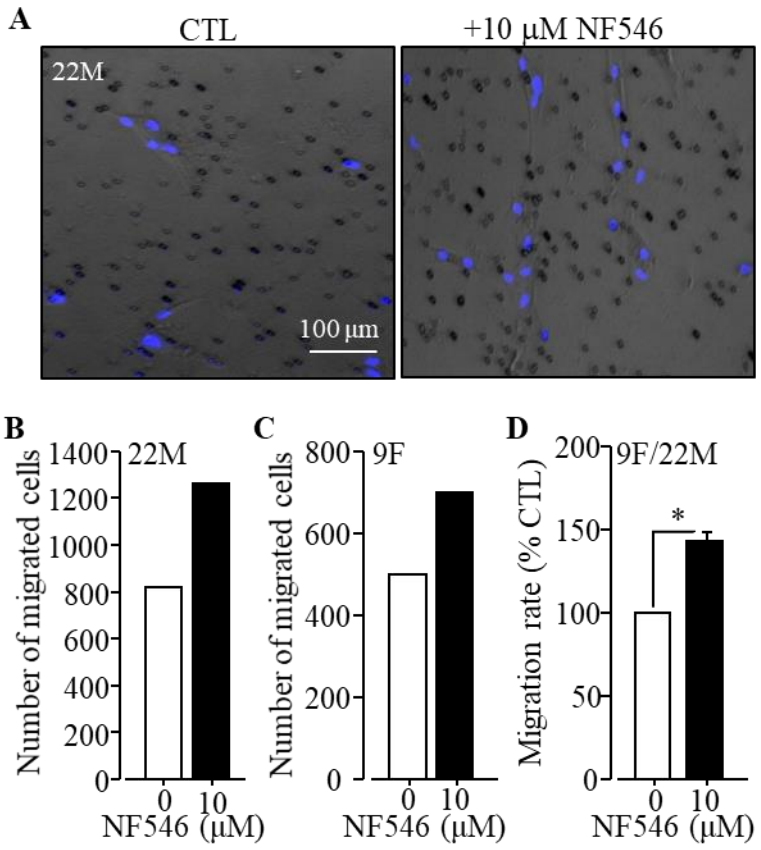

Figure 3.8 NF546 stimulates hDP-MSC migration in trans-well migration assay.
(A) Representative images of trans-well migration assay showing migration of cells from 22M stained with Hoechst 33342 in the absence of (CTL) and presence of 10 μM NF546 in the culture medium. (B, C) Quantitative analysis of the number of migrated cells in 5 random fields from 22M (N = 2 wells) (B) and 9F (N = 2 wells) (C) in 1 set of experiment. (D) Summary of the cell migration rate by expressing the migrated cell number as percentage of that under control conditions from 3 independent experiments using cells from 22M and 9F. *, $p < 0.05$ compared to control cells.

3.2.4 Effect of CaMKII inhibitor KN-93 on ATP-induced cell migration

Next, I investigated the role of CaMKII in mediating ATP-induced hDP-MSC migration by examining the effect of treatment with KN-93, a CaMKII inhibitor, on ATP-induced cell migration. Treatment with 0.3 μM KN-93, prior to and during exposure to 30 μM ATP, reduced ATP-induced cell migration in hDP-MSCs from 9F assessed using the wound healing assay at 24, 48 and 72 hours (Figure 3.9A-B). Similar results were obtained in cells from 22M (Figure 3.9C). Figure 3.9D summarizes the mean results from 6 independent experiments in hDP-MSCs from these two donors and shows that KN-93 strongly reduced ATP-induced cell migration. Treatment with KN-93 alone in the absence of ATP showed no inhibition of cell migration in cells from 22M (Figure 3.9E) and 32F. Collectively, these results suggest an important role for CaMKII in ATP-induced stimulation of hDP-MSC migration.

3.2.5 Effect of PKC inhibitor chelerythrine chloride in ATP-induced cell migration

To determine whether PKC is a downstream signalling molecule in ATP-induced cell migration in hDP-MSCs, I tested the effect of chelerythrine chloride (CTC), a PKC inhibitor, on ATP-induced hDP-MSC migration. As shown in Figure 3.10A, treatment with 1 μM CTC, prior to and during exposure to 30 μM ATP, suppressed ATP-induced increase in cell migration (Figure 3.10A and B) at 24, 48 and 72 hours. Figure 3.10C summarizes the mean results from 4 independent experiments in hDP-MSCs from 9F, and shows that treatment with CTC largely abolished ATP-induced an increase in cell migration. Treatment with 1 μM CTC alone showed no inhibition on cell migration in cells from 32F (Figure 3.10D). These results, therefore, provide evidence to suggest a critical engagement of PKC in ATP-induced stimulation of hDP-MSC migration.

3.2.6 Effect of PYK2 inhibitor PF431396 on ATP-induced cell migration

I also examined the role of PYK2 in mediating ATP-induced increase in hDP-MSC migration by performing wound healing assay of hDP-MSCs from 9F treated with 10 nM PF431396, a PYK2 inhibitor, prior to and during exposure to 30 μM ATP (Figure 3.11A and B). Figure 3.11C summarizes the mean results from 4 independent experiments in

hDP-MSCs from 9F and shows that PF431396 prevented ATP-induced increase in cell migration at 24, 48 and 72 hours. Treatment with 10 nM PF431396 alone showed no effect on cell migration in cells from 32F (Figure 3.11D). These results suggest that PYK2 can act as a Ca^{2+}-dependent signalling mechanism in ATP-induced stimulation of hDP-MSC migration.

3.2.7 Effect of MEK/ERK inhibitor U0126 in ATP-induced cell migration

The MEK/ERK signalling pathway was suggested to mediate endogenously released ATP-induced P2Y-mediated increase in the wound healing of *in vivo* ischemic model (Weihs et al., 2014). In this set of experiments, I examined the role of MEK/ERK signalling pathway in ATP-induced increase in hDP-MSC migration by determining the effect of treatment with U0126, an inhibitor of MEK that phosphorylates and thereby activate ERK (Hotokezaka et al., 2002). Treatment with 1 µM U0126, prior to and during exposure to 30 µM ATP, suppressed ATP-induced migration of hDP-MSCs from 9F at 24, 48 and 72 hours (Figure 3.12A and B). Figure 3.12C summarizes the mean results from 6 independent experiments in hDP-MSCs from 9F and shows that treatment with U0126 significantly reduced ATP-induced increase in cell migration. Treatment with 1 µM U0126 alone tested in cells from 32F was without effect on cell migration (Figure 3.12D). These results, therefore, provide evidence to suggest that the MEK/ERK signalling pathway plays an important role in ATP -induced increase in hDP-MSC migration.

3.2.8 Effect of p38 kinase inhibitor SB202190 on ATP-induced cell migration

Studies have reported that the p38 kinase MAPK signalling pathway plays a role in regulating cell functions of MSCs, including cell migration (Yuan et al., 2012; Yuan et al., 2013; Lin et al., 2016). Accordingly, it was interesting to examine whether the p38 signalling pathway was involved in ATP-induced stimulation of hDP-MSC migration. SB202190 is a selective and potent inhibitor of p38 kinase and treatment with 1 µM SB202190, prior to and during exposure to ATP, resulted in strong inhibition of hDP-MSC migration at 24, 48 and 72 hours (Figure 3.13A and B). Analysis of the mean results

from 3 independent experiments using hDP-MSCs from 9F shows inhibition by treatment with SB202190 at 24 and 48 hours reached a significant level (Figure 3.13C). Treatment with 1 μM SB303190 in the absence of ATP showed no inhibition on cell migration in cells from 32F (Figure 3.13D). These findings suggest that the p38 kinase signalling pathway can be involved in ATP-induced stimulation of hDP-MSC migration.

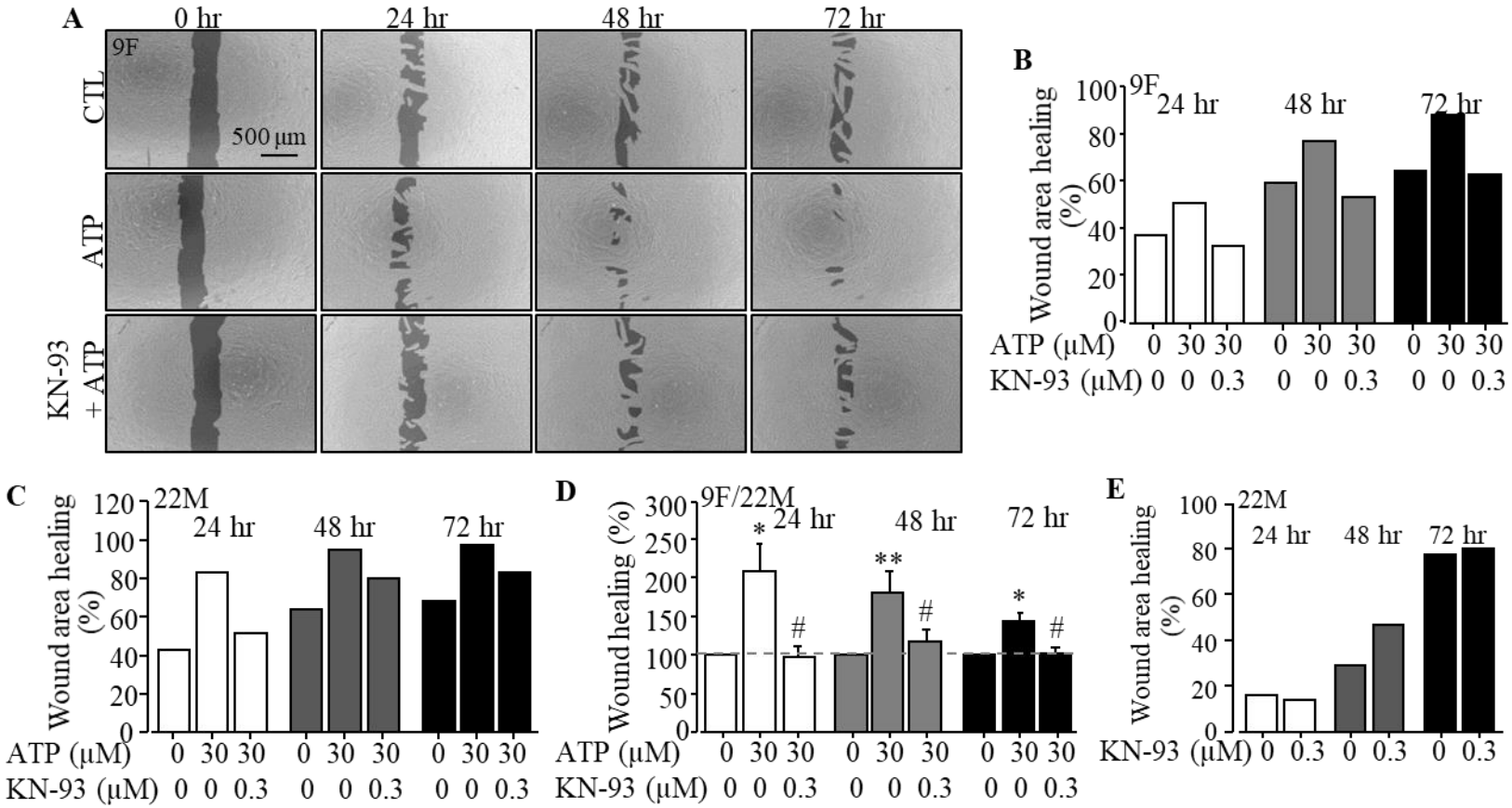

Figure 3.9 Inhibition of ATP-induced hDP-MSC migration by KN-93.

(A) Representative images showing wound areas at 24, 48 and 72 hours, using cells from 9F in the absence (CTL) and presence of 30 µM ATP without or with prior treatment with 0.3 µM KN-93. (B, C) Quantitative analysis of wound healing in cells from 9F (N = 2 wells) (B) and 22M (N = 2 wells) (C) in 1 set of experiment. (D) Summary of the mean wound healing, as percentage of that under control conditions at the same time points in parallel experiments, from 6 independent experiments using cells from 9F and 22M. (E) Quantitative analysis of wound healing from 2 wells in 1 set of experiment using cells from 22M in the absence of and presence of 0.3 µM KN-93 alone. *, $p < 0.05$; **, $p < 0.01$ compared to control cells. #, $p < 0.05$ compared to cells treated with ATP alone.

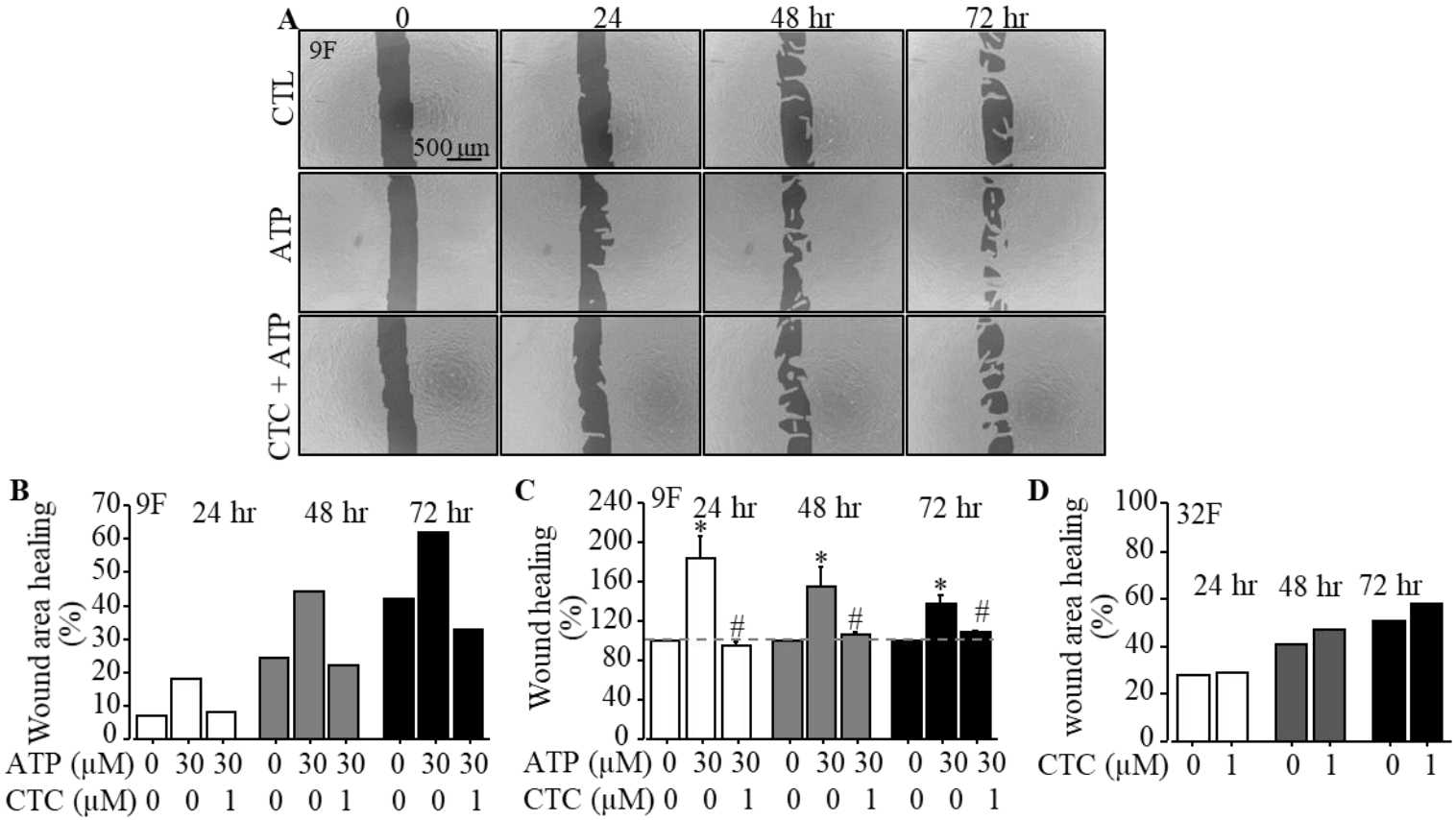

Figure 3.10 Inhibition of ATP-induced hDP-MSC migration by CTC.

(A) Representative images showing wound areas at 0, 24, 48 and 72 hours, using cells from 9F in the absence (CTL) and presence of 30 µM ATP without or with prior treatment with 1 µM chelerythrine chloride (CTC). (B) Quantitative analysis of wound area healing using cells from 9F (N = 2 wells) in 1 set of experiment. (C) Summary of the mean wound healing, as percentage of that under control conditions at the same time points in parallel experiments, from 4 independent experiments using cells from 9F. (D) Quantitative analysis of wound area healing from 2 wells in 1 set of experiment using cells from 32F in the absence and presence of 1 µM CTC alone. *, $p < 0.05$; **, $p < 0.01$ compared to control cells. #, $p < 0.05$ compared to cells treated with ATP alone.

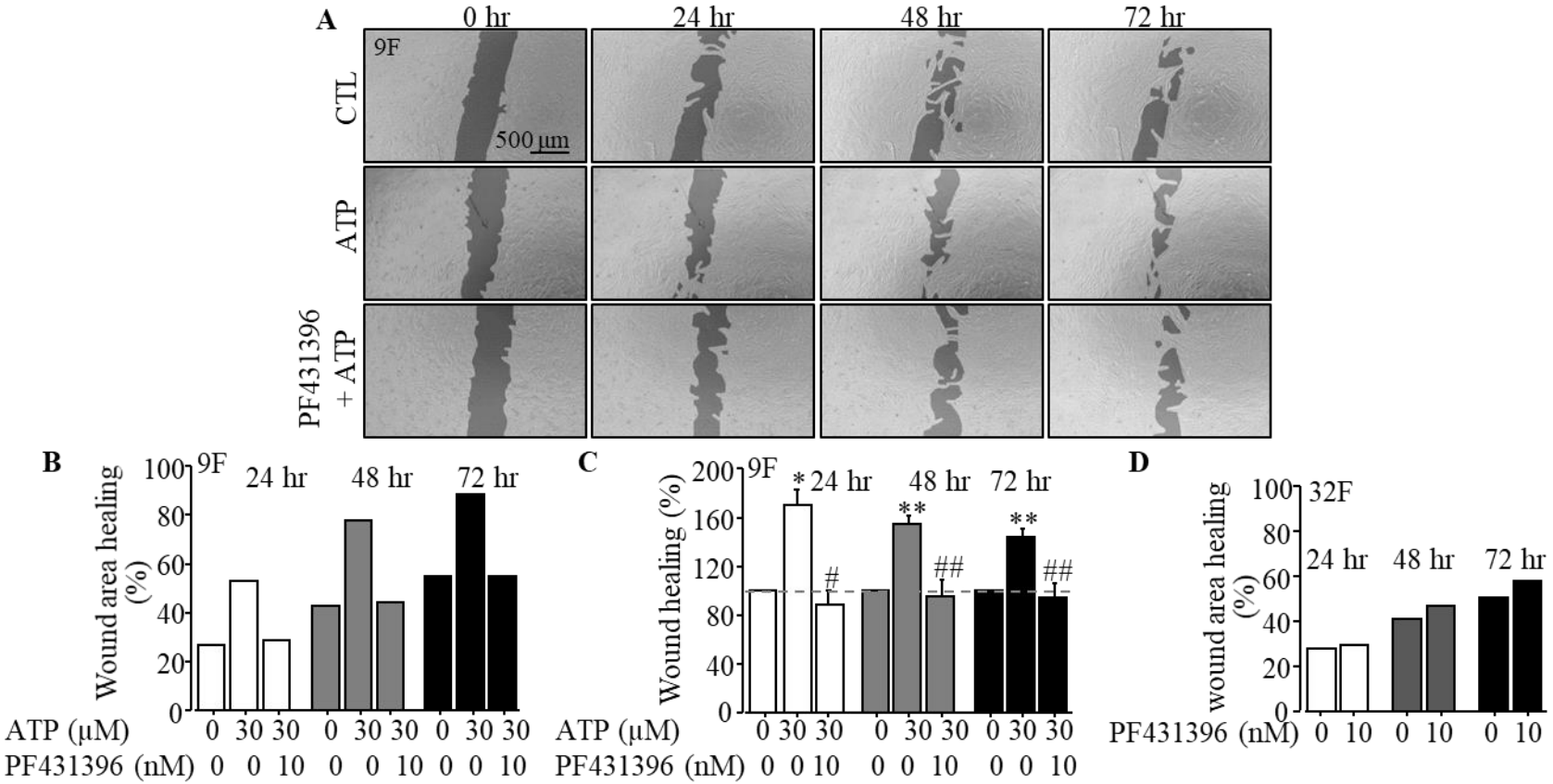

Figure 3.11 Inhibition of ATP-induced hDP-MSC migration by PF431396.

(A) Representative images showing wound areas at 0, 24, 48 and 72 hours, using cells from 9F in the absence (CTL) and presence of 30 µM ATP without or with prior treatment with 10 nM PF431396. (B) Quantitative analysis of wound area healing using cells from 9F (N = 2 wells) in 1 set of experiment. (C) Summary of the mean wound healing, as percentage of that under control conditions at the same time points in parallel experiments, from 4 independent experiments using cells from 9F. (D) Quantitative analysis of wound area healing from 2 wells in 1 set of experiment using hDP-MSCs from 32F in the absence and presence of 10 nM PF431396 alone in basal media. *, $p < 0.05$; **, $p < 0.01$ compared to control cells. #, $p < 0.05$; ##, $p < 0.01$ compared to cells treated with ATP alone.

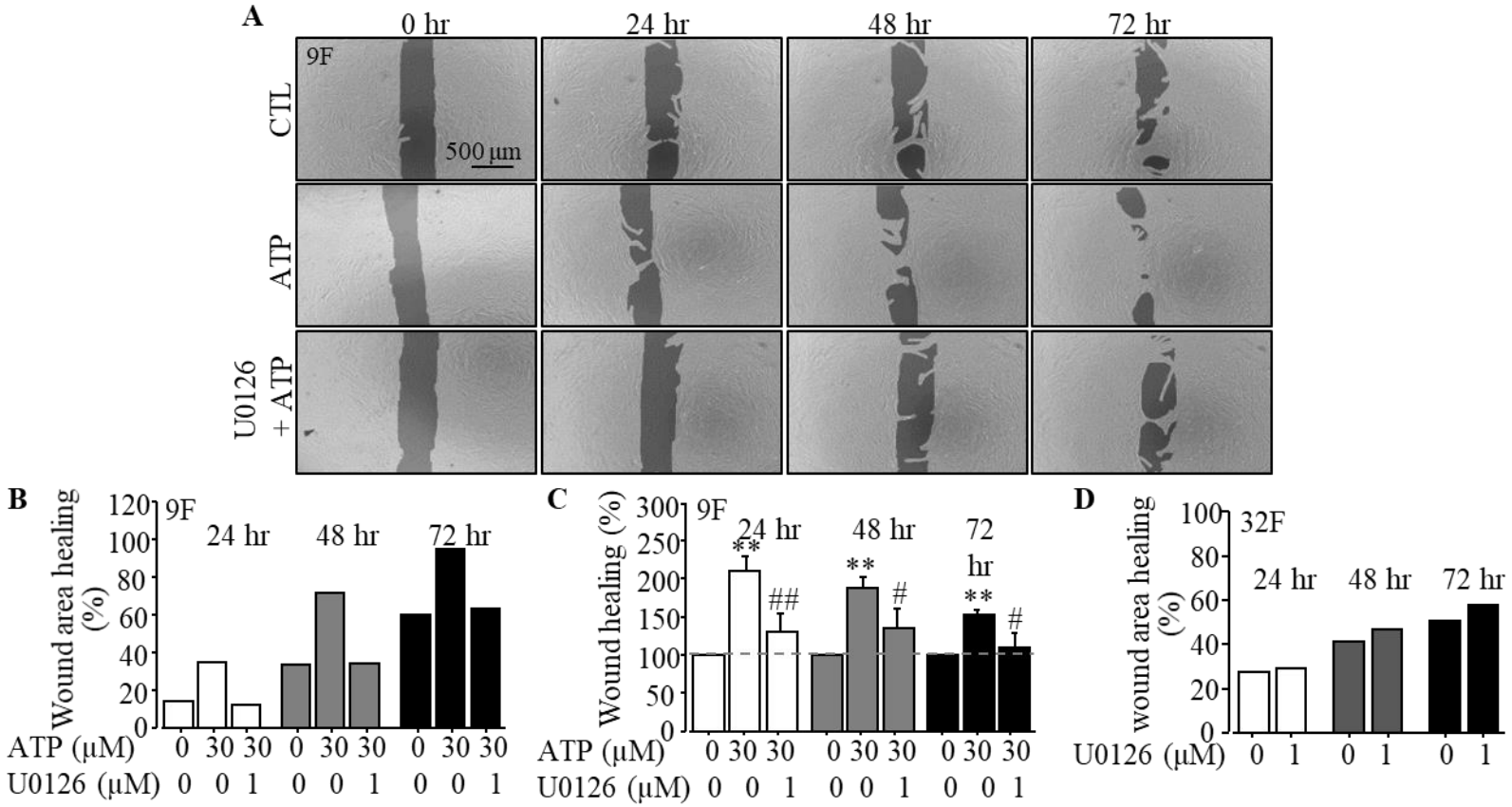

Figure 3.12 Inhibition of ATP-induced hDP-MSC migration by U0126.

(A) Representative images showing wound areas at 24, 48 and 72 hours, using cells from 9F in the absence (CTL) and presence of 30 µM ATP without or with prior treatment with 1 µM U0126. (B) Quantitative analysis of wound area healing using cells from 9F (N = 2 wells) in 1 set of experiment. (C) Summary of the mean wound healing, as % of that under control conditions at the same time points in parallel experiments, from 6 independent experiments using cells from 9F. (D) Quantitative analysis of wound area healing from 2 wells in 1 set of experiment using cells from 32F in the absence and presence 1 µM U0126 alone in the culture medium. **, $p < 0.01$ compared to the control without ATP. **, $p < 0.01$ compared to control cells. #, $p < 0.05$; ##, $p < 0.01$ compared to cells treated with ATP alone.

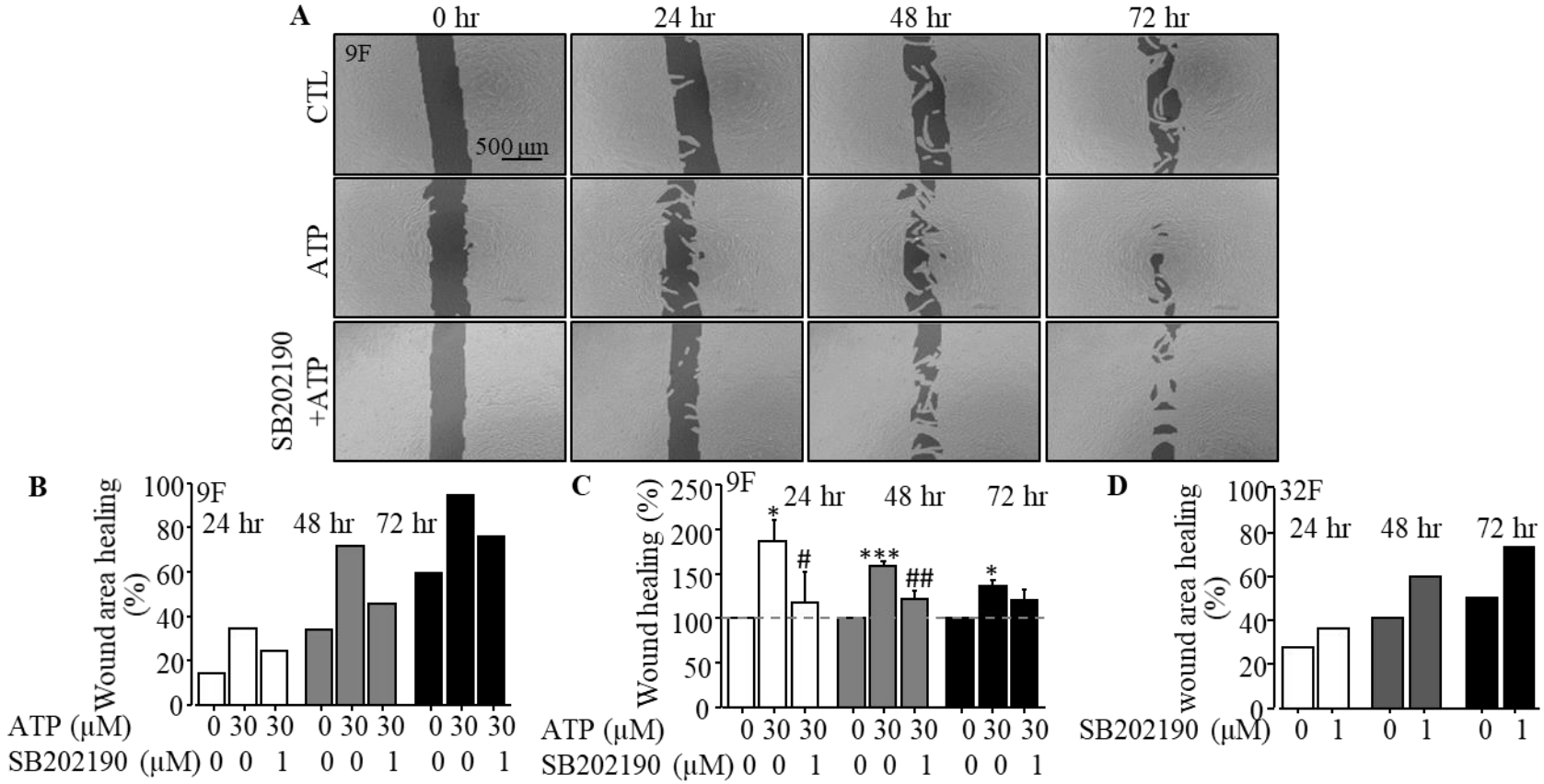

Figure 3.13 Inhibition of ATP-induced hDP-MSC migration by SB202190

(A) Representative images showing wound areas at 24, 48 and 72 hours, using cells from 9F in the absence (CTL) and presence of 30 µM ATP without or with prior treatment with 1 µM SB202190. (B) Quantitative analysis of wound area healing using hDP-MSCs from 9F (N = 2 wells) in 1 set of experiment. (C) Summary of the mean wound healing, as percentage of that under control conditions at the same time points in parallel experiments, from 3 independent experiments using hDP-MSCs from 9F. (D) Quantitative analysis of wound area healing from 2 wells in 1 set of experiment using hDP-MSCs from 32F in the absence and presence 1 µM SB202190 alone in the basal medium. *, $p < 0.05$; **, $p < 0.01$; compared to the control without ATP. #, $p < 0.05$; ##, $p < 0.01$ compared to ATP alone.

3.3 Discussion

The study presented in this chapter provides further evidence to support our recent findings that ATP stimulates cell migration in hDP-MSCs and the P2X7, P2Y1 and P2Y11 receptors are involved in mediating such ATP-induced effect on cell migration (Peng et al., 2016). Moreover, the study suggests that CaMKII, PYK2 and PKC and downstream MEK/ERK and p38 MAPK signalling pathways are engaged in mediating ATP-induced stimulation of cell migration in hDP-MSCs.

Our recent study demonstrates that ATP induces strong Ca^{2+} responses and the P2X7, P2Y1 and P2Y11 receptors are expressed in hDP-MSCs and mediate ATP-induced Ca^{2+} signalling, using FLEX-Station measurement, and further show that exposure to ATP stimulates cell migration and the P2X7, P2Y1 and P2Y11 receptors participate in mediating ATP-induced effect on cell migration, using wound healing assay (Peng et al., 2016). The present study showed that ATP stimulated hDP-MSC migration, using trans-well assay (Figure 3.1) as well as using wound healing assay (Figure 3.2). Furthermore, the present study using both cell migration assays demonstrated that treatment with PPADS prevented ATP-induced increase in cell migration (Figure 3.3 and Figure 3.4) without effect on cell migration in the absence of ATP (Figure 3.5 and Figure 3.6), indicating a critical role of the P2 receptors in mediating ATP-induced increase in cell migration. Our recent study has concluded that ATP stimulates hDP-MSC migration via activating the P2X7, P2Y1 and P2Y11 receptors (Peng et al., 2016). This conclusion is consistent with the observation in the present study that BzATP, which is known to activate the P2X7, P2Y1 and P2Y11 receptors (Communi et al., 1999; Burnstock, 2007; Ilatovskaya et al., 2013; Jacobson et al., 2015; von Kügelgen and Hoffmann, 2016), was effective in stimulating hDP-MSC migration (Figure 3.7). The present study further demonstrated activation of the P2Y11 receptor with NF546 stimulated hDP-MSC migration (Figure 3.8). Taken together, the present study provides further evidence to support a significant role of the P2X7, P2Y1 and P2Y11 receptors in ATP-induced stimulation of hDP-MSC migration (Peng et al., 2016).

Ca^{2+} signalling is considered to be important in hBM-MSC migration (Ding et al., 2012). As shown in our recent study (Peng et al., 2016), ATP-induced activation of the P2X7, P2Y1 and P2Y11 receptors give rise to a strong increase in the $[Ca^{2+}]_i$. As discussed in section 1.8, it is known that Ca^{2+}-sensitive signalling molecules are critical in mediating Ca^{2+} signalling regulation of cell migration (Shin et al., 2008; Schwab et al., 2012; Tang et al., 2012; Song et al., 2013; Lin et al., 2015). One major finding of the present study is that CaMKII, PKC and PYK2 are important in ATP-induced stimulation of hDP-MSC migration. As introduced above, CaMKII is a kinase activated by Ca^{2+} and CaM, and is known to play a role in regulating cell migration (Shin et al., 2008; Song et al., 2010; Umemura et al., 2014; Chi et al., 2016). The present study showed that treatment with KN-93 strongly inhibited hDP-MSC migration in the presence of ATP (Figure 3.9A-D), without a significant effect on cell migration in the absence of ATP (Figure 3.9E). These results suggest that CaMKII has a critical role in mediating ATP-induced stimulation of hDP-MSC migration. PKC and PYK2 are Ca^{2+}-sensitive. Recent studies have reported that inhibition of Ca^{2+}-induced activation of PKC reduced ACh-induced rBM-MSC migration (Tang et al., 2012), IL-1β- (Lin et al., 2015) and LPA-induced hUC-MSC migration (Ryu and Han, 2015). Similarly, the present study found that inhibition of PKC with CTC prevented ATP-induced stimulation of hDP-MSC migration (Figure 3.10A-C) without significant effect on cell migration in the absence of ATP (Figure 3.10D). The present and previous studies thus provide consistent evidence to support that activation of PKC is important in mediating stimulation of MSC migration induced by various stimuli. The role of PYK2 in the regulation of MSC migration is unknown. Treatment with PF431396 largely prevented ATP-induced increase in hDP-MSC migration (Figure 3.11A-C) without effect on cell migration in the absence of ATP (Figure 3.11D). These results are consistent with previous studies showing that genetic or pharmacological intervention of PYK2 activation reduced migration of epithelial cells (Block et al., 2010) and breast cancer cells (Fan and Guan, 2011). Taken together, the present study provides evidence to suggest a critical role of CaMKII, PKC and PYK2 in mediating ATP-induced stimulation of hDP-MSC migration. Of notice, treatment with each individual kinase inhibitor resulted in strong or complete loss of ATP-induced stimulation, raising the possibility that these signalling molecules, instead of working independently of each other,

are more likely to act in concert or cross-talk to each other in mediating ATP-induced stimulation of hDP-MSC migration.

The MAPK signalling pathways are crucial in transducing extracellular signals to cell functions, including cell migration. MEK/ERK has been well documented to act as a signalling pathway downstream of Ca^{2+}-stimulated activation of CaMKII (Umemura et al., 2014), PKC (Farshori et al., 2003; Hodges et al., 2006; Tang et al., 2012; Lin et al., 2015) and PYK2 (Lev et al., 1995; Wu et al., 2002; Farshori et al., 2003; Hodges et al., 2006; Louis and Zahradka, 2010; Chen et al., 2011). The present study showed that inhibition of MEK/ERK with U0126 strongly suppressed ATP-induced hDP-MSC migration (Figure 3.12A-C) without effect on cell migration in the absence of ATP (Figure 3.12D), suggesting a critical role for the MEK/ERK signalling pathway. This finding is consistent with previous studies showing a positive role of MEK/ERK in mediating hUC-MSC migration stimulated by stromal cell-derived factor-1 (Ryu et al., 2010b), netrin-1 (Lee et al., 2014) and IL-1β (Lin et al., 2015) and also ACh-induced rBM-MSC migration (Tang et al., 2012). However, an early study reported that inhibition of the ERK signalling pathway had no significant effect on TNF-α-induced rBM-MSC migration (Fu et al., 2009). It has also been reported that p38 kinase signalling pathway has a positive role in regulating MSC migration (Fu et al., 2009; Ryu et al., 2010b; Yuan et al., 2012; Yuan et al., 2013; Oh et al., 2015; Lin et al., 2016). The present study showed that blockage of p38 kinase with SB202190 strongly inhibited ATP-induced increase in hDP-MSC migration (Figure 3.13A-C) without effect on cell migration in the absence of ATP (Figure 3.13D). These results suggest that the p38 kinase plays a significant role in ATP-induced stimulation of hDP-MSC migration. PMA-induced PKC activation was reported to induce the p38 kinase signalling pathway during cell migration (Nomura et al., 2007; Wu et al., 2019). As discussed above (section 1.8), MEK/ERK and p38 kinase are important signalling pathways downstream of PKC, PYK2 or CaMKII. Therefore, it is highly likely that MEK/ERK and p38 kinase as signalling pathways downstream of PKC, PYK2 and/or CaMKII mediate ATP-induced stimulation of hDP-MSC migration, although further investigations are required to provide the supporting evidence.

In summary, the results presented in this chapter provide further evidence to support that extracellular ATP stimulates hDP-MSC migration via Ca^{2+} signalling mechanisms mediated by the P2X7, P2Y1 and P2Y11 receptors. Furthermore, as illustrated in Figure 3.14, the results provide evidence to suggest a critical role for CaMKII, PKC, PYK2 and MEK/ERK and p38 MAPK signalling pathways as downstream Ca^{2+}-dependent signalling mechanisms in ATP-induced stimulation of cell migration in hDP-MSCs.

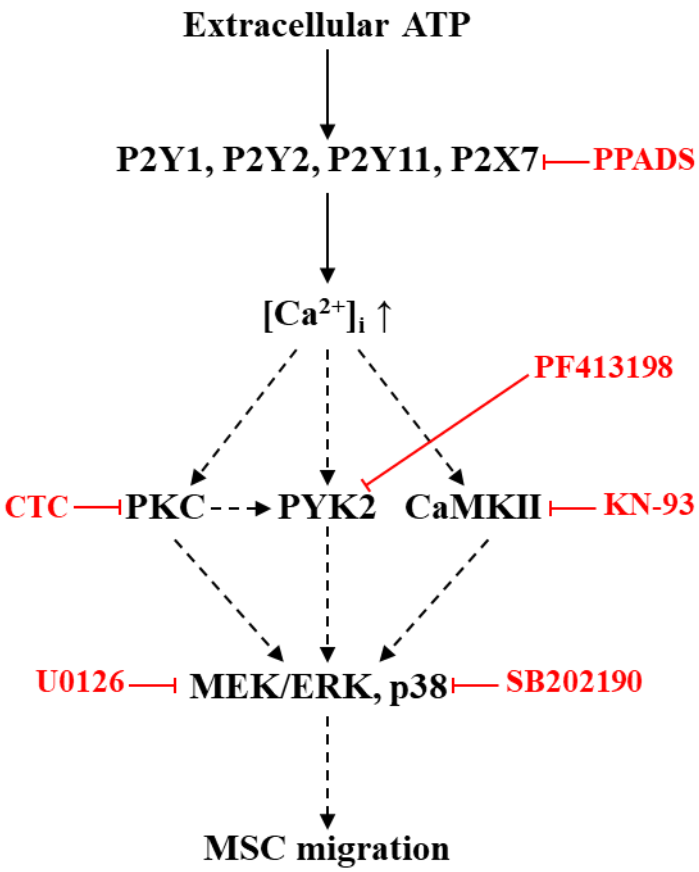

Figure 3.14 Proposed Ca^{2+} signalling mechanisms that mediate ATP-induced increase in hDP-MSC migration.
Exposure of hDP-MSCs to extracellular ATP activates ATP-sensitive P2 receptors (P2X7, P2Y1, P2Y2 and P2Y11), resulting in an increase in the concentration of intracellular Ca^{2+} ($[Ca^{2+}]_i$). Such Ca^{2+} signalling induces activation of protein kinase C (PKC), protein tyrosine kinase 2 (PYK2) that can also be activated by PKC, and Ca^{2+}/calmodulin-dependent protein kinase II (CaMKII), and further mitogen-activated protein kinase kinase/extracellular signal-regulated kinase (MEK/ERK) and p38 kinase as downstream signalling pathways. Activation of such Ca^{2+}-dependent signalling mechanisms drives ATP-induced stimulation of cell migration. The inhibitors used to target various signalling molecules used in the present study are highlighted in red.

CHAPTER 4

Expression of Piezo1 channel in hDP-MSCs and its role in regulating cell migration via ATP release and P2 purinergic signalling

4.1 Introduction

The results from our recent study (Peng et al, 2016) and the results described in chapter 3 provide evidence to show that extracellular ATP promotes cell migration through the P2X7, P2Y1 and P2Y11 purinergic receptors in hDP-MSCs. The results presented in chapter 3 also suggest that Ca^{2+}-dependent downstream signalling pathways mediated by CaMKII, PKC, PYK2 and downstream MEK/ERK and p38 kinase pathways are engaged in transducing ATP-induced regulation of cell migration. As discussed in the Introduction chapter (section 1.3), there is increasing evidence that MSCs release ATP in response to mechanical stimulation (Riddle et al., 2007; Sun et al., 2013; Weihs et al., 2014). For example, exposure to shockwaves can promote hBM-MSC osteogenesis (Sun et al., 2013), and proliferation of hBM-MSCs and AT-MSCs (Riddle et al., 2007; Weihs et al., 2014). Such mechanical regulation of hMSC functions is mediated via ATP release and subsequent activation of P2 receptor-mediated Ca^{2+} signalling mechanisms (Riddle et al., 2007; Sun et al., 2013; Weihs et al., 2014). However, the molecular mechanisms for ATP release from MSC are not well elucidated (Jiang et al., 2017a). Interestingly, recent studies examining urothelial cells (Miyamoto et al., 2014), red blood cells (Cinar et al., 2016) and endothelial cells (Wang et al., 2016; Albarrán-Juárez et al., 2018) provide compelling evidence to indicate that the Piezo1 channel can transduce various mechanical stimuli into intracellular Ca^{2+} signals via regulating ATP release and P2 receptor-mediated purinergic Ca^{2+} signalling.

As discussed in the Introduction chapter (section 1.1.3), Piezo1 functions as a newly identified mechanosensitive or mechanically activated Ca^{2+}-permeable channel and upon activation mediates Ca^{2+} influx to increase the $[Ca^{2+}]_i$ (Coste et al., 2010; Miyamoto et al., 2014; Syeda et al., 2015; Hung et al., 2016). There is increasing evidence to support a role for the Piezo1 channel in regulating cell migration (McHugh et al., 2012; Li et al., 2014;

Hung et al., 2016; Zhang et al., 2017). The Piezo1 channel is expressed in MSCs. One recent study has recently proposed that activation of the Piezo1 channel stimulates cell proliferation in rDP-MSCs via the ERK signalling pathway (Gao et al., 2017). The same study, however, suggests that LIPUS-induced activation of the Piezo1 channel promotes rPDLSC proliferation via the p38 signalling pathway (Gao et al., 2017). Another recent study examining MSC-like cells, UE7T-13 and SDP11, has demonstrated that activation of the Piezo1 channel by HP loading or Yoda1 enhances osteogenesis and conversely suppresses adipogenesis via the ERK and p38 kinase signalling pathways (Sugimoto et al., 2017). These results suggest that the Piezo1 channel in MSCs plays an important role in regulating cell proliferation, osteogenesis and adipogenesis through inducing the MAPK signalling pathways.

However, the role of the Piezo1 channel in MSC migration remains unclear. Therefore, the aims of the study described in this chapter were to examine the expression of the Piezo1 channel in hDP-MSC and, furthermore, to test the hypothesis that activation of the Piezo1 channel stimulates hDP-MSC migration and such stimulation occurs via inducing ATP release and subsequent activation of the P2 receptors and downstream Ca^{2+}-dependent signalling pathways.

4.2 Results

4.2.1 Piezo1 expression in hDP-MSCs

The Piezo1 mRNA expression in hDP-MSCs was examined using real-time RT-PCR. As shown in Figure 4.1A, the mRNA transcript for Piezo1 was consistently detected in hDP-MSCs from four donors examined (9F, 20M, 22M and 32F) (Figure 4.1A). The mean mRNA expression levels for Piezo1 relative to that of β-actin in hDP-MSCs from each donor are shown in Figure 4.1B. There are some variations in the mRNA expression level among the four donors, which seem unrelated to the age or gender of the donors (Figure 4.1B). Next, immunostaining was used to examine the Piezo1 protein expression in hDP-MSCs. Consistently with the detectable mRNA expression, there was positive immunoreactivity for Piezo1 in hDP-MSCs from all the donors that were labelled with an

anti-Piezo1 primary antibody, whereas such immunostaining was not observed in cells only labeled with the secondary antibody (Figure 4.1C).

4.2.2 Ca^{2+} responses to Yoda1

As introduced above, the Piezo1 Ca^{2+}-permeable channel can be chemically activated using Yoda1 and its activation can lead to an increase the $[Ca^{2+}]_i$. Therefore, to demonstrate the functional expression and properties of the Piezo1 channel in hDP-MSCs, I performed Fura 2-based ratiometric measurements of the change in the $[Ca^{2+}]_i$ in response to exposure to Yoda1 at different concentrations. Yoda1 at 0.1, 0.3, 1, 3 and 10 μM in extracellular Ca^{2+}-containing solution induced a concentration-dependent increase in the $[Ca^{2+}]_i$ in hDP-MSC from each of the four donors (Figure 4.1D). Yoda1 at 3 μM was used in further experiments. In contrast with the robust increases in the $[Ca^{2+}]_i$ in extracellular Ca^{2+}-containing solution, exposure to 3 μM Yoda1 evoked no noticeable Ca^{2+} response in extracellular Ca^{2+}-free solution in hDP-MSCs from any of the four donors (Figure 4.2), clearly indicating that Yoda1-induced increase in the $[Ca^{2+}]_i$ results from extracellular Ca^{2+} influx. Taken together, these results provide molecular, biochemical and functional evidence that consistently show expression of Piezo1 as a Ca^{2+}-permeable channel on the cell surface in hDP-MSCs.

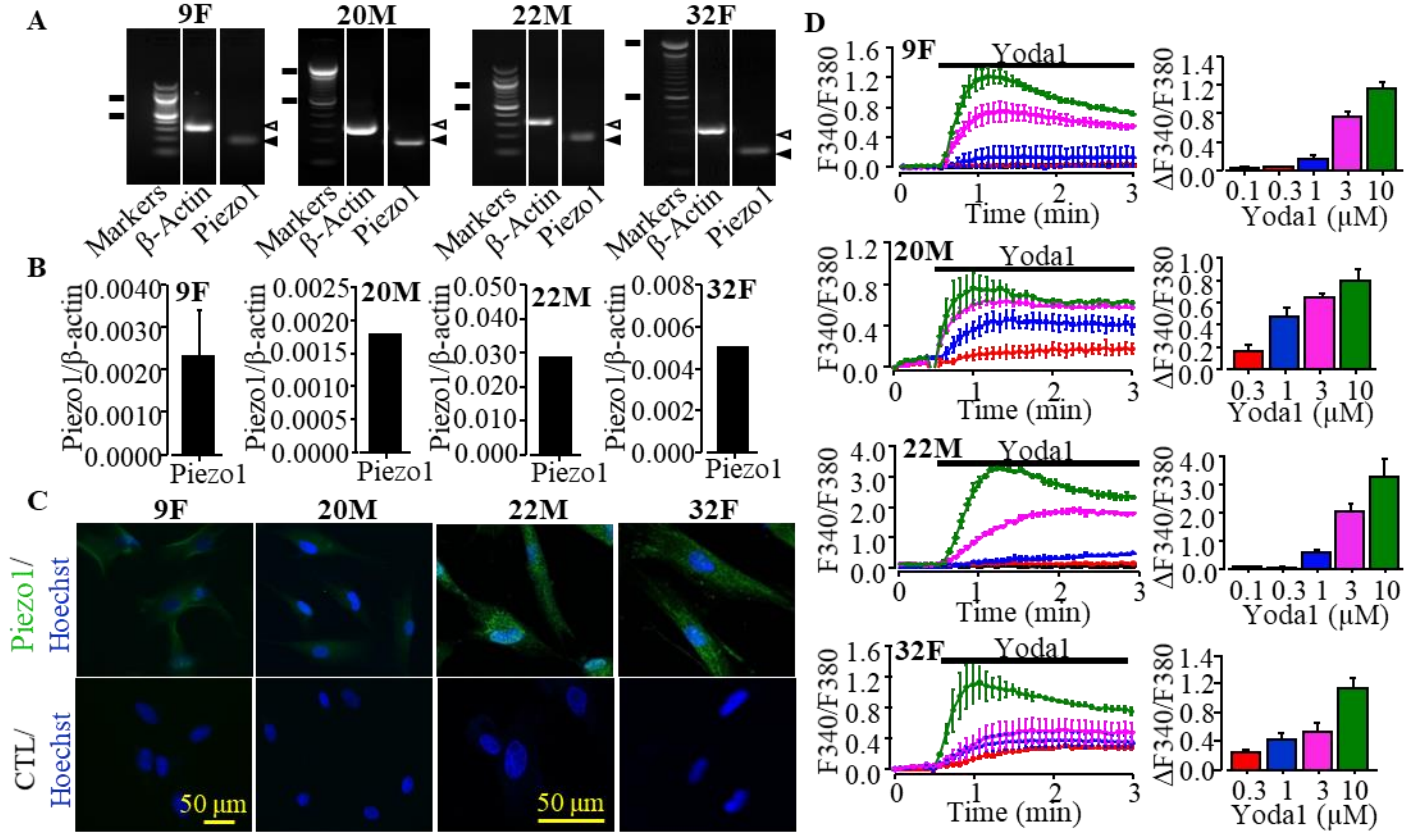

Figure 4.1 Expression of Piezo1 in hDP-MSCs.
(A) Representative agarose gel images showing real-time RT-PCR products of Piezo1 and β-actin mRNA expression in 9F, 20M, 22M and 32F. The double lines on the left of each gel indicate 1.0 kb and 0.5 kb DNA markers. The hollow and solid arrowheads on the right indicate β-actin and Piezo1 PCR products, respectively. (B) The mean Piezo1/β-actin ratio from independent mRNA preparations from 3 wells from 9F, and 2 wells from each of 20M, 22M, and 32F. (C) Representative microscopic images showing immunofluorescence in cells from each of the 4 donors labelled with the anti-Piezo1 antibody (Piezo1, top) or only with the second antibody (CTL, bottom) and counterstained with Hoechst 33342. (D) Representative intracellular Ca^{2+} responses to different concentrations of Yoda1 (left) and the peak Ca^{2+} responses (right) in cells from each of the 4 donors, presented as mean ± sem values of 4 wells from 1 set of experiments.

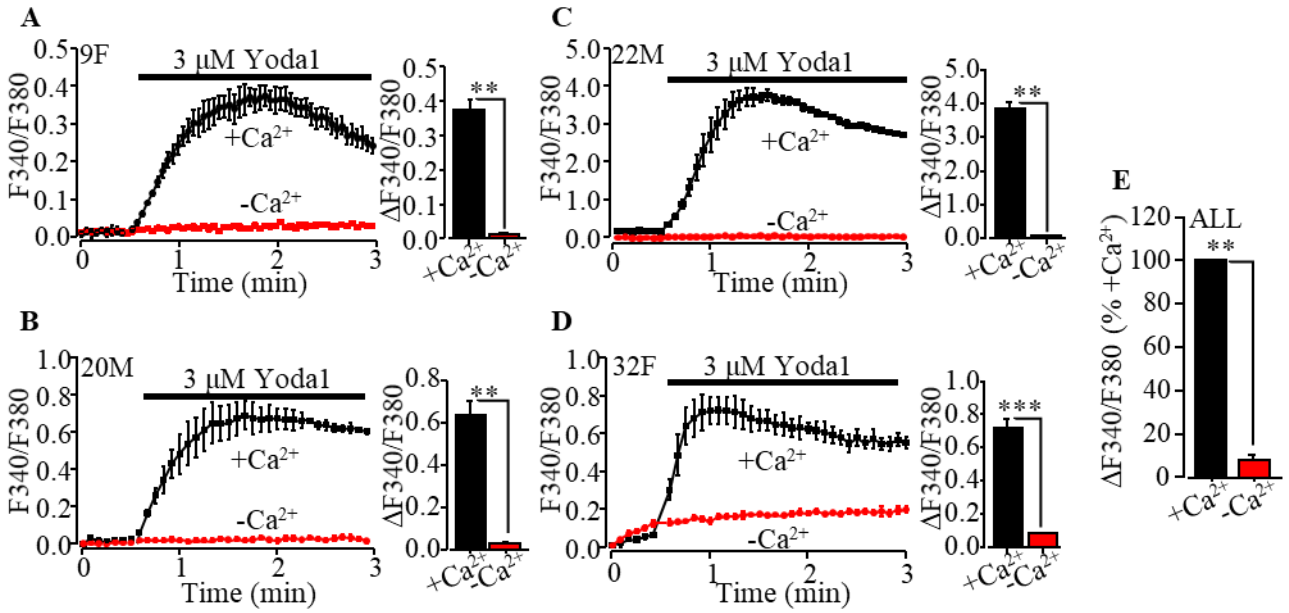

Figure 4. 2 Yoda1 induces Ca^{2+} responses via extracellular Ca^{2+} influx in hDP-MSCs.
(A-D) Representative Yoda1-induced intracellular Ca^{2+} peak responses in extracellular Ca^{2+}-containing ($+Ca^{2+}$) or Ca^{2+}-free ($-Ca^{2+}$) solutions in parallel experiments (left) and the mean peak Ca^{2+} responses (right) in cells from 9F (N = 4 wells) (A), 20M (N = 4 wells) (B), 22M (N = 4 wells) (C) and 32F (N = 4 wells) (D), presented with mean ± sem value from one set of experiment using four wells of cells for each condition. (E) Summary of the mean peak Ca^{2+} responses in Ca^{2+}-containing ($+Ca^{2+}$) and Ca^{2+}-free ($-Ca^{2+}$) solutions from four independent experiments from all the donors. The peak Ca^{2+} response was expressed as percentage of the peak Ca^{2+} responses in extracellular Ca^{2+}-containing in parallel experiments. **, $p < 0.01$ and ***, $p < 0.001$.

4.2.3 Effects of inhibiting Piezo1 channel in Yoda1-induced Ca^{2+} responses

There is evidence suggests that Yoda1 may act on other unknown targets than the Piezo1 channel (Dela Paz and Frangos, 2018). To provide evidence to show that Yoda1-induced Ca^{2+} influx in hDP-MSCs was mediated by the Piezo1 channel, I examined the effect of RR, which is known to suppress the Piezo1 channel activity (Coste et al., 2010), on Yoda1-induced Ca^{2+} responses. Consistently, in hDP-MSCs from three donors examined (9F, 20M and 32F), treatment of hDP-MSCs with RR at 10 and 30 μM for 5 minutes had no or little effect on the basal Ca^{2+} level but significantly attenuated Yoda1-induced increase in the $[Ca^{2+}]_i$ (Figure 4.3).

I also tested the effect of GsMTx4, a spider peptide known to inhibit the Piezo1 channel with better specificity (Bae et al., 2011), on Yoda1-induced Ca^{2+} responses. Pre-treatment with GsMTx4 at 0.3, 1 and 3 μM for 30 minutes resulted in a concentration-dependent reduction in Yoda1-induced increase in the $[Ca^{2+}]_i$ in hDP-MSCs from the two donors examined (9F and 20M) (Figure 4.4).

Finally, I examined the effect of siRNA-mediated knockdown of the Piezo1 expression on Yoda1-induced Ca^{2+} responses. Transfection of hDP-MSCs from 9F, 20M and 32F with Piezo1-specific siRNA (siPiezo1) reduced the Piezo1 mRNA expression as determined by real-time RT-PCR (Figure 4.5A-C). On average, transfection with siPiezo1 reduced the Piezo1 mRNA expression by approximately 60% (Figure 4.5D). Such siRNA-mediated knockdown of the Piezo1 expression strongly suppressed Yoda1-induced increase in the $[Ca^{2+}]_i$ (Figure 4.6A-C). The mean peak Yoda1-induced Ca^{2+} responses in hDP-MSCs from 9F, 20M and 32F transfected with siPiezo1 was reduced by approximately 40% as compared to that in cells transfected with siCTL (Figure 4.6D).

In summary, the results from pharmacological and genetic interventions provide further and consistent evidence to support the notion that Yoda1 acts on and activates the Piezo1 Ca^{2+}-permeable channel in hDP-MSCs.

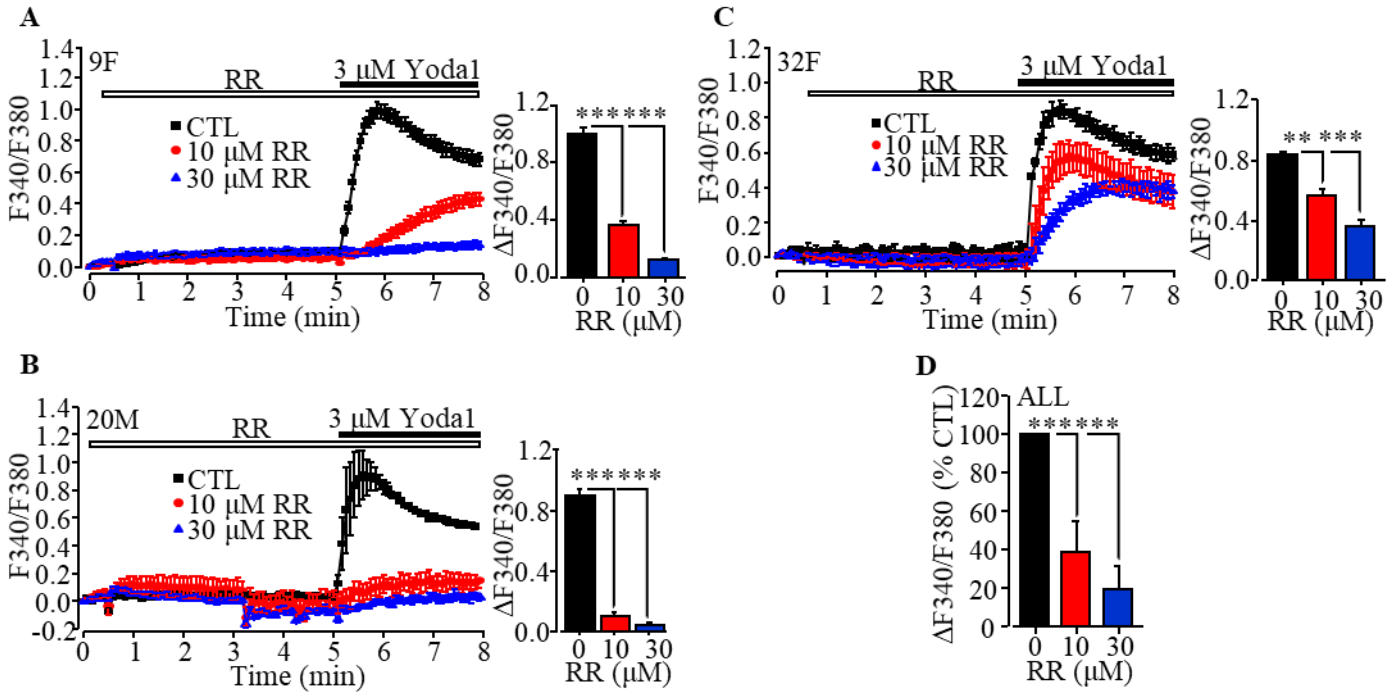

Figure 4. 3 Inhibition of Yoda1-induced Ca^{2+} responses in hDP-MSCs by ruthenium red.
(A-C) Representative Yoda1-induced intracellular Ca^{2+} responses (left) and peak Ca^{2+} responses (right) in cells from 9F (N = 4 wells) (A), 20M(N = 4 wells) (B) and 32F (N = 4 wells) (C) without (CTL) and with treatment with 10 or 30 μM ruthenium red (RR) for 5 min before and duration exposure to 3 μM Yoda1, presented as mean ± sem values from one set of experiments using four wells of cells for each condition. (D) Summary of the mean Yoda1-induced peak Ca^{2+} responses in cells treated with RR, from three independent experiments from 9F, 20M and 32F, with the peak Ca^{2+} responses expressed as percentage of that in cells under control conditions in parallel experiments. **, $p < 0.01$ and ***, $p < 0.001$, compared to control cells.

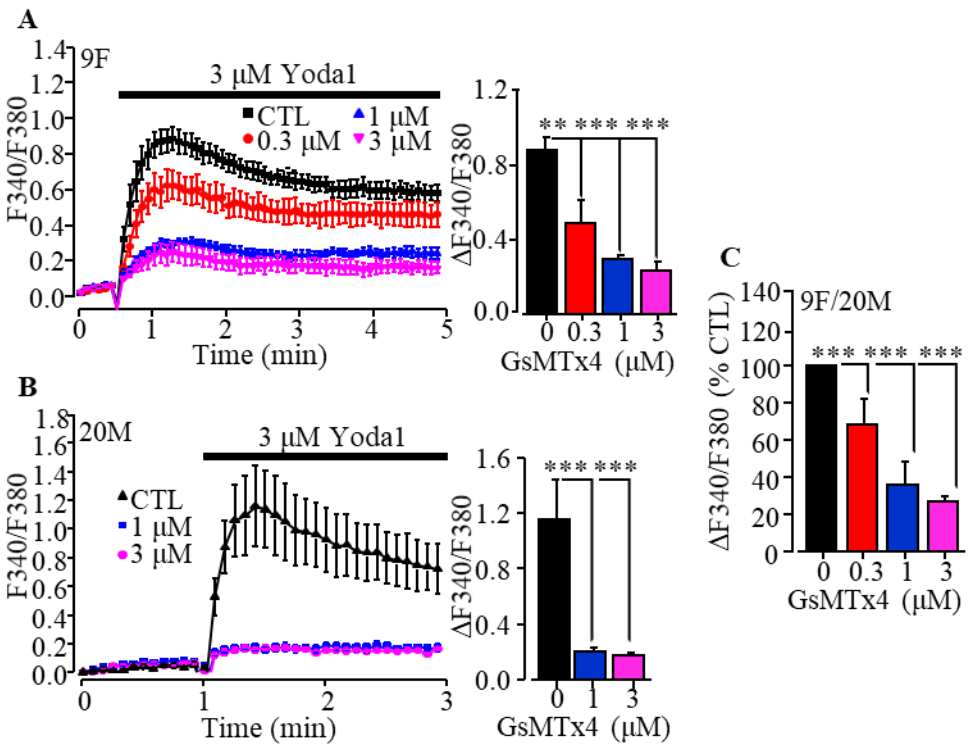

Figure 4. 4 Inhibition of Yoda1-induced Ca^{2+} responses in hDP-MSCs by GsMTx4. (A-B) Representative intracellular Ca^{2+} responses to 3 μM Yoda1 in cells without (CTL) and with treatment with indicated concentrations of GsMTx4 for 30 min prior to and during exposure to Yoda1 (left), and Yoda1-induced peak Ca^{2+} responses (right) in cells from 9F (N = 4 wells) (A) and 20M (N = 4 wells) (B) presented as mean ± sem values from one set of experiments using four wells of cells for each condition. (C) Summary of the mean Yoda1-induced peak Ca^{2+} responses in cells treated with GsMTx4, from 4 independent experiments from 9F and 20M, with the peak Ca^{2+} responses expressed as percentage of that in cells under control conditions in parallel experiments. **, $p < 0.01$ and ***, $p < 0.001$ compared to control cells.

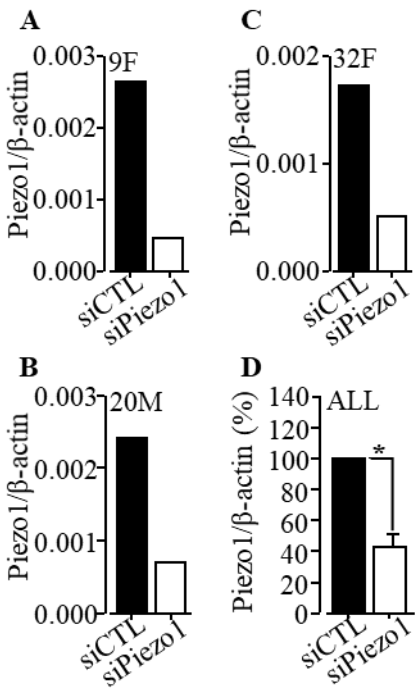

Figure 4. 5 siRNA-mediated knockdown of Piezo1 expression in hDP-MSCs.
(A-C) Summary of the Piezo1/β-actin mRNA ratio detected by real-time RT-PCR in 1 set of experiment using cells from 9F (N = 2 wells) (A), 20M (N = 2 wells) (B) and 32F (N = 2 wells) (C) transfected with control siRNA (siCTL) or Piezo1-specific siRNA (siPiezo1) in parallel experiments. (D) Summary of the mean Piezo1/β-actin mRNA ratio in cells transfected with siCTL or siPiezo1 from three independent experiments from 9F, 20M and 32F. The Piezo1/β-actin ratio expressed as percentage of that in siCTL-transfected cells in parallel experiments. *, $p < 0.05$.

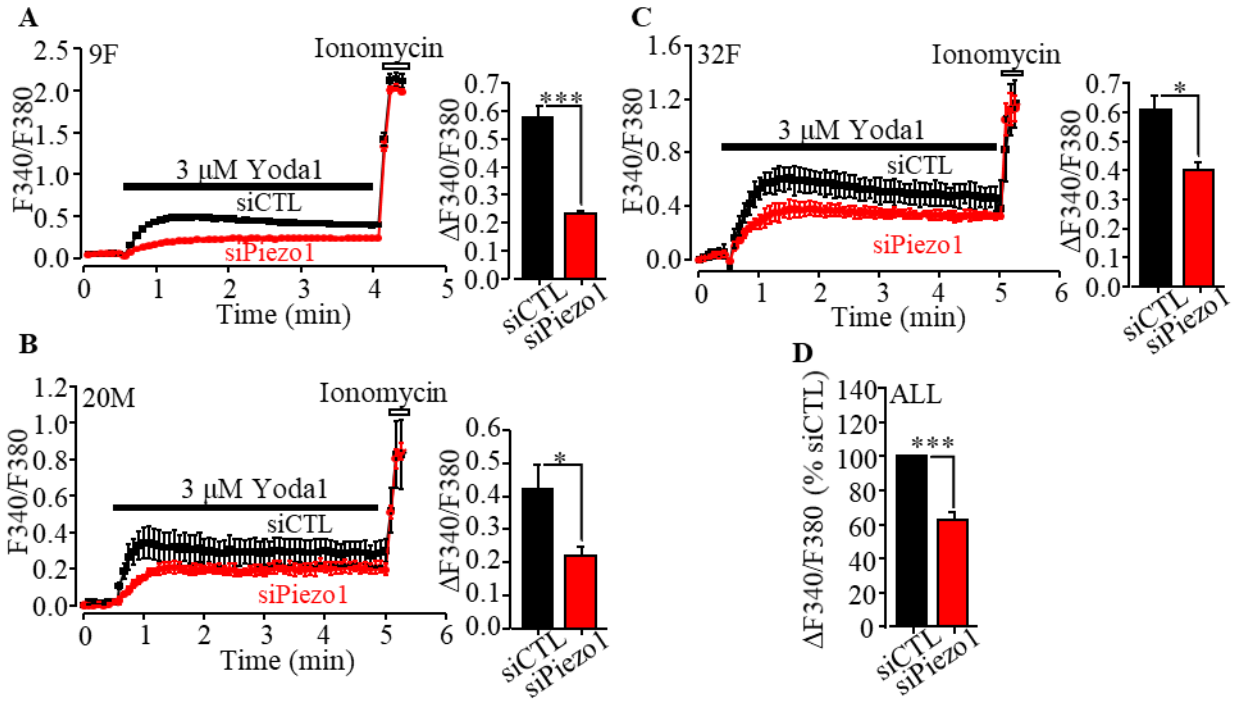

Figure 4. 6 Effect of siRNA-mediated knockdown of Piezo1 on Yoda1-induced Ca^{2+} responses in hDP-MSCs.
(A-C) Representative intracellular Ca^{2+} responses to 3 μM Yoda1 (left) and the mean peak Ca^{2+} responses (right) in cells from 9F (N = 4 wells) (A), 20M (N = 4 wells) (B) and 32F (N = 4 wells) (C) transfected with siCTL or siPiezo1, from 1 set of experiment using four wells of cells for each condition. Cells were exposed to 5 μM ionomycin at the end of recordings. (D) Summary of mean peak Yoda1-induced Ca^{2+} responses from 5 independent experiments in transfected cells from all donors, with the Ca^{2+} response expressed as percentage of that in siCTL-transfected cells in parallel experiments. *, $p < 0.05$ and ***, $p < 0.001$.

4.2.4 Effect of Yoda1 on cell migration

Several recent studies have reported a critical role of the Piezo1 channels in mediating cell migration in cancer and endothelial cells (McHugh et al., 2012; Li et al., 2014; Hung et al., 2016; Zhang et al., 2017). To investigate the Piezo1 channel has a similar role in regulating hDP-MSC migration, I performed wound healing assay to determine the effects of exposure to Yoda1 on hDP-MSC migration. Figure 4.7A illustrates representative images of the wound areas at 0, 24, 48 and 72 hours for cells from 9F in the absence and in the presence of 0.1, 0.3 and 1 μM Yoda1. Figure 4.7B-E shows quantitative analysis of wound healing at 24, 48 and 72 hours for hDP-MSCs from 9F, 20M, 22M and 32F. Figure 4.7F summarizes the mean results from 8 independent experiments from cells of all four donors. The results, albeit with some variations among the donors show that exposure to Yoda1 resulted in a concentration-dependent increase in cell migration, with the increase induced by 0.3 and 1 μM Yoda1 reaching significance (Figure 4.7F).

4.2.5 Effect of siRNA knockdown of Piezo1 on Yoda1-induced cell migration

To further demonstrate the role of the Piezo1 channels in Yoda1-induced hDP-MSC migration, I examined the effect of exposure to 0.3 μM Yoda1 on cell migration in hDP-MSCs transfected with siPiezo1 and siCTL. Of notice, as compared to transfection with siCTL, transfection with siPiezo1 appeared to affect cell migration in the absence of Yoda1, and the effects were variable from no change in cells from 9F (Figures 4.8A), an increase in cells from 20M and 22M (Figures 4.8B and C) and a reduction in cells from 32F (Figure 4.8D). The mean results from 5 independent experiments for cells from all donors are thus presented as percentage of cell migration in the absence of Yoda1 (Figure 4.8E). It is clear that Yoda1 still significantly increased cell migration in hDP-MSCs transfected with siCTL and, in contrast, Yoda1-induced increase in cell migration was largely abolished in cells transfected with siPiezo1 (Figures 4.8E). The results provide evidence to support a role of the Piezo1 channel in mediating Yoda-1induced increase in hDP-MSC migration.

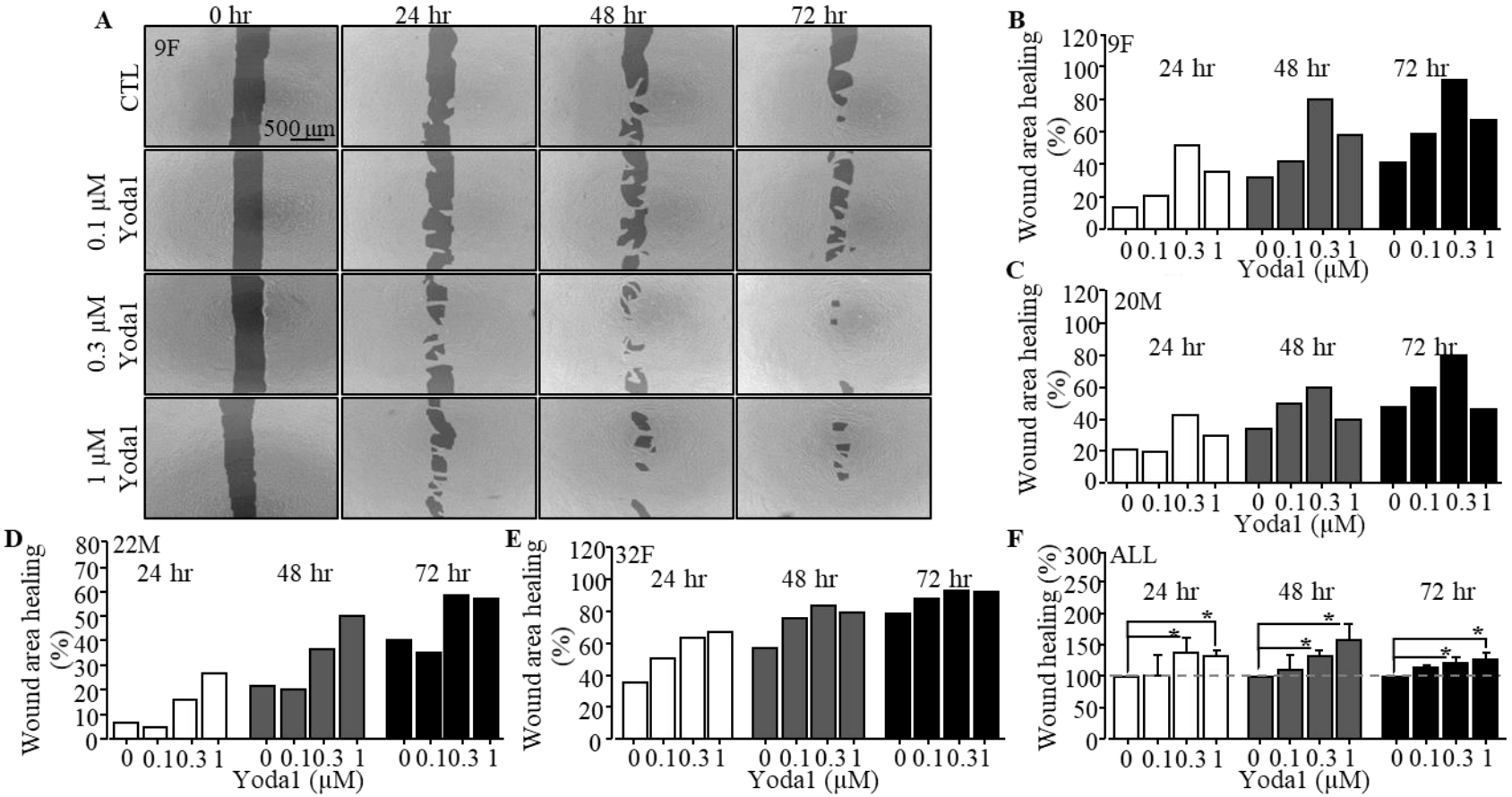

Figure 4. 7 Yoda1 stimulates hDP-MSC migration.

(A) Representative images illustrating the wound areas at 0, 24, 48 and 72 hours, using cells from 9F in the absence (CTL) and presence of indicated concentrations of Yoda1 in the culture medium. (B-E) Quantitative analysis of wound area healing at 24, 48 and 72 hours, using cells from 9F (N = 2 wells) (B), 20M (N = 2 wells) (C) 22M (N = 2 wells) (D) and 32F (N = 2 wells) (E) in 1 set of experiment. (F) Summary of the mean wound narrowing, as percentage of that under control conditions at the same time points in parallel experiments, from 8 independent experiments using cells from all donors. *, $p < 0.05$ compared to control condition at the same time points.

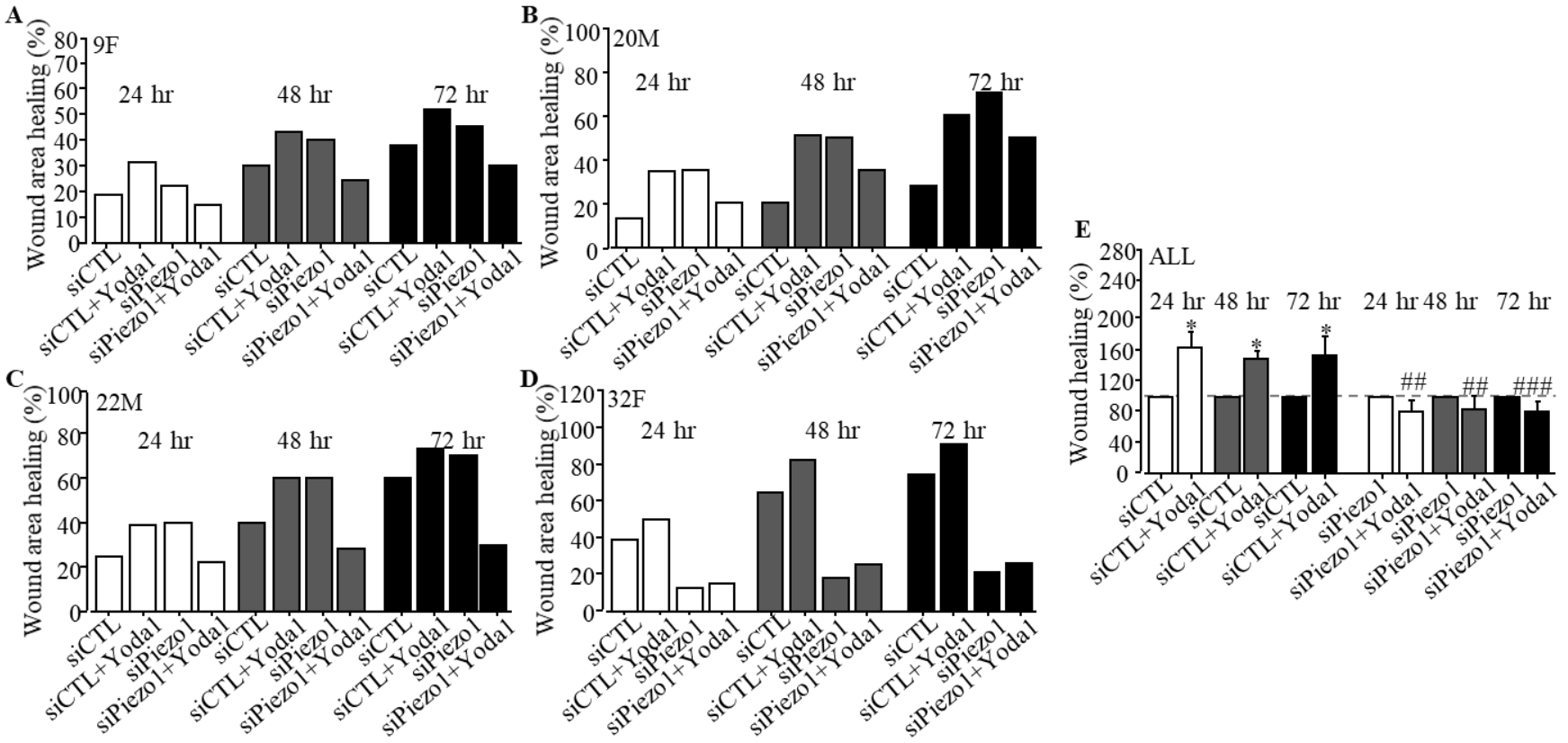

Figure 4. 8 Effect of siRNA-mediated knockdown of Piezo1 on Yoda1-induced hDP-MSC migration.
(A-D) Quantitative analysis of wound area healing 24, 48 and 72 hours, using cells from 9F (N = 2 wells) (A), 20M (N = 2 wells) (B) 22M (N = 2 wells) (C) and 32F (N = 2 wells) (D) transfected with siCTL and siPiezo1 in the absence and presence of 0.3 μM Yoda1 in 1 set of experiment. (E) Summary of the mean wound narrowing, as percentage of that under control conditions at the same time points in parallel experiments, from 5 independent experiments using cells from all donors. *, $p < 0.05$ compared to siCTL-transfected cells under control condition at the same time points. ##, $p < 0.01$ and ###, $p < 0.001$ compared to siCTL-transfected cells treated with Yoda1 at the same time points.

4.2.6 Effects of PPADS and apyrase on Yoda1-induced cell migration

As discussed in the Introduction chapter (section 1.5) and briefly recapitulated in the Introduction to this chapter (section 4.1), it has been shown that mechanical stimuli can regulate MSC functions via inducing ATP release and activation of the P2 receptors. There is also increasing evidence that the Piezo1 channel mediates mechanical induction of ATP release (Miyamoto et al., 2014; Cinar et al., 2016; Wang et al., 2016; Albarrán-Juárez et al., 2018) and activation of the P2 receptors (Wang et al., 2016). These findings lead to the hypothesis that Yoda1-induced activation of the Piezo1 channel stimulated hDP-MSC migration via promoting ATP release and subsequent activation of P2 receptors. Our recent study (Peng et al., 2016) and the results shown in chapter 3 show that ATP-induced stimulation promotes hDP-MSC migration were sensitive to blockage by treatment with 30 μM PPADS. Therefore, to test the above hypothesis, I firstly determined whether treatment with PPADS was also effective in blocking Yoda1-induced increase in cell migration. As I showed in chapter 3 (Figure 3.3), treatment with 30 μM PPADS in the absence of Yoda1 was without effect on cell migration but, interestingly, largely prevented Yoda1-induced increase in cell migration of hDP-MSCs (Figure 4.9).

To further examine whether Yoda1-induced activation of the Piezo1 channel indeed induces release of ATP and, in turn, activates ATP-sensitive P2 receptors, I next determined the effect of treatment with ATP-hydrolyzing enzyme apyrase on Yoda1-induced increase in hDP-MSC migration. Indeed, inclusion of 0.3 and 1 U/ml apyrase, while resulting in no effect on cell migration on its own, inhibited Yoda1-induced increase in hDP-MSC migration (Figure 4.10). Quantitative analysis of the mean data shows that treatment with 0.3 U/ml apyrase significantly reduced Yoda1-induced increase in cell migration at 24 hour and treatment with 1 U/ml apyrase prevented Yoda1-induced stimulation of cell migration at 24, 48 and 72 hours (Figure 4.10C).

In summary, these results provide strong evidence to suggest that Yoda1-induced Piezo1 channel activation stimulates hDP-MSC migration via ATP release and subsequent activation of the P2 receptors.

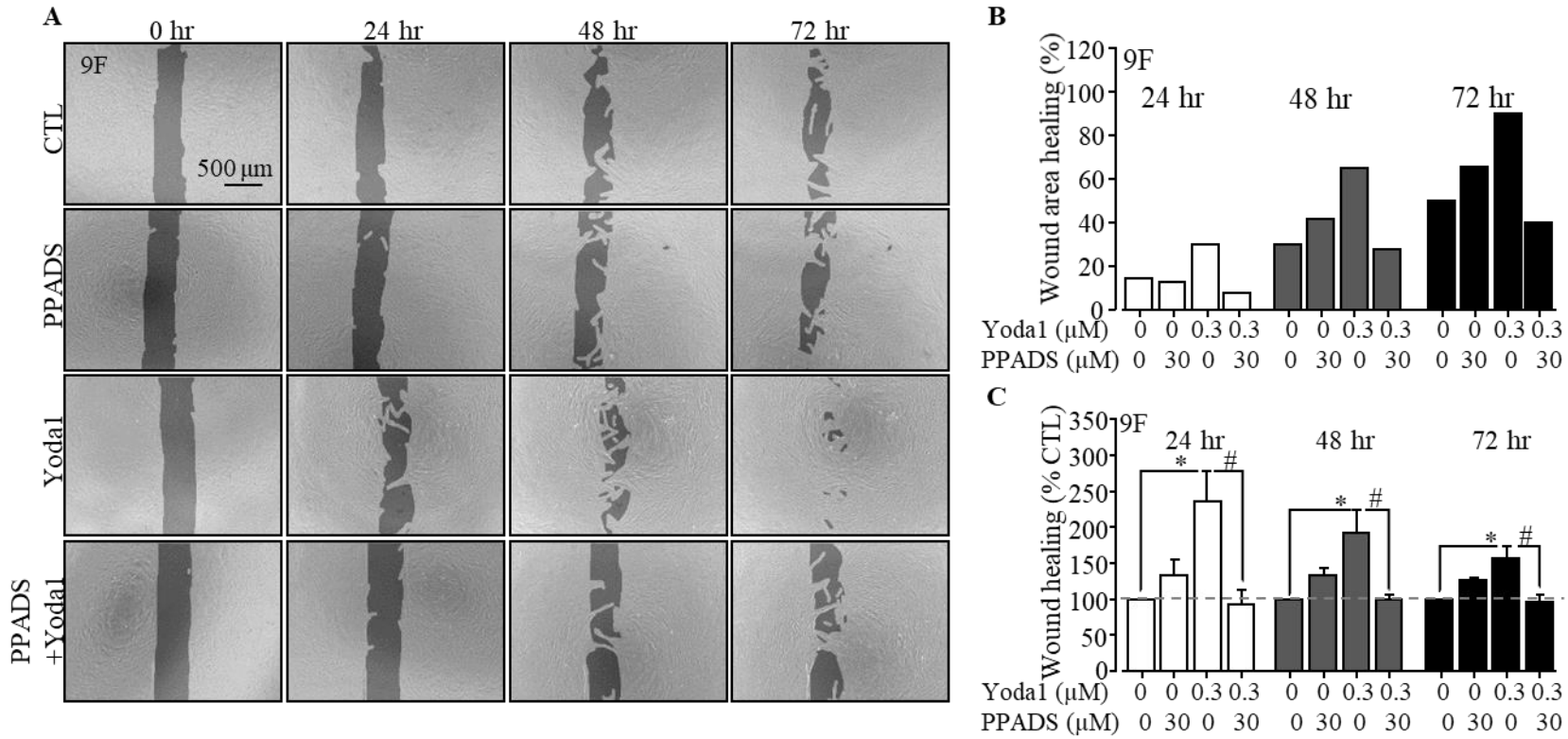

Figure 4. 9 Inhibition of Yoda1-induced hDP-MSC migration by PPADS.
(A) Representative images showing wound areas in wound healing assay at 24, 48 and 72 hours, using cells from 9F pre-treated with 30 µM of PPADS in the absence and presence of 0.3 µM Yoda1. (B) Quantitative analysis of wound area healing under the same experimental concentrations as shown in A (N = 2 wells). (C) Summary of the mean wound narrowing, as percentage of that under control conditions at the same time points in parallel experiments, from 3 independent experiments using cells from 9F. *, $p < 0.05$ compared to control condition at the same time points; #, $p < 0.05$ compared to cells exposed to Yoda1 alone at the same time points.

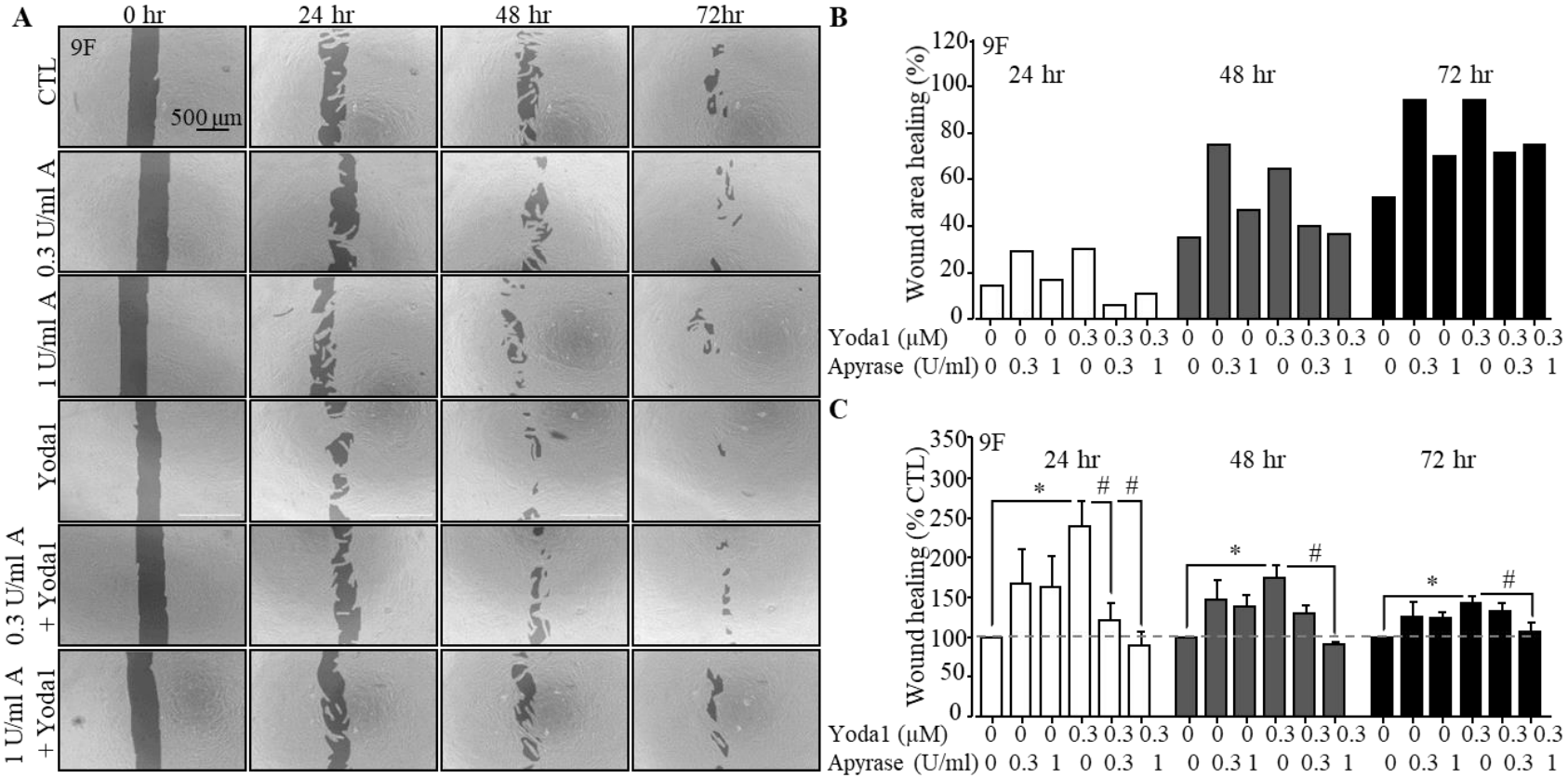

Figure 4. 10 Inhibition of Yoda1-induced hDP-MSC migration by treatment with apyrase.
(A) Representative images showing wound areas in wound healing assay at 0, 24, 48 and 72 hours, using 9F pre-treated with apyrase at indicated concentrations in the absence and presence of 0.3 µM Yoda1. (B) Quantitative analysis of wound area healing under the same experimental concentrations as shown in A (N = 2 wells). (C) Summary of the mean wound narrowing, as percentage of that under control conditions at the same time points in parallel experiments, from 3 independent experiments using cells from 9F. *, $p < 0.05$ compared to control condition at the same time points; #, $p < 0.05$ compared to cells exposed to Yoda1 alone at the same time points.

4.2.7 Effect of CaMKII inhibitor KN-93 on Yoda1-induced cell migration

The results described in the previous chapter show involvement of CaMKII, PKC, PYK2 and MAPKs as Ca^{2+}-dependent downstream signalling pathways in ATP-induced increase in hDP-MSC migration. It is interesting to test whether these signalling pathways are also involved in Yoda1-induced Piezo1-mediated increase in hDP-MSC migration. I firstly examined the effect of KN-93 on Yoda1-induced hDP-MSC migration. Pre-treatment with 0.3 μM KN-93 prior to and during exposure to 0.3 μM Yoda1 reduced cell migration of hDP-MSCs from 32F (Figure 4.11A and B). Similar results were obtained for cells from 9F and 20M (Figure 4.11C and D). Figure 4.11E summarizes the mean data from 4 independent experiments using hDP-MSCs from all the three donors and shows that treatment with KN-93 largely abolished Yoda1-induced increase in cell migration. These results suggest a role for CaMKII as a Ca^{2+}-dependent signalling mechanism downstream of Piezo1 channel activation in mediating hDP-MSC migration.

4.2.8 Effect of PKC inhibitor CTC on Yoda1-induced cell migration

To determine whether PKC is involved in mediating Piezo1-mediated stimulation of hDP-MSC migration, I tested the effect of CTC on Yoda1-induced hDP-MSC migration. As shown in Figure 4.13A, migration of hDP-MSC from 32F was reduced by treatment with 1 μM CTC prior to and during exposure to Yoda1, as examined at 24, 48 and 72 hours (Figure 4.12A and B). Similar results were obtained for cells from 9F and 20M (Figure 4.12C-D). Figure 4.12E summarizes the mean data from 4 independent experiments using hDP-MSCs from all three donors and shows that inhibition of PKC strongly suppressed Yoda1-induced increase in cell migration. These results, therefore, suggest a significant role for the activation of PKC in transducing Piezo1 channel-mediated hDP-MSC migration.

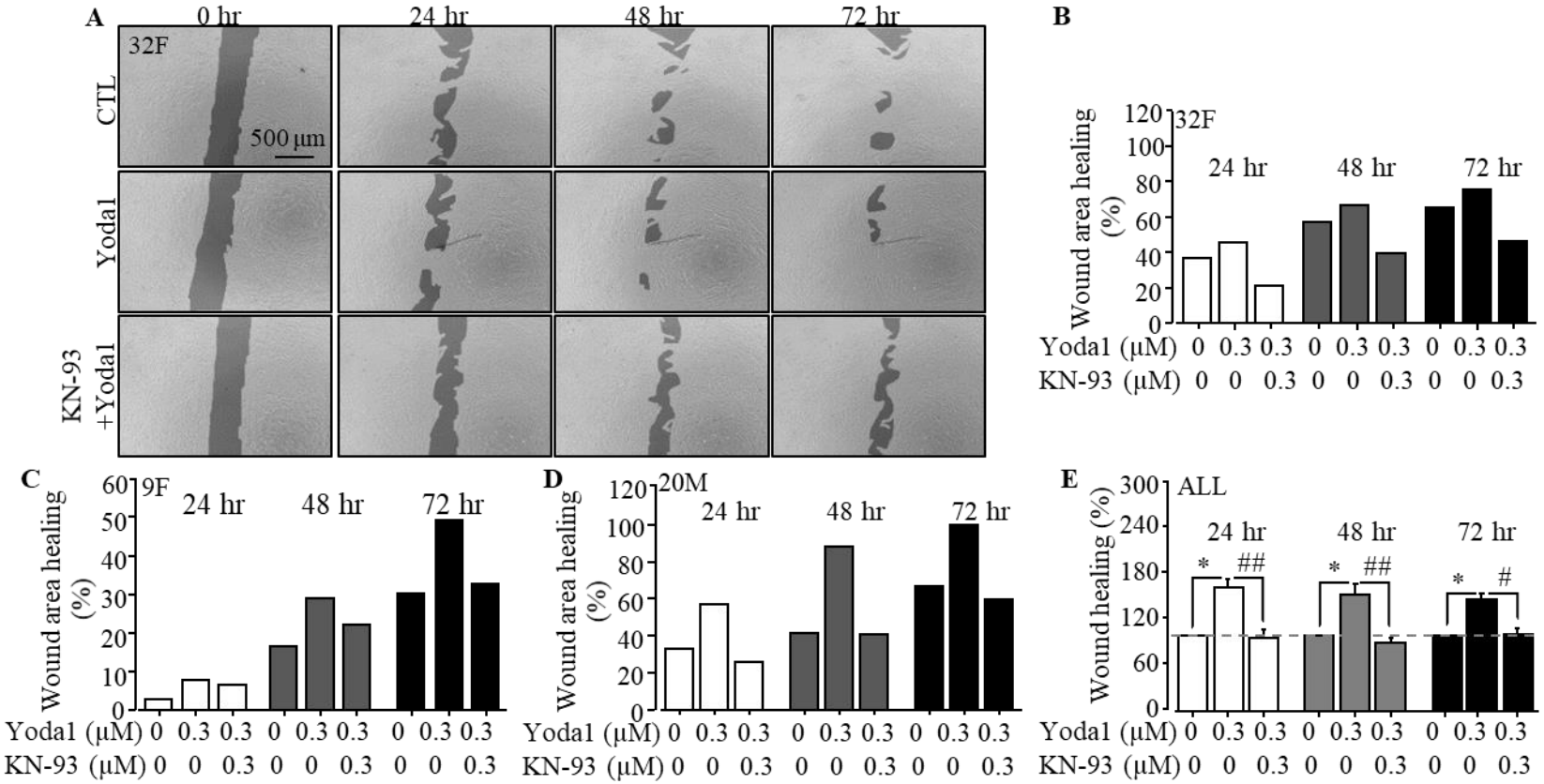

Figure 4.11 Inhibition of Yoda1-induced hDP-MSC migration by KN-93.

(A) Representative images showing wound areas at 0, 24, 48 and 72 hours, using cells from 32F in the absence (CTL) and presence of 0.3 µM Yoda1 without or with prior treatment with 0.3 µM KN-93. (B-D) Quantitative analysis of wound area healing at 24, 48 and 72 hours, using cells from 32F (N = 2 wells) (B), 9F (N = 2 wells) (C) and 20M (N = 2 wells) (D) in 1 set of experiment, under the same experimental concentrations as shown for 32F in A. (E) Summary of the mean wound narrowing, as % of that under control conditions at the same time points in parallel experiments, from 4 independent experiments using cells from 9F, 20M and 32F. *, $p < 0.05$ compared to control condition at the same time points; #, $p < 0.05$ and ##, $p < 0.01$ compared to cells exposed to Yoda1 alone at the same time points.

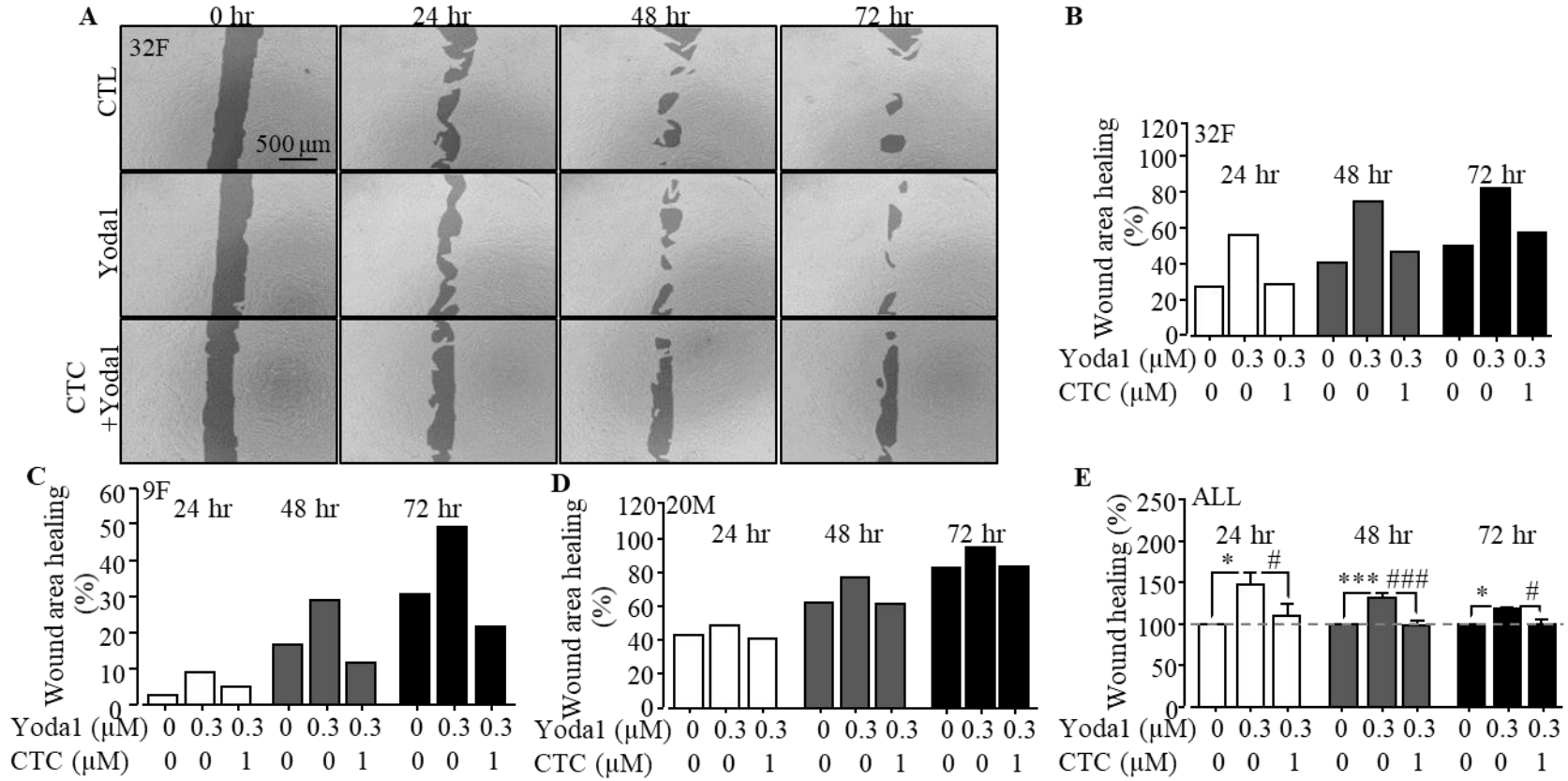

Figure 4. 12 Inhibition of Yoda1-induced hDP-MSC migration by CTC.

(A) Representative images showing wound areas at 0, 24, 48 and 72 hours, using 32F in the absence (CTL) and presence of 0.3 µM Yoda1 without or with prior treatment with 1 µM chelerythrine chloride (CTC). (B-D) Quantitative analysis of wound areas using 32F (N = 2 wells) (B), 9F (N = 2 wells) (C) and 20M (N = 2 wells) (D) in 1 set of experiment, under the same experimental concentrations as shown in A. (E) Summary of the mean wound narrowing, as % of that under control condition at the same time points in parallel experiments, from 4 independent experiments from 9F, 20M and 32F. *, $p < 0.05$ and ***, $p < 0.001$ compared to control condition at the same time points; #, $p < 0.05$ and ###, $p < 0.001$ compared to cells exposed to Yoda1 alone at the same time points.

4.2.9 Effect of PYK2 inhibitor PF431396 on Yoda1-induced cell migration

The involvement of PYK2 in Yoda1-induced cell migration was also investigated by using PF431396. Figures 4.13A illustrates representative images showing wound healing of hDP-MSCs from 32F that were treated with 10 nM PF431396 prior to and during exposure to Yoda1, and Figure 4.13B show quantitative analysis of wound healing or migration at 24, 48 and 72 hours. Similar results were obtained for cells from 9F and 20M (Figure 4.13C and D). Figure 4.13E summarizes the mean data from 3 independent experiments using hDP-MSCs from all the three donors and shows that inhibition of PYK2 almost completely abolished Yoda1-induced increase in cell migration, therefore, suggesting that activation of PYK2 plays an important role in transducing Piezo1 channel-mediated hDP-MSC migration.

4.2.10 Effect of MEK/ERK inhibitor U0126 on Yoda1-induced cell migration

The role of MEK/ERK in Yoda1-induced stimulation of cell migration was examined using U0126. Treatment with 1 μM U0126 prior to and during exposure to Yoda1 resulted in complete loss of Yoda1-induced increase in cell migration in hDP-MSCs from 32F (Figure 4.14A and B). Similar results were obtained for cells from 9F and 20M (Figure 4.14C and D). Figure 4.14E summarizes the mean data from 3 independent experiments using hDP-MSCs from all the three donors and shows that treatment with U0126 prevented Yoda1-induced stimulation of cell migration (Figure 4.14E). These results, therefore, provide evidence to suggest the engagement of MEK/ERK as a downstream signalling pathway in Piezo1 channel-mediated hDP-MSC migration.

4.2.11 Effect of p38 kinase inhibitor SB202190 on Yoda1-induced cell migration

Finally, the role of p38 signalling pathway was investigated in Yoda1-induced hDP-MSC migration. Figure 4.15A illustrates representative images showing wound healing of hDP-MSCs from 9F that were treated with 1 μM SB202190 prior to and during exposure to Yoda1, and Figure 4.15B shows quantitative analysis of wound healing or migration at 24, 48 and 72 hours. Figure 4.15C summarizes the mean data from 3 independent experiments using hDP-MSCs from 9F cells and shows that inhibition of p38 kinase

resulted in no significant inhibition of Yoda1-induced cell migration (Figure 4.15C), suggest that the p38 kinase signalling pathway is involved in Piezo1 channel-mediated cell migration in hDP-MSCs.

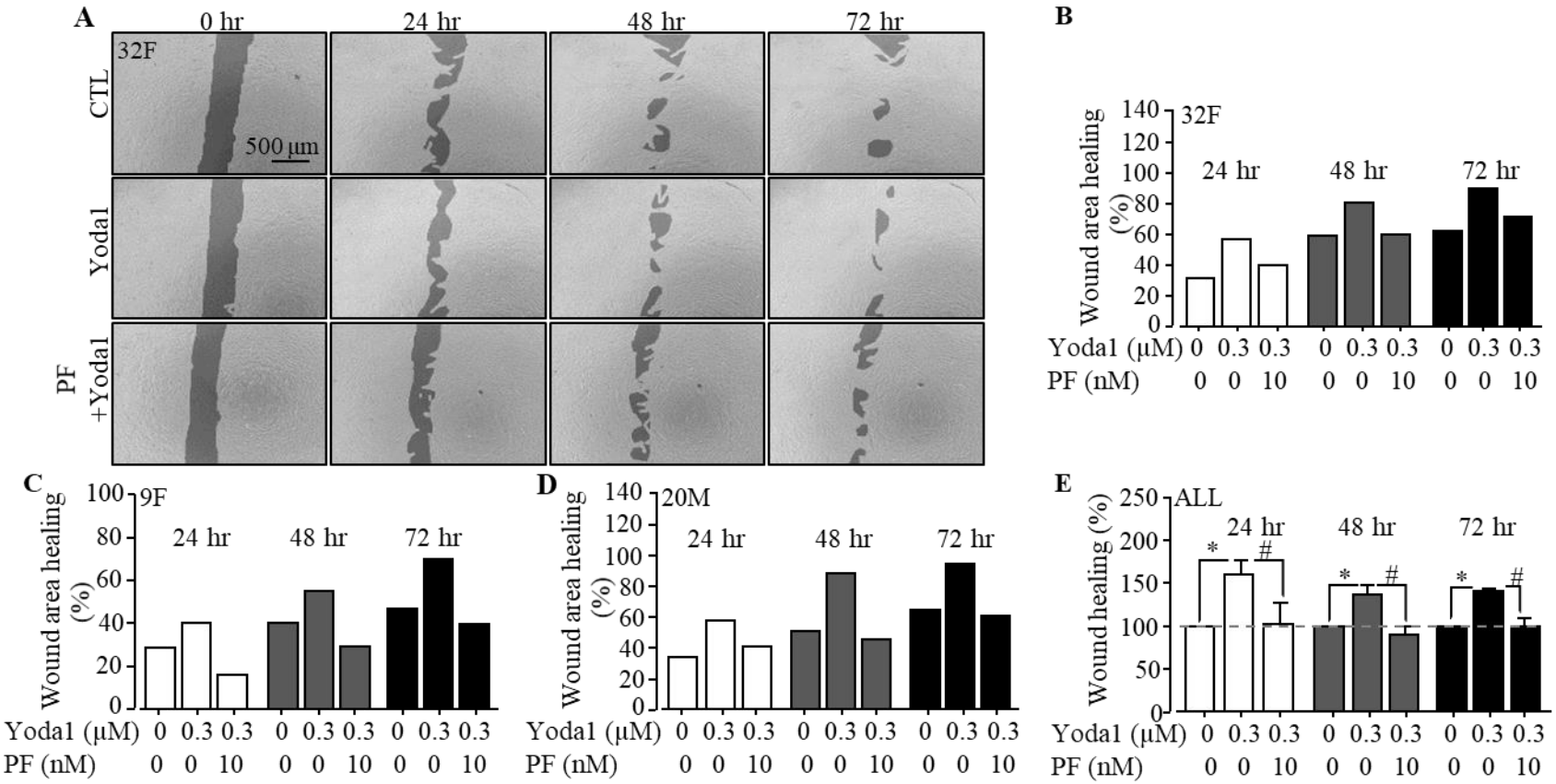

Figure 4. 13 Inhibition of Yoda1-induced hDP-MSC migration by PF431396.

(A) Representative images showing wound areas at 0, 24, 48 and 72 hours, using cells from 32F in the absence (CTL) and presence of 0.3 μM Yoda1 without or with prior treatment with 10 nM PF431396 (PF). (B-D) Quantitative analysis of wound area healing using cells from 32F (N = 2 wells) (B), 9F (N = 2 wells) (C) and 20M (N = 2 wells) (D) in 1 set of experiment, under the same experimental concentrations as shown in A. (E) Summary of the mean wound narrowing, as percentage of that under control conditions at the same time points in parallel experiments, from 3 independent experiments using cells from 9F, 20M and 32F. *, $p < 0.05$ compared to control condition at the same time points; #, $p < 0.05$ compared to cells exposed to Yoda1 alone at the same time points.

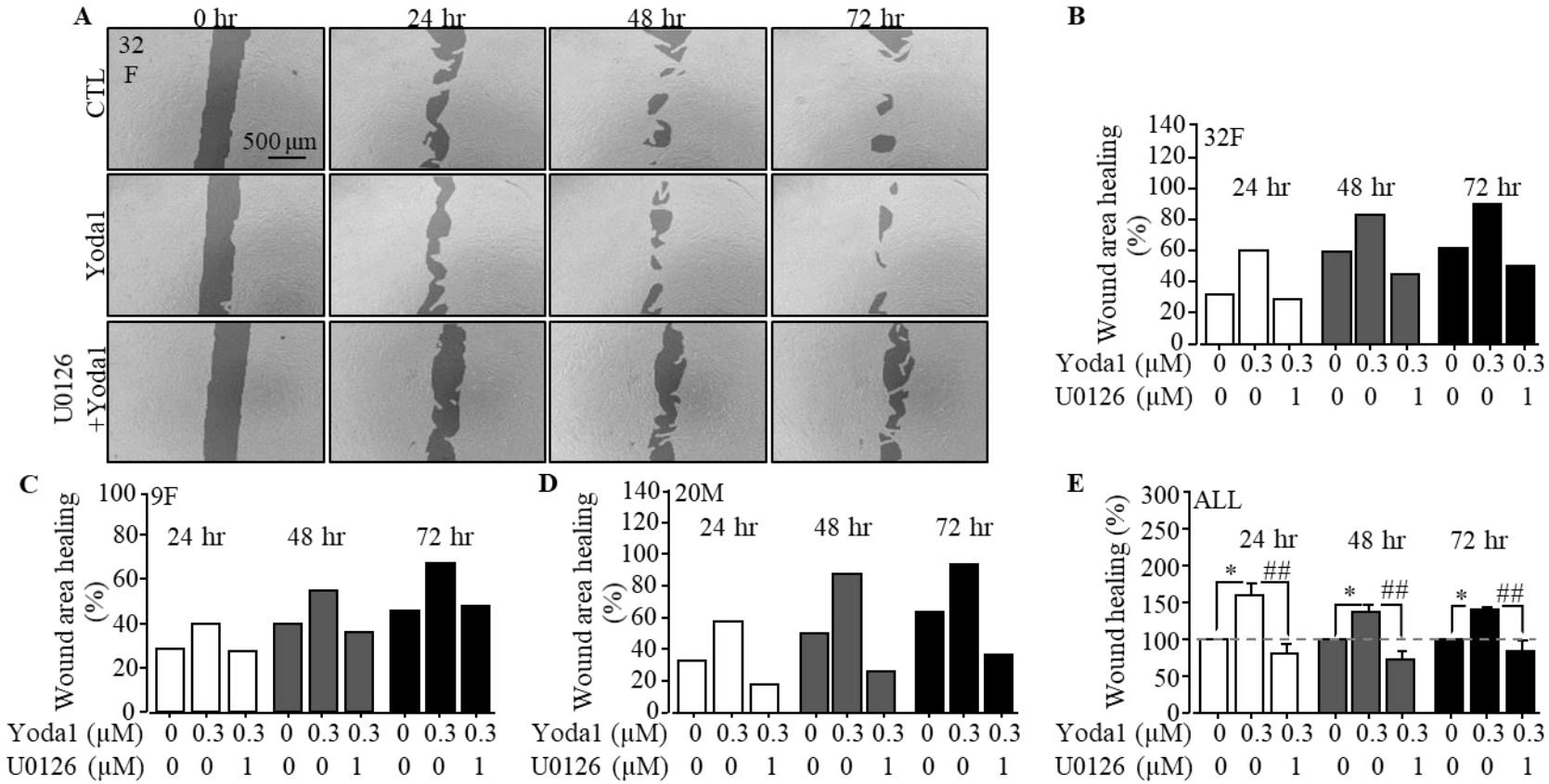

Figure 4. 14 Inhibition of Yoda1-induced hDP-MSC migration by U0126.

(A) Representative images showing wound areas at 24, 48 and 72 hours, using cells from 32F in the absence (CTL) and presence of 0.3 μM Yoda1 without or with prior treatment with 1 μM U0126. (B-D) Quantitative analysis of wound area healing using cells from 32F (N = 2 wells) (B), 9F (N = 2 wells) (C) and 20M (N = 2 wells) (D) in 1 set of experiment, under the same experimental concentrations as shown in A. (E) Summary of the mean wound narrowing, as percentage of that under control conditions at the same time points in parallel experiments, from 3 independent experiments using cells from 9F, 20M and 32F. *, $p < 0.05$ compared to control condition at the same time points; ##, $p < 0.01$ compared to cells exposed to Yoda1 alone at the same time points.

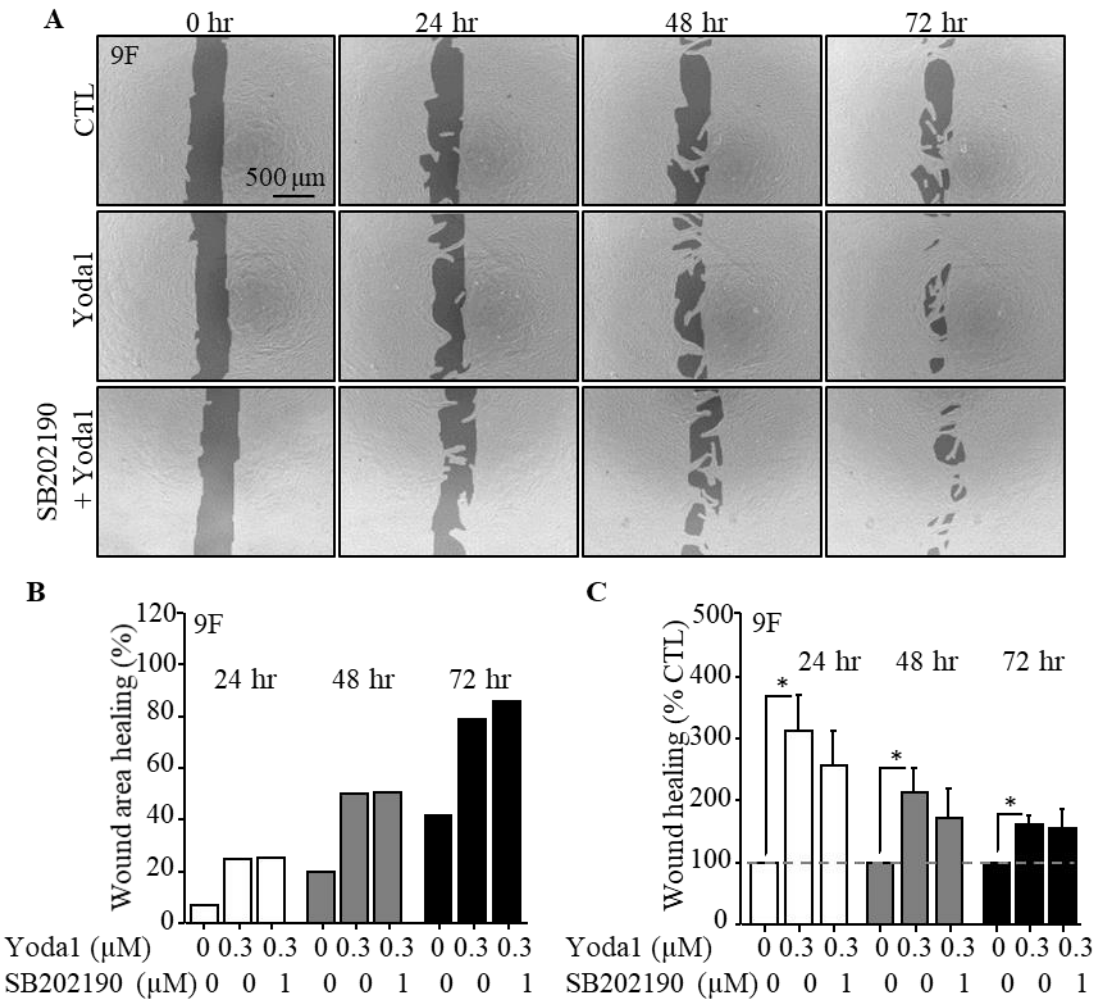

Figure 4. 15 No inhibition of Yoda1-induced hDP-MSC migration by SB202190.
(A) Representative images showing wound areas in wound healing assay at 0, 24, 48 and 72 hours, using cells from 9F in the absence (CTL) and presence of 0.3 µM Yoda1 without or with prior treatment with 1 µM SB202190, and (B) quantitative analysis of wound area healing at 24, 48 and 72 hours under the same experimental concentrations (N = 2 wells) in 1 set of experiment as shown in A. (C) Summary of the mean wound narrowing, as percentage of that under control conditions at the same time points in parallel experiments, from 3 independent experiments using cells from 9F. *, $p < 0.05$ compared to control condition at the same time points.

4.3 Discussion

The study described in this chapter has made several findings regarding the mechanosensitive Piezo1 channel in hDP-MSCs. First of all, the Piezo1 mRNA and protein expression are detected, and chemical activation of the Piezo1 channel results in Ca^{2+} influx leading to an increase in the $[Ca^{2+}]_i$. Secondly, Piezo1 channel activation stimulates cell migration. Thirdly, Piezo1 channel activation induces ATP release and subsequent activation of the P2 receptors. Finally, CaMKII, PKC, PYK2 and downstream MEK/ERK signalling pathways are engaged as Ca^{2+}-dependent signalling mechanisms in Piezo1 channel-mediated stimulation of cell migration.

My study provides clear evidence to support the expression of the Piezo1 channel in hDP-MSCs. The Piezo1 expression at the mRNA (Figure 4.1A-B) and protein level (Figure 4.1C) was detected in hDP-MSCs from all donors. Consistently, exposure to Yoda1 evoked robust increases in the $[Ca^{2+}]_i$ (Figure 4.1D) via extracellular Ca^{2+} influx (Figure 4.2). Yoda1-induced increase in the $[Ca^{2+}]_i$ was strongly inhibited by treatment with RR (Figure 4.3) and GsMTx4 (Figure 4.4). Furthermore, Yoda1-induced increases in the $[Ca^{2+}]_i$ were also significantly attenuated by siRNA-mediated knockdown of Piezo1 expression (Figure 4.6). These results from pharmacological and genetic interventions provide compelling evidence to show that the Piezo1 channel is functionally expressed on the cell surface with a significant role in mediating Ca^{2+} influx in hDP-MSCs. This finding is consistent with a recent study reporting expression of the Piezo1 channels in hBM-MSCs (Sugimoto et al., 2017). In addition to the Piezo1 channel being mainly localized in the plasma membrane (Coste et al., 2010; Miyamoto et al., 2014; Etem et al., 2018), there is some evidence to suggest that Piezo1 channel is also present in intracellular organelles such as ER (McHugh et al, 2010; McHugh et al, 2012). Furthermore, the Piezo1 channel was reported to regulate cell adhesion in epithelial cells by mediating ER Ca^{2+} release and subsequent activation of Ca^{2+}-activated calpain (McHugh et al., 2012).

Several studies show the role for the mechanically activated Piezo1 channel in regulating cell migration in CHO-α4WT cells (Hung et al., 2016), endothelial cells (Li et al., 2014), gastric cancer cells (Yang et al., 2014) and small cell lung cancer (McHugh et al., 2012).

The results present in this chapter demonstrated that hDP-MSC migration was significantly stimulated by exposure to 0.3 or 1 μM Yoda1 for 24-72 hours (Figure 4.7). Moreover, siRNA-mediated knockdown of Piezo1 expression significantly attenuated Yoda1-induced cell migration (Figure 4.8). These results suggest chemical activation of the Piezo1 channel stimulates hDP-MSC migration. Therefore, the present study together with recent studies from other researchers (Gao et al., 2017; Sugimoto et al., 2017) suggest that the Piezo1 channel plays an important role in regulating cell proliferation, osteogenesis and adipogenesis and migration of MSCs. A previous study by Yuan et al. (2012) reported that a low level of shear stress (0.2 pascals) induced hMSC migration in a wound healing assay. It remains to be established whether such mechanical stimulus is sufficient to activate the Piezo1 channel to stimulate cell migration in hDP-MSCs.

Our recent study (Peng et al., 2016) and the study described in chapter 3 have shown that ATP stimulates hDP-MSC migration by activation of P2 receptor-mediated purinergic Ca^{2+} signalling in hDP-MSCs. In the present study, treatment with P2 generic antagonist PPADS (Figure 4.9) or ATP scavenging enzyme apyrase (Figure 4.10) effectively prevented Yoda1-induced hDP-MSC migration. Neither treatment with PPADS (Figure 3.6 and Figure 4.9) nor apyrase in the absence of Yoda1 resulted in significant effect on cell migration (Figure 4.10). Taken together, these results provide strong evidence to support the hypothesis that activation of the Piezo1 channel induces ATP release and activation of P2 receptors. This is consistent with recent findings that Piezo1 channel mediates mechanical induction of ATP release and subsequent activation of P2 receptors in urothelial cells (Miyamoto et al., 2014), red blood cells (Cinar et al., 2016) and endothelial cells (Wang et al., 2016; Albarrán-Juárez et al., 2018). Previous studies reported that mechanical regulation of BM-MSC proliferation and differentiation is mediated by ATP release and subsequent activation of purinergic Ca^{2+} signalling mechanisms (Riddle et al., 2007; Sun et al., 2013; Weihs et al., 2014). It is interesting to investigate whether the Piezo1 channel plays a role in such mechanical regulation of MSC proliferation and differentiation via inducing ATP release and subsequent activation of purinergic Ca^{2+} signalling mechanisms.

Previous studies showed that mechanical stimulation induced an increase in the $[Ca^{2+}]_i$ and consequent activation of PYK2 and downstream MAPK signalling pathways in osteoblast-like cell proliferation (Boutahar et al., 2004). As discussed above in the Introduction section, recent studies have reported that activation of the Piezo1 channel induces proliferation of rDP-MSCs via the ERK downstream signalling pathway (Gao et al., 2017), and enhances osteogenic, while inhibiting adipogenic, differentiation of hBM-MSCs by stimulating the ERK and p38 kinase signalling pathways (Sugimoto et al., 2017). The present study showed pharmacological inhibition of CaMKII (Figure 4.11), PKC (Figure 4.12), PYK2 (Figure 4.13) and MEK/ERK (Figure 4.14), but not p38 kinase (Figure 4.15) strongly inhibited or completely prevented Yoda1-induced increase in cell migration, provide evidence to suggest critical engagement of these kinases as Ca^{2+}-dependent signalling mechanisms in Piezo1 channel-mediated stimulation of hDP-MSC migration. As shown in chapter 3, pharmacological intervention of these signalling molecules resulted in a similar inhibition of ATP-induced P2 receptor-mediated stimulation of hDP-MSC migration, highly consistent with the notion that activation of the Piezo1 channel induces ATP release and activation of P2 receptor and downstream Ca^{2+}-dependent signalling pathways in stimulating hDP-MSC migration.

As summarized in Figure 4.17, the results presented in this chapter provide evidence to show expression of the Piezo1 channel in hDP-MSCs and support the hypothesis that activation of the Piezo1 channel stimulates hDP-MSC migration via promoting ATP release and subsequent activation of P2 receptor-mediated purinergic Ca^{2+} signalling, CaMKII, PKC, PYK2 and MEK/ERK signalling mechanisms.

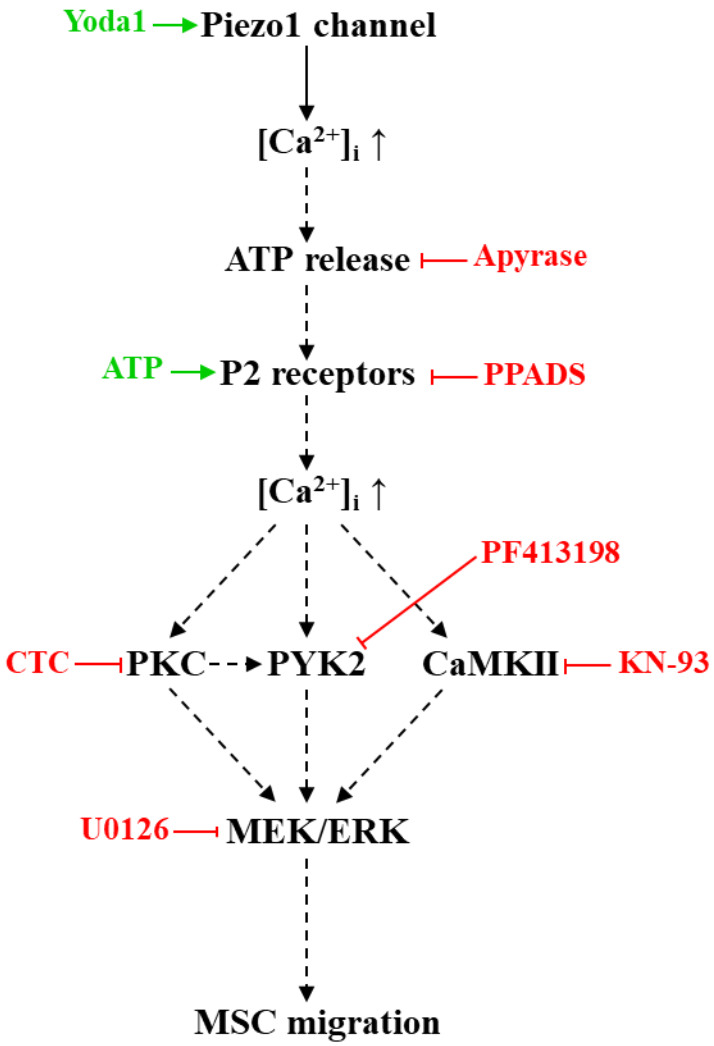

Figure 4.16 Proposed signalling mechanisms mediating Piezo1 channel-mediated stimulation of hDP-MSC migration.

Summary of the signalling mechanisms that mediate Piezo1 channel-dependent stimulation of hDP-MSC migration. Activation of the Piezo1 channel by Yoda1 induces ATP release and, in turn, ATP activates the P2 receptors (possibly P2X7, P2Y1, P2Y2 and/or P2Y11) to evoke an increase in the concentration of intracellular Ca^{2+} ($[Ca^{2+}]_i$), which induces activation of protein kinase C (PKC), protein tyrosine kinase 2 (PYK2) and Ca^{2+}/calmodulin-dependent protein kinase II (CaMKII). Activation of PYK2, PKC and/or CaMKII further triggers mitogen-activated protein kinase kinase/extracellular signal-regulated kinase (MEK/ERK). Activation of such signalling pathways is important in Yoda1-induced Piezo1-mediated increase in hDP-MSC migration. The activators and inhibitors used in my study to target various signalling molecules are highlighted in green and red, respectively.

CHAPTER 5

Expression of ATP-sensitive P2 receptors during adipogenesis of hDP-MSCs

5.1 Introduction

As discussed in the Introduction chapter (sections 1.5 and 1.6), the expression of the P2 purinergic receptors, both P2X and P2Y, and their roles in ATP-induced signalling mechanisms have been well documented in MSCs from different species and tissues. Our recent study supports a role for the P2X7, P2Y1, P2Y2, and P2Y11 receptors in mediating ATP-induced Ca^{2+} signalling in hDP-MSCs (Peng et al., 2016). MSCs are known to commit differentiation along different lineages, including adipogenesis. There is evidence to indicate changes in the expression of both P2X and P2Y receptors during adipogenic differentiation. For example, expression of the P2Y11 receptor at the mRNA and protein levels was increased after adipogenic differentiation of hAT-MSCs (Zippel et al., 2012). In rBM-MSCs cultured in adipogenic differentiation medium, the P2X7 mRNA and protein expression were down-regulated (Li et al., 2015b), whereas the P2Y2 mRNA expression was up-regulated (Li et al., 2016). There is evidence to suggest a significant role of the P2Y1, but not the P2X7, P2Y2 and P2Y11 receptors in ATP-induced stimulation of hBM-MSC adipogenic differentiation (Ciciarello et al., 2013). However, a recent study has proposed a role for the P2Y2 receptor in mediating UTP-induced adipogenic differentiation of rBM-MSCs (Li et al., 2016). Taken together, there is a noticeable discrepancy in the literature with respect to whether the expression of ATP-sensitive P2X and P2Y receptors changes during adipogenic differentiation of MSCs and the role they play in regulating adipogenic differentiation.

As discussed and demonstrated in previous chapters, intracellular Ca^{2+} acts as a second messenger mediating activation of various Ca^{2+}-dependent downstream signalling pathways. An earlier study showed that ATP-induced increases in the $[Ca^{2+}]_i$ in hBM-MSCs promoted activation and translocation of Ca^{2+}-dependent transcription factor NFAT from the cytoplasm into the nucleus to initiate expression of genes involved in the

regulation of adipogenic differentiation (Kawano et al., 2006). An earlier study reported that activation of CaMKII suppressed adipogenic differentiation and enhanced osteogenic differentiation of MSC-like cells, ST2 cells (Takada et al., 2007). A recent study has shown that pharmacological inhibition of CaMKII reduced lipid accumulation and expression of PPARγ and CEBPα during adipogenesis of pBM-MSCs (Zhang et al., 2018b). It was reported that inhibition of ERK promoted adipogenic differentiation of hBM-MSCs, while activation of ERK stimulated osteogenic differentiation (Jaiswal et al., 2000). However, a recent study suggests that activation of ERK, but not JNK or p38 kinase, downstream of UTP-induced activation of the P2Y2 receptor, mediates up-regulation of the early stage of adipogenic differentiation of rBM-MSCs (Li et al., 2016). Another study from the same group also shows that ERK and JNK, but not p38 kinase, play an important role in BzATP-induced P2X7-mediated down-regulation of adipogenic differentiation of rBM-MSCs (Li et al., 2015b). Clearly, more investigation is required to better understand the Ca^{2+}-dependent signalling mechanisms in extracellular nucleotide regulation of MSC adipogenic differentiation.

The study presented in this chapter aimed to understand how ATP regulates adipogenic differentiation of hDP-MSCs and the potential role of P2X and P2Y receptors in such regulation. I started with examining the expression of the P2X7, P2Y1, P2Y2 and P2Y11 receptors in hDP-MSCs. I, then, studied the effect of ATP on adipogenic differentiation and the expression of the aforementioned P2 receptors during adipogenic differentiation. Finally, I investigated the role of CaMKII and PYK2 in mediating ATP-induced adipogenic differentiation of hDP-MSCs.

5.2 Results

5.2.1 Purinergic agonists-induced Ca^{2+} responses in hDP-MSCs

The expression of P2X and ATP-sensitive P2Y receptors was firstly examined by measuring the intracellular Ca^{2+} responses to ATP and other purinergic agonists. Figure 5.1A-C illustrate the Ca^{2+} responses to 300 μM ATP in extracellular Ca^{2+}-containing solution in hDP-MSCs from 9F, 22M and 22M. ATP-induced Ca^{2+} responses, albeit some

variations in the amplitude and kinetics, were consistently observed in cells from all the three donors (Figure 5.1D). Treatment with 30 μM PPADS had no significant effect on the basal $[Ca^{2+}]_i$ but strongly reduced ATP-induced increase in the $[Ca^{2+}]_i$ in hDP-MSCs from all three donors (Figure 5.2).

I performed further experiments to compare ATP-induced Ca^{2+} responses in extracellular Ca^{2+}-containing and Ca^{2+}-free solutions to determine the contribution of P2X and P2Y receptors. There were some noticeable differences in ATP-induced Ca^{2+} responses. In hDP-MSCs from 9F, ATP evoked strong but transient Ca^{2+} responses in Ca^{2+}-free solution (Figure 5.3A). The peak amplitude of ATP-induced Ca^{2+} response was not significantly different in Ca^{2+}-containing and Ca^{2+}-free solutions, but the sustained ATP-induced Ca^{2+} response in Ca^{2+}-containing solution was significantly higher (Figure 5.3A and D). In contrast, the mean amplitude of both the peak and sustained ATP-evoked Ca^{2+} responses in Ca^{2+}-containing solution was significantly higher than in Ca^{2+}-free solution in hDP-MSCs from 20M (Figure 5.3B and E) and 22M (Figure 5.3C and F). These results are consistent with our recent study hosing various expression of ATP-sensitive P2 receptors in hDP-MSCs from different donors, including P2X7, P2Y1 and P2Y11 that represent the major receptors in ATP- Ca^{2+} responses (Peng et al., 2016).

I also measured the intracellular Ca^{2+} responses to BzATP, ADP and NF546 in extracellular Ca^{2+}-containing solution to further characterize the expression of P2X and P2Y receptors. As introduced in Introduction chapter (sections 1.2.2 and 1.2.3), BzATP activates the P2X7 receptor with greater potency than ATP, and it also activates the P2Y1 and P2Y11 receptors. ADP preferentially acts as an agonist at the P2Y1 receptor, and NF546 at the P2Y11 receptor. Exposure to 300 μM BzATP induced strong Ca^{2+} responses in hDP-MSCs from 9F, 20M and 22M (Figure 5.4). Moreover, parallel experiments show that the peak amplitude of BzATP-induced Ca^{2+} responses was significantly greater than that of ATP-induced Ca^{2+} responses in hDP-MSCs from all the three donors (Figure 5.4), consistent with the expression of the P2X7 receptor. I also compared BzATP-induced Ca^{2+} responses in Ca^{2+}-containing and Ca^{2+}-free solutions. BzATP induced measurable Ca^{2+} responses in Ca^{2+}-free solutions, supporting the expression of the P2Y1 and P2Y11

receptors. Overall, like ATP-induced Ca^{2+} responses, there were some variations in BzATP-induced Ca^{2+} responses in hDP-MSCs from different donors. In hDP-MSCs from 9F, the peak amplitude of BzATP-induced Ca^{2+} responses in Ca^{2+}-containing and Ca^{2+}-free solutions showed no significant difference, but the amplitude of the sustained component in Ca^{2+}-containing solution was significantly greater than in Ca^{2+}-free solution (Figure 5.5A and D). BzATP induced strong Ca^{2+} response in Ca^{2+}-containing solutions but very small Ca^{2+} responses in Ca^{2+}-free solutions in hDP-MSCs from 20M and 22M (Figure 5.5B and C). Exposure to 100 μM ADP consistently induced an increase in the $[Ca^{2+}]_i$ in and Ca^{2+}-containing solution in hDP-MSCs from 9F, 20M and 22M, supporting the expression of the P2Y1 receptor (Figure 5.6). Likewise, exposure to 10 μM NF546 readily induced strong Ca^{2+} responses in hDP-MSCs from 9F, 20M and 22M (Figure 5.7). Taken together, these results support that P2X7, P2Y1 and P2Y11 receptors are expressed, albeit with variations, in hDP-MSCs, as reported in our recent study (Peng et al., 2016).

5.2.2 Effect of ATP on adipogenic differentiation

I next carried out experiments to examine the effect of exposure to ATP on adipogenic differentiation of hDP-MSCs using cells from 9F and 22M. Cells were cultured for 21 days in basal medium and also in adipogenic differentiation medium without or with 30 μM ATP. Adipogenic differentiation was assessed using oil red O staining which shows red staining of lipid droplets found in adipocytes (Figure 5.8A-B). Determination of the DNA content, an indicator of cell number, showed that reduced cell growth or proliferation under adipogenesis-inducing conditions, and exposure to ATP further reduced cell growth (Figure 5.8C-D). As illustrated in Figure 5.8 A and B, there were more cells exhibiting oil red O staining under adipogenesis-inducing conditions and exposure to ATP noticeably increased oil red O staining, which were consistently observed in cells from both donors. Adipogenic differentiation was further analyzed by extracting oil red O stain and normalized by the DNA content or cell number (Figure 5.8E-G). Overall, the results clearly demonstrated that extracellular ATP can significantly enhance the adipogenic differentiation of hDP-MSCs.

5.2.3 Expression of the P2Y1, P2Y2, P2Y11 and P2X7 receptors in hDP-MSC after adipogenic differentiation

As mentioned above, there is evidence to show considerable changes in the expression of both P2X and P2Y receptors during adipogenic differentiation. I, therefore, performed real-time RT-PCR to determine the expression of P2X7, and all ATP-sensitive P2Y receptors, P2Y1, P2Y2 and P2Y11, in hDP-MSCs from 9F cultured in basal and adipogenic differentiation inducing media without or with 30 μM ATP, as described above for the experiments examining the effect of ATP on adipogenic differentiation. The mRNA expression for P2Y1, P2Y2, P2Y11 and P2X7 was detected. The P2Y1 mRNA level was significantly up-regulated in hDP-MSCs after adipogenic differentiation (Figure 5.9A-B). Conversely, the P2Y2 mRNA expression was strongly down-regulated in cells after cultured in adipogenic differentiation medium (Figure 5.9C-D). Exposure to ATP resulted in no further change in the mRNA expression level for the P2Y1 and P2Y2 receptors (Figure 5.9A-D). The P2Y11 mRNA expression remained unaltered in cells after cultured in adipogenic differentiation medium, but significantly up-regulated by exposure to ATP (Figure 5.9E-F). Finally, the P2X7 mRNA expression showed no significant change during adipogenic differentiation and remained the same after exposure to ATP (Figure 5.9G-H). These results show upregulation of the P2Y1 receptor, down-regulation of the P2Y2 receptor, and no change for the P2Y11 and P2X7 receptors during adipogenic differentiation of hDP-MSCs and that ATP up-regulates the P2Y11 receptor without no effect on the P2Y1, P2Y2 and P2X7 receptors.

5.2.4 Effects of PYK2 and CaMKII inhibitors on ATP-induced up-regulation of adipogenic differentiation

Recent studies have shown that purinergic Ca^{2+} signalling can regulate MSC adipogenic differentiation via activation of downstream Ca^{2+}-dependent signalling pathways (Li et al., 2015b; Li et al., 2016). I was interested in the role of PYK2 and CaMKII in mediating ATP-induced up-regulation of adipogenic differentiation of hDP-MSCs. Figure 5.10A illustrates representative images showing oil red O staining of hDP-MSCs from 9F incubated in basal medium and adipogenic differentiation inducing medium and treated with 10 nM PF431396, prior to and during exposure to 30 μM ATP. Treatment with

PF431396 slightly increased the DNA content or cell growth (Figure 5.10B), and reduced oil red O staining in cells after cultured in adipogenic differentiation inducing medium in the presence of ATP (Figure 5.10A). Similar results were obtained with cells from 22M (Figure 5.10C). Figure 5.10D summarizes the mean data from 9F and 22M from 3 independent experiments and show that treatment with PF431396 significantly attenuated ATP-induced up-regulation of adipogenesis. Likewise, as shown for hDP-MSCs from 9F (Figure 5.11A and B) and 22M (Figure 5.11C) and the mean data from both donors from 3 independent experiments (Figure 5.11D), treatment with 0.3 μM KN-93, prior to and during exposure to ATP, reduced ATP-induced increase in adipogenic differentiation. These results suggest an important role of PYK2 and CaMKII in mediating ATP-induced upregulation of adipogenic differentiation of hMSCs.

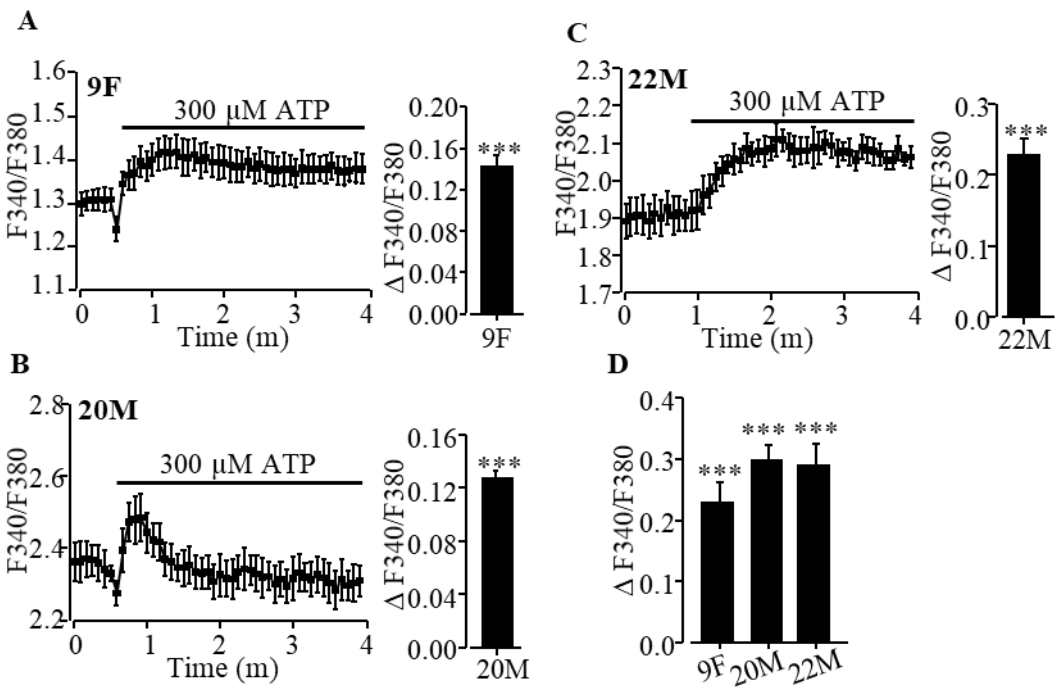

Figure 5.1 ATP-induced intracellular Ca^{2+} responses in hDP-MSCs.
(A-C) Representative recordings of the change in F340/F380 (the $[Ca^{2+}]_i$) by 300 μM ATP in extracellular Ca^{2+}-containing solution from (left) 9F (N = 4 wells) (A), 20M (N = 4 wells) (B) and 22M (N = 4 wells) (C) and summary of the mean maximum change in the $[Ca^{2+}]_i$ induced by ATP in cells for each donor (right) from 4 wells in 1 set of experiment. (D) Summary of the mean changes in the $[Ca^{2+}]_i$ in 6 independent experiments for cells from each donor. ***, $p < 0.001$ indicates significant increase in the Ca^{2+} responses after addition of ATP.

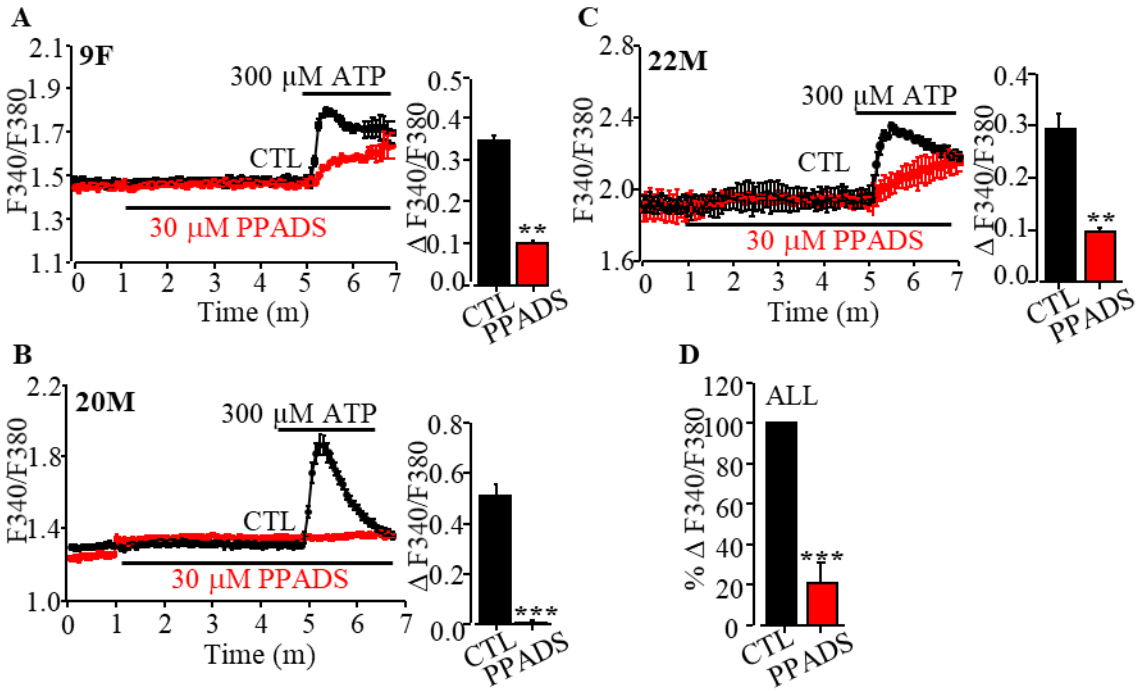

Figure 5.2 Inhibition by PPADS of ATP-induced increase in the $[Ca^{2+}]_i$ in hDP-MSCs.
(A-C) Representative recordings of the change in F340/F380 (the $[Ca^{2+}]_i$) induced by 300 µM ATP in cells pre-treated with (red) and without (black) 30 µM PPADS (left) from 9F (N = 4 wells) (A), 20M (N = 4 wells) (B) and 22M (N = 4 wells) (C), and summary of the mean maximum change in the $[Ca^{2+}]_i$ induced by ATP in cells for each donor (right) from 4 wells in 1 set of experiment. (D) Summary of the mean percentage of inhibition by PPADS in 5 independent experiments from all three donors. **, $p < 0.01$, ***, $p < 0.001$ compared to control cells treated with ATP alone.

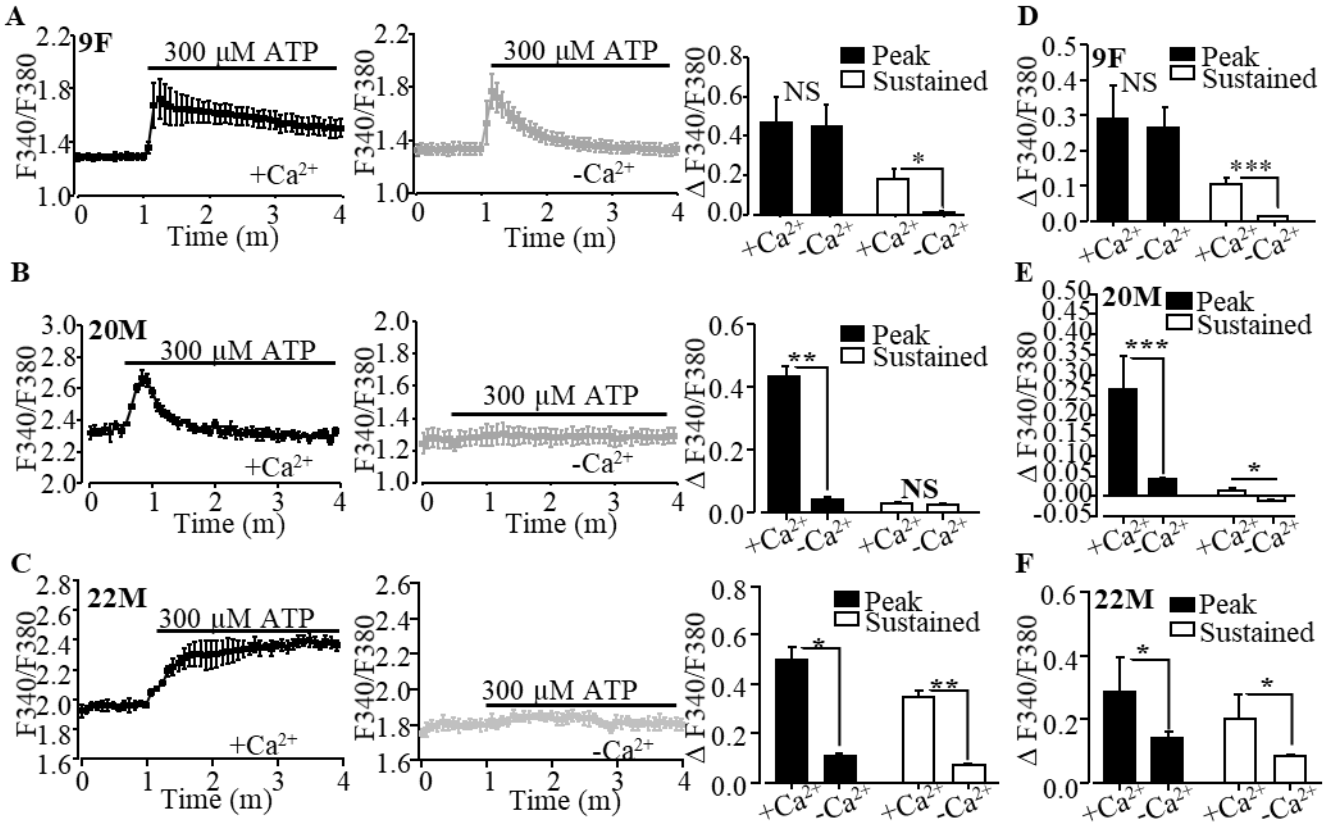

Figure 5.3 ATP-induced intracellular Ca^{2+} responses in extracellular Ca^{2+}-free solution in hDP-MSCs.

(A-C) Representative recordings of the change in F340/F380 (the $[Ca^{2+}]_i$) induced by 300 μM ATP in extracellular Ca^{2+}-containing and Ca^{2+}-free solutions (left) from 9F (N = 4 wells) (A), 20M (N = 4 wells) (B) and 22M (N = 4 wells) (C), and summary of the mean maximum change in the $[Ca^{2+}]_i$ in cells for each donor (right) from 4 wells in 1 set of experiment. (D-F) Summary of the average change in the $[Ca^{2+}]_i$ induced by ATP in cells in extracellular Ca^{2+}-containing and Ca^{2+}-free solutions in 3 independent experiments for each of the 9F (D), 20M (E) and 22M (F). *, $p < 0.05$, ***, $p < 0.001$ compared Ca^{2+} responses in extracellular Ca^{2+}-containing and Ca^{2+}-free solutions at the same time points. NS, no significant difference.

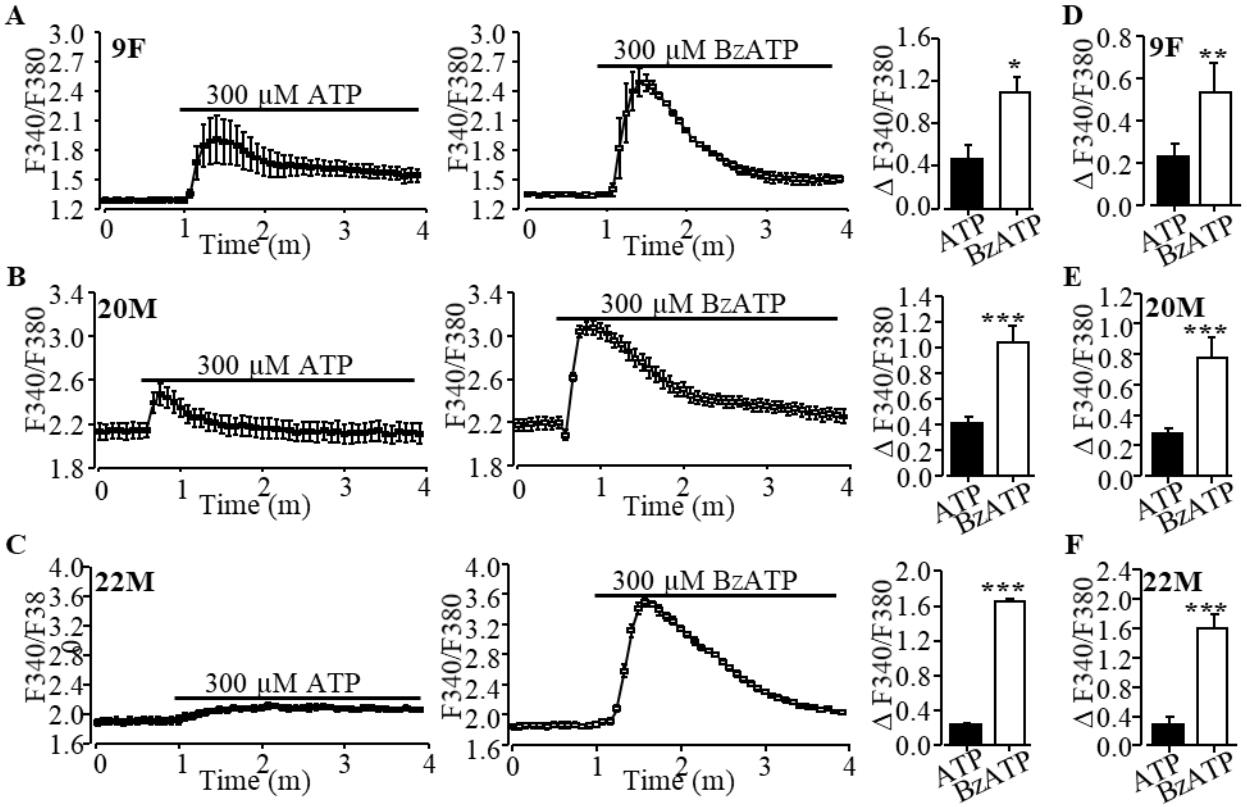

Figure 5.4 BzATP-induced intracellular Ca^{2+} responses in hDP-MSCs.
(A-C) Representative recordings of the changes in F340/F380 (the $[Ca^{2+}]_i$) by 300 μM ATP and BzATP in extracellular Ca^{2+}-containing solution from (left) 9F (N = 4 wells) (A), 20M (N = 4 wells) (B) and 22M (N = 4 wells) (C), and summary of the mean maximum change in the F340/F380 in cells for each donor (right) from 4 wells in 1 set of experiment. (D-F) summary of the changes in the $[Ca^{2+}]_i$ induced by ATP and BzATP in 6 independent experiments for 9F (D), 9 independent experiments for 20M (E) and 7 independent experiments for 22M (F). *, $p < 0.05$, **, $p < 0.01$, ***, $p < 0.001$ compared to ATP.

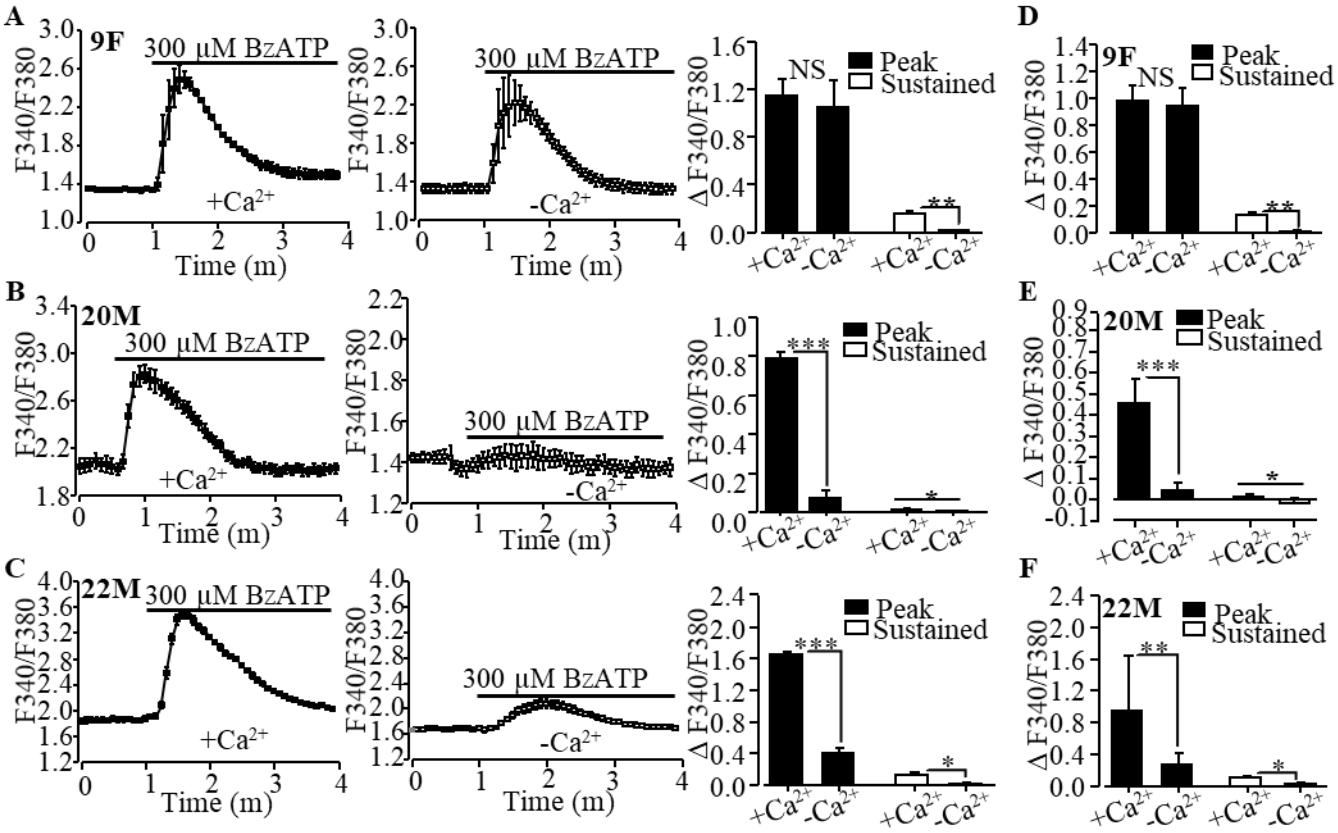

Figure 5.5 BzATP-induced intracellular Ca^{2+} responses in the presence and absence of extracellular Ca^{2+} in hDP-MSCs.
(A-C) Representative recordings of the change in F340/F380 ($[Ca^{2+}]_i$) induced by 300 μM BzATP in extracellular Ca^{2+}-containing and Ca^{2+}-free solutions (left) from 9F (N = 4 wells) (A), 20M (N = 4 wells) (B) and 22M (N = 4 wells) (C), and summary of the mean maximum change in the $[Ca^{2+}]_i$ in cells for each donor (right) from 4 wells in 1 set of experiment. (D-F) Summary of the average change in the $[Ca^{2+}]_i$ induced by BzATP in cells in extracellular Ca^{2+}-containing and Ca^{2+}-free solutions in 4 independent experiments for the 20M (E), and 2 independent experiments for each of the 9F (D) and 22M (F). *, $p < 0.05$, **, $p < 0.01$, ***, $p < 0.001$ compared Ca^{2+} responses in Ca^{2+}-containing and Ca^{2+}-free solutions at the same time points. NS, no significant difference.

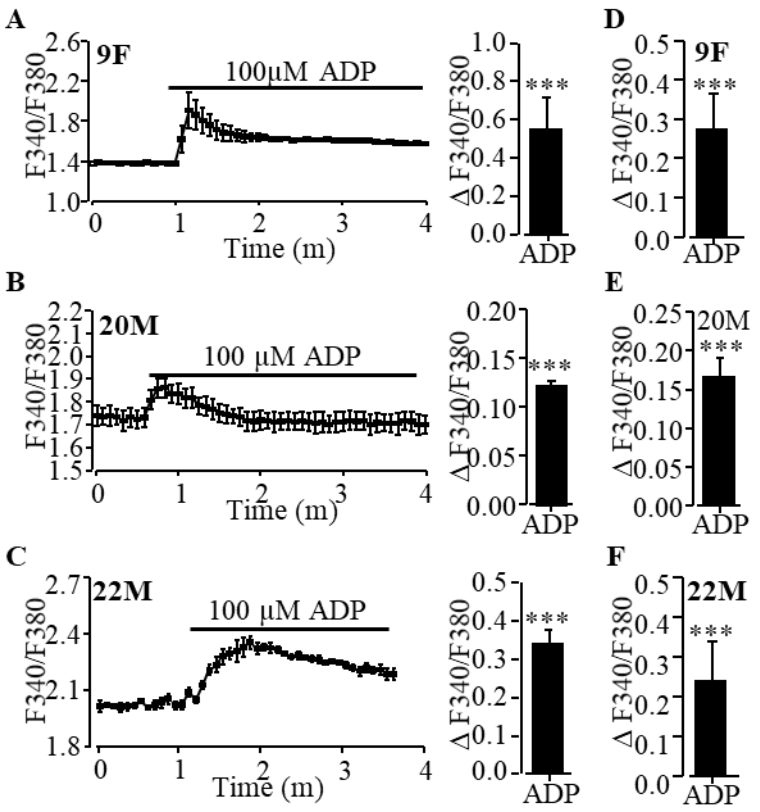

Figure 5.6 ADP-induced intracellular Ca^{2+} responses in hDP-MSCs
(A-C) Representative recordings of the change in F340/F380 (the $[Ca^{2+}]_i$) induced by 100 μM ADP in extracellular Ca^{2+}-containing solutions (left) from 9F (N = 4 wells) (A), 20M (N = 4 wells) (B) and 22M (N = 4 wells) (C), and summary of the mean maximum change in the $[Ca^{2+}]_i$ in cells for each donor (right) from 4 wells in 1 set of experiment. (D-F) Summary of ADP-induced changes in the $[Ca^{2+}]_i$ from 4 independent experiments for the 9F (D) and 20M (E), and 2 experiments for the 22M (F). ***, $p < 0.001$ indicates a significant increase in the $[Ca^{2+}]_i$ after addition of ADP.

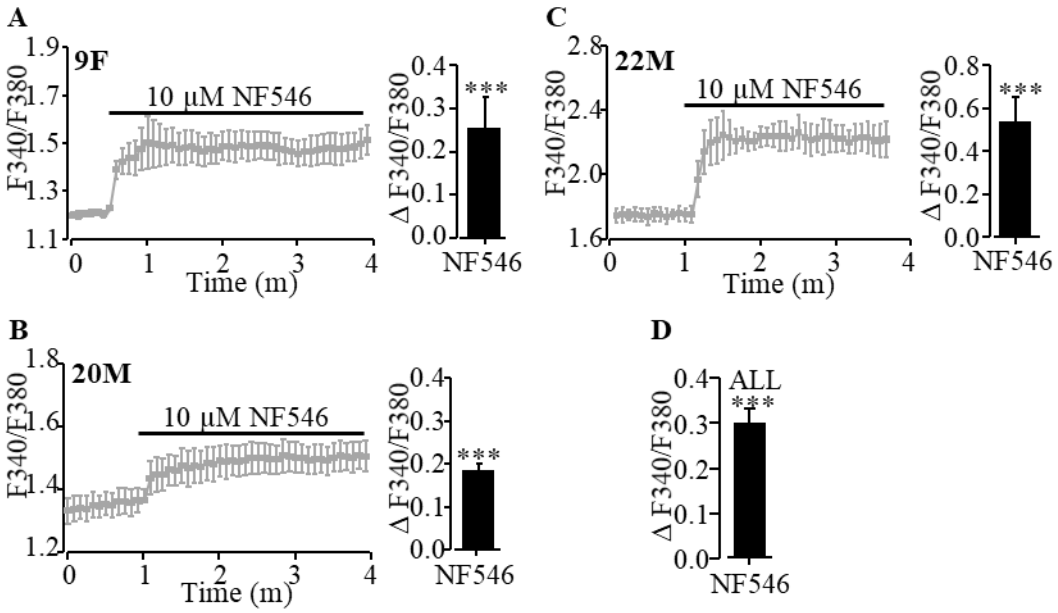

Figure 5.7 NF546-induced intracellular Ca^{2+} responses in hDP-MSCs.
(A-C) Representative recordings of the change in F340/F380 (the $[Ca^{2+}]_i$) induced by 10 μM NF546 in extracellular Ca^{2+}-containing solutions (left) from 9F (N = 4 wells) (A), 20M (N = 4 wells) (B), 22M (N = 4 wells) (C), and summary of the mean maximum change in the $[Ca^{2+}]_i$ in cells for each donor (right) from 4 wells in 1 set of experiment. (D) Summary of NF546-induced changes in the $[Ca^{2+}]_i$ in 5 independent experiments for hDP-MSCs from all three donors; 9F, 20M and 22M. ***, $p < 0.001$ indicates a significant increase in the $[Ca^{2+}]_i$ after addition of NF546.

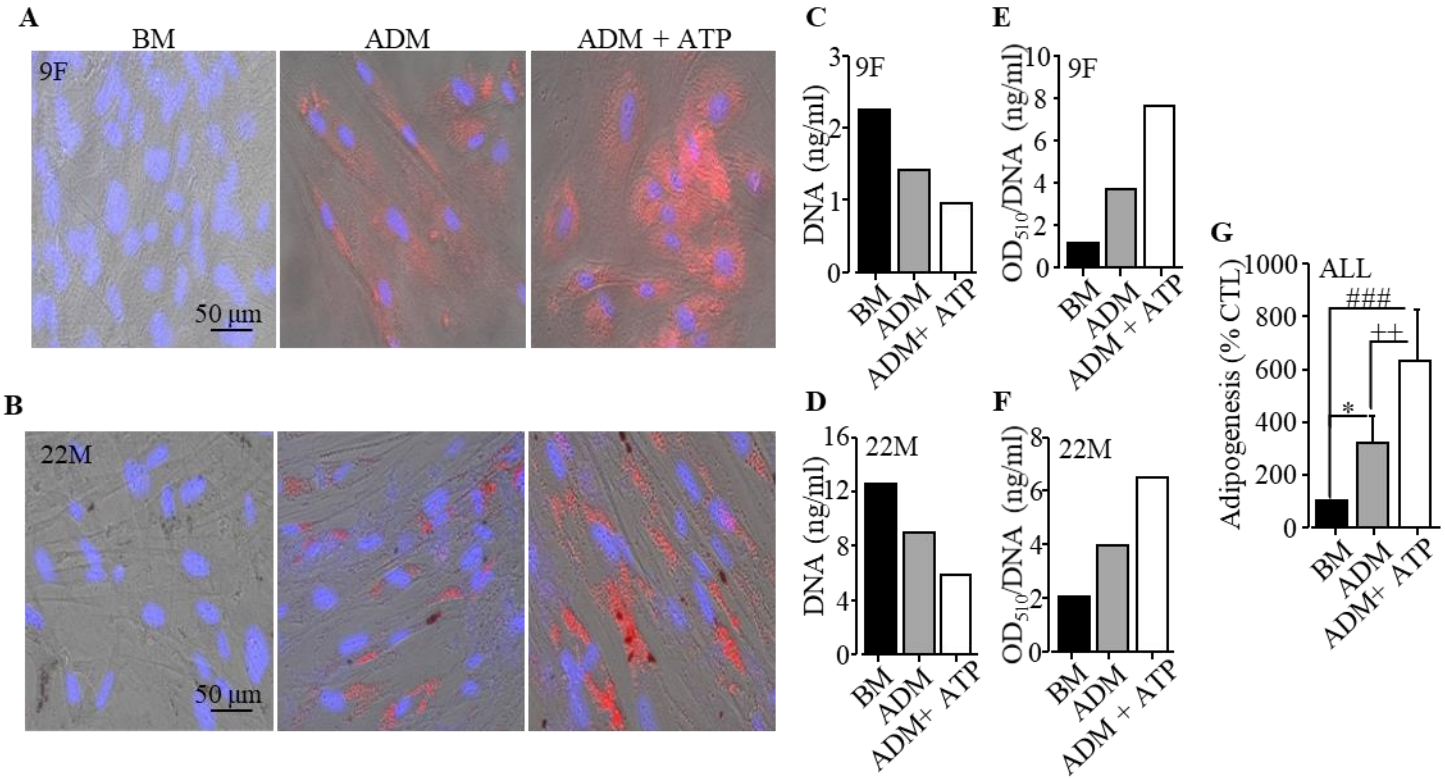

Figure 5.8 Effect of ATP on adipogenic differentiation of hDP-MSCs.
(A-B) Representative images showing typical oil red O staining (fat droplets in red indicating fat-containing adipocytes) and Hoechst 33342 staining (nuclei in blue) after cells (A: 9F and B: 22M) cultured for 21 days in basal medium (BM) and adipogenic differentiation medium (ADM) with or without 30 µM ATP. (C-D) Summary of the DNA content (ng/ml) in cells (C: 9F and D: 22M) cultured in the indicated conditions in 1 set of experiment. (E-F) Summary of oil red O staining determined by the OD_{510} value normalized by the DNA content (ng/ml) related to the number of cells (E: 9F and F: 22M) under the conditions indicated in 1 set of experiment. (G) Summary of adipogenic differentiation of hDP-MSCs in ADM with or without ATP as compared to cells in BM for 4 independent experiments from 9F and 22M. *, $p < 0.05$ compared to ADM. ###, $p < 0.001$ compared to ADM and ATP. ++, $p < 0.01$ compared to ATP.

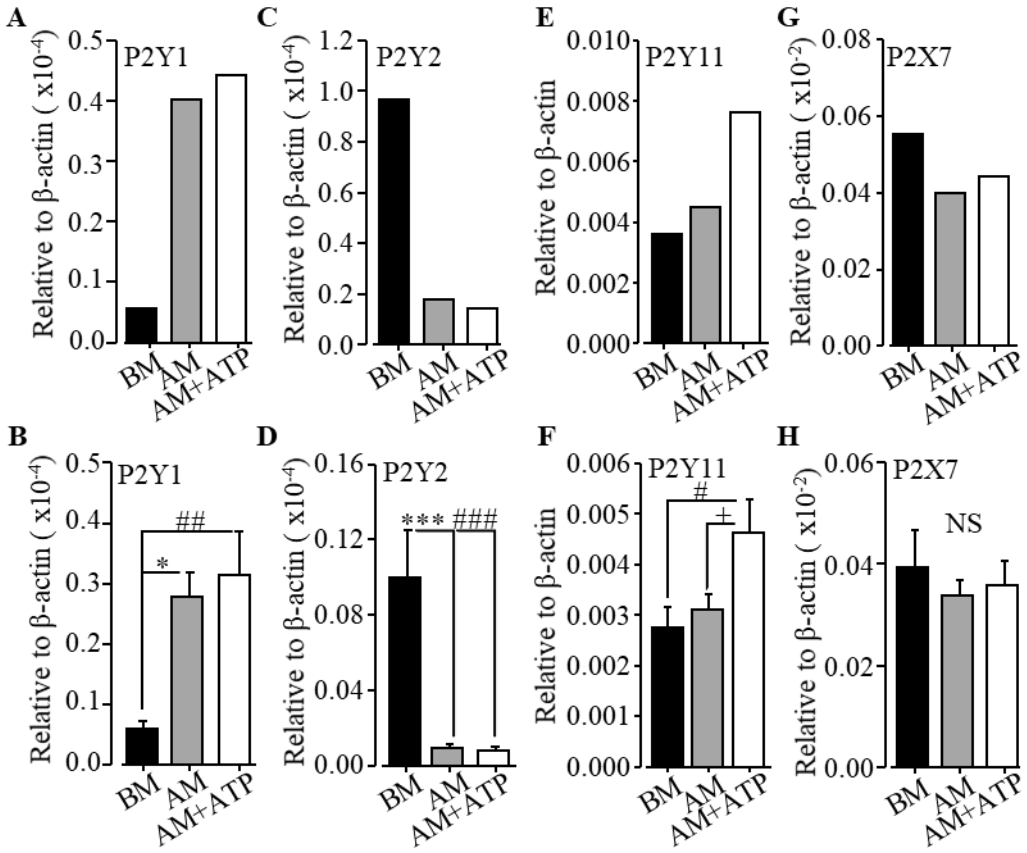

Figure 5.9 The mRNA expression of P2Y1, P2Y2, P2Y11 and P2X7 during adipogenic differentiation of hDP-MSCs.
Real-time RT-PCR analysis of the mRNA expression for P2Y1 (A), P2Y2 (C), P2Y11 (E) and P2X7 (G) receptors relative to that of β-actin from 2 wells in 1 set of experiment using 9F cells under indicated conditions. Summary of the mean mRNA expression levels of P2Y1 (B), P2Y2 (D), P2Y11 (F) and P2X7 (H) receptors/β-actin from 4 independent mRNA preparations from 9F cells. *, $p < 0.05$, *, $p < 0.05$, ***, $p < 0.001$ compared to control cells in BM. #, $p < 0.05$, ##, $p < 0.01$, ###, $p < 0.001$ compared to cells in ADM treated with ATP. +, $p < 0.05$ compared to ATP. NS, no significant difference. BM, basal medium, ADM, adipogenic differentiation medium.

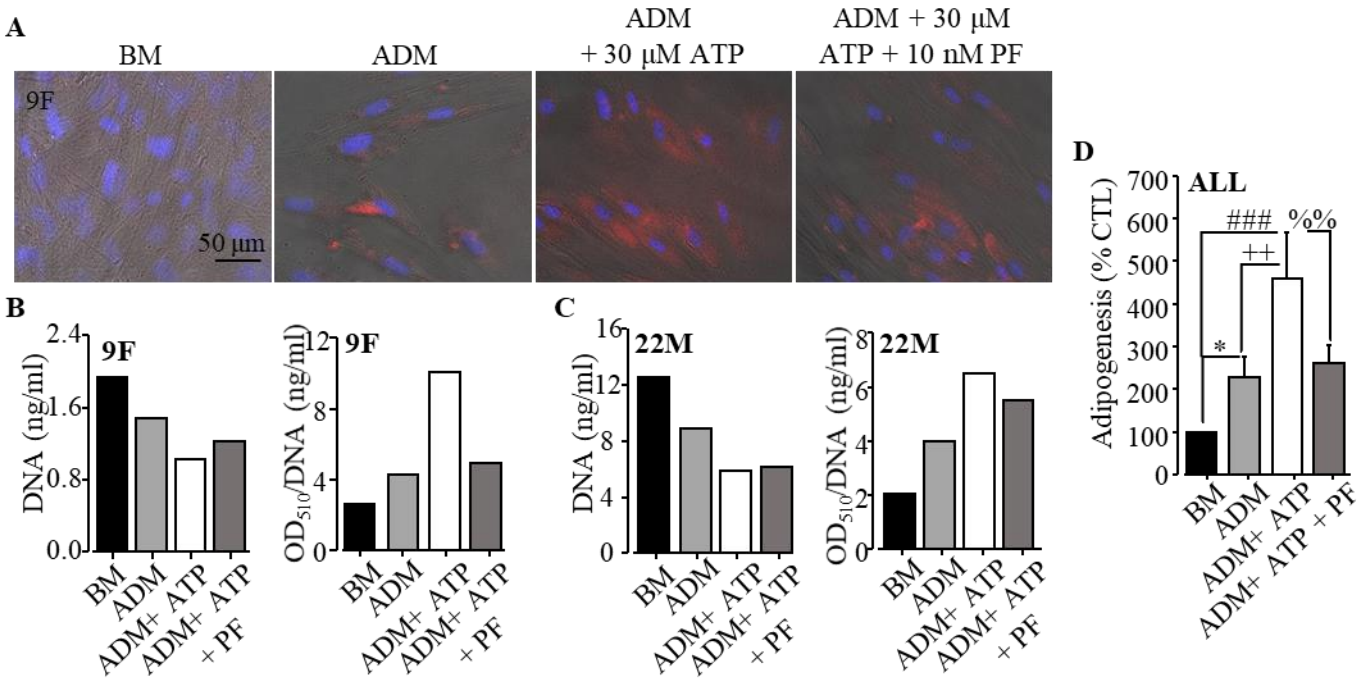

Figure 5.10 Effect of inhibiting PYK2 on adipogenic differentiation of hDP-MSCs.
(A) Representative images showing typical oil red O staining (fat droplets in red indicating fat-containing cells) and Hoechst 33342 staining (nuclei in blue) after hDP-MSCs from 9F donor cultured for 21 days in basal medium (BM) and adipogenic differentiation medium (ADM) without or with 30 µM ATP or together with 10 nM PF431396. (B-C) Summary of the DNA content and summary of the oil red O staining determined by the OD_{510} value per DNA (ng/ml) in cells (B: 9F and C: 22M) under the indicated conditions in 1 set of experiment. (D) Summary of adipogenic differentiation of hDP-MSCs under indicated conditions from 3 independent experiments from 9F and 22M. *, $p < 0.05$ compared to control cells in BM. ###, $p < 0.001$ compared to cells in ADM treated with ATP. ++, $p < 0.01$ compared to ATP. %%, $p < 0.01$ compared to cell treated with PF431396.

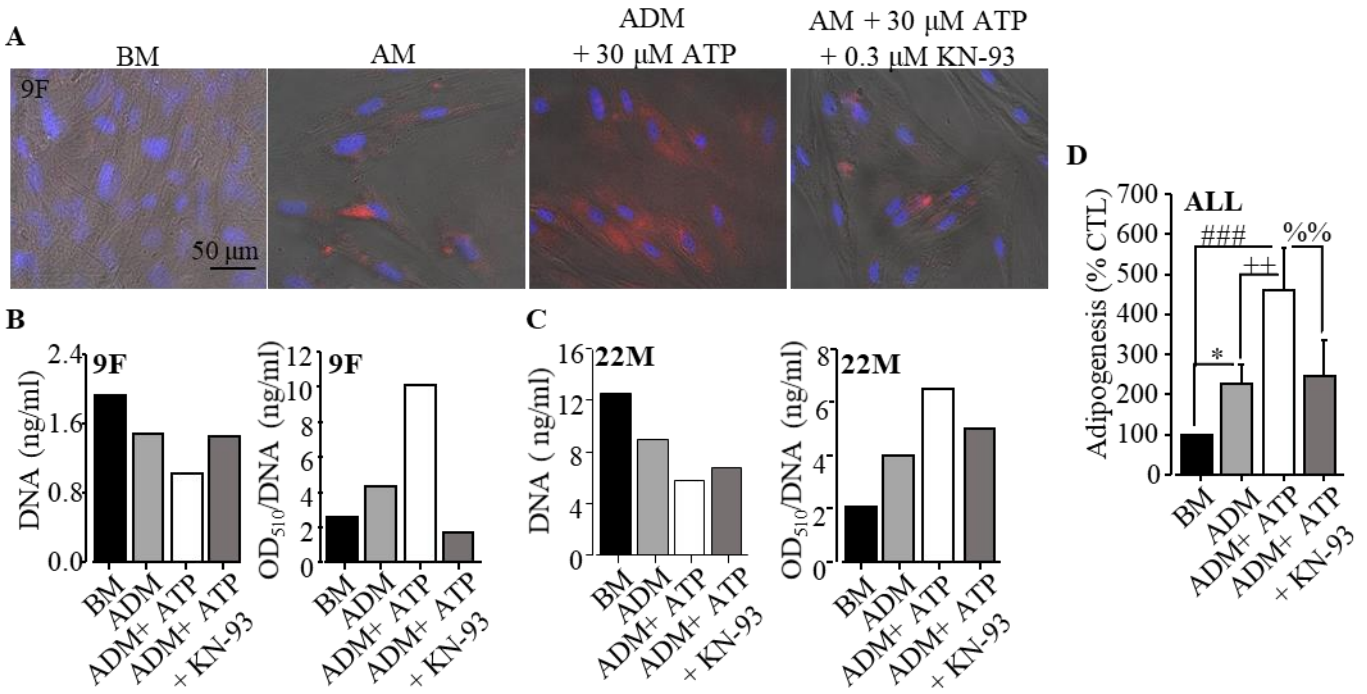

Figure 5.11 Effect of inhibiting CaMKII on adipogenic differentiation of hDP-MSCs.
(A) Representative images showing typical oil red O staining (fat droplets in red indicating fat-containing cells) and Hoechst 33342 staining (nuclei in blue) after hDP-MSCs from 9F donor cultured for 21 days in basal medium (BM) and adipogenic differentiation medium (ADM) without or with 30 µM ATP or together with 0.3 µM KN-93. (B-C) Summary of the DNA content (ng/ml) and summary of the oil red O staining determined by the OD_{510} value per DNA (ng/ml) in cells (B: 9F and C: 22M) under the indicated conditions in 1 set of experiment. (D) Summary of adipogenic differentiation of hDP-MSCs under indicated conditions from 3 independent experiments from 9F and 22M donors. *, $p < 0.05$ compared to control cells in BM. ###, $p < 0.001$ compared to cells in ADM treated with ATP. ++, $p < 0.01$ compared to ATP. %%, $p < 0.01$ compared to cell treated with KN-93.

5.3 Discussion

The results described in this chapter provide evidence to support that the P2Y1, P2Y2, P2Y11 and P2X7 receptors are expressed in hDP-MSCs and that the P2Y1, P2Y11 and P2X7 receptors are engaged in ATP-induced Ca^{2+} signalling, with variations among three donors, 9F, 20M and 22M. Based on the cells from one donor, 9F, the P2Y1 expression is up-regulated and the P2Y2 expression is down-regulated, whereas the expression of P2Y11 and P2X7 remain unchanged after adipogenic differentiation; exposure to ATP during adipogenic differentiation enhanced the P2Y11 expression without effect on the other three receptors. ATP enhanced adipogenic differentiation, depending on the activation of PYK2 and CaMKII in hDP-MSCs from two donors, 9F and 22M.

Similar to previous studies on MSCs from other tissues or origins (Zippel et al., 2012; Ferrari et al., 2011), the present study showed that ATP induced robust increases in the $[Ca^{2+}]_i$ in extracellular Ca^{2+}-containing solution in hDP-MSCs (Figure 5.1). ATP-induced Ca^{2+} responses were, however, noticeably different among three donors examined, being sustained in cells from 9F and 22M (Figure 5.1A and C) and much transient in cells from 20M (Figure 5.1B). Regardless, ATP-induced Ca^{2+} responses were strongly inhibited by treatment with PPADS (Figure 5.2), supporting the importance of P2 receptors in mediating such ATP-induced Ca^{2+} signalling in hDP-MSCs.

As discussed in the Introduction chapter, ATP can increase the $[Ca^{2+}]_i$ through the P2X and P2Y receptors (Figure 1.5). ATP-induced Ca^{2+} responses in Ca^{2+}-containing solution, albeit variable responses among donors, were greater in amplitude and/or more sustained in kinetics than those in Ca^{2+}-free solution in hDP-MSCs (Figure 5.3), suggesting expression of the P2X receptors and/or CRAC channels with a significant role in ATP-induced Ca^{2+} influx (Peng et al., 2016). BzATP, known to be more potent than ATP at the P2X7 receptor (Jarvis and Khakh, 2009), induced significantly stronger Ca^{2+} responses in Ca^{2+}-containing solution than ATP at the same concentration (300 μM) in Ca^{2+}-containing solution in cells from all three donors (Figure 5.4), consistent with expression of the P2X7 receptor. BzATP can also activate the P2Y1 (Ilatovskaya et al., 2013) and P2Y11 receptors (Communi et al., 1999), and

evoked considerable Ca^{2+} responses in cells from all three donors in Ca^{2+}-free solutions (Figure 5.5). Both ADP, preferentially activating the P2Y1 receptor (Lambrecht, 2000; Burnstock, 2007; Jacobson et al., 2015), and NF546, a P2Y11-selective agonist (Meis et al., 2010), induced substantial Ca^{2+} responses in Ca^{2+}-containing solutions in hDP-MSCs from all three donors (Figure 5.6 and Figure 5.7). These results obtained using hDP-MSC from multiple donors provide further evidence to support the expression of the P2Y1, P2Y11 and P2X7 receptors in hDP-MSCs and their contribution in ATP-induced Ca^{2+} signalling (Peng et al., 2016).

An important finding from the present study is that exposure to ATP during adipogenic differentiation of hDP-MSCs from 9F and 22M donors significantly increased fat droplet formation (Figure 5.8), indicating that ATP stimulates adipogenic differentiation, consistent with the previous study examining ATP-pretreated hBM-MSCs cultured in adipogenic differentiation medium (Ciciarello et al., 2013). Real-time RT-PCR analysis of the expression of the P2Y1, P2Y2, P2Y11 and P2X7 receptors in hDP-MSCs from 9F donor after adipogenic differentiation, revealed an increase in the P2Y1 expression, a decrease in the P2Y2 expression, and no alteration in the expression of the P2Y11 and P2X7 receptors, in comparison to non-induced hDP-MSCs (Figure 5.9). These results strongly support the notion that the expression of the P2X and/or P2Y receptors changes during adipogenic differentiation (Zippel et al., 2012; Li et al., 2015b; Li et al., 2016). For example, in adipogenesis inducing medium, mRNA expression of the P2Y2 receptor was up-regulated in rBM-MSCs (Li et al., 2016), P2Y11 receptor was up-regulated in hAT-MSCs (Zippel et al., 2012), and P2X7 receptor was down-regulated in rBM-MSCs (Li et al., 2015b). Such discrepancies could be attributed to different species and origins of MSC preparations. In the present study, exposure to ATP during adipogenic differentiation significantly up-regulated the P2Y11 mRNA expression in hDP-MSCs from 9F donor, without effect on the mRNA expression of the P2Y1, P2Y2 and P2X7 receptors, in comparison to hDP-MSCs cultured in adipogenesis inducing medium in the absence of application of exogenous ATP (Figure 5.9). A recent study also reported that UTP exposure had no effect on the P2Y2 expression in rBM-MSCs during adipogenic differentiation (Li et al., 2016).

Another noticeable finding from the present study is to reveal the role of PYK2 and CaMKII in ATP-induced up-regulation of adipogenic differentiation of hDP-MSCs. The present study showed that pharmacological inhibition of PYK2 reduced ATP-induced stimulation of adipogenic differentiation of hDP-MSCs, suggesting that activation of PYK2 enhanced adipogenic differentiation (Figure 5.10). It was reported that hMSCs transfected by adenovirus-expressing PYK2-targeted short-hairpin RNA or catalytically inactive PYK2 mutant increased osteogenic differentiation (Buckbinder et al., 2007), suggesting that activation of PYK2 suppress osteogenic differentiation of MSCs. It is known that adipogenesis and osteogenesis of MSC are mutually excluded (Chen et al., 2016). The present and previous studies are thus consistent with the notion that activation of PYK2 stimulates adipogenesis and suppresses osteogenesis. The present study also found that pharmacological inhibition of CaMKII reduced ATP-induced stimulation of adipogenic differentiation of hDP-MSCs (Figure 5.11). A recent study reports that pharmacological inhibition of CaMKII reduced lipid accumulation and expression of PPARγ and CEBPα during adipogenesis of pBM-MSCs (Zhang et al., 2018b). However, an earlier study reported that Ca^{2+}/CaMKII suppressed adipogenic differentiation and promoted osteogenic differentiation of MSC-like cells, ST2 (Takada et al., 2007). Evidently, further investigations are required to better understand the role of CaMKII in regulating differentiation of MSCs including adipogenesis.

In summary, the present study shows that ATP enhances adipogenesis of hDP-MSC, accompanied with changes in the expression of P2Y1, P2Y2 and P2Y11 receptors and suggests an important role for PYK2 and CaMKII in mediating ATP-stimulated adipogenic differentiation of hDP-MSCs. Such information should help to better understand the signalling pathways determining and regulating the differentiation of MSCs.

CHAPTER 6

General discussion and conclusions

MSCs are multipotent adult stem cells that reside in a diversity of tissues, such as bone marrow, umbilical cord, adipose tissue and dental pulp (Liu et al., 2009; Kaebisch et al., 2015; Sudulaguntla et al., 2016). Thus, MSCs have highly desirable attributes such as wide access to tissues, ease isolation and expansion *in vitro*. In addition, MSCs have a multitude of the functional properties, including the ability of migrating and homing to the site of injury, differentiating into multiple cell types, secreting stimulatory molecules to facilitate regeneration or recovery of injured tissues, modulating the immune response, and lacking immunogenicity (Wang et al., 2012). Altogether, MSCs provide promising cell sources for regeneration medicines, including tissue engineering and cell-based therapy (Ghoraishizadeh et al., 2014). However, translational uses of MSCs remain inefficacious in part due to their limited capability of migrating and homing to the target sites (Liu et al., 2009; Rombouts and Ploemacher, 2003; Maijenburg et al., 2012). It is known that the stem cell niches in tissues provide essential extrinsic signals and associated intrinsic signalling mechanisms to support the stem cell functions (Ghoraishizadeh et al., 2014), but the current knowledge towards such signalling mechanisms in stem cells including MSCs is limited. A better understanding of the signalling mechanisms determining or regulating hMSC functions will facilitate applications of hMSCs in regenerative medicines. Intracellular Ca^{2+} is a ubiquitous signalling molecule in determining or regulating a wide arrange of cell functions. Thus, extracellular chemical, physical and biological signals are transduced via specified receptors to an intracellular Ca^{2+} signal and thereby activation of intrinsic signalling mechanisms (Bootman, 2012; Kim et al., 2015; Artemenko et al., 2018). The studies presented in this thesis examined the Ca^{2+} signalling mechanisms and downstream Ca^{2+}-dependent signalling pathways, and their roles in regulating migration and differentiation in hDP-MSCs. This chapter will summarize the key findings and discuss the future directions.

6.1 General discussion

6.1.1 Ca^{2+} signalling mechanisms in ATP-induced cell migration

Extracellular ATP is a well-known signalling molecule leading to an increase in the $[Ca^{2+}]_i$ by activating ligand-gated ion channel P2X receptors to mediate extracellular Ca^{2+} entry, and/or G-protein-coupled P2Y receptors to induce Ca^{2+} release following activation of the $G_{\alpha,q/11}$-PLC-IP_3R signalling pathway (Figure 1.5) (Burnstock and Ulrich, 2011). Our recent study (Peng et al., 2016) and the study described in chapter 5, examining ATP-induced Ca^{2+} signalling mechanisms in hDP-MSC using pharmacological and genetic interventions, demonstrate that the P2X7, P2Y1 and P2Y11 receptors mediate ATP-induced Ca^{2+} signalling and play a significant role in ATP-induced stimulation of cell migration. The study presented in chapter 3 provides further evidence to support this finding. The results from using wound healing and trans-well cell migration assays consistently supported that exposure to ATP enhanced hDP-MSC migration (Figure 3.1 and Figure 3.2). Treatment with PPADS blocked ATP-induced hDP-MSC migration (Figure 3.3 and Figure 3.4), without affecting cell migration in the absence of ATP (Figure 3.5, Figure 3.6 and Figure 4.9). The present study investigated the potential role of the P2X7, P2Y1 and P2Y11 receptors in ATP-induced stimulation of hDP-MSC migration using receptor subtype specific agonists. Like ATP, BzATP, a synthetic ATP analogue that activates the P2X7, P2Y1 and P2Y11 receptors, also stimulated hDP-MSC migration (Figure 3.7). NF546, a P2Y11 selective agonist, was also effective in stimulating hDP-MSC migration (Figure 3.8). These results in the present study have supported the hypothesis stated that ATP-sensitive P2 receptors regulate MSC migration and provide further evidence to confirm or support the finding that the P2X7, P2Y1 and P2Y11 receptors participate in mediating ATP-induced stimulation of hDP-MSC cell migration, as reported in our recent study (Peng et al., 2016).

Intracellular Ca^{2+}-dependent signalling pathways have been shown to be engaged in cell migration. Therefore, the study presented in chapter 3 further investigated the hypothesis that Ca^{2+}-dependent downstream signalling pathways are involved in transducing ATP-induced Ca^{2+} signalling to cell migration. My study focused on the role of CaMKII, PKC and PYK2, which have been shown in regulating cell migration in many cell types by various stimuli. Inhibition of CaMKII with KN-93 strongly

suppressed ATP-induced hDP-MSC migration (Figure 3.9). Similarly, inhibition of PKC with CTC prevented ATP-induced hDP-MSC migration (Figure 3.10), providing consistent evidence with other studies reported that inhibition of PKC reduced cell migration of hUC-MSCs (Lee et al., 2014; Lin et al., 2015; Ryu and Han, 2015) and rBM-MSCs (Tang et al., 2012; Song et al., 2013). In addition, inhibition of PYK2 with PF431396 reduced ATP-induced cell migration of hDP-MSCs (Figure 3.11). There was no significant effect of these inhibitors on cell migration under the basal condition, that is, in the absence of ATP (Figure 3.9, Figure 3.10 and Figure 3.11). PYK2 is a Ca^{2+}-dependent tyrosine kinase and can also be activated by PKC (Lev et al., 1995; Wu et al., 2002), it remains possible that activation of PYK2 in the present study occurs downstream of PKC activation. As discussed in chapter 1 (section 1.8), activation of PKC, PYK2 and CaMKII can initiate downstream signalling pathways, particularly MEK/ERK and p38 MAPK, to regulate cell migration. There is increasing evidence to support involvement of MEK/ERK in in regulating MSC migration in hUC-MSCs (Ryu et al., 2010b; Lee et al., 2014; Lin et al., 2015) and rBM-MSCs (Tang et al., 2012) or p38 in hUC-MSCs (Ryu et al., 2010b; Oh et al., 2015), hBM-MSCs (Yuan et al., 2012; Yuan et al., 2013; Lin et al., 2016) and rBM-MSCs (Fu et al., 2009). Therefore, the study went on to investigate the role of these MAPKs in ATP-induced stimulation of hDP-MSC migration. Inhibition of MEK/ERK with U0126 (Figure 3.12) or p38 with SB202190 (Figure 3.13) reduced ATP-induced hDP-MSC migration. Collectively, these results presented in chapter 3 have supported the hypothesis stated that Ca^{2+}-dependent downstream signalling pathways involve in transducing ATP-induced cell migration and suggest a significant role of intracellular Ca^{2+}-dependent signalling pathways, engaging CaMKII, PKC and PYK2 and downstream MER/ERK and p38, in transducing ATP-induced Ca^{2+} signalling to an increase in hDP-MSC migration.

6.1.2 Ca^{2+} signalling mechanisms in Piezo1 activation-induced cell migration

Mechanical stimulation represents one of the common physical signals to mammalian cells, and it is also well documented to evoke intracellular Ca^{2+} signalling but the underlying mechanosensitive Ca^{2+} mechanisms remained elusive until recent identification of the Piezo1 channel. There is compelling evidence to demonstrate that the Piezo1 channel functions as a mechanically-activated Ca^{2+}-permeable channel that

can mediate mechanical induction of an increase in the $[Ca^{2+}]_i$. Interestingly, evidence has emerged to support a role for the Piezo1 channel in mediating mechanical induction of ATP release from cells such as endothelial cell (Wang et al., 2016; Albarrán-Juárez et al., 2018), urothelial cell (Miyamoto et al., 2014) and red blood cell (Cinar et al., 2015). MSCs can release ATP in response to mechanical stimulation (Riddle et al., 2007; Sun et al., 2013; Weihs et al., 2014). However, mechanical stimulation-induced ATP release from hMSCs remains poorly understood phenomena (Jiang et al., 2017a). Recent studies have reported expression of the Ca^{2+}-permeable Piezo1 channel in hBM-MSCs (Sugimoto et al., 2017) and rDP-MSCs (Gao et al., 2017). As discussed above, exposure to ATP induces hDP-MSC migration via inducing P2 receptor-mediated purinergic Ca^{2+} signalling. Taken together, these findings support the hypothesis that activation of the Piezo1 channel can regulate MSC migration via inducing ATP release, activation of P2 receptors and regulation of downstream Ca^{2+}-dependent proteins.

The study presented in chapter 4, therefore, examined the above hypothesis. Real-time RT-PCR and immunostaining showed the expression of Piezo1 at the mRNA (Figure 4.1A-B) and protein (Figure 4.1C) in hDP-MSCs. Consistently, exposure to the Piezo1 channel activator Yoda1 induced an increase in the $[Ca^{2+}]_i$ (Figure 4.1D), due to Ca^{2+} influx (Figure 4.2), which was strongly inhibited by treatment with RR, and GsMTx4, and also by siRNA-mediated knockdown of the Piezo1 expression (Figure 4.3, Figure 4.4 and Figure 4.6). These results provide pharmacological and genetic evidence to indicate functional expression of the Piezo1 channel in hDP-MSCs. This is consistent with recent studies suggesting expression of the Piezo1 channel in hBM-MSCs (Sugimoto et al., 2017) and rDP-MSCs and rPDLSCs (Gao et al., 2017), and these studies support the expression of the Piezo1 channel in MSC of different tissues and species. In addition, Yoda1-induced increase in the $[Ca^{2+}]_i$ in hDP-MSCs was abolished by removing extracellular Ca^{2+} (Figure 4.2), suggesting that Piezo1 functions as a Ca^{2+}-permeable channel in the plasma membrane, as described in bladder urothelial cancer cells (Miyamoto et al., 2014; Etem et al., 2018) and Neuro2A cells (Coste et al., 2010).

Recent studies have revealed an important role for the Piezo1 channel in mediating mechanical regulation of cell migration in endothelial cells (Li et al., 2014; Zhang et al., 2017) and numerous types of cancer cells (McHugh et al., 2012; Yang et al., 2014; Li et al., 2015a; Hung et al., 2016; Zhang et al., 2018a). The study presented in this chapter provides evidence to suggest that the Piezo1 channel plays a similar role in regulating hDP-MSC migration. Exposure to Yoda1 increased hDP-MSC migration (Figure 4.7), which was suppressed by Piezo1-specific siRNA (Figure 4.8). Yoda1-induced stimulation of hDP-MSC migration was lost in the presence of apyrase, a potent ATP-scavenger (Figure 4.10), indicating ATP release mediates Yoda1-induced Piezo1 channel-dependent regulation of cell migration. This is the first evidence to suggest that activation of the Piezo1 channel induces ATP release from MSCs, and provide a plausible mechanism for mechanical induction of ATP release from MSCs reported in previous studies (Riddle et al., 2007; Sun et al., 2013; Weihs et al., 2014). Furthermore, Yoda1-induced Piezo1-dependent stimulation of hDP-MSC migration was strongly inhibited by treatment with PPADS (Figure 4.9). Neither treatment with PPADS (Figure 3.6 and Figure 4.9) nor with apyrase resulted in significant effect on cell migration in the absence of Yoda1 (Figure 4.10). Collectively, these results strongly support the hypothesis that the Piezo1 channel activation stimulates hDP-MSC migration via inducing ATP release and subsequent activation of P2 receptor purinergic signalling.

The Piezo1 channel in rDP-MSCs and rPDLSCs (Gao et al., 2017) as well as MSC-like cells, UE7T-13 and SDP11 (Sugimoto et al., 2017) was proposed to mediate mechanical induction of the MEK/ERK and p38 MAPK signalling pathways, resulting in regulation of MSC proliferation (Gao et al., 2017) and differentiation (Sugimoto et al., 2017). In the final part of the study present in chapter 4 investigated the role of intracellular Ca^{2+} signalling pathways mediated by CaMKII, PKC, PYK2 and downstream MEK/ERK and p38 MAPK signalling pathways in mediating Yoda1-induced Piezo1 channel-dependent stimulation of hDP-MSCs migration. Inhibition of CaMKII with KN-93 strongly suppressed Yoda1-induced hDP-MSC migration (Figure 4.11). Inhibition of PKC with CTC also prevented Yoda1-induced hDP-MSC migration (Figure 4.12). Inhibition of PYK2 with PF431396 reduced Yoda1-induced cell migration (Figure 4.13). Furthermore, inhibition of MEK/ERK with U0126 significantly reduced Yoda1-induced hDP-MSC migration (Figure 4.14). As shown in

the study examining the effects of these inhibitors on ATP-induced stimulation of hDP-MSC migration, there was no significant effect of treatment with these inhibitors on cell migration under the basal condition or in the absence of Yoda1 (Figure 3.9, Figure 3.10, Figure 3.11 and Figure 3.12). These results suggest a significant role for CaMKII, PKC, PYK2 and downstream MEK/ERK signalling pathway in Yoda1-induced Piezo1 channel-dependent stimulation of hDP-MSCs migration. Considered that such signalling mechanisms, as the discussion above, are important for ATP-induced P2 receptor-mediated stimulation of hDP-MSC migration, these findings are consistent with the hypothesis that the Piezo1 channel activation stimulates hDP-MSC migration via inducing ATP release and subsequent activation of P2 receptors. However, in contrast with ATP-induced hDP-MSC migration (Figure 3.13), inhibition of p38 with SB202190 did not significantly reduce Yoda1-induced hDP-MSC migration (Figure 4.15). The exact reasons for this difference require further investigation. The experiments with apyrase strongly indicate Yoda1-induced ATP release via activation of the Piezo1 channel (Figure 4.10), and while the ATP concentration in the culture medium was not determined, it was anticipated to be lower than exogenous ATP applied (30 μM) in the study presented in chapter 3, which may reduce the activation of the P2 receptors, particularly P2X7 receptor. This is consistent with a previous study showing that activation of the P2X7 receptor by shockwaves or exogenous application of ATP is coupled to the p38 signalling pathway in hBM-MSCs (Sun et al., 2013).

6.1.3 Ca^{2+} signalling mechanisms in ATP-induced adipogenesis

Our recent study supports a role for the P2Y1, P2Y11 and P2X7 receptors in mediating ATP-induced Ca^{2+} signalling in hDP-MSCs (Peng et al., 2016). The unpublished results from my laboratory suggest that extracellular ATP promoted adipogenic differentiation of hDP-MSCs via activation of the P2Y1 and P2Y11, but not P2X7 receptor. As discussed in chapter 1 (section 1.6.3.1), increasing evidence suggests changes in the expression of both P2X and P2Y receptors during adipogenic differentiation of MSCs (Zippel et al., 2012; Li et al., 2015b; Li et al., 2016). In addition, it has been suggested or proposed that an increase in the $[Ca^{2+}]_i$ has been reported to promote activation of Ca^{2+}-dependent proteins such as PYK2 (Buckbinder, 2007; Eleniste et al., 2016) and CaMKII (Takada et al., 2007; Zhang et al., 2018b) in the

regulation of adipogenic differentiation of MSCs. Therefore, the study presented in chapter 5 examined demonstrate a change in the mRNA expression of the P2Y1, P2Y2, P2Y11 and P2X7 receptors during adipogenic differentiation in the absence or presence of ATP and, in addition, a role of PYK2 and CaMKII in ATP-induced stimulation of adipogenic differentiation of hDP-MSCs.

The results present in chapter 5, first of all, provide pharmacological evidence to further support the functional expression of the P2X7, P2Y1, P2Y2 and P2Y11 receptors in hDP-MSCs reported in our recent study (Peng et al., 2016). Exposure to ATP evoked strong increases in the $[Ca^{2+}]_i$ in the Ca^{2+}-containing solution (Figure 5.1), and transient Ca^{2+} responses in the Ca^{2+}-free solution (Figure 5.3), albeit with noticeably different kinetics, in hDP-MSCs from different donors. ATP-induced Ca^{2+} responses in the Ca^{2+}-containing solution were strongly inhibited by treatment with PPADS (Figure 5.2). Exposure to BzATP induced robust Ca^{2+} responses with a greater amplitude than ATP in the Ca^{2+}-containing solution (Figure 5.4). BzATP can activate the P2Y1 (Ilatovskaya et al., 2013) and P2Y11 receptors (Communi et al., 1999) and induced transient Ca^{2+} responses in the Ca^{2+}-free solution (Figure 5.5). Consistently, exposure to P2Y1 agonist ADP (Figure 5.6) or P2Y11 selective agonist NF546 (Figure 5.7) evoked significant Ca^{2+} responses in hDP-MSCs. Overall, these results support the conclusion of our previous study (Peng et al., 2016) that the expression of the P2X7, P2Y1 and P2Y11 receptors in ATP-induced Ca^{2+} signalling in hDP-MSCs. The variations in the amplitude and kinetics of agonist-induced Ca^{2+} responses among different donors are likely due to the different expression level of the P2 receptors.

The study presented in chapter 5 also provides evidence to show that hDP-MSCs from 9F and 22M donors are potentially capable to differentiate into adipocytes using well-defined inducing protocol. When cultured in adipogenic differentiation medium, cells grew slowly, and exhibited dramatic changes in their morphology from the fibroblast-like or spindle-shaped morphology, which was maintained in non-induced cells, to the oval-like adipocyte appearance. Adipogenic differentiation was identified by staining fat droplets with oil red O. Altogether, these observations indicate hDP-MSC differentiation into adipocytes. Moreover, the present study shows that ATP promoted adipogenic differentiation of hDP-MSCs (Figure 5.8), consistent with what was

reported in a previous study that ATP enhanced adipogenic differentiation in hBM-MSCs (Ciciarello et al., 2013). Real-time RT-PCR analysis revealed an increase in the P2Y1 expression and a decrease in the P2Y2 expression but no alteration in the expression of the P2Y11 and P2X7 receptors in hDP-MSC after cultured in adipogenesis inducing medium (Figure 5.9). Exposure to ATP during adipogenesis resulted in significant up-regulation of the P2Y11 expression with no effect on the P2Y1, P2Y2 and P2X7 receptors (Figure 5.9). There is evidence to show that ATP-induced stimulation of adipogenesis was not influenced by treatment with hP2X7 selective antagonist KN-62, largely excluding a possible role of the P2X7 receptor in mediating ATP-induced regulation of hBM-MSCs adipogenic differentiation (Ciciarello et al., 2013). Further experiments are required to provide a better understanding of the role of the above-mentioned P2 receptors in ATP-induced stimulation of hDP-MSC adipogenesis.

The results presented in the last chapter showed that inhibition of PYK2 significantly reduced adipogenic differentiation of hDP-MSCs in the presence of ATP (Figure 5.10), providing evidence to support the notion that PYK2 may act as a positive regulator of adipogenesis in hMSCs (Buckbinder et al., 2007; Eleniste et al., 2016). Inhibition of CaMKII also significantly reduced adipogenic differentiation of hDP-MSCs in the presence of ATP (Figure 5.11), consistent with a recent study reporting that inhibition of CaMKII reduced adipogenic differentiation of pBM-MSCs (Zhang et al., 2018b). Taken together, the present study supports the hypothesis that PYK2 and CaMKII have an important role in mediating ATP-stimulated adipogenic differentiation of hDP-MSCs.

6.2 Summary of the major findings

In summary, the study described in this thesis has made the following major findings. First of all, the study shows exposure to ATP stimulated cell migration in hDP-MSCs via sequential activation of the P2 receptors, particularly the P2X7, P2Y1 and P2Y11 receptors, and downstream Ca^{2+}-dependent signalling mechanisms engaging CaMKII, PKC and PYK2 and MAPK signalling pathways. Secondly, the study reveals a critical role for activation of the mechanosensitive Piezo1 channel in stimulating hDP-MSC migration and furthermore suggests such Piezo1 channel-dependent stimulation is

mediated by ATP release and activation of the P2 receptors and the above-described Ca^{2+}-dependent signalling mechanisms. Finally, the study demonstrates exposure to ATP promotes adipogenesis of hDP-MSC, which also depends on the activation of CaMKII and PYK2. The study also shows significant changes in the mRNA expression of the P2Y1 and P2Y2 receptors, not the P2X7 and P2Y11 receptors, during adipogenesis of hDP-MSCs, and in the P2Y11 expression following exposure to ATP during adipogenesis. Such information should be useful in developing better applications of MSCs in tissue engineering and cell-based therapy. The cell migration/homing capacity of *in vitro* expanded MSCs to the lesion sites after *in vivo* transplantation is limited but critical for the development of better applications of MSC-based therapy. The Ca^{2+} signalling mechanisms such as those presented in this thesis can be harnessed to improve the low or poor homing capacity of MSCs and thereby the efficacy of promising applications of MSC-based tissue engineering and therapies. Moreover, the findings in chapter 5 showed that ATP enhanced MSC adipogenic differentiation via the P2Y receptors and downstream signal pathways. Such information is useful for therapeutic applications that depend on MSC adipogenesis. Indeed, several studies have examined the potential roles of MSC adipogenesis in managing osteoporosis and obesity-associated metabolic syndromes, such as dyslipidemia and diabetes, that are characterized by an increase in adipocyte cell number (Matsushita, 2016; Picke et al., 2018) and reported that the signalling pathways governing MSC adipogenesis is a highly complex and the molecular mechanisms linking adipogenesis with health conditions, especially obesity-related complications, remain unclear (Matsushita, 2016). On the other hand, directing MSCs to adipogenic differentiation may instead be beneficial in case when reconstructive surgery (lipofilling) is required after cancer surgery (Oliver-De La Cruz et al., 2019).

6.3 Future directions

The Ca^{2+} signalling mechanisms and Ca^{2+}-dependent downstream signalling pathways play a key role in transducing extracellular signals to intracellular events to drive cell functions such as migration and differentiation. While the study presented in this thesis provide significant insights in Ca^{2+} signalling mechanisms and Ca^{2+}-dependent downstream signalling pathways in the regulation of cell migration and adipogenic

differentiation of hDP-MSCs, there are limitations and more investigations can help to gain a more comprehensive understanding of such Ca^{2+} signalling mechanisms.

The present and previous studies provide clear evidence that ATP-induced P2 receptor-mediated purinergic Ca^{2+} signalling mechanisms and downstream signalling pathways play an important role in determining and/or regulating cell differentiation and migration. Identification of such ATP-induced signalling pathways could facilitate the application of MSC-based therapies and MSC transplantation. With regard to ATP-induced stimulation of hDP-MSC migration, our previous study (Peng et al., 2016) reported that pharmacological and genetic inhibition of the P2X7, P2Y1 and/or P2Y11 reduced ATP-induced hDP-MSC migration. The present study shows that pharmacological inhibition of Ca^{2+}-dependent signalling pathways, PKC, PYK2, CaMKII and downstream MEK/ERK and p38 MAPKs, reduced ATP-induced hDP-MSC migration. Therefore, future experiments could include siRNA knockdown of particular ATP-sensitive P2 receptor to investigate their role in inducing activation of these Ca^{2+}-dependent downstream signalling pathways using western blotting analysis of the phosphorylation. Ca^{2+} chelators also can be applied to provide more direct supporting evidence to show the involvement of Ca^{2+} in activating such downstream signalling pathways. As discussed in the Introduction chapter, conventional PKCs are activated by Ca^{2+} and DAG, however, the PKC inhibitor used in the present study, CTC, is a broad PKC inhibitor targeting conventional, novel and atypical PKCs. Therefore, pharmacological inhibition using conventional PKC specific inhibitors, and/or genetic inhibition using siRNA transfection, will inform the PKC types and isoforms that are involved in ATP-induced cell migration. Likewise, siRNA knockdown of PYK2, CaMKII as well as MEK/ERK and p38 MAPKs can provide supporting evidence for their role in mediating ATP-induced cell migration. As mentioned earlier, PKC, PYK2 and CaMKII can act upstream of the MAPK signalling pathways. Thus, siRNA knockdown of such Ca^{2+}-dependent proteins can be applied to evaluate, using western blotting, their effects on regulating the activity of MEK/ERK and p38 MAPKs. A study carried out by Ferrari et al. (2011) has reported that hMSC pre-treated with ATP increased their homing capacity to the bone marrow of immune-deficient mice (Ferrari et al., 2011). It is of high interest to evaluate the importance of Ca^{2+}-dependent signalling mechanisms present in this thesis on hDP-

MSC homing capacity *in vivo*. Application of siRNA knockdown of the P2X7, P2Y1 and P2Y11 can be considered in future experiments to investigate their effects of on the *in vivo* homing capacity of hDP-MSCs pre-treated with ATP.

As discussed earlier, MSCs are mechanosensitive that can sense a variety of external mechanical cues in the microenvironments, such as shear force, osmotic stress and stretch, as well as cell-generated intracellular traction forces via actin-myosin contraction in the absence of extracellular mechanical stimuli. The Piezo1 channel has been shown to be directly gated in response to extracellular mechanical stimuli (Pathak et al., 2014; Murthy et al., 2017) and intracellular cytoskeleton components in the absence of extracellular mechanical stimuli (Pathak et al., 2014; Nourse and Pathak, 2017; Ellefsen et al., 2019). Accordingly, it is interesting to test whether external mechanical stimuli such as fluid flow-induced shear stress as well as application of Yoda1 can evoke the Piezo1 channel activation using patch-clamp recording and furthermore, to study their effect of mechanical stimuli on MSC migration. My study provided clear evidence to support that Piezo1 channel activation results in ATP release from hDP-MSCs. However, further experiments by measuring ATP release following mechanical stimulation and exposure to Yoda1 and the effects of siRNA-mediated knockdown of Piezo1 expression on the ATP release will provide more definitive evidence. There is evidence that intracellular Ca^{2+} can trigger the vesicular release of ATP (Striedinger et al., 2007; Praetorius and Leipziger, 2009; Dou et al., 2012). Therefore, application of Ca^{2+} chelators could be considered. Due to the limitation of the pharmacological inhibitor, PPADS, used in the present study, experiments should be repeated after selective inhibition of the P2X7, P2Y1 or P2Y11 receptor, using selective receptor inhibitors or siRNA knockdown. Such experiments can clarify which P2 receptor(s) are activated by ATP released upon Piezo1 channel activation and lead to increased hMSC migration. In this regard, it was noted that p38 MAPK has a significant role in ATP-induced cell migration but not in Yoda1-induced cell migration. It was shown that ATP-induced P2X7 receptor led to activation of the p38 in hBM-MSCs (Sun et al., 2016). One possibility is the level of ATP released following the Piezo1 channel activation was relatively lower and, thus, insufficient to activate the P2X7 receptor. Furthermore, siRNA-mediated inhibition of each of the Ca^{2+}-dependent signalling pathway can be applied to verify their role in mediating Piezo1-dependent hMSC migration.

In terms of ATP-induced adipogenic differentiation of hDP-MSCs is mediated through ATP-sensitive P2 receptors, the findings in the present study can be further strengthened by experiments using siRNA-mediated knockdown of the P2X7, P2Y1, P2Y2 or P2Y11 receptor. In addition, to profile the adipogenesis gene expression as well as fat droplet formation should provide more information regarding ATP-induced upregulation of adipogenesis. Moreover, the role of Ca^{2+}-dependent proteins in ATP-stimulated adipogenic differentiation of hDP-MSCs can further be investigated by siRNA-mediated knockdown. To further demonstrate the significance of the findings presented in this thesis, *in vivo* experiments are valuable to examine the effects of hMSCs pre-treated with ATP on *in vivo* adipogenic differentiation. Such experiments can provide a better understanding of the molecular mechanisms underlying ATP-induced regulation of adipogenic differentiation in hMSCs and the translational potential and importance of such findings.

References

Abbracchio, M.P., Burnstock, G., Boeynaems, J.-M., Barnard, E.A., Boyer, J.L., Kennedy, C., Knight, G.E., Fumagalli, M., Gachet, C., Jacobson, K.A. and Weisman, G.A. 2006. International union of pharmacology LVIII: Update on the P2Y G protein-coupled nucleotide receptors: from molecular mechanisms and pathophysiology to therapy. *Pharmacological Reviews*. **58**(3), pp.281–341.

Agell, N., Bachs, O., Rocamora, N. and Villalonga, P. 2002. Modulation of the Ras/Raf/MEK/ERK pathway by Ca^{2+}, and calmodulin. *Cellular Signalling*. **14**(8), pp.649–654.

Agresti, C., Meomartini, M.E., Amadio, S., Ambrosini, E., Serafini, B., Franchini, L., Volonté, C., Aloisi, F. and Visentin, S. 2005b. Metabotropic P2 receptor activation regulates oligodendrocyte progenitor migration and development: Metabotropic P2 receptor regulation of OP migration and development. *Glia*. **50**(2), pp.132–144.

Agresti, C., Meomartini, M.E., Amadio, S., Ambrosini, E., Volonté, C., Aloisi, F. and Visentin, S. 2005a. ATP regulates oligodendrocyte progenitor migration, proliferation, and differentiation: Involvement of metabotropic P2 receptors. *Brain Research Reviews*. **48**(2), pp.157–165.

Albarrán-Juárez, J., Iring, A., Wang, S., Joseph, S., Grimm, M., Strilic, B., Wettschureck, N., Althoff, T.F. and Offermanns, S. 2018. Piezo1 and G_q /G_{11} promote endothelial inflammation depending on flow pattern and integrin activation. *Journal of Experimental Medicine*. **215**(10), pp.2655–2672.

Ali, S., Turner, J. and Fountain, S.J. 2018. P2Y2 and P2Y6 receptor activation elicits intracellular calcium responses in human adipose-derived mesenchymal stromal cells. *Purinergic Signalling*. **14**(4), pp.371–384.

Argentati, C., Morena, F., Bazzucchi, M., Armentano, I., Emiliani, C. and Martino, S. 2018. Adipose stem cell translational applications: From bench-to-bedside. *International Journal of Molecular Sciences*. **19**(11), p.3475.

Artemenko, Y., Axiotakis, L., Borleis, J., Iglesias, P.A. and Devreotes, P.N. 2016. Chemical and mechanical stimuli act on common signal transduction and cytoskeletal networks. *Proceedings of the National Academy of Sciences of the United States of America*. **113**(47), pp.E7500–E7509.

Augello, A., Tasso, R., Negrini, S.M., Cancedda, R. and Pennesi, G. 2007. Cell therapy using allogeneic bone marrow mesenchymal stem cells prevents tissue damage in collagen-induced arthritis. *Arthritis & Rheumatism*. **56**(4), pp.1175–1186.

Bae, C., Sachs, F. and Gottlieb, P.A. 2011. The mechanosensitive ion channel Piezo1 is inhibited by the peptide GsMTx4. *Biochemistry*. **50**(29), pp.6295–6300.

Bae, C., Suchyna, T.M., Ziegler, L., Sachs, F. and Gottlieb, P.A. 2016. Human PIEZO1 ion channel functions as a split protein. *PloS One*. **11**(3), p.e0151289.

Bagriantsev, S.N., Gracheva, E.O. and Gallagher, P.G. 2014. Piezo proteins: Regulators of mechanosensation and other cellular processes. *Journal of Biological Chemistry*. **289**(46), pp.31673–31681.

Baroja-Mazo, A., Barberà-Cremades, M. and Pelegrín, P. 2013. The participation of plasma membrane hemichannels to purinergic signalling. *Biochimica et Biophysica Acta (BBA) - Biomembranes*. **1828**(1), pp.79–93.

Basseri, S., Lhoták, Š., Sharma, A.M. and Austin, R.C. 2009. The chemical chaperone 4-phenylbutyrate inhibits adipogenesis by modulating the unfolded protein response. *Journal of Lipid Research*. **50**(12), pp.2486–2501.

Berridge, M.J., Bootman, M.D. and Roderick, H.L. 2003. Calcium signalling: dynamics, homeostasis and remodelling. *Nature Reviews Molecular Cell Biology*. **4**(7), pp.517–529.

Berridge, M.J., Lipp, P. and Bootman, M.D. 2000. The versatility and universality of calcium signalling. *Nature Reviews Molecular Cell Biology*. **1**(1), pp.11–21.

Bhartiya, D., Unni, S., Parte, S. and Anand, S. 2013. Very small embryonic-like stem cells: Implications in reproductive biology. *BioMed Research International*. **2013**, pp.1–10.

Biver, G., Wang, N., Gartland, A., Orriss, I., Arnett, T.R., Boeynaems, J.-M. and Robaye, B. 2013. Role of the P2Y13 receptor in the differentiation of bone marrow stromal cells into osteoblasts and adipocytes: P2Y13 receptor and BMSCs differentiation. *Stem Cells*. **31**(12), pp.2747–2758.

Black, A.R. and Black, J.D. 2012. Protein kinase C signalling and cell cycle regulation. *Frontiers in Immunology*. **3**, p.423.

Blaukat, A., Ivankovic-Dikic, I., Grönroos, E., Dolfi, F., Tokiwa, G., Vuori, K. and Dikic, I. 1999. Adaptor proteins Grb2 and Crk couple Pyk2 with activation of specific mitogen-activated protein kinase cascades. *Journal of Biological Chemistry*. **274**(21), pp.14893–14901.

Block, E.R., Tolino, M.A. and Klarlund, J.K. 2010. Pyk2 Activation triggers epidermal growth factor receptor signalling and cell motility after wounding sheets of epithelial cells. *Journal of Biological Chemistry*. **285**(18), pp.13372–13379.

Bodin, P. and Burnstock, G. 2001. Purinergic signalling: ATP release. *Neurochemical Research*. **26**(8–9), pp.959–969.

Bootman, M.D. 2012. Calcium signalling. *Cold Spring Harbor Perspectives in Biology*. **4**(7), pp.a011171–a011171.

Boutahar, N., Guignandon, A., Vico, L. and Lafage-Proust, M.-H. 2004. Mechanical strain on osteoblasts activates autophosphorylation of focal adhesion kinase and proline-rich tyrosine kinase 2 tyrosine sites involved in ERK activation. *Journal of Biological Chemistry*. **279**(29), pp.30588–30599.

Bowler, W.B., Buckley, K.A., Gartland, A., Hipskind, R.A., Bilbe, G. and Gallagher, J.A. 2001. Extracellular nucleotide signalling: a mechanism for integrating local and systemic responses in the activation of bone remodeling. *Bone*. **28**(5), pp.507–512.

Bowman, C.L., Gottlieb, P.A., Suchyna, T.M., Murphy, Y.K. and Sachs, F. 2007. Mechanosensitive ion channels and the peptide inhibitor GsMTx-4: History, properties, mechanisms and pharmacology. *Toxicon*. **49**(2), pp.249–270.

Brandao-Burch, A., Key, M.L., Patel, J.J., Arnett, T.R. and Orriss, I.R. 2012. The P2X7 receptor is an important regulator of extracellular ATP levels. *Frontiers in Endocrinology*. **3**, p41.

Buckbinder, L., Crawford, D.T., Qi, H., Ke, H.Z., Olson, L.M., Long, K.R., Bonnette, P.C., Baumann, A.P., Hambor, J.E., Grasser, W.A., Pan, L.C., Owen, T.A., Luzzio, M.J., Hulford, C.A., Gebhard, D.F., Paralkar, V.M., Simmons, H.A., Kath, J.C., Roberts, W.G., Smock, S.L., Guzman-Perez, A., Brown, T.A. and Li, M. 2007. Proline-rich tyrosine kinase 2 regulates osteoprogenitor cells and bone formation, and offers an anabolic treatment approach for osteoporosis. *Proceedings of the National Academy of Sciences of the United States of America*. **104**(25), pp.10619–10624.

Burnstock, G. 2018. Purine and purinergic receptors. *Brain and Neuroscience Advances*. **2**, p.239821281881749.

Burnstock, G. 2007. Purine and pyrimidine receptors. *Cellular and Molecular Life Sciences*. **64**(12), pp.1471–1483.

Burnstock, G. 2013. Purinergic signalling: pathophysiology and therapeutic potential. *The Keio Journal of Medicine*. **62**(3), pp.63–73.

Burnstock, G., Dumsday, B. and Smythe, A. 1972. Atropine resistant excitation of the urinary bladder: the possibility of transmission via nerves releasing a purine nucleotide. *British Journal of Pharmacology*. **44**(3), pp.451–461.

Burnstock, G., Fredholm, B.B., North, R.A. and Verkhratsky, A. 2010. The birth and postnatal development of purinergic signalling: Purinergic signalling: historic overview. *Acta Physiologica*. **199**(2), pp.93–147.

Burnstock, G. and Ulrich, H. 2011. Purinergic signalling in embryonic and stem cell development. *Cellular and Molecular Life Sciences*. **68**(8), pp.1369–1394.

Burnstock, G. and Verkhratsky, A. 2009. Evolutionary origins of the purinergic signalling system. *Acta Physiologica*. **195**(4), pp.415–447.

Caplan, A.I. 1991. Mesenchymal stem cells. *Journal of Orthopaedic Research*. **9**(5), pp.641–650.

Chadet, S., Jelassi, B., Wannous, R., Angoulvant, D., Chevalier, S., Besson, P. and Roger, S. 2014. The activation of P2Y2 receptors increases MCF-7 breast cancer cells migration through the MEK-ERK1/2 signalling pathway. *Carcinogenesis*. **35**(6), pp.1238–1247.

Chagastelles, P.C. and Nardi, N.B. 2011. Biology of stem cells: an overview. *Kidney International Supplements*. **1**(3), pp.63–67.

Chang, S.-J., Tzeng, C.-R., Lee, Y.-H. and Tai, C.-J. 2008. Extracellular ATP activates the PLC/PKC/ERK signalling pathway through the P2Y2 purinergic receptor leading to the induction of early growth response 1 expression and the inhibition of viability in human endometrial stromal cells. *Cellular Signalling*. **20**(7), pp.1248–1255.

Chen, Q., Shou, P., Zheng, C., Jiang, M., Cao, G., Yang, Q., Cao, J., Xie, N., Velletri, T., Zhang, X., Xu, C., Zhang, L., Yang, H., Hou, J., Wang, Y. and Shi, Y. 2016. Fate decision of mesenchymal stem cells: adipocytes or osteoblasts? *Cell Death and Differentiation*. **23**(7), pp.1128–1139.

Chen, Y.-F., Chiu, W.-T., Chen, Y.-T., Lin, P.-Y., Huang, H.-J., Chou, C.-Y., Chang, H.-C., Tang, M.-J. and Shen, M.-R. 2011. Calcium store sensor stromal-interaction molecule 1-dependent signalling plays an important role in cervical cancer growth, migration, and angiogenesis. *Proceedings of the National Academy of Sciences of the United States of America*. **108**(37), pp.15225–15230.

Chi, M., Evans, H., Gilchrist, J., Mayhew, J., Hoffman, A., Pearsall, E.A., Jankowski, H., Brzozowski, J.S. and Skelding, K.A. 2016. Phosphorylation of calcium/calmodulin-stimulated protein kinase II at T286 enhances invasion and migration of human breast cancer cells. *Scientific Reports*. **6**(1).

Choi, B., Chun, J.S., Lee, Y.S., Sonn, J.K. and Kang, S.S. 1995. Expression of protein kinase C isozymes that are required for chondrogenesis of chick limb bud mesenchymal cells. *Biochemical and Biophysical Research Communications*. **216**(3), pp.1034–1040.

Choi, Y.H., Choi, J.-H., Oh, J.-W. and Lee, K.-Y. 2013. Calmodulin-dependent kinase II regulates osteoblast differentiation through regulation of Osterix. *Biochemical and Biophysical Research Communications*. **432**(2), pp.248–255.

Ciciarello, M., Zini, R., Rossi, L., Salvestrini, V., Ferrari, D., Manfredini, R. and Lemoli, R.M. 2013. Extracellular purines promote the differentiation of human bone marrow-derived mesenchymal stem cells to the osteogenic and adipogenic lineages. *Stem Cells and Development*. **22**(7), pp.1097–1111.

Cinar, E., Zhou, S., DeCourcey, J., Wang, Y., Waugh, R.E. and Wan, J. 2015. Piezo1 regulates mechanotransductive release of ATP from human RBCs. *Proceedings of the National Academy of Sciences of the United States of America*. **112**(38), pp.11783–11788.

Clapham, D.E. 2007. Calcium signalling. *Cell*. **131**(6), pp.1047–1058.

Clark, J.A., Black, A.R., Leontieva, O.V., Frey, M.R., Pysz, M.A., Kunneva, L., Woloszynska-Read, A., Roy, D. and Black, J.D. 2004. Involvement of the ERK signalling cascade in protein kinase C-mediated cell cycle arrest in intestinal epithelial cells. *Journal of Biological Chemistry*. **279**(10), pp.9233–9247.

Communi, D., Robaye, B. and Boeynaems, J.M. 1999. Pharmacological characterization of the human P2Y11 receptor. *British Journal of Pharmacology*. **128**(6), pp.1199–1206.

Coppi, E., Pugliese, A.M., Urbani, S., Melani, A., Cerbai, E., Mazzanti, B., Bosi, A., Saccardi, R. and Pedata, F. 2007. ATP modulates cell proliferation and elicits two different electrophysiological responses in human mesenchymal stem cells. *Stem Cells*. **25**(7), pp.1840–1849.

Coste, B., Mathur, J., Schmidt, M., Earley, T.J., Ranade, S., Petrus, M.J., Dubin, A.E. and Patapoutian, A. 2010. Piezo1 and Piezo2 are essential components of distinct mechanically activated cation channels. *Science*. **330**(6000), pp.55–60.

Coste, B., Xiao, B., Santos, J.S., Syeda, R., Grandl, J., Spencer, K.S., Kim, S.E., Schmidt, M., Mathur, J., Dubin, A.E., Montal, M. and Patapoutian, A. 2012. Piezo proteins are pore-forming subunits of mechanically activated channels. *Nature*. **483**(7388), pp.176–181.

Costessi, A., Pines, A., D'Andrea, P., Romanello, M., Damante, G., Cesaratto, L., Quadrifoglio, F., Moro, L. and Tell, G. 2005. Extracellular nucleotides activate Runx2 in the osteoblast-like HOBIT cell line: A possible molecular link between mechanical stress and osteoblasts' response. *Bone*. **36**(3), pp.418–432.

Dela Paz, N.G. and Frangos, J.A. 2018. Yoda1-induced phosphorylation of Akt and ERK1/2 does not require Piezo1 activation. *Biochemical and Biophysical Research Communications*. **497**(1), pp.220–225.

Di Virgilio, F. and Adinolfi, E. 2017. Extracellular purines, purinergic receptors and tumor growth. *Oncogene*. **36**(3), pp.293–303.

Ding, F., Zhang, G., Liu, L., Jiang, L., Wang, R., Zheng, Y., Wang, G., Xie, M. and Duan, Y. 2012. Involvement of cationic channels in proliferation and migration of human mesenchymal stem cells. *Tissue and Cell*. **44**(6), pp.358–364.

Dolmetsch, R.E., Xu, K. and Lewis, R.S. 1998. Calcium oscillations increase the efficiency and specificity of gene expression. *Nature*. **392**(6679), pp.933–936.

Dominici, M., Le Blanc, K., Mueller, I., Slaper-Cortenbach, I., Marini, F.C., Krause, D.S., Deans, R.J., Keating, A., Prockop, D.J. and Horwitz, E.M. 2006. Minimal criteria for defining multipotent mesenchymal stromal cells. The International Society for Cellular Therapy position statement. *Cytotherapy*. **8**(4), pp.315–317.

Donnelly-Roberts, D.L., Namovic, M.T., Han, P. and Jarvis, M.F. 2009. Mammalian P2X7 receptor pharmacology: comparison of recombinant mouse, rat and human P2X7 receptors. *British Journal of Pharmacology*. **157**(7), pp.1203–1214.

Dou, Y., Wu, H., Li, H., Qin, S., Wang, Y., Li, J., Lou, H., Chen, Z., Li, X., Luo, Q. and Duan, S. 2012. Microglial migration mediated by ATP-induced ATP release from lysosomes. *Cell Research*. **22**(6), pp.1022–1033.

Easley, C.A., Brown, C.M., Horwitz, A.F. and Tombes, R.M. 2008. CaMK-II promotes focal adhesion turnover and cell motility by inducing tyrosine dephosphorylation of FAK and paxillin. *Cell Motility and the Cytoskeleton*. **65**(8), pp.662–674.

Egbuniwe, O., Grover, S., Duggal, A.K., Mavroudis, A., Yazdi, M., Renton, T., Di Silvio, L. and Grant, A.D. 2014. TRPA1 and TRPV4 activation in human odontoblasts stimulates ATP release. *Journal of Dental Research*. **93**(9), pp.911–917.

Eleniste, P.P., Patel, V., Posritong, S., Zero, O., Largura, H., Cheng, Y.-H., Himes, E.R., Hamilton, M., Baughman, J., Kacena, M.A. and Bruzzaniti, A. 2016. Pyk2 and megakaryocytes regulate osteoblast differentiation and migration via distinct and overlapping mechanisms: Pyk2 and megakaryocytes regulate osteoblast activity. *Journal of Cellular Biochemistry*. **117**(6), pp.1396–1406.

Ellefsen, K.L., Chang, A., Nourse, J.L., Holt, J.R., Arulmoli, J., Mekhdjian, A., Abuwarda, H., Tombola, F., Flanagan, L.A., Dunn, A.R., Parker, I. and Pathak, M.M. 2019. Myosin-II mediated traction forces evoke localized Piezo1 Ca^{2+} flickers. *Communications Biology. 2:298*

Engler, A.J., Sen, S., Sweeney, H.L. and Discher, D.E. 2006. Matrix elasticity directs stem cell lineage specification. *Cell*. **126**(4), pp.677–689.

Etem, E.Ö., Ceylan, G.G., Özaydın, S., Ceylan, C., Özercan, I. and Kuloğlu, T. 2018. The increased expression of Piezo1 and Piezo2 ion channels in human and mouse bladder carcinoma. *Advances in Clinical and Experimental Medicine: Official Organ Wroclaw Medical University*. **27**(8), pp.1025–1031.

Fan, H. and Guan, J.-L. 2011. Compensatory function of Pyk2 protein in the promotion of focal adhesion kinase (FAK)-null mammary cancer stem cell tumorigenicity and metastatic activity. *Journal of Biological Chemistry*. **286**(21), pp.18573–18582.

Farini, A., Sitzia, C., Erratico, S., Meregalli, M. and Torrente, Y. 2014. Clinical applications of mesenchymal stem cells in chronic diseases. *Stem Cells International*. **2014**, pp.1–11.

Faroni, A., Rothwell, S.W., Grolla, A.A., Terenghi, G., Magnaghi, V. and Verkhratsky, A. 2013. Differentiation of adipose-derived stem cells into Schwann cell phenotype induces expression of P2X receptors that control cell death. *Cell Death & Disease*. **4**(7), pp.e743–e743.

Farshori, P.Q., Shah, B.H., Arora, K.K., Martinez-Fuentes, A. and Catt, K.J. 2003. Activation and nuclear translocation of PKCδ, Pyk2 and ERK1/2 by gonadotropin releasing hormone in HEK293 cells. *Journal of Steroid Biochemistry and Molecular Biology*. **85**(2–5), pp.337–347.

Ferrari, D., Gulinelli, S., Salvestrini, V., Lucchetti, G., Zini, R., Manfredini, R., Caione, L., Piacibello, W., Ciciarello, M., Rossi, L., Idzko, M., Ferrari, S., Di Virgilio, F. and Lemoli, R.M. 2011. Purinergic stimulation of human mesenchymal stem cells potentiates their chemotactic response to CXCL12

and increases the homing capacity and production of proinflammatory cytokines. *Experimental Hematology*. **39**(3), pp.360-374.e5.

Fleming, I., MacKenzie, S.J., Vernon, R.G., Anderson, N.G., Houslay, M.D. and Kilgour, E. 1998. Protein kinase C isoforms play differential roles in the regulation of adipocyte differentiation. *Biochemical Journal*. **333**(3), pp.719–727.

Fruscione, F., Scarfì, S., Ferraris, C., Bruzzone, S., Benvenuto, F., Guida, L., Uccelli, A., Salis, A., Usai, C., Jacchetti, E., Ilengo, C., Scaglione, S., Quarto, R., Zocchi, E. and De Flora, A. 2011. Regulation of human mesenchymal stem cell functions by an autocrine loop involving NAD^+ release and P2Y11-mediated signalling. *Stem Cells and Development*. **20**(7), pp.1183–1198.

Fu, X., Han, B., Cai, S., Lei, Y., Sun, T. and Sheng, Z. 2009. Migration of bone marrow-derived mesenchymal stem cells induced by tumor necrosis factor-α and its possible role in wound healing. *Wound Repair and Regeneration*. **17**(2), pp.185–191.

Fuchs, E., Tumbar, T. and Guasch, G. 2004. Socializing with the neighbors: stem cells and their niche. *Cell*. **116**(6), pp.769–778.

Gadjanski, I. and Vunjak-Novakovic, G. 2013. Purinergic responses of chondrogenic stem cells to dynamic loading. *Journal of the Serbian Chemical Society*. **78**(12), pp.1865–1874.

Gao, Q., Cooper, P.R., Walmsley, A.D. and Scheven, B.A. 2017. Role of Piezo channels in ultrasound-stimulated dental stem cells. *Journal of Endodontics*. **43**(7), pp.1130–1136.

Gao, X., Balan, V., Tai, G. and Raz, A. 2014. Galectin-3 induces cell migration via a calcium-sensitive MAPK/ERK1/2 pathway. *Oncotarget*. **5**(8), pp.2077–2084.

Gattazzo, F., Urciuolo, A. and Bonaldo, P. 2014. Extracellular matrix: A dynamic microenvironment for stem cell niche. *Biochimica et Biophysica Acta (BBA) - General Subjects*. **1840**(8), pp.2506–2519.

Ge, J., Li, W., Zhao, Q., Li, N., Chen, M., Zhi, P., Li, R., Gao, N., Xiao, B. and Yang, M. 2015. Architecture of the mammalian mechanosensitive Piezo1 channel. *Nature*. **527**(7576), pp.64–69.

Ghayor, C., Rey, A. and Caverzasio, J. 2005. Prostaglandin-dependent activation of ERK mediates cell proliferation induced by transforming growth factor β in mouse osteoblastic cells. *Bone*. **36**(1), pp.93–100.

Ghoraishizadeh, P., Raikar, S., Ghorishizadeh, A., Boroojerdi, M.H. and Daneshvar, N. 2014. Biology, properties and clinical application of mesenchymal stem cells. *Russian Open Medical Journal*. **3**(2), p.0202.

Glaser, T., Cappellari, A.R., Pillat, M.M., Iser, I.C., Wink, M.R., Battastini, A.M.O. and Ulrich, H. 2012. Perspectives of purinergic signalling in stem cell

differentiation and tissue regeneration. *Purinergic Signalling*. **8**(3), pp.523–537.

Gnanasambandam, R., Ghatak, C., Yasmann, A., Nishizawa, K., Sachs, F., Ladokhin, A.S., Sukharev, S.I. and Suchyna, T.M. 2017. GsMTx4: Mechanism of inhibiting mechanosensitive ion channels. *Biophysical Journal*. **112**(1), pp.31–45.

Goetzke, R., Sechi, A., De Laporte, L., Neuss, S. and Wagner, W. 2018. Why the impact of mechanical stimuli on stem cells remains a challenge. *Cellular and Molecular Life Sciences*. **75**(18), pp.3297–3312.

Gronthos, S., Brahim, J., Li, W., Fisher, L.W., Cherman, N., Boyde, A., DenBesten, P., Robey, P.G. and Shi, S. 2002. Stem cell properties of human dental pulp stem cells. *Journal of Dental Research*. **81**(8), pp.531–535.

Gronthos, S., Mankani, M., Brahim, J., Robey, P.G. and Shi, S. 2000. Postnatal human dental pulp stem cells (DPSCs) in vitro and invivo. *Proceedings of the National Academy of Sciences of the United States of America*. **97**(25), pp.13625–13630.

Grottkau, B.E., Purudappa, P.P. and Lin, Y. 2010. Multilineage differentiation of dental pulp stem cells from green fluorescent protein transgenic mice. *International Journal of Oral Science*. **2**(1), pp.21–27.

Gudipaty, S.A., Lindblom, J., Loftus, P.D., Redd, M.J., Edes, K., Davey, C.F., Krishnegowda, V. and Rosenblatt, J. 2017. Mechanical stretch triggers rapid epithelial cell division through Piezo1. *Nature*. **543**(7643), pp.118–121.

Guo, Y.R. and MacKinnon, R. 2017. Structure-based membrane dome mechanism for Piezo mechanosensitivity. *eLife*. **6**, p.e33660.

Hattori, M. and Gouaux, E. 2012. Molecular mechanism of ATP binding and ion channel activation in P2X receptors. *Nature*. **485**(7397), pp.207–212.

Hatzistergos, K.E., Quevedo, H., Oskouei, B.N., Hu, Q., Feigenbaum, G.S., Margitich, I.S., Mazhari, R., Boyle, A.J., Zambrano, J.P., Rodriguez, J.E., Dulce, R., Pattany, P.M., Valdes, D., Revilla, C., Heldman, A.W., McNiece, I. and Hare, J.M. 2010. Bone marrow mesenchymal stem cells stimulate cardiac stem cell proliferation and differentiation. *Circulation Research*. **107**(7), pp. 913-922.

Hawryluk, G.W.J., Mothe, A., Wang, J., Wang, S., Tator, C. and Fehlings, M.G. 2012. An In Vivo Characterization of Trophic Factor Production Following Neural Precursor Cell or Bone Marrow Stromal Cell Transplantation for Spinal Cord Injury. *Stem Cells and Development*. **21**(12), pp.2222–2238.

Heckman, C.A., Pandey, P., Cayer, M.L., Biswas, T., Zhang, Z.-Y. and Boudreau, N.S. 2017. The tumor promoter-activated protein kinase Cs are a system for regulating filopodia. *Cytoskeleton*. **74**(8), pp.297–314.

Heid, C.A., Stevens, J., Livak, K.J. and Williams, P.M. 1996. Real time quantitative PCR. *Genome Research*. **6**(10), pp.986–994.

Hodges, R.R., Rios, J.D., Vrouvlianis, J., Ota, I., Zoukhri, D. and Dartt, D.A. 2006. Roles of protein kinase C, Ca^{2+}, Pyk2, and c-Src in agonist activation of rat lacrimal gland p42/p44 MAPK. *Investigative Opthalmology & Visual Science*. **47**(8), p.3352.

Hoebertz, A., Mahendran, S., Burnstock, G. and Arnett, T.R. 2002. ATP and UTP at low concentrations strongly inhibit bone formation by osteoblasts: A novel role for the P2Y2 receptor in bone remodeling. *Journal of Cellular Biochemistry*. **86**(3), pp.413–419.

Hofstetter, C.P., Schwarz, E.J., Hess, D., Widenfalk, J., El Manira, A., Prockop, D.J. and Olson, L. 2002. Marrow stromal cells form guiding strands in the injured spinal cord and promote recovery. *Proceedings of the National Academy of Sciences of the United States of America*. **99**(4), pp.2199–2204.

Hotokezaka, H., Sakai, E., Kanaoka, K., Saito, K., Matsuo, K., Kitaura, H., Yoshida, N. and Nakayama, K. 2002. U0126 and PD98059, specific inhibitors of MEK, accelerate differentiation of RAW264.7 cells into osteoclast-like cells. *Journal of Biological Chemistry*. **277**(49), pp.47366–47372.

Hu, Y., Tan, H.B., Wang, X.M., Rong, H., Cui, H.P. and Cui, H. 2013. Bone marrow mesenchymal stem cells protect against retinal ganglion cell loss in aged rats with glaucoma. *Clinical Interventions in Aging*. **8**, pp.1467–1470.

Huang, G.T.-J., Gronthos, S. and Shi, S. 2009. Mesenchymal stem cells derived from dental tissues *vs* those from other sources: Their biology and role in regenerative medicine. *Journal of Dental Research*. **88**(9), pp.792–806.

Hung, W.-C., Yang, J.R., Yankaskas, C.L., Wong, B.S., Wu, P.-H., Pardo-Pastor, C., Serra, S.A., Chiang, M.-J., Gu, Z., Wirtz, D., Valverde, M.A., Yang, J.T., Zhang, J. and Konstantopoulos, K. 2016. Confinement sensing and signal optimization via Piezo1/PKA and myosin II pathways. *Cell Reports*. **15**(7), pp.1430–1441.

Ilatovskaya, D.V., Palygin, O., Levchenko, V. and Staruschenko, A. 2013. Pharmacological characterization of the P2 receptors profile in the podocytes of the freshly isolated rat glomeruli. *American Journal of Physiology-Cell Physiology*. **305**(10), pp.C1050–C1059.

Iwasaki, H., Yoshimoto, T., Sugiyama, T. and Hirata, Y. 2003. Activation of cell adhesion kinase β by mechanical stretch in vascular smooth muscle cells. *Endocrinology*. **144**(6), pp.2304–2310.

Jacobson, K.A., Ivanov, A.A., de Castro, S., Harden, T.K. and Ko, H. 2009. Development of selective agonists and antagonists of P2Y receptors. *Purinergic Signalling*. **5**(1), pp.75–89.

Jacobson, K.A., Paoletta, S., Katritch, V., Wu, B., Gao, Z.-G., Zhao, Q., Stevens, R.C. and Kiselev, E. 2015. Nucleotides acting at P2Y receptors: Connecting structure and function. *Molecular Pharmacology*. **88**(2), pp.220–230.

Jaiswal, R.K., Jaiswal, N., Bruder, S.P., Mbalaviele, G., Marshak, D.R. and Pittenger, M.F. 2000. Adult human mesenchymal stem cell differentiation to the osteogenic or adipogenic lineage is regulated by mitogen-activated protein kinase. *Journal of Biological Chemistry*. **275**(13), pp.9645–9652.

Janebodin, K., Horst, O.V., Ieronimakis, N., Balasundaram, G., Reesukumal, K., Pratumvinit, B. and Reyes, M. 2011. Isolation and characterization of neural crest-derived stem cells from dental pulp of neonatal mice. *PloS One*. **6**(11), p.e27526.

Jarvis, M.F. and Khakh, B.S. 2009. ATP-gated P2X cation-channels. *Neuropharmacology*. **56**(1), pp.208–215.

Jiang, L.-H. 2012. P2X receptor-mediated ATP purinergic signalling in health and disease. *Cell Health and Cytoskeleton*. p.83.

Jiang, L.-H., Mousawi, F., Yang, X. and Roger, S. 2017a. ATP-induced Ca^{2+}-signalling mechanisms in the regulation of mesenchymal stem cell migration. *Cellular and Molecular Life Sciences*. **74**(20), pp.3697–3710.

Jiang, L.-H., Hao, Y., Mousawi, F., Peng, H. and Yang, X. 2017b. Expression of P2 purinergic receptors in mesenchymal stem cells and their roles in extracellular nucleotide regulation of cell functions: P2 receptors in MSC functions. *Journal of Cellular Physiology*. **232**(2), pp.287–297.

Jiang, L.H., Mackenzie, A.B., North, R.A. and Surprenant, A. 2000. Brilliant blue G selectively blocks ATP-gated rat P2X7 receptors. *Molecular Pharmacology*. **58**(1), pp.82–88.

Jin, Y., Li, J., Wang, Y., Ye, R., Feng, X., Jing, Z. and Zhao, Z. 2015. Functional role of mechanosensitive ion channel Piezo1 in human periodontal ligament cells. *The Angle Orthodontist*. **85**(1), pp.87–94.

Kaebisch, C., Schipper, D., Babczyk, P. and Tobiasch, E. 2015. The role of purinergic receptors in stem cell differentiation. *Computational and Structural Biotechnology Journal*. **13**, pp.75–84.

Kang, J.-H. 2014. Protein kinase C (PKC) isozymes and cancer. *New Journal of Science*. **2014**, pp.1–36.

Katz, S., Boland, R. and Santillán, G. 2006. Modulation of ERK 1/2 and p38 MAPK signalling pathways by ATP in osteoblasts: Involvement of mechanical stress-activated calcium influx, PKC and Src activation. *The International Journal of Biochemistry & Cell Biology*. **38**(12), pp.2082–2091.

Katz, S., Boland, R. and Santillán, G. 2008. Purinergic (ATP) signalling stimulates JNK1 but not JNK2 MAPK in osteoblast-like cells: Contribution of intracellular Ca^{2+} release, stress activated and L-voltage-dependent calcium influx, PKC and Src kinases. *Archives of Biochemistry and Biophysics*. **477**(2), pp.244–252.

Kawano, S., Otsu, K., Kuruma, A., Shoji, S., Yanagida, E., Muto, Y., Yoshikawa, F., Hirayama, Y., Mikoshiba, K. and Furuichi, T. 2006. ATP autocrine/paracrine signalling induces calcium oscillations and NFAT activation in human mesenchymal stem cells. *Cell Calcium*. **39**(4), pp.313–324.

Kawano, S., Shoji, S., Ichinose, S., Yamagata, K., Tagami, M. and Hiraoka, M. 2002. Characterization of Ca^{2+} signalling pathways in human mesenchymal stem cells. *Cell Calcium*. **32**(4), pp.165–174.

Kennedy, C., Qi, A.-D., Herold, C.L., Harden, T.K. and Nicholas, R.A. 2000. ATP, an agonist at the rat P2Y4 receptor, is an antagonist at the human P2Y4 receptor. *Molecular Pharmacology*. **57**(5), p.926.

Kim, D.-H., Wong, P.K., Park, J., Levchenko, A. and Sun, Y. 2009. Microengineered platforms for cell mechanobiology. *Annual Review of Biomedical Engineering*. **11**(1), pp.203–233.

Kim, E.K. and Choi, E.-J. 2010. Pathological roles of MAPK signalling pathways in human diseases. *Biochimica et Biophysica Acta*. **1802**(4), pp.396–405.

Kim, N. and Cho, S.-G. 2013. Clinical applications of mesenchymal stem cells. *The Korean Journal of Internal Medicine*. **28**(4), p.387.

Kim, N. and Cho, S.-G. 2015. New strategies for overcoming limitations of Mesenchymal stem cell-based immune modulation. *International Journal of Stem Cells*. **8**(1), pp.54–68.

Kim, T.-J., Joo, C., Seong, J., Vafabakhsh, R., Botvinick, E.L., Berns, M.W., Palmer, A.E., Wang, N., Ha, T., Jakobsson, E., Sun, J. and Wang, Y. 2015. Distinct mechanisms regulating mechanical force-induced Ca^{2+} signals at the plasma membrane and the ER in human MSCs. *eLife*. **4**, p. e04876.

Király, M., Porcsalmy, B., Pataki, Á., Kádár, K., Jelitai, M., Molnár, B., Hermann, P., Gera, I., Grimm, W.-D., Ganss, B., Zsembery, Á. and Varga, G. 2009. Simultaneous PKC and cAMP activation induces differentiation of human dental pulp stem cells into functionally active neurons. *Neurochemistry International*. **55**(5), pp.323–332.

Ko, H., Carter, R.L., Cosyn, L., Petrelli, R., de Castro, S., Besada, P., Zhou, Y., Cappellacci, L., Franchetti, P., Grifantini, M., Van Calenbergh, S., Harden, T.K. and Jacobson, K.A. 2008. Synthesis and potency of novel uracil nucleotides and derivatives as P2Y2 and P2Y6 receptor agonists. *Bioorganic & Medicinal Chemistry*. **16**(12), pp.6319–6332.

Kotova, P.D., Bystrova, M.F., Rogachevskaja, O.A., Khokhlov, A.A., Sysoeva, V. Y., Tkachuk, V.A. and Kolesnikov, S.S. 2018. Coupling of P2Y receptors to Ca^{2+} mobilization in mesenchymal stromal cells from the human adipose tissue. *Cell Calcium*. **71**, pp.1–14.

Kretlow, J.D., Jin, Y.-Q., Liu, W., Zhang, W., Hong, T.-H., Zhou, G., Baggett, L.S., Mikos, A.G. and Cao, Y. 2008. Donor age and cell passage affects

differentiation potential of murine bone marrow-derived stem cells. *BMC Cell Biology*. **9**(1), p.60.

von Kügelgen, I. and Hoffmann, K. 2016. Pharmacology and structure of P2Y receptors. *Neuropharmacology*. **104**, pp.50–61.

Kuwabara, K., Nakaoka, T., Sato, K., Nishishita, T., Sasaki, T. and Yamashita, N. 2004. Differential regulation of cell migration and proliferation through proline-rich tyrosine kinase 2 in endothelial cells. *Endocrinology*. **145**(7), pp.3324–3330.

Kwon, H.J. 2012. Extracellular ATP signalling via P2X4 receptor and cAMP/PKA signalling mediate ATP oscillations essential for prechondrogenic condensation. *Journal of Endocrinology*. **214**(3), pp.337–348.

Lacroix, J.J., Botello-Smith, W.M. and Luo, Y. 2017. Chemical gating of the mechanosensitive Piezo1 channel by asymmetric binding of its agonist Yoda1. *bioRxiv*., p.169516.

Laird, D.J., von Andrian, U.H. and Wagers, A.J. 2008. Stem cell trafficking in tissue development, growth, and disease. *Cell*. **132**(4), pp.612–630.

Lambrecht, G. 2000. Agonists and antagonists acting at P2X receptors: selectivity profiles and functional implications. *Naunyn-Schmiedeberg's Archives of Pharmacology*. **362**(4–5), pp.340–350.

Lazarowski, E.R. 2003. Mechanisms of release of nucleotides and integration of their action as P2X- and P2Y-receptor activating molecules. *Molecular Pharmacology*. **64**(4), pp.785–795.

Lazarowski, E.R. 2012. Vesicular and conductive mechanisms of nucleotide release. *Purinergic Signalling*. **8**(3), pp.359–373.

Lazarowski, E.R., Watt, W.C., Stutts, M.J., Boucher, R.C. and Harden, T.K. 1995. Pharmacological selectivity of the cloned human P2U-purinoceptor: potent activation by diadenosine tetraphosphate. *British Journal of Pharmacology*. **116**(1), pp.1619–1627.

Lee, D.A., Knight, M.M., Campbell, J.J. and Bader, D.L. 2011. Stem cell mechanobiology. *Journal of Cellular Biochemistry*. **112**(1), pp.1–9.

Lee, S.-J., Jung, Y.H., Oh, S.Y., Yong, M.S., Ryu, J.M. and Han, H.J. 2014. Netrin-1 induces MMP-12-dependent E-cadherin degradation via the distinct activation of PKCα and FAK/Fyn in promoting mesenchymal stem cell motility. *Stem Cells and Development*. **23**(16), pp.1870–1882.

Leeanansaksiri, W., Rattananinsruang, P. and Dechsukhum, C. 2016. Human embryonic stem cells and induced pluripotent stem cells: The promising tools for insulin-producing cell generation, *Pluripotent Stem Cells - From the Bench to the Clinic* [Online]. InTech. Available from: http://www.intechopen.com/books/pluripotent-stem-cells-from-the-bench-to-

the-clinic/human-embryonic-stem-cells-and-induced-pluripotent-stem-cells-the-promising-tools-for-insulin-produc.

Lembong, J., Sabass, B. and Stone, H.A. 2017. Calcium oscillations in wounded fibroblast monolayers are spatially regulated through substrate mechanics. *Physical Biology*. **14**(4), p.045006.

Lev, S., Moreno, H., Martinez, R., Canoll, P., Peles, E., Musacchio, J.M., Plowman, G.D., Rudy, B. and Schlessinger, J. 1995. Protein tyrosine kinase PYK2 involved in Ca^{2+}-induced regulation of ion channel and MAP kinase functions. *Nature*. **376**(6543), pp.737–745.

Lewis, A.H. and Grandl, J. 2015. Mechanical sensitivity of Piezo1 ion channels can be tuned by cellular membrane tension. *eLife*. **4**, p.e12088.

Li, C., Rezania, S., Kammerer, S., Sokolowski, A., Devaney, T., Gorischek, A., Jahn, S., Hackl, H., Groschner, K., Windpassinger, C., Malle, E., Bauernhofer, T. and Schreibmayer, W. 2015a. Piezo1 forms mechanosensitive ion channels in the human MCF-7 breast cancer cell line. *Scientific Reports*. **5**(1).

Li, J., Hou, B., Tumova, S., Muraki, K., Bruns, A., Ludlow, M.J., Sedo, A., Hyman, A.J., McKeown, L., Young, R.S., Yuldasheva, N.Y., Majeed, Y., Wilson, L.A., Rode, B., Bailey, M.A., Kim, H.R., Fu, Z., Carter, D.A.L., Bilton, J., Imrie, H., Ajuh, P., Dear, T.N., Cubbon, R.M., Kearney, M.T., Prasad, K.R., Evans, P.C., Ainscough, J.F.X. and Beech, D.J. 2014. Piezo1 integration of vascular architecture with physiological force. *Nature*. **515**(7526), pp.279–282.

Li, N., Wang, C., Wu, Y., Liu, X. and Cao, X. 2009. Ca^{2+}/calmodulin-dependent protein kinase II promotes cell cycle progression by directly activating MEK1 and subsequently modulating p27 phosphorylation. *Journal of Biological Chemistry*. **284**(5), pp.3021–3027.

Li, S., Wang, J., Han, Y., Li, X., Liu, C., Lv, Z., Wang, X., Tang, X. and Wang, Z. 2018. Carbenoxolone inhibits mechanical stress-induced osteogenic differentiation of mesenchymal stem cells by regulating p38 MAPK phosphorylation. *Experimental and Therapeutic Medicine*. **15**(3), pp.2798–2803.

Li, W., Li, G., Zhang, Y., Wei, S., Song, M., Wang, W., Yuan, X., Wu, H. and Yang, Y. 2015b. Role of P2X7 receptor in the differentiation of bone marrow stromal cells into osteoblasts and adipocytes. *Experimental Cell Research*. **339**(2), pp.367–379.

Li, W., Wei, S., Liu, C., Song, M., Wu, H. and Yang, Y. 2016. Regulation of the osteogenic and adipogenic differentiation of bone marrow-derived stromal cells by extracellular uridine triphosphate: The role of P2Y2 receptor and ERK1/2 signalling. *International Journal of Molecular Medicine*. **37**(1), pp.63–73.

Lim, Y.-B., Kang, S.-S., An, W.G., Lee, Y.-S., Chun, J.-S. and Sonn, J.K. 2003. Chondrogenesis induced by actin cytoskeleton disruption is regulated via

protein kinase C-dependent p38 mitogen-activated protein kinase signalling. *Journal of Cellular Biochemistry*. **88**(4), pp.713–718.

Lin, C.-Y., Zu, C.-H., Yang, C.-C., Tsai, P.-J., Shyu, J.-F., Chen, C.-P., Weng, Z.-C., Chen, T.-H. and Wang, H.-S. 2015. IL-1β-induced mesenchymal stem cell migration involves MLCK activation via PKC signalling. *Cell Transplantation*. **24**(10), pp.2011–2028.

Lin, F., Zhang, W., Xue, D., Zhu, T., Li, J., Chen, E., Yao, X. and Pan, Z. 2016. Signalling pathways involved in the effects of HMGB1 on mesenchymal stem cell migration and osteoblastic differentiation. *International Journal of Molecular Medicine*. **37**(3), pp.789–797.

Liu, J., Liao, Z., Camden, J., Griffin, K.D., Garrad, R.C., Santiago-Pérez, L.I., González, F.A., Seye, C.I., Weisman, G.A. and Erb, L. 2004. Src homology 3 binding sites in the P2Y2 nucleotide receptor interact with Src and regulate activities of Src, proline-rich tyrosine kinase 2, and growth factor receptors. *Journal of Biological Chemistry*. **279**(9), pp.8212–8218.

Liu, J., Someren, E., Mentink, A., Licht, R., Dechering, K., van Blitterswijk, C. and de Boer, J. 2010. The effect of PKC activation and inhibition on osteogenic differentiation of human mesenchymal stem cells. *Journal of Tissue Engineering and Regenerative Medicine*. **4**(5), pp.329–339.

Liu, Y.-S. and Lee, O.K. 2014. In search of the pivot point of mechanotransduction: Mechanosensing of stem cells. *Cell Transplantation*. **23**(1), pp.1–11.

Liu, Z.-J., Zhuge, Y. and Velazquez, O.C. 2009. Trafficking and differentiation of mesenchymal stem cells. *Journal of Cellular Biochemistry*. **106**(6), pp.984–991.

Livak, K.J. and Schmittgen, T.D. 2001. Analysis of relative gene expression data using real-time quantitative PCR and the $2^{-\Delta\Delta CT}$ method. *Methods*. **25**(4), pp.402–408.

Lohman, A.W. and Isakson, B.E. 2014. Differentiating connexin hemichannels and pannexin channels in cellular ATP release. *FEBS Letters*. **588**(8), pp.1379–1388.

Louis, S.F. and Zahradka, P. 2010. Vascular smooth muscle cell motility: From migration to invasion. *Experimental and Clinical Cardiology*. **15**(4), pp.e75-85.

Luan, X., Dangaria, S., Ito, Y., Walker, C.G., Jin, T., Schmidt, M.K., Galang, M.T. and Druzinsky, R. 2009. Neural crest lineage segregation: A blueprint for periodontal regeneration. *Journal of Dental Research*. **88**(9), pp.781–791.

Maijenburg, M.W., van der Schoot, C.E. and Voermans, C. 2012. Mesenchymal stromal cell migration: Possibilities to improve cellular therapy. *Stem Cells and Development*. **21**(1), pp.19–29.

Malandraki-Miller, S., Lopez, C. A., Al-Siddiqi, H., and Carr, C. A. 2018. Changing metabolism in differentiating cardiac progenitor cells-can stem cells become metabolically flexible cardiomyocytes? *Frontiers in Cardiovascular Medicine*. **5**, p.119.

Mansoor, S.E., Lü, W., Oosterheert, W., Shekhar, M., Tajkhorshid, E. and Gouaux, E. 2016. X-ray structures define human P2X3 receptor gating cycle and antagonist action. *Nature*. **538**(7623), pp.66–71.

del Mármol, J.I., Touhara, K.K., Croft, G. and MacKinnon, R. 2018. Piezo1 forms a slowly-inactivating mechanosensory channel in mouse embryonic stem cells. *eLife*. **7**, p. e33149.

Matsushita K. 2016. Mesenchymal stem cells and netabolic syndrome: Current understanding and potential clinical implications. *Stem Cells International*. **2016**, 2892840.

McHugh, B.J., Buttery, R., Lad, Y., Banks, S., Haslett, C. and Sethi, T. 2010. Integrin activation by Fam38A uses a novel mechanism of R-Ras targeting to the endoplasmic reticulum. *Journal of Cell Science*. **123**(1), pp.51–61.

McHugh, B.J., Murdoch, A., Haslett, C. and Sethi, T. 2012. Loss of the integrin-activating transmembrane protein Fam38A (Piezo1) promotes a switch to a reduced integrin-dependent mode of cell migration. *PloS One*. **7**(7), p.e40346.

Meis, S., Hamacher, A., Hongwiset, D., Marzian, C., Wiese, M., Eckstein, N., Royer, H.-D., Communi, D., Boeynaems, J.-M., Hausmann, R., Schmalzing, G. and Kassack, M.U. 2010. NF546 [4,4'-(Carbonylbis(imino-3,1-phenylene-carbonylimino-3,1-(4-methyl-phenylene)-carbonylimino))-bis(1,3-xylene- , '-diphosphonic Acid) tetrasodium salt] is a non-nucleotide P2Y11 agonist and stimulates release of interleukin-8 from human monocyte-derived dendritic cells. *Journal of Pharmacology and Experimental Therapeutics*. **332**(1), pp.238–247.

Miyamoto, T., Mochizuki, T., Nakagomi, H., Kira, S., Watanabe, M., Takayama, Y., Suzuki, Y., Koizumi, S., Takeda, M. and Tominaga, M. 2014. Functional role for Piezo1 in stretch-evoked Ca^{2+} influx and ATP release in urothelial cell cultures. *Journal of Biological Chemistry*. **289**(23), pp.16565–16575.

Moreschi, I., Bruzzone, S., Nicholas, R.A., Fruscione, F., Sturla, L., Benvenuto, F., Usai, C., Meis, S., Kassack, M.U., Zocchi, E. and De Flora, A. 2006. Extracellular NAD^+ is an agonist of the human $P2Y_{11}$ purinergic receptor in human granulocytes. *Journal of Biological Chemistry*. **281**(42), pp.31419–31429.

Morrell, A.E., Brown, G.N., Robinson, S.T., Sattler, R.L., Baik, A.D., Zhen, G., Cao, X., Bonewald, L.F., Jin, W., Kam, L.C. and Guo, X.E. 2018. Mechanically induced Ca^{2+} oscillations in osteocytes release extracellular vesicles and enhance bone formation. *Bone Research*. **6**(1), p.6.

Murthy, S.E., Dubin, A.E. and Patapoutian, A. 2017. Piezos thrive under pressure: mechanically activated ion channels in health and disease. *Nature Reviews Molecular Cell Biology*. **18**(12), pp.771–783.

Narsinh, K.H., Plews, J. and Wu, J.C. 2011. Comparison of human induced pluripotent and embryonic stem cells: Fraternal or identical twins? *Molecular Therapy*. **19**(4), pp.635–638.

Nishimura, A., Sunggip, C., Oda, S., Numaga-Tomita, T., Tsuda, M. and Nishida, M. 2017. Purinergic P2Y receptors: Molecular diversity and implications for treatment of cardiovascular diseases. *Pharmacology & Therapeutics*. **180**, pp.113–128.

Nishizuka, M., Koyanagi, A., Osada, S. and Imagawa, M. 2008. Wnt4 and Wnt5a promote adipocyte differentiation. *FEBS Letters*. **582**(21–22), pp.3201–3205.

Nishizuka, Y. 1992. Intracellular signalling by hydrolysis of phospholipids and activation of protein kinase C. *Science*. **258**(5082), pp.607–614.

Nomura, N., Nomura, M., Sugiyama, K. and Hamada, J.-I. 2007. Phorbol 12-myristate 13-acetate (PMA)-induced migration of glioblastoma cells is mediated via p38MAPK/Hsp27 pathway. *Biochemical Pharmacology*. **74**(5), pp.690–701.

Noronha-Matos, J.B., Coimbra, J., Sá-e-Sousa, A., Rocha, R., Marinhas, J., Freitas, R., Guerra-Gomes, S., Ferreirinha, F., Costa, M.A. and Correia-de-Sá, P. 2014. P2X7-induced zeiosis promotes osteogenic differentiation and mineralization of postmenopausal bone marrow-derived mesenchymal stem cells. *The FASEB Journal*. **28**(12), pp.5208–5222.

Noronha-Matos, J.B., Costa, M.A., Magalhães-Cardoso, M.T., Ferreirinha, F., Pelletier, J., Freitas, R., Neves, J.M., Sévigny, J. and Correia-de-Sá, P. 2012. Role of ecto-NTPDases on UDP-sensitive P2Y6 receptor activation during osteogenic differentiation of primary bone marrow stromal cells from postmenopausal women. *Journal of Cellular Physiology*. **227**(6), pp.2694–2709.

North, R.A. 2002. Molecular physiology of P2X receptors. *Physiological Reviews*. **82**(4), pp.1013–1067.

North, R.A. and Jarvis, M.F. 2013. P2X receptors as drug targets. *Molecular Pharmacology*. **83**(4), pp.759–769.

Nourse, J.L. and Pathak, M.M. 2017. How cells channel their stress: Interplay between Piezo1 and the cytoskeleton. *Seminars in Cell & Developmental Biology*. **71**, pp.3–12.

Oh, S.Y., Lee, S.-J., Jung, Y.H., Lee, H.J. and Han, H.J. 2015. Arachidonic acid promotes skin wound healing through induction of human MSC migration by MT3-MMP-mediated fibronectin degradation. *Cell Death & Disease*. **6**, p.e1750.

Oliver-De La Cruz, J., Nardone, G., Vrbsky, J., Pompeiano, A., Perestrelo, A.R., Capradossi, F., Melajová, K., Filipensky, P. and Forte G. 2019. Substrate mechanics controls adipogenesis through YAP phosphorylation by dictating cell spreading. *Biomaterials*. **205**, pp.64-80.

Orriss, I.R., Knight, G.E., Utting, J.C., Taylor, S.E.B., Burnstock, G. and Arnett, T.R. 2009. Hypoxia stimulates vesicular ATP release from rat osteoblasts. *Journal of Cellular Physiology*. **220**(1), pp.155–162.

Park, C.Y., Hoover, P.J., Mullins, F.M., Bachhawat, P., Covington, E.D., Raunser, S., Walz, T., Garcia, K.C., Dolmetsch, R.E. and Lewis, R.S. 2009. STIM1 clusters and activates CRAC channels via direct binding of a cytosolic domain to Orai1. *Cell*. **136**(5), pp.876–890.

Parpaite, T. and Coste, B. 2017. Piezo channels. *Current Biology*. **27**(7), pp.R250–R252.

Pasek, J.G., Wang, X. and Colbran, R.J. 2015. Differential CaMKII regulation by voltage-gated calcium channels in the striatum. *Molecular and Cellular Neurosciences*. **68**, pp.234–243.

Pathak, M.M., Nourse, J.L., Tran, T., Hwe, J., Arulmoli, J., Le, D.T.T., Bernardis, E., Flanagan, L.A. and Tombola, F. 2014. Stretch-activated ion channel Piezo1 directs lineage choice in human neural stem cells. *Proceedings of the National Academy of Sciences of the United States of America*. **111**(45), pp.16148–16153.

Peng, H., Hao, Y., Mousawi, F., Roger, S., Li, J., Sim, J.A., Ponnambalam, S., Yang, X. and Jiang, L.-H. 2016. Purinergic and store-operated Ca^{2+} signalling mechanisms in mesenchymal stem cells and their roles in ATP-induced stimulation of cell migration: ATP-induced Ca^{2+} signalling in MSC migration. *Stem Cells*. **34**(8), pp.2102–2114.

Perry, B.C., Zhou, D., Wu, X., Yang, F.-C., Byers, M.A., Chu, T.-M.G., Hockema, J.J., Woods, E.J. and Goebel, W.S. 2008. Collection, cryopreservation, and characterization of human dental pulp–derived mesenchymal stem cells for banking and clinical use. *Tissue engineering part C: Methods*. **14**(2), pp.149–156.

Picke, A.K., Campbell, G.M., Blüher, M., Krügel, U., Schmidt, F.N., Tsourdi, E., Winzer, M., Rauner, M., Vukicevic, V., Busse, B., Salbach-Hirsch, J., Tuckermann, J.P., Simon, J.C., Anderegg, U., Hofbauer, L.C. and Saalbach, A. 2018. Thy-1 (CD90) promotes bone formation and protects against obesity. *Science Translational Medicine*. **10**(453), eaao680.

Pittenger, M.F., Mackay, A.M., Beck, S.C., Jaiswal, R.K., Douglas, R., Mosca, J.D., Moorman, M.A., Simonetti, D.W., Craig, S. and Marshak, D.R. 1999. Multilineage potential of adult human mesenchymal stem cells. *Science*. **284**(5411), pp.143–147.

Planat-Bénard, V., Menard, C., André, M., Puceat, M., Perez, A., Garcia-Verdugo, J.M., Pénicaud, L. and Casteilla, L. 2004. Spontaneous cardiomyocyte

differentiation from adipose tissue stroma cells. *Circulation Research.* **94**(2), pp.223-229.

Praetorius, H.A. and Leipziger, J. 2009. ATP release from non-excitable cells. *Purinergic Signalling*. **5**(4), pp.433–446.

Qu, F., Zhao, Z., Yuan, B., Qi, W., Li, C., Shen, X., Liu, C., Li, H., Zhao, G., Wang, J., Guo, Q. and Liu, Y. 2015. CaMKII plays a part in the chondrogenesis of bone marrow-derived mesenchymal stem cells. *International Journal of Clinical and Experimental Pathology*. **8**(5), pp.5981–5987.

Rácz, G.Z., Szűcs, Á., Szlávik, V., Vág, J., Burghardt, B., Elliott, A.C. and Varga, G. 2006. Possible role of duration of PKC-induced ERK activation in the effects of agonists and phorbol esters on DNA synthesis in panc-1 cells. *Journal of Cellular Biochemistry*. **98**(6), pp.1667–1680.

Rafehi, M., Burbiel, J.C., Attah, I.Y., Abdelrahman, A. and Müller, C.E. 2017. Synthesis, characterization, and in vitro evaluation of the selective P2Y2 receptor antagonist AR-C118925. *Purinergic Signalling*. **13**(1), pp.89–103.

Ralevic, V. and Burnstock, G. 1998. Receptors for purines and pyrimidines. *Pharmacological Reviews*. **50**(3), pp.413–492.

Ranade, S.S., Qiu, Z., Woo, S.-H., Hur, S.S., Murthy, S.E., Cahalan, S.M., Xu, J., Mathur, J., Bandell, M., Coste, B., Li, Y.-S.J., Chien, S. and Patapoutian, A. 2014. Piezo1, a mechanically activated ion channel, is required for vascular development in mice. *Proceedings of the National Academy of Sciences of the United States of America*. **111**(28), pp.10347–10352.

Ranade, S.S., Syeda, R. and Patapoutian, A. 2015. Mechanically activated ion channels. *Neuron*. **87**(6), pp.1162–1179.

Rastegar, F., Shenaq, D., Huang, J., Zhang, W., Zhang, B.-Q., He, B.-C., Chen, L., Zuo, G.-W., Luo, Q., Shi, Q., Wagner, E.R., Huang, E., Gao, Y., Gao, J.-L., Kim, S.H., Zhou, J.-Z., Bi, Y., Su, Y., Zhu, G., Luo, J., Luo, X., Qin, J., Reid, R.R., Luu, H.H., Haydon, R.C., Deng, Z.-L. and He, T.-C. 2010. Mesenchymal stem cells: Molecular characteristics and clinical applications. *World Journal of Stem Cells*. **2**(4), pp.67–80.

Rettinger, J., Schmalzing, G., Damer, S., Müller, G., Nickel, P. and Lambrecht, G. 2000. The suramin analogue NF279 is a novel and potent antagonist selective for the P2X1 receptor. *Neuropharmacology*. **39**(11), pp.2044–2053.

Reyland, M.E. 2009. Protein kinase C isoforms: Multi-functional regulators of cell life and death. *Frontiers in Bioscience (Landmark Edition)*. **14**, pp.2386–2399.

Riddle, R.C., Taylor, A.F., Rogers, J.R. and Donahue, H.J. 2007. ATP release mediates fluid flow-induced proliferation of human bone marrow stromal cells. *Journal of Bone and Mineral Research*. **22**(4), pp.589–600.

Rodrigues, C., de Assis, A.M., Moura, D.J., Halmenschlager, G., Saffi, J., Xavier, L.L., da Cruz Fernandes, M. and Wink, M.R. 2014. New therapy of skin repair

combining adipose-derived mesenchymal stem cells with sodium carboxymethylcellulose scaffold in a pre-clinical rat model. *PLoS One*. **9**(5), p.e96241.

Rombouts, W.J.C. and Ploemacher, R.E. 2003. Primary murine MSC show highly efficient homing to the bone marrow but lose homing ability following culture. *Leukemia*. **17**(1), pp.160–170.

Ryu, C.H., Park, S.A., Kim, S.M., Lim, J.Y., Jeong, C.H., Jun, J.A., Oh, J.H., Park, S.H., Oh, W.-I. and Jeun, S.-S. 2010b. Migration of human umbilical cord blood mesenchymal stem cells mediated by stromal cell-derived factor-1/CXCR4 axis via Akt, ERK, and p38 signal transduction pathways. *Biochemical and Biophysical Research Communications*. **398**(1), pp.105–110.

Ryu, J.M. and Han, H.J. 2015. Autotaxin-LPA axis regulates hMSC migration by adherent junction disruption and cytoskeletal rearrangement via LPAR1/3-dependent PKC/GSK3β/β-catenin and PKC/Rho GTPase pathways: Effect of ATX/LPA on hMSC motility. *Stem Cells*. **33**(3), pp.819–832.

Ryu, J.M., Lee, M.Y., Yun, S.P. and Han, H.J. 2010a. High glucose regulates cyclin D1/E of human mesenchymal stem cells through TGF-beta1 expression via Ca^{2+}/PKC/MAPKs and PI3K/Akt/mTOR signal pathways. *Journal of Cellular Physiology*. **224**(1), pp.59–70.

Samtleben, S., Jaepel, J., Fecher, C., Andreska, T., Rehberg, M. and Blum, R. 2013. Direct imaging of ER calcium with targeted-esterase induced dye loading (TED). *Journal of Visualized Experiments*. **75**, p. e50317

Saotome, K., Murthy, S.E., Kefauver, J.M., Whitwam, T., Patapoutian, A. and Ward, A.B. 2018. Structure of the mechanically activated ion channel Piezo1. *Nature*. **554**(7693), pp.481–486.

Scadden, D.T. 2006. The stem-cell niche as an entity of action. *Nature*. **441**(7097), pp.1075–1079.

Scarfì, S. 2014. Purinergic receptors and nucleotide processing ectoenzymes: Their roles in regulating mesenchymal stem cell functions. *World Journal of Stem Cells*. **6**(2), p.153.

Schwab, A., Fabian, A., Hanley, P.J. and Stock, C. 2012. Role of ion channels and transporters in cell migration. *Physiological Reviews*. **92**(4), pp.1865–1913.

Schwiebert, E.M. 2001. ATP release mechanisms, ATP receptors and purinergic signalling along the nephron. *Clinical and Experimental Pharmacology & Physiology*. **28**(4), pp.340–350.

Scintu, F., Reali, C., Pillai, R., Badiali, M., Sanna, M.A., Argiolu, F., Ristaldi, M.S. and Sogos, V. 2006. Differentiation of human bone marrow stem cells into cells with a neural phenotype: diverse effects of two specific treatments. *BMC Neuroscience*. **7**, p.14.

Seo, J.H., Jin, Y.-H., Jeong, H.M., Kim, Y.-J., Jeong, H.G., Yeo, C.-Y. and Lee, K.-Y. 2009. Calmodulin-dependent kinase II regulates Dlx5 during osteoblast differentiation. *Biochemical and Biophysical Research Communications*. **384**(1), pp.100–104.

Shibukawa, Y., Sato, M., Kimura, M., Sobhan, U., Shimada, M., Nishiyama, A., Kawaguchi, A., Soya, M., Kuroda, H., Katakura, A., Ichinohe, T. and Tazaki, M. 2015. Odontoblasts as sensory receptors: transient receptor potential channels, pannexin-1, and ionotropic ATP receptors mediate intercellular odontoblast-neuron signal transduction. *Pflügers Archiv - European Journal of Physiology*. **467**(4), pp.843–863.

Shin, M.K., Kim, M.-K., Bae, Y.-S., Jo, I., Lee, S.-J., Chung, C.-P., Park, Y.-J. and Min, D.S. 2008. A novel collagen-binding peptide promotes osteogenic differentiation via Ca^{2+}/calmodulin-dependent protein kinase II/ERK/AP-1 signalling pathway in human bone marrow-derived mesenchymal stem cells. *Cellular Signalling*. **20**(4), pp.613–624.

Singh, R.K., Kumar, S., Gautam, P.K., Tomar, M.S., Verma, P.K., Singh, S.P., Kumar, S. and Acharya, A. 2017. Protein kinase C-α and the regulation of diverse cell responses. *Biomolecular Concepts*. **8**(3–4).

Soltoff, S.P., Avraham, H., Avraham, S. and Cantley, L.C. 1998. Activation of P2Y2 receptors by UTP and ATP stimulates mitogen-activated kinase activity through a pathway that involves related adhesion focal tyrosine kinase and protein kinase C. *Journal of Biological Chemistry*. **273**(5), pp.2653–2660.

Song, B.-W., Chang, W., Hong, B.-K., Kim, I.-K., Cha, M.-J., Lim, S., Choi, E.J., Ham, O., Lee, S.-Y., Lee, C.Y., Park, J.-H., Choi, E., Song, H., Jang, Y. and Hwang, K.-C. 2013. Protein kinase C activation stimulates mesenchymal stem cell adhesion through activation of focal adhesion kinase. *Cell Transplantation*. **22**(5), pp.797–809.

Song, H.Y., Lee, M.J., Kim, M.Y., Kim, K.H., Lee, I.H., Shin, S.H., Lee, J.S. and Kim, J.H. 2010. Lysophosphatidic acid mediates migration of human mesenchymal stem cells stimulated by synovial fluid of patients with rheumatoid arthritis. *Biochimica et Biophysica Acta (BBA) - Molecular and Cell Biology of Lipids*. **1801**(1), pp.23–30.

Steward, A.J., Kelly, D.J. and Wagner, D.R. 2016. Purinergic signalling regulates the transforming growth factor-β3-induced chondrogenic response of mesenchymal stem cells to hydrostatic pressure. *Tissue Engineering Part A*. **22**(11–12), pp.831–839.

Stokes, L., Jiang, L.-H., Alcaraz, L., Bent, J., Bowers, K., Fagura, M., Furber, M., Mortimore, M., Lawson, M., Theaker, J., Laurent, C., Braddock, M. and Surprenant, A. 2006. Characterization of a selective and potent antagonist of human P2X7 receptors, AZ11645373. *British Journal of Pharmacology*. **149**(7), pp.880–887.

Stokes, L., Layhadi, J.A., Bibic, L., Dhuna, K. and Fountain, S.J. 2017. P2X4 receptor function in the nervous system and current breakthroughs in pharmacology. *Frontiers in Pharmacology*. **8**, p.291

Striedinger, K., Meda, P. and Scemes, E. 2007. Exocytosis of ATP from astrocyte progenitors modulates spontaneous Ca^{2+} oscillations and cell migration. *Glia*. **55**(6), pp.652–662.

Suadicani, S.O. 2006. P2X7 receptors mediate ATP release and amplification of astrocytic intercellular Ca^{2+} signalling. *Journal of Neuroscience*. **26**(5), pp.1378–1385.

Suchyna, T.M., Johnson, J.H., Hamer, K., Leykam, J.F., Gage, D.A., Clemo, H.F., Baumgarten, C.M. and Sachs, F. 2000. Identification of a peptide toxin from *Grammostola spatulata* spider venom that blocks cation-selective stretch-activated channels. *Journal of General Physiology*. **115**(5), pp.583–598.

Sudulaguntla, A., Gurung, S., Nanjwade, B. and Kumar Tamang, J. 2016. A review: Stem cells and classification of stem cells based on their origin. *World Journal of Pharmacy and Pharmaceutical Sciences*. **5**, pp.534–556.

Sugasawa, M., Erostegui, C., Blanchet, C. and Dulon, D. 1996. ATP activates non-selective cation channels and calcium release in inner hair cells of the guinea-pig cochlea. *Journal of Physiology*. **491 (Pt 3)**, pp.707–718.

Sugimoto, A., Miyazaki, A., Kawarabayashi, K., Shono, M., Akazawa, Y., Hasegawa, T., Ueda-Yamaguchi, K., Kitamura, T., Yoshizaki, K., Fukumoto, S. and Iwamoto, T. 2017. Piezo type mechanosensitive ion channel component 1 functions as a regulator of the cell fate determination of mesenchymal stem cells. *Scientific Reports*. **7**(1), p.17696

Suhr, F., Delhasse, Y., Bungartz, G., Schmidt, A., Pfannkuche, K. and Bloch, W. 2013. Cell biological effects of mechanical stimulations generated by focused extracorporeal shock wave applications on cultured human bone marrow stromal cells. *Stem Cell Research*. **11**(2), pp.951–964.

Sumagin, R., Robin, A.Z., Nusrat, A. and Parkos, C.A. 2013. Activation of PKCβII by PMA facilitates enhanced epithelial wound repair through increased cell spreading and migration. *PLoS One*. **8**(2), p.e55775.

Sun, C.K., Man, K., Ng, K.T., Ho, J.W., Lim, Z.X., Cheng, Q., Lo, C.-M., Poon, R.T. and Fan, S.-T. 2008. Proline-rich tyrosine kinase 2 (Pyk2) promotes proliferation and invasiveness of hepatocellular carcinoma cells through c-Src/ERK activation. *Carcinogenesis*. **29**(11), pp.2096–2105.

Sun, D., Junger, W.G., Yuan, C., Zhang, W., Bao, Y., Qin, D., Wang, C., Tan, L., Qi, B., Zhu, D., Zhang, X. and Yu, T. 2013. Shockwaves induce osteogenic differentiation of human mesenchymal stem cells through ATP release and activation of P2X7 receptors. *Stem Cells*. **31**(6), pp.1170–1180.

Swarthout, J.T., Doggett, T.A., Lemker, J.L. and Partridge, N.C. 2001. Stimulation of extracellular signal-regulated kinases and proliferation in rat osteoblastic cells

by parathyroid hormone is protein kinase C-dependent. *Journal of Biological Chemistry*. **276**(10), pp.7586–7592.

Syed, N.-H. and Kennedy, C. 2012. Pharmacology of P2X receptors. *Wiley Interdisciplinary Reviews: Membrane Transport and Signalling*. **1**(1), pp.16–30.

Syeda, R., Florendo, M.N., Cox, C.D., Kefauver, J.M., Santos, J.S., Martinac, B. and Patapoutian, A. 2016. Piezo1 channels are inherently mechanosensitive. *Cell Reports*. **17**(7), pp.1739–1746.

Syeda, R., Xu, J., Dubin, A.E., Coste, B., Mathur, J., Huynh, T., Matzen, J., Lao, J., Tully, D.C., Engels, I.H., Petrassi, H.M., Schumacher, A.M., Montal, M., Bandell, M. and Patapoutian, A. 2015. Chemical activation of the mechanotransduction channel Piezo1. *eLife*. **4**.

Szabo, E., Feng, T., Dziak, E. and Opas, M. 2009. Cell adhesion and spreading affect adipogenesis from embryonic stem cells: The role of calreticulin. *Stem Cells*. **27**(9), pp.2092–2102.

Takada, I., Mihara, M., Suzawa, M., Ohtake, F., Kobayashi, S., Igarashi, M., Youn, M.-Y., Takeyama, K., Nakamura, T., Mezaki, Y., Takezawa, S., Yogiashi, Y., Kitagawa, H., Yamada, G., Takada, S., Minami, Y., Shibuya, H., Matsumoto, K. and Kato, S. 2007. A histone lysine methyltransferase activated by non-canonical Wnt signalling suppresses PPAR-γ transactivation. *Nature Cell Biology*. **9**(11), pp.1273–1285.

Takahashi, K. and Yamanaka, S. 2006. Induction of pluripotent stem cells from mouse embryonic and adult fibroblast cultures by defined factors. *Cell*. **126**(4), pp.663–676.

Tang, J.-M., Yuan, J., Li, Q., Wang, J.-N., Kong, X., Zheng, F., Zhang, L., Chen, L., Guo, L.-Y., Huang, Y.-H., Yang, J.-Y. and Chen, S.-Y. 2012. Acetylcholine induces mesenchymal stem cell migration via Ca^{2+}/PKC/ERK1/2 signal pathway. *Journal of Cellular Biochemistry*. **113**(8), pp.2704–2713.

Tatullo, M., Marrelli, M., Shakesheff, K.M. and White, L.J. 2015. Dental pulp stem cells: function, isolation and applications in regenerative medicine: Function, isolation and applications of dental pulp stem cells. *Journal of Tissue Engineering and Regenerative Medicine*. **9**(11), pp.1205–1216.

Tolhurst, G., Vial, C., Léon, C., Gachet, C., Evans, R.J. and Mahaut-Smith, M.P. 2005. Interplay between P2Y1, P2Y12, and P2X1 receptors in the activation of megakaryocyte cation influx currents by ADP: evidence that the primary megakaryocyte represents a fully functional model of platelet P2 receptor signalling. *Blood*. **106**(5), pp.1644–1651.

Toma, C., Pittenger, M.F., Cahill, K.S., Byrne, B.J. and Kessler, P.D. 2002. Human mesenchymal stem cells differentiate to a cardiomyocyte phenotype in the adult murine heart. *Circulation*. **105**(1), pp.93–98.

Trubiani, O., Horenstein, A.L., Caciagli, F., Caputi, S., Malavasi, F. and Ballerini, P. 2014. Expression of P2X7 ATP receptor mediating the IL8 and CCL20 release in human periodontal ligament stem cells: P2X7 and periodontal ligament stem cells. *Journal of Cellular Biochemistry*. **115**(6), pp.1138–1146.

Tsai, T.-L., Manner, P.A. and Li, W.-J. 2013. Regulation of mesenchymal stem cell chondrogenesis by glucose through protein kinase C/transforming growth factor signalling. *Osteoarthritis and Cartilage*. **21**(2), pp.368–376.

Tsolaki, E. and Yannaki, E. 2015. Stem cell-based regenerative opportunities for the liver: State of the art and beyond. *World Journal of Gastroenterology*. **21**(43), pp.12334–12350.

Tu, J., Yang, F., Wan, J., Liu, Yunhui, Zhang, J., Wu, B., Liu, Yafeng, Zeng, S. and Wang, L. 2014. Light-controlled astrocytes promote human mesenchymal stem cells toward neuronal differentiation and improve the neurological deficit in stroke rats: Light-controlled astrocytes promote MSCs to neuronal cells. *Glia*. **62**(1), pp.106–121.

Tu, M.-T., Luo, S.-F., Wang, C.-C., Chien, C.-S., Chiu, C.-T., Lin, C.-C. and Yang, C.-M. 2000. P2Y2 receptor-mediated proliferation of C_6 glioma cells *via* activation of Ras/Raf/MEK/MAPK pathway. *British Journal of Pharmacology*. **129**(7), pp.1481–1489.

Tuan, R.S., Boland, G. and Tuli, R. 2003. Adult mesenchymal stem cells and cell-based tissue engineering. *Arthritis Research & Therapy*. **5**(1), pp.32–45.

Tzameret, A., Sher, I., Belkin, M., Treves, A.J., Meir, A., Nagler, A., Levkovitch-Verbin, H., Barshack, I., Rosner, M. and Rotenstreich, Y. 2014. Transplantation of human bone marrow mesenchymal stem cells as a thin subretinal layer ameliorates retinal degeneration in a rat model of retinal dystrophy. *Experimental Eye Research*. **118**, pp.135–144.

Ullmann, H., Meis, S., Hongwiset, D., Marzian, C., Wiese, M., Nickel, P., Communi, D., Boeynaems, J.-M., Wolf, C., Hausmann, R., Schmalzing, G. and Kassack, M.U. 2005. Synthesis and structure-activity relationships of suramin-derived P2Y11 receptor antagonists with nanomolar potency. *Journal of Medicinal Chemistry*. **48**(22), pp.7040–7048.

Umemura, M., Baljinnyam, E., Feske, S., De Lorenzo, M.S., Xie, L.-H., Feng, X., Oda, K., Makino, A., Fujita, T., Yokoyama, U., Iwatsubo, M., Chen, S., Goydos, J.S., Ishikawa, Y. and Iwatsubo, K. 2014. Store-operated Ca^{2+} entry (SOCE) regulates melanomapProliferation and cell migration. *PLoS One*. **9**(2), p.e89292.

Van Kolen, K. and Slegers, H. 2006. Integration of P2Y receptor-activated signal transduction pathways in G protein-dependent signalling networks. *Purinergic Signalling*. **2**(3), pp.451–469.

Via, A.G., Frizziero, A. and Oliva, F. 2012. Biological properties of mesenchymal Stem Cells from different sources. *Muscles, Ligaments and Tendons Journal*. **2**(3), pp.154–162.

Virginio, C., MacKenzie, A., North, R.A. and Surprenant, A. 1999. Kinetics of cell lysis, dye uptake and permeability changes in cells expressing the rat P2X7 receptor. *Journal of Physiology*. **519 (2)**, pp.335–346.

Visweswaran, M., Pohl, S., Arfuso, F., Newsholme, P., Dilley, R., Pervaiz, S. and Dharmarajan, A. 2015. Multi-lineage differentiation of mesenchymal stem cells – To Wnt, or not Wnt. *The International Journal of Biochemistry & Cell Biology*. **68**, pp.139–147.

Wang, C., Li, N., Liu, X., Zheng, Y. and Cao, X. 2008. A novel endogenous human CaMKII inhibitory protein suppresses tumor growth by inducing cell cycle arrest via p27 stabilization. *Journal of Biological Chemistry*. **283**(17), pp.11565–11574.

Wang, H. and Reiser, G. 2003. The role of the Ca^{2+}-sensitive tyrosine kinase Pyk2 and Src in thrombin signalling in rat astrocytes. *Journal of Neurochemistry*. **84**(6), pp.1349–1357.

Wang, H., Ubl, J.J., Stricker, R. and Reiser, G. 2002. Thrombin (PAR-1)-induced proliferation in astrocytes via MAPK involves multiple signalling pathways. *American Journal of Physiology-Cell Physiology*. **283**(5), pp.C1351–C1364.

Wang, S., Chennupati, R., Kaur, H., Iring, A., Wettschureck, N. and Offermanns, S. 2016. Endothelial cation channel PIEZO1 controls blood pressure by mediating flow-induced ATP release. *Journal of Clinical Investigation*. **126**(12), pp.4527–4536.

Wang, S., Qu, X. and Zhao, R. 2012. Clinical applications of mesenchymal stem cells. *Journal of Hematology & Oncology*. **5**(1), p.19.

Webb, B.L.J., Hirst, S.J. and Giembycz, M.A. 2000. Protein kinase C isoenzymes: a review of their structure, regulation and role in regulating airways smooth muscle tone and mitogenesis. *British Journal of Pharmacology*. **130**(7), pp.1433–1452.

Webb, T.E., Feolde, E., Vigne, P., Neary, J.T., Runberg, A., Frelin, C. and Barnard, E.A. 1996. The P2Y purinoceptor in rat brain microvascular endothelial cells couple to inhibition of adenylate cyclase. *British Journal of Pharmacology*. **119**(7), pp.1385–1392.

Wei, F., Wang, T.Z., Zhang, J., Yuan, Z.Y., Tian, H.Y., Ni, Y.J., Zhuo, X.Z., Han, K., Liu, Y., Lu, Q., Bai, H.Y. and Ma, A.Q. 2012. Mesenchymal stem cells neither fully acquire the electrophysiological properties of mature cardiomyocytes nor promote ventricular arrhythmias in infarcted rats. *Basic Research in Cardiology*. **107**, p.274.

Wei, L., Caseley, E., Li, D. and Jiang, L.-H. 2016. ATP-induced P2X receptor-dependent large pore formation: How much do we know? *Frontiers in Pharmacology*. **7**, p.5.

Weihs, A.M., Fuchs, C., Teuschl, A.H., Hartinger, J., Slezak, P., Mittermayr, R., Redl, H., Junger, W.G., Sitte, H.H. and Rünzler, D. 2014. Shock wave treatment

enhances cell proliferation and improves wound healing by ATP release-coupled extracellular signal-regulated kinase (ERK) activation. *Journal of Biological Chemistry*. **289**(39), pp.27090–27104.

Wiedon, A., Tölle, M., Bastine, J., Schuchardt, M., Huang, T., Jankowski, V., Jankowski, J., Zidek, W. and van der Giet, M. 2012. Uridine adenosine tetraphosphate (Up4A) is a strong inductor of smooth muscle cell migration via activation of the P2Y2 receptor and cross-communication to the PDGF receptor. *Biochemical and Biophysical Research Communications*. **417**(3), pp.1035–1040.

Williams, A. R., Hatzistergos, K. E., Addicott, B., McCall, F., Carvalho, D., Suncion, V., Morales, A.R., Da Silva, J., Sussman, M.A., Heldman, A.W. and Hare, J.M. 2013. Enhanced effect of combining human cardiac stem cells and bone marrow mesenchymal stem cells to reduce infarct size and to restore cardiac function after myocardial infarction. *Circulation*. **127**(2), pp.213–223.

Wu, D. and Mori, N. 1999. Extracellular ATP-induced inward current in isolated epithelial cells of the endolymphatic sac. *Biochimica et Biophysica Acta*. **1419**(1), pp.33–42.

Wu, J., Lewis, A.H. and Grandl, J. 2017. Touch, Tension, and Transduction – The function and regulation of Piezo ion channels. *Trends in Biochemical Sciences*. **42**(1), pp.57–71.

Wu, S.S., Chiu, T. and Rozengurt, E. 2002. ANG II and LPA induce Pyk2 tyrosine phosphorylation in intestinal epithelial cells: role of Ca^{2+}, PKC, and Rho kinase. *American Journal of Physiology-Cell Physiology*. **282**(6), pp.C1432–C1444.

Wu, T.-C., Chang, C.-C., Leu, H.-B., Huang, P.-H., Lin, S.-J. and Chen, J.-W. 2019. Phorbol ester-induced angiogenesis of endothelial progenitor cells: The role of NADPH oxidase-mediated, redox-related matrix metalloproteinase pathways. *PLoS One*. **14**(1), p.e0209426.

Xie, Y., Hong, Y., Ma, X.-Y., Ren, X.-R., Ackerman, S., Mei, L. and Xiong, W.-C. 2006. DCC-dependent phospholipase C signalling in netrin-1-induced neurite elongation. *Journal of Biological Chemistry*. **281**(5), pp.2605–2611.

Xu, X.-Y., He, X.-T., Wang, J., Li, X., Xia, Y., Tan, Y.-Z. and Chen, F.-M. 2019. Role of the P2X7 receptor in inflammation-mediated changes in the osteogenesis of periodontal ligament stem cells. *Cell Death & Disease*. **10**(1), p.20.

Xu, X.Z.S. 2016. Demystifying mechanosensitive Piezo ion channels. *Neuroscience Bulletin*. **32**(3), pp.307–309.

Yang, X.-N., Lu, Y.-P., Liu, J.-J., Huang, J.-K., Liu, Y.-P., Xiao, C.-X., Jazag, A., Ren, J.-L. and Guleng, B. 2014. Piezo1 is as a novel trefoil factor family 1 binding protein that promotes gastric cancer cell mobility in vitro. *Digestive Diseases and Sciences*. **59**(7), pp.1428–1435.

Yegutkin, G.G. 2008. Nucleotide- and nucleoside-converting ectoenzymes: Important modulators of purinergic signalling cascade. *Biochimica et Biophysica Acta (BBA) - Molecular Cell Research*. **1783**(5), pp.673–694.

Yuan, L., Sakamoto, N., Song, G. and Sato, M. 2012. Migration of human mesenchymal stem cells under low shear stress mediated by mitogen-activated protein kinase signalling. *Stem Cells and Development*. **21**(13), pp.2520–2530.

Yuan, L., Sakamoto, N., Song, G. and Sato, M. 2013. Low-level shear stress induces human mesenchymal stem cell migration through the SDF-1/CXCR4 axis via MAPK signalling pathways. *Stem Cells and Development*. **22**(17), pp.2384–2393.

Yun, S.P., Lee, M.Y., Ryu, J.M., Song, C.H. and Han, H.J. 2009. Role of HIF-1α and VEGF in human mesenchymal stem cell proliferation by 17β-estradiol: involvement of PKC, PI3K/Akt, and MAPKs. *American Journal of Physiology-Cell Physiology*. **296**(2), pp.C317–C326.

Zamponi, G.W. and Currie, K.P.M. 2013. Regulation of CaV2 calcium channels by G protein coupled receptors. *Biochimica et Biophysica Acta (BBA) - Biomembranes*. **1828**(7), pp.1629–1643.

Zayzafoon, M. 2006. Calcium/calmodulin signalling controls osteoblast growth and differentiation. *Journal of Cellular Biochemistry*. **97**(1), pp.56–70.

Zayzafoon, M., Fulzele, K. and McDonald, J.M. 2005. Calmodulin and calmodulin-dependent kinase IIα regulate osteoblast differentiation by controlling c-*fos* expression. *Journal of Biological Chemistry*. **280**(8), pp.7049–7059.

Zhang, D., Gao, Z.-G., Zhang, K., Kiselev, E., Crane, S., Wang, J., Paoletta, S., Yi, C., Ma, L., Zhang, W., Han, G.W., Liu, H., Cherezov, V., Katritch, V., Jiang, H., Stevens, R.C., Jacobson, K.A., Zhao, Q. and Wu, B. 2015. Two disparate ligand-binding sites in the human P2Y1 receptor. *Nature*. **520**(7547), pp.317–321.

Zhang, F., Ye, J., Meng, Y., Ai, W., Su, H., Zheng, J., Liu, F., Zhu, X., Wang, L., Gao, P., Shu, G., Jiang, Q. and Wang, S. 2018. Calcium supplementation enhanced adipogenesis and improved glucose homeostasis through activation of Camkii and PI3K/Akt signalling pathway in porcine bone marrow mesenchymal stem cells (pBMSCs) and mice fed high fat diet (HFD). *Cellular Physiology and Biochemistry*. **51**(1), pp.154–172.

Zhang, J., Zhou, Y., Huang, T., Wu, F., Liu, L., Kwan, J.S.H., Cheng, A.S.L., Yu, J., To, K.F. and Kang, W. 2018. PIEZO1 functions as a potential oncogene by promoting cell proliferation and migration in gastric carcinogenesis. *Molecular Carcinogenesis*. **57**(9), pp.1144–1155.

Zhang, S., Ye, D., Ma, L., Ren, Y., Dirksen, R.T. and Liu, X. 2019. Purinergic signalling modulates survival/proliferation of human dental pulp stem cells. *Journal of Dental Research*. **98**(2), pp.242–249.

Zhang, S.L., Yu, Y., Roos, J., Kozak, J.A., Deerinck, T.J., Ellisman, M.H., Stauderman, K.A. and Cahalan, M.D. 2005. STIM1 is a Ca^{2+} sensor that activates CRAC channels and migrates from the Ca^{2+} store to the plasma membrane. *Nature*. **437**(7060), pp.902–905.

Zhang, T., Chi, S., Jiang, F., Zhao, Q. and Xiao, B. 2017. A protein interaction mechanism for suppressing the mechanosensitive Piezo channels. *Nature Communications*. **8**(1), p1797.

Zhao, Q., Wu, K., Geng, J., Chi, S., Wang, Y., Zhi, P., Zhang, M. and Xiao, B. 2016. Ion permeation and mechanotransduction mechanisms of mechanosensitive Piezo channels. *Neuron*. **89**(6), pp.1248–1263.

Zhao, Q., Zhou, H., Li, X. and Xiao, B. 2019. The mechanosensitive Piezo1 channel: a three-bladed propeller-like structure and a lever-like mechanogating mechanism. *FEBS Journal.* **286(13)**, pp.2461-2470.

Zippel, N., Limbach, C.A., Ratajski, N., Urban, C., Luparello, C., Pansky, A., Kassack, M.U. and Tobiasch, E. 2012. Purinergic receptors influence the differentiation of human mesenchymal stem cells. *Stem Cells and Development*. **21**(6), pp.884–900.

Zuk, P.A., Zhu, M., Ashjian, P., De Ugarte, D.A., Huang, J.I., Mizuno, H., Alfonso, Z.C., Fraser, J.K., Benhaim, P. and Hedrick, M.H. 2002. Human adipose tissue is a source of multipotent stem cells. *Molecular Biology of the Cell*. **13**(12), pp.4279–4295.